

Optimization of Solid Phase Microextraction for Determination of Disinfection By-products in Water

by

Farhad Riazi Kermani

A thesis
presented to the University of Waterloo
in fulfillment of the
thesis requirement for the degree of
Doctor of Philosophy
in
Chemistry

Waterloo, Ontario, Canada, 2012

© Farhad Riazi Kermani 2012

Author's Declaration

I hereby declare that I am the sole author of this thesis. This is a true copy of the thesis,
including any required final revisions, as accepted by my examiners.

I understand that my thesis may be made electronically available to the public.

Abstract

A new technique for sample preparation and trace analysis of organic pollutants in water using mixed-phase thin film (MPTF) devices, combined with direct thermal desorption, cold trapping, gas chromatography-mass spectrometry (GC-MS) is presented for the first time. Two novel analytical devices, Carboxen/polydimethylsiloxane (CAR/PDMS) and polydimethylsiloxane/divinylbenzene (PDMS/DVB) TF samplers were fabricated using spin coating technique and glass wool fabric mesh as substrate. The samplers were easily tailored in size and shape by cutting tools. Good durability and flat-shape stability were observed during extractions and stirring in water. The latter characteristic obviates the need for an extra framed holder for rapid thin film microextraction (TFME) and makes the samplers more robust and user-friendly. The analytical performance of the MPTF devices was satisfactorily illustrated and compared with those of solid phase microextraction (SPME) fibers and PDMS thin film membrane using water samples spiked with seven N-nitrosamines (NAs), known as disinfection by-products (DBPs) in drinking water. Marked enhancement of extraction efficiencies (typically more than one order of magnitude) for the N-nitrosamines, including the hydrophilic ones, was obtained with the MPTF devices under generally pre-equilibrium conditions, compared to the SPME fibers and PDMS thin film membrane. The analytical results obtained in this study, including linearity, repeatability and detection levels at low ng/L for the tested compounds, indicate that the new thin film devices are promising for rapid sampling and sample preparation of trace levels of polar organic pollutants in water with sensitivities higher than SPME fibers and with a wide application range typical of mixed-phase coatings. The user-friendly format and robustness of the novel devices are also advantageous for on-site applications, which is the ultimate use of thin film samplers. Moreover, the thin film fabrication approach developed in this study offers the possibility of making other novel samplers with PDMS or different absorptive polymers such as polyacrylate (PA) and polyethylene glycol (PEG) as particle-free, or as particle-loaded thin films with a variety of adsorptive solid particles.

In another development in the course of this research, the performance and accuracy of the SPME fiber approach for sample preparation of selected DBPs were demonstrated and compared with the conventional liquid-liquid extraction (LLE) method by real drinking water

samples analysis in collaboration with Health Canada. Four regulated trihalomethanes (THMs) and seven other DBPs known as priority by-products, including four haloacetonitriles, two haloketones and chloropicrin, were analyzed in real samples during two separate comparative studies. In each study, duplicate samples from several water treatment and distribution systems in Canada, collected and stabilized under the same protocol, were analyzed in parallel by two independent labs; in the University of Waterloo by an optimized headspace SPME-GC-MS and in Health Canada by a LLE-GC-ECD (electron capture detection) method equivalent to EPA 551.1. The values for the concentration of the analytes in the samples obtained by the two methods were in good agreement with each other in majority of the cases indicating that SPME affords the promise of a dependable sample preparation technique for rapid DBPs analysis. In particular, it was shown that the SPME fiber approach combined with GC-MS is a fast reliable alternative to the LLE-GC-ECD (EPA 551.1) method for analysis of the regulated THMs in the concentration ranges that are typical and relevant for drinking water samples.

Acknowledgements

Thanks are due to many people who supported, offered comments or helped in other ways during this thesis. Firstly, my supervisor, Professor Janusz Pawliszyn, for giving me the opportunity to do research within his group and for his guidance throughout my PhD work. Secondly, my advisory committee members, Professors Tadeusz Gorecki, Wojciech Gabryelski and Romek Pawluczyk for support and constructive comments during my research. Thirdly, Professors Jack Rosenfeld and Ken Stark for accepting to be the external and internal/external examiners and for their helpful comments on my thesis.

Then are the people who I worked with while undertaking experiments and who showed me new techniques or equipments. Dr. Vadoud Niri and Dr. In-Yong Eom for assistance at early stages of my research, Dr. Suresh Seethapathy for sharing his valuable GC/MS experiences and helping out in various other ways, Dr. Shokouh H. Haddadi and Dr. Maria Rowena Monton for helpful comments, and my other colleagues in Prof. Pawliszyn's group and Prof. Gorecki's group who supported me in other ways and shared their friendship.

Thanks are also due to the staff of the Chemistry Department and the Science Shop in University of Waterloo, especially Cathy Van Esch, Heide Flatt, Jacek Szubra, Krunomir Dvorski, and particularly Harmen Vander Heide who was always resourceful and addressed my technical needs in the shortest possible time.

My special gratitude is extended to Dr. Anca-Maria Tugulea and her colleagues at Exposure and Biomonitoring Division, and Chemicals Management Plan, Health Canada, for collaboration in providing water samples and financial support on the joint research works.

Additionally, I would like to thank Robert Shirey and Supelco for supplying particles and advice on my research.

I also thank my former supervisor Professor I. Yavari, for inspiration, encouragement and continued support throughout the years.

Finally, I would like to thank my parents, my wife and my son for their love, care and encouragement. This thesis would never have been possible without their support.

Dedication

To my loving parents, my wife and Kayvan

Table of Contents

| | |
|--|------|
| Author's Declaration | ii |
| Abstract | iii |
| Acknowledgements | v |
| Dedication | vi |
| Table of Contents | vii |
| List of Tables | xiii |
| List of Figures | xv |
| List of Abbreviations | xx |
| | |
| Chapter 1: Introduction | 1 |
| 1.1 Disinfection by-products in drinking water | 1 |
| 1.2 Analytical methodologies for DBPs studies | 6 |
| 1.2.1 Instrumental approaches | 6 |
| 1.2.2 Sample collection considerations | 7 |
| 1.2.3 Conventional methods for sample preparation | 8 |
| 1.2.4 Trends in new sample preparation techniques | 12 |
| 1.3 Microextraction techniques | 13 |
| 1.3.1 Liquid phase microextraction (LPME) | 13 |
| 1.3.1.1 Single drop microextraction (SDME) | 14 |
| 1.3.1.2 Hollow-fiber liquid phase microextraction (HFLPME) | 16 |
| 1.3.1.3 Dispersive liquid-liquid microextraction (DLLME) | 19 |
| 1.3.2 Solid phase microextraction (SPME) | 20 |
| 1.3.2.1 Theoretical and practical aspects | 21 |
| 1.3.2.1.1 SPME device | 21 |

| | | |
|-----------|---|----|
| 1.3.2.1.2 | Procedure and modes of extraction | 23 |
| 1.3.2.1.3 | Equilibrium extraction | 24 |
| 1.3.2.1.4 | Pre-equilibrium extraction | 27 |
| 1.3.2.1.5 | Matrix effect | 28 |
| 1.3.2.1.6 | Kinetics | 29 |
| 1.3.2.1.7 | Adsorption versus absorption extraction | 34 |
| 1.3.2.1.8 | Calibration and quantification | 37 |
| 1.3.2.2 | Method development | 41 |
| 1.3.2.2.1 | Fiber coating | 41 |
| 1.3.2.2.2 | Analyte derivatization | 45 |
| 1.3.2.2.3 | Extraction mode | 45 |
| 1.3.2.2.4 | Sample and headspace volumes | 46 |
| 1.3.2.2.5 | Matrix conditions | 48 |
| 1.3.2.2.6 | Agitation method | 49 |
| 1.3.2.2.7 | Extraction time | 50 |
| 1.3.2.2.8 | Desorption conditions | 51 |
| 1.3.2.3 | Stir-bar sorptive configuration | 51 |
| 1.3.2.4 | Thin film membrane configuration | 53 |
| 1.3.2.4.1 | Methods for thin film preparation | 54 |
| 1.3.2.4.2 | Spin coating | 55 |
| 1.4 | Research Objectives | 60 |
| 1.5 | Reference | 61 |

| | |
|--|-----|
| Chapter 2: Solid phase microextraction of N–nitrosamines in water: Development of mixed-phase (particle-loaded) thin films as novel sampling and sample preparation devices | 87 |
| 2.1 Introduction | 87 |
| 2.2 Experimental | 91 |
| 2.2.1 Safety considerations | 91 |
| 2.2.2 Chemicals and supplies | 91 |
| 2.2.3 GC-MS analysis | 92 |
| 2.2.4 Spin coating instrument | 93 |
| 2.2.5 Fabrication of mixed-phase thin films (MPTFs) | 93 |
| 2.2.6 Scanning electron microscopy (SEM) | 95 |
| 2.2.7 SPME procedure | 95 |
| 2.2.8 TFME set-up and procedure | 95 |
| 2.3 Results and Discussion | 98 |
| 2.3.1 Analytes description and properties | 98 |
| 2.3.2 Separation and identification | 100 |
| 2.3.3 SPME fibers evaluation | 100 |
| 2.3.4 Extraction mode (CAR/PDMS fiber) | 102 |
| 2.3.5 Extraction time (CAR/PDMS fiber) | 104 |
| 2.3.6 pH effect | 105 |
| 2.3.7 Salt addition effect | 106 |
| 2.3.8 Thermal degradation on CAR/PDMS coating | 107 |
| 2.3.9 Analytical parameters (CAR/PDMS fiber) | 109 |
| 2.3.10 Precision and quality of spin coating | 109 |
| 2.3.11 Development of MPTF devices | 112 |

| | | |
|--|---|------------|
| 2.3.12 | Thin film reinforcement by incorporation of glass wool fabric mesh | 117 |
| 2.3.13 | Analytical performance of MPTF technique | 117 |
| 2.3.13.1 | Stability and extraction repeatability of MPTFs | 117 |
| 2.3.13.2 | Extraction time profiles of N-nitrosamines using MPTFs | 118 |
| 2.3.13.3 | Extraction efficiencies of MPTFs versus SPME fibers and PDMS thin film | 118 |
| 2.3.13.4 | Linearity and lowest detectable levels using MPTFs | 123 |
| 2.4 | Conclusions | 123 |
| 2.5 | References | 126 |
| Chapter 3: Solid phase microextraction of trihalomethanes in drinking water | | 132 |
| 3.1 | Introduction | 132 |
| 3.2 | Experimental | 134 |
| 3.2.1 | HS-SPME-GC-MS method | 134 |
| 3.2.1.1 | Chemicals and supplies | 134 |
| 3.2.1.2 | Instrumentation | 135 |
| 3.2.1.3 | SPME procedure | 136 |
| 3.2.2 | LLE -GC-ECD method | 136 |
| 3.2.2.1 | Chemicals and supplies | 136 |
| 3.2.2.2 | Instrumentation | 137 |
| 3.2.2.3 | LLE extraction | 137 |
| 3.2.3 | Water samples | 138 |
| 3.3 | Results and Discussion | 138 |
| 3.3.1 | Analytes description and properties | 138 |
| 3.3.2 | Separation and identification | 140 |

| | | |
|-------|-----------------------------|-----|
| 3.3.3 | Fiber selection | 141 |
| 3.3.4 | Extraction time | 142 |
| 3.3.5 | Desorption time | 142 |
| 3.3.6 | Salt addition | 143 |
| 3.3.7 | Analytical parameters | 143 |
| 3.3.8 | Sample analysis | 146 |
| 3.4 | Conclusions | 149 |
| 3.5 | References | 150 |

| | | |
|-------------------|---|------------|
| Chapter 4: | Solid phase microextraction of haloacetonitriles, haloketones and chloropicrin in drinking water | 154 |
| 4.1 | Introduction | 154 |
| 4.2 | Experimental | 156 |
| 4.2.1 | HS-SPME-GC-MS method | 156 |
| 4.2.1.1 | Chemicals and supplies | 156 |
| 4.2.1.2 | Instrumentation | 157 |
| 4.2.1.3 | SPME procedure | 157 |
| 4.2.2 | LLE -GC-ECD method | 158 |
| 4.2.2.1 | Chemicals and supplies | 158 |
| 4.2.2.2 | Instrumentation | 159 |
| 4.2.2.3 | LLE extraction | 159 |
| 4.2.3 | Water samples | 159 |
| 4.3 | Results and Discussion | 160 |
| 4.3.1 | Analytes description and properties | 160 |
| 4.3.3 | Fiber selection | 160 |

| | | |
|---|-----------------------------|------------|
| 4.3.4 | Extraction time | 163 |
| 4.3.5 | Desorption time | 164 |
| 4.3.6 | Chemical ionization | 164 |
| 4.3.7 | Analytical parameters | 165 |
| 4.3.8 | Sample analysis | 165 |
| 4.4 | Conclusions | 173 |
| 4.5 | References | 174 |
| Chapter 5: Summary and future directions | | 178 |
| 4.1 | Summary | 178 |
| 4.1 | Future directions | 181 |
| Appendix A Video Illustration I | | 183 |
| Appendix B Video Illustration II | | 184 |
| Appendix C Video Illustration III | | 185 |

List of Tables

| | |
|---|-----|
| Table 1.1 Major classes of DBPs, their occurrence, genotoxicity and carcinogenicity..... | 4 |
| Table 1.2 Physical characteristics of common adsorbents used in SPME fibers | 43 |
| Table 2.1 Description and properties of N–nitrosamines (EPA 521) | 99 |
| Table 2.2 Analytical data for SPME-GC-MS of the N–nitrosamines (EPA 521) in water using CAR/PDMS fiber | 110 |
| Table 2.3 Precision of PDMS thin film preparation by spin coating | 111 |
| Table 2.3 Analytical data for TFME-GC-MS of the N–nitrosamines (EPA 521) in water using mixed-phase thin films | 125 |
| Table 3.1 Description and properties of commonly found trihalomethanes (THMs) in drinking water | 139 |
| Table 3.2 Analytical data for selected trihalomethanes (THMs) in water | 145 |
| Table 3.3 Characteristics of the Canadian drinking water samples (Winter 2009) | 147 |
| Table 3.4 Results of drinking water sample analysis by the LLE and the SPME methods | 148 |
| Table 4.1 Description and properties of chloropicrin and commonly found haloacetonitriles and haloketones in drinking water | 161 |
| Table 4.2 Analytical parameters using spiked water samples | 168 |

Table 4.3 Characteristics of the Canadian drinking water samples (Winter 2010) 169

Table 4.4 Results of drinking water sample analysis by the LLE and the SPME methods
..... 171

List of Figures

| | |
|---|----|
| Figure 1.1 Schematic diagram of the formation of DBPs from disinfectants and/or organic and inorganic precursors | 2 |
| Figure 1.2 Design of the commercial SPME device made by Supelco (Sigma-Aldrich)..... | 22 |
| Figure 1.3 (A) Direct immersion and (B) headspace SPME | 23 |
| Figure 1.4 Universal profile of mass extracted versus time for a perfectly agitated sample solution of infinite volume; a , bare fiber radius; b , coated fiber radius; $(b-a)$, fiber thickness; D_f , analyte diffusion coefficient in the fiber coating; $t_{95\%}$, practical equilibrium extraction time | 30 |
| Figure 1.5 Boundary layer model configuration; regions and concentrations versus radius profile | 31 |
| Figure 1.6 Universal extraction time profile for a practically agitated sample solution of infinite volume, when the boundary layer controls the extraction rate; δ , boundary layer thickness; K_{fs} , distribution coefficient of the analyte between the fiber coating and the sample; $(b-a)$, fiber thickness; D_s , analyte diffusion coefficient in the sample; $t_{95\%}$, practical equilibrium extraction time | 32 |
| Figure 1.7 Comparison of (A) absorption and (B, C) adsorption extractions (cross-sections of the support or bare fiber). Diagrams on the upper side illustrate the initial stages of the extractions. Diagrams on the lower side illustrate the equilibrium condition | 36 |
| Figure 1.8 Schematic drawing of a tapered pore in a Carboxen 1006 particle | 44 |
| Figure 1.9 Schematic representation of stages in spin coating process | 56 |

| | |
|--|-----|
| Figure 2.1 Schematic representation of thin film fabrication; (A) coating fluid deposition, (B) spin coated GW fabric mesh | 94 |
| Figure 2.2 (A) Schematic representations and (B) images of house-shape thin film sampler with cotter pin and Teflon-made holder. | 96 |
| Figure 2.3 Schematic representation and image of set-up for thin film extraction | 97 |
| Figure 2.4 Schematic representation of thin film desorption in TDU-CIS-GC system | 98 |
| Figure 2.5 Typical liquid injection GC-MS chromatogram of N–nitrosamines | 100 |
| Figure 2.6 Comparison of different SPME fiber coatings for the extraction of selected N–nitrosamines; 50 µg/L spiked water sample, 30 min direct extraction at 30°C, n = 3 | 101 |
| Figure 2.7 Direct versus headspace extraction of N–nitrosamines with CAR/PDMS fiber; 2µg/L spiked water sample, 30 min extraction at 30°C, n = 3 | 102 |
| Figure 2.8 Headspace extraction of N–nitrosamines at different temperatures with CAR/PDMS fiber; 2 µg/L spiked water sample, 30 min extraction, n = 3 | 103 |
| Figure 2.9 Direct versus headspace extraction (elevated temperature) of N–nitrosamines with CAR/PDMS fiber; 2 µg/L spiked water sample, 30 min extraction, n = 3 | 104 |
| Figure 2.10 Extraction time profile of N–nitrosamines for direct immersion SPME with CAR/PDMS fiber; 2 µg/L spiked water sample, extraction temperature 30°C, 250 rpm stirring rate | 105 |
| Figure 2.11 Effect of pH on the extraction of N–nitrosamines with CAR/PDMS fiber; 2µg/L spiked water sample, 30 min headspace extraction at 30°C, n = 3 | 106 |

| | |
|--|-----|
| Figure 2.12 Effect of salt addition on the extraction of N–nitrosamines with CAR/PDMS fiber; 2 µg/L spiked water sample, 30 min extraction at 30°C, n = 3 | 107 |
| Figure 2.13 Thermal desorption efficiency of N–nitrosamines (25 ng), <i>p</i> -xylene and mesitylene (5 ng) from SPME fibers; direct loading, n = 3 | 108 |
| Figure 2.14 PDMS thin film sample cut weight/thickness versus spin speed (n = 5) | 111 |
| Figure 2.15 SEM surface images of PDMS/DVB thin films; (A) 0.15 w/w, (B) 0.20 w/w particle-to-PDMS ratio | 113 |
| Figure 2.16 SEM images of CAR/PDMS mixed-phase thin film device using GW fabric mesh; particle-to-PDMS ratio equal to that of the commercial fiber coating | 114 |
| Figure 2.17 SEM surface images of CAR/PDMS mixed-phase thin film device; particle-to-PDMS ratio equal to that of the similar commercial fiber coating | 115 |
| Figure 2.18 SEM surface images of PDMS/DVB mixed-phase thin film device; particle-to-PDMS ratio equal to that of the similar commercial fiber coating | 116 |
| Figure 2.19 Repeatability of extraction using MPTF devices; (A) CAR/PDMS TF, (B) PDMS/DVB TF; 2 µg/L N–nitrosamines in water, 30 min extraction room temp., n = 7 ... | 119 |
| Figure 2.20 Extraction time profiles of N–nitrosamines in water with MPTF devices; (A) CAR/PDMS TF, (B) PDMS/DVB TF; 500 ng/L spiked water sample, room temp, 250 rpm | 120 |
| Figure 2.21 Extraction efficiencies of MPTF device vs. SPME fiber; (A) CAR/ PDMS coating, (B) PDMS/ DVB coating; 500 ng/L N–nitrosamines in water, 16 h, room temp. | 121 |

| | |
|--|-----|
| Figure 2.22 (A) Extraction time profiles of NDPA and NDBA in water with commercial PDMS thin film; (B) Extraction efficiency of PDMS/DVB TF vs. commercial PDMS TF; (A, B) 100 ng/L spiked water sample, 250 rpm; (B) 16 h, room temp. | 122 |
| Figure 3.1 HS-SPME-GC-MS chromatogram of THMs in spiked water sample (1µg/L) using 100µm PDMS fiber | 140 |
| Figure 3.2 Comparison of different SPME fiber coatings for the extraction of selected THMs; 4 µg/L spiked water sample, 15 min headspace extraction at 30°C, n = 3 | 142 |
| Figure 3.3 Extraction time profiles of THMs in water for HS-SPME with 100µm PDMS fiber; 1µg/L spiked water sample, extraction temperature 30°C | 143 |
| Figure 3.4 Effect of salt addition (NaCl 25% w/w) on HS-SPME extraction of THMs from water with PDMS fiber; 1 µg/L spiked water sample, extraction temperature 30°C | 144 |
| Figure 3.5 Scatter plot of the amounts of TCB, BDCM, DBCM and TBM detected in some Canadian water samples measured by HS-SPME-GC-MS and LLE-GC-ECD | 146 |
| Figure 4.1 Evaluation of different SPME fibers for extraction of TCAN, DCAN, BCAN, DBAN, CP, 1,1-DCP and 1,1,1-TCP in water; 20 µg/L spiked water samples, 15 min headspace extraction at 30°C, n = 3 | 162 |
| Figure 4.2 SEM image (95 magnifications) of the custom-made PDMS/DVB-NVP fiber | 163 |
| Figure 4.3 HS-SPME extraction time profiles of TCAN, DCAN, BCAN, DBAN, CP, 1,1-DCP and 1,1,1-TCP in water; DVB/CAR/PDMS fiber; 20µg/L spiked water samples, extraction temperature 30°C | 164 |

Figure 4.4 GC chromatograms and MS spectra of 1,1-DCP for 50 µg/L spiked water samples; EI (top) and CI (bottom). Molecular ion not observed in EI mode, signal-to-noise ratio significantly increased in CI mode 166

Figure 4.5 GC chromatograms and MS spectra of 1,1,1-TCP for 50 µg/L spiked water samples; EI (top) and CI (bottom). Molecular ion not observed in EI mode, signal-to-noise ratio significantly increased in CI mode 167

Figure 4.6 Scatter plot of amounts of TCAN, DCAN, BCAN, DBAN, CP, 1,1-DCP and 1,1,1-TCP detected in some Canadian water samples measured by HS-SPME-GC-MS and LLE-GC-ECD 170

List of Abbreviations

| | |
|--------|---|
| CAR | Carboxen 1006 |
| CASRN | Chemical Abstract Service Registry Number |
| CDHS | California Department of Health Services |
| CE | capillary electrophoresis |
| CI | chemical ionization |
| CIS | cooled injection system |
| CW | Carbowax |
| DBPs | disinfection by-products |
| DI | direct immersion |
| DVB | divinylbenzene |
| DWSP | Drinking Water Surveillance Program |
| ECD | electron capture detector |
| EI | electron impact ionization |
| ELCD | electrolytic conductivity detector |
| EU | European Union |
| FID | flame ionization detector |
| GC | gas chromatography |
| GC/MS | gas chromatography/mass spectrometry |
| HAAs | haloacetic acids |
| HAMs | haloamides |
| HANs | haloacetonitriles |
| HFLPME | hollow fiber liquid-phase microextraction |
| HFM | hollow fiber membrane |
| HKs | haloketones |
| HNMs | halonitromethanes |
| HOCS | hydrophobic organic compounds |
| HPLC | high performance liquid chromatography |
| HRMS | high-resolution mass spectrometry |
| HS | headspace |
| ID | inner diameter |

| | |
|--------|--|
| IL | ionic liquid |
| IS | internal standard |
| LC | liquid chromatography |
| LC/MS | liquid chromatography/mass spectrometry |
| LDL | lowest detectable level |
| LLE | liquid-liquid extraction |
| LPME | liquid-phase microextraction |
| MAC | maximum acceptable concentration |
| MCL | maximum contamination level |
| MDL | method detection limit |
| MOEE | Ontario Ministry of Environment and Energy |
| MS | mass spectrometry |
| MS/MS | tandem mass spectrometry |
| MW | molecular weight |
| NAs | N–nitrosamines |
| NCD | nitrogen chemiluminescence detector |
| ND | not detected |
| NDBA | N–nitrosodibutylamine |
| N-DBPs | nitrogenous disinfection by-products |
| NDEA | N–nitrosodiethylamine |
| NDMA | N–nitrosodimethylamine |
| NDPA | N–nitrosodipropylamine |
| NDPHA | N–nitrosodiphenylamine |
| NIST | National Institute of Standards and Technology |
| NMEA | N–nitrosomethylethylamine |
| NMOR | N–nitrosomorpholine |
| NPD | nitrogen–phosphorus detector |
| NPIP | N–nitrosopiperidine |
| NPYR | N–nitrosopyrrolidine |
| OSF | organic solvent film |
| PA | polyacrylate |

| | |
|----------|--|
| PAHs | polycyclic aromatic hydrocarbons |
| PDMS | polydimethylsiloxane |
| PEG | polyethylene glycol |
| PID | photoionization detector |
| P&T | purge-and-trap |
| PTV | programmed temperature vaporizer |
| rpm | revolutions per minute |
| RSD | relative standard deviation |
| RT | retention time |
| SBME | solvent bar microextraction |
| SBSE | stir bar sorptive extraction |
| SD | standard deviation |
| SDME | single-drop microextraction |
| SEM | scanning electron microscopy |
| SFODME | solidified floating organic drop microextraction |
| SLM | supported liquid membrane |
| SPE | solid phase extraction |
| SPME | solid phase microextraction |
| TDS | thermal desorption system |
| TDU | thermal desorption unit |
| TEA | thermal energy analyzer |
| TFM | thin film membrane |
| TFME | thin film microextraction |
| THMs | trihalomethanes |
| TOX | total organic halides |
| UCMR | Unregulated Contaminants Monitoring Rule |
| UPLC | ultra-high performance liquid chromatography |
| U.S. EPA | United States Environmental Protection Agency |
| VOCs | volatile organic compounds |

Chapter 1

Introduction

1.1 Disinfection by-products in drinking water

Disinfection of water supplies is among the most successful public health measures ever implemented to control pathogens and protect the public from infectious water-borne diseases. Millions of people worldwide receive quality drinking water every day from their public water systems.

While disinfectants (chlorine, chlorine dioxide, chloramines and ozone) are effective for killing harmful microorganisms in drinking water, their highly reactive oxidizing nature causes interaction with organic and/or inorganic substances naturally present in most source waters (rivers, lakes, and many ground waters). As a result, unintended harmful compounds known as disinfection by-products (DBPs) are formed in drinking water. The DBPs concentrations may vary by orders of magnitude depending on factors such as the type of disinfectant, dosage used, contact time, quality of source water and reaction conditions, e.g. temperature and pH. A schematic diagram of the formation of DBPs from disinfectants and organic and/or inorganic precursors is shown in Fig. 1.1.

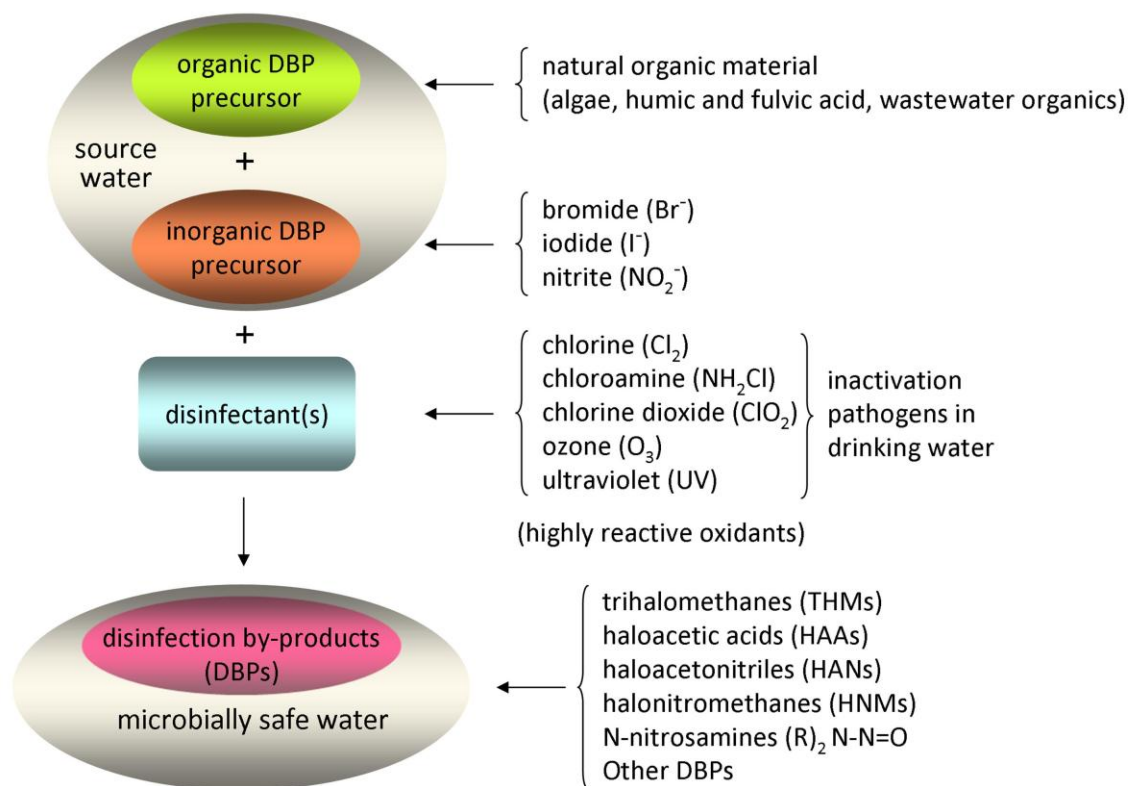


Figure 1.1 Schematic diagram of the formation of DBPs from disinfectants and organic and/or inorganic precursors.

It was in the early 1970s that scientists first became aware of DBPs. In 1974, Rook¹ and Bellar² reported the identification of the first DBPs in chlorinated drinking water; chloroform and other trihalomethanes (THMs). In 1976, the U.S. Environmental Protection Agency (U.S. EPA) published the results of a national survey that showed that chloroform and the other THMs were very common in chlorinated drinking water³. In the same year, the U.S. National Cancer Institute published a report that chloroform was carcinogenic in laboratory animals⁴. Also, the first reports appeared in the late 1970s showing that organic extracts of drinking water were mutagenic in the *Salmonella* mutagenicity assay⁵. Based on these observations, an important public health issue was recognized; DBPs may cause developmental, reproductive and carcinogenic effects.

From that point onwards there have been significant research efforts towards elucidating the formation, control, occurrence and health risks of DBPs. As analytical techniques and detection capabilities advanced, it was realized that many different products could arise from the reactions between the precursors in source waters and chemical disinfectants. Hence, the focus has moved from solely THMs to incorporate other classes of DBPs. By 1980, it was found that another group of DBPs, the haloacetic acids (HAAs) could occur in drinking water at levels similar to, or above those of THMs⁶. Since then more than 600 other DBPs representing several chemical classes have been identified in drinking water⁷, of which certain numbers are known to be animal carcinogens or mutagenic in bacterial assays⁸⁻¹² and thus potentially harmful to humans. Research studies have shown that the THMs and HAAs are the most prevalent classes of DBPs in chlorinated water, accounting for almost 25% of the halogenated DBPs in drinking water^{13, 14}. The THMs were regulated in Canada in 1978 and then in the USA in 1979 to limit the risk they pose to human health. Since 1998 the HAAs have also been regulated in the USA. Currently, the maximum acceptable concentration (MAC) of total THMs in drinking water in Canada and the European Union (EU) is 100 µg/L. The present consents in the USA are 80 and 60 µg L⁻¹ for the THMs and HAAs, respectively¹⁵.

In addition to halogenated DBPs, non-halogenated and nitrogen-containing DBPs (N-DBPs) have been identified. Table 1.1 presents the major classes of currently known DBPs, the most important individuals of each class and the relevant toxicity data. In terms of health hazards, the recently identified N-DBPs such as N-nitrosamines, haloacetonitriles (HANs) and halonitromethanes (HNMs) are found to have greater toxicity to mammalian cells than the regulated DBPs¹⁴. N-DBPs are particularly found in drinking water when chloramines are used as secondary residuals in the distribution networks to prevent regrowth of pathogens prior to consumption¹⁶. Although there are provincial guidelines for some of these DBPs, they have not yet been regulated federally for several reasons, including poor understanding of formation processes, analytical difficulties, lack of adequate toxicity data and most importantly the issue of the need for rigorous and reliable disinfection process. The risks from waterborne pathogens are far more clear and immediate than long term adverse health effects of DBP in drinking water.

Table 1.1 Major classes of DBPs, their occurrence, genotoxicity and carcinogenicity

| DBP Class | Individual DBPs | Formula | Occurrence ^a | Genotoxicity ^b | Carcinogenicity ^b |
|----------------------------|------------------------------------|---|-------------------------|---------------------------|------------------------------|
| <i>Regulated</i> | | | | | |
| Trihalomethanes (THMs) | Chloroform | CHCl ₃ | ***** | – | + |
| | Bromodichloromethane | CHCl ₂ Br | **** | + | + |
| | Dibromochloromethane | CHClBr ₂ | **** | + | + |
| | Bromoform | CHBr ₃ | **** | + | + |
| Haloacetic acids (HAAs) | Monochloroacetic acid | CH ₂ ClCOOH | *** | + | – |
| | Dichloroacetic acid | CHCl ₂ COOH | ***** | + | + |
| | Trichloroacetic acid | CCl ₃ COOH | ***** | – | + |
| | Monobromoacetic acid | CH ₂ BrCOOH | *** | + | |
| | Dibromoacetic acid | CHBr ₂ COOH | ***** | + | + |
| Oxyhalides | Bromate | BrO ₃ [–] | **** | + | + |
| | Chlorite | ClO ₂ [–] | ***** | | – |
| <i>Unregulated</i> | | | | | |
| Other THMs | Dichloromethane | CH ₂ Cl ₂ | *** | + | |
| | Iodoform | CHI ₃ | *** | + | |
| Other HAAs | Tribromoacetic acid | CBr ₃ COOH | ***** | + | |
| | Monoiodoacetic acid | CH ₂ I ₂ COOH | *** | + | |
| | Bromoiodoacetic acid | CH ₂ BrICOOH | *** | + | |
| Other Oxyhalides | Chlorate | ClO ₃ [–] | ***** | + | + |
| Haloacetonitriles | Trichloroacetonitrile | CCl ₃ CN | *** | + | |
| | Dichloroacetonitrile | CHCl ₂ CN | *** | + | |
| | Bromochloroacetonitrile | CHBrClCN | *** | + | |
| | Dibromoacetonitrile | CHBr ₂ CN | *** | + | |
| <i>N</i> -nitrosamines | <i>N</i> -nitrosodimethylamine | (CH ₃) ₂ -N (NO) | ** | + | + |
| | <i>N</i> -nitrosomethylethyleamine | (CH ₃)(C ₂ H ₅)-N (NO) | | + | + |
| | <i>N</i> -nitrosodiethylamine | (C ₂ H ₅) ₂ -N (NO) | | + | + |
| | <i>N</i> -nitrosopyrrolidine | C ₄ H ₈ -N (NO) | * | + | + |
| | <i>N</i> -nitrosodipropylamine | (C ₃ H ₇) ₂ -N (NO) | | + | + |
| | <i>N</i> -nitrosopiperidine | C ₅ H ₁₀ -N (NO) | * | + | + |
| | <i>N</i> -nitrosodibutylamine | (C ₄ H ₉) ₂ -N (NO) | | + | + |

... continued ...

Table 1.1 (continued)

| DBP Class | Individual DBPs | Formula | Occurrence ^a | Genotoxicity ^b | Carcinogenicity ^b |
|------------------------------|---------------------------|---|-------------------------|---------------------------|------------------------------|
| Haloketones | 1,1-Dichloroacetone | CHCl ₂ COCH ₃ | *** | + | |
| | 1,1,1-Trichloroacetone | CCl ₃ COCH ₃ | *** | + | |
| Halonnitromethanes (HNMs) | Trichloronitromethane | CCl ₃ NO ₂ | ** | + | |
| | Tribromonitromethane | CBr ₃ NO ₂ | ** | + | |
| | Chloronitromethane | CH ₂ ClNO ₂ | ** | + | |
| | Bromonitromethane | CH ₂ BrNO ₂ | *** | + | |
| | Dichloronitromethane | CHCl ₂ NO ₂ | ** | + | |
| | Dibromonitromethane | CHBr ₂ NO ₂ | **** | + | |
| | Bromochloronitromethane | CHBrClNO ₂ | *** | + | |
| | Bromodichloronitromethane | CBrCl ₂ NO ₂ | *** | + | |
| | Dibromochloronitromethane | CBr ₂ ClNO ₂ | *** | + | |
| Haloamides | Chloroacetamide | CH ₂ ClCONH ₂ | *** | + | |
| | Bromoacetamide | CH ₂ BrCONH ₂ | *** | + | |
| | Iodoacetamide | CH ₂ ICONH ₂ | | + | |
| | Dichloroacetamide | CHCl ₂ CONH ₂ | *** | + | |
| | Bromochloroacetamide | CHBrClCONH ₂ | *** | + | |
| | Dibromoacetamide | CHBr ₂ CONH ₂ | *** | + | |
| | Bromoiodoacetamide | CHBrI CONH ₂ | *** | + | |
| | Trichloroacetamide | CCl ₃ CONH ₂ | *** | + | |
| | Bromodichloroacetamide | CBrCl ₂ CONH ₂ | *** | + | |
| | Dibromochloroacetamide | CBr ₂ ClCONH ₂ | *** | + | |
| | Tribromoacetamide | CBr ₃ CONH ₂ | *** | + | |
| | Diiodoacetamide | CHI ₂ CONH ₂ | | + | |
| | Chloroiodoacetamide | CHClI CONH ₂ | | + | |
| Halopyrroles | 2,3,5-Tribromopyrrole | C ₄ H ₂ Br ₃ N | ** | + | |
| Aldehydes | Formaldehyde | HCHO | *** | + | + |
| | Acetaldehyde | CH ₃ CHO | *** | + | + |
| | Chloroacetaldehyde | CH ₂ ClCHO | *** | | + |
| | Chloral hydrate | CCl ₃ C(OH) ₂ | **** | + | + |

^a Key to occurrence symbols: * low nanogram per liter (low-ng/L) levels; ** ng/L to sub-µg/L levels; *** sub- to low-µg/L levels; **** low-µg/L levels; ***** low- to mid µg/L levels; ***** high µg/L levels.

^b Toxicity data adapted from US EPA Integrated Risk Information System (IRIS) database and Ref. 14.

It is noteworthy to point out that of more than 600 DBPs currently known, only a small number have been investigated for their quantitative occurrence and health effects. Also, the known DBPs only account for less than 50% of total organic halides (TOX) during disinfection¹⁴. Therefore, a significant portion of the TOX is still unaccounted for.

1.2 Analytical methodologies for DBPs studies

The dual responsibility of protection of the public from the acute health effects of waterborne diseases and also the chronic effects of long term exposure to DBPs requires increasing research to advance understanding of DBPs nature, formation, concentrations and health hazards. Analytical methodologies for monitoring drinking water serve a number of related purposes, including occurrence studies in community water systems, determination of the DBPs of various water treatment approaches and identification of new species. These activities, in turn, form the supporting bases for toxicology studies and drinking water regulations.

1.2.1 Instrumental approaches

Clearly, the choice of separation method is primarily dictated by analyte properties; with gas chromatography (GC) most suitable for volatile and semi-volatile analytes, and liquid chromatography (LC) most suitable for highly polar, non-volatile and thermally unstable analytes. GC offers inherent advantages of high resolution, rapid separation, low cost and easy linkage with sensitive and selective detectors. To date, analytical measurements of DBPs have predominantly been carried out using GC combined with electron-capture detector (ECD), photoionization (PID) and electrolytic conductivity detector (ELCD) in series, and mass spectrometry (MS). The GC-MS approach in particular has played a pivotal role in the discovery of DBPs in drinking water. The technique provides the advantage of confirmation capability, the option of soft chemical ionization (CI) versus electron ionization (EI) for less fragmentation, molecular weight information, and the tandem mass spectrometry (MS/MS) which increase the selectivity and sensitivity of the detection.

The application of liquid chromatography has often been hampered with difficulties such as specific operating parameters for different analytes, expensive instrumental equipment and lack of LC/MS libraries which makes compound identification very challenging. Recently, there has been growing interest in the application of the LC/MS technique for direct measurement of the highly polar hydrophilic DBPs, which are difficult or impossible to extract from water, and for the exploration of high molecular weight types which are not directly detectable by GC. It is thought that these species account for the significant portion of the unexplained TOX and the missing DBPs fraction¹⁷.

1.2.2 Sample collection considerations

Although separation and detection are important parts of DBPs analysis, the key role of preliminary steps such as sampling and sample preparation cannot be neglected. In fact, the quality of these steps significantly affects precision and accuracy of results. As regards sample collection, there are two aspects that must not be overlooked if analytes concentrations are to be preserved prior to analysis. First, continued formation of DBPs and all other reactions should be stopped at the time of sample collection. This is achieved by pH adjustment¹⁸ and addition of a preservative in the field to quench residual disinfectant and preclude changing the concentration of the target analytes in the sample. Typical residual chlorine quenching agents include ammonia salts that form chloramines with free chlorine. For those DBPs more commonly produced during chloramination, such as cyanogen halides, iodinated DBPs and nitrosamines, ascorbic acid is usually the quenching reagent of choice. Under somewhat controlled conditions it is possible to use this reagent for quenching both chlorine and chloramine¹⁹. Nonetheless, care should be taken when selecting type and quality of the quenching agent. Some sources of ammonium chloride contain sufficient bromide contamination that residual chlorine can generate hypobromite as well as bromamines that can react with naturally organic compounds after quenching²⁰. Dihalogenated HAAs can form in chloraminated waters and ammonia salts can enhance the process²¹. Also, some DBPs such as brominated analogues of trichloroacetonitrile and chloropicrin are unstable in the presence of even a slight excess of ascorbic acid^{22, 23}. Therefore, an evaluation of the stability of the DBPs in quenched samples should be done before using the reagent in the

field. In some cases, a holding time study can determine the maximum length of time and conditions under which samples can be stored before analysis.

The second control for analyte preservation requires that no degradation of the target DBPs can occur during sample holding. Temperature increase, exposure to light and inappropriate use of quenching agents can lead to degradation of the analytes. Data from recent Health Canada studies indicate that 1,1,1-trichloro-2-propanone and trihalogenated aldehydes²⁴ will degrade in water to their corresponding THMs at increased pH and temperature. However, they are stable in water at sampling/storage conditions (pH 4.5, 4°C). Some DBPs are biodegradable, especially dihalogenated acetic acids, aldehydes and acids, and in the absence of a disinfectant residual after quenching require a biocide to prevent bacterial regrowth²⁵.

1.2.3 Conventional methods for sample preparation

The concentrations of DBPs in drinking water samples are usually in the range of nanogram or picogram per milliliter. Additionally, most analytical instruments cannot handle direct injection of water samples. Therefore, a sample preparation step is necessary prior to analysis, which serves a number of purposes including elimination or reduction of disturbing components of the sample matrix (clean-up), trace concentration of analytes (enrichment), medium exchange (gas phase, solvent or sorbent) for introduction to analytical instruments and, if needed, analytes conversion to more suitable form for separation and detection (derivatization)²⁶. Compared with other sample matrices such as biological and waste water samples, sample preparation of drinking water with relatively clean matrix and low amounts of DBPs is usually less cumbersome and often restricted to extraction and preconcentration of analytes from aqueous medium. However, challenges still arise from hydrophilicity, high polarity, non-volatility and instability of some analytes, which renders their efficient extraction and detection difficult to achieve. Obviously, the more soluble the analytes in water, the greater is the difficulty to extract them. Non-volatile highly polar analytes may need an extra derivatization step to transform to volatile species amenable to GC separation. So, depending on the nature and concentration of target analytes different sample pretreatments and strategies may be required.

The conventional sample preparation techniques for analysis of micropollutants in water, including DBPs, are liquid-liquid extraction (LLE), static headspace, purge-and-trap, and solid phase extraction (SPE). Liquid-liquid extraction has been the primary choice for sample preparation as it is a versatile reliable technique. It is based on the partitioning of analytes between aqueous sample and an immiscible organic solvent. The technique is simple, straightforward and allows a large number of analytes in a single extracts including polar analytes. It also offers large linear range, high reproducibility and minimum carryover and memory effects, which sometimes arise from glassware equipment. The large selection of available solvents with a wide range of selectivity properties is often claimed as an inherent advantage of LLE. When the partition coefficients are small and analytes concentrations are very low, larger volumes of solvent must be handled and continuous extraction should be used. Salt addition is a strategy that may be used to reduce the solubility of analytes in the aqueous phase. The technique has been prescribed in many standard analytical methods for water analysis, including for example US EPA method 551 (determination of chlorination disinfection by-products and chlorinated solvents in drinking water by LLE/GC/ECD, 1990) and method 552 (determination of haloacetic acids in drinking water by LLE, derivatization, and GC/ECD, 1990). Health Canada also uses LLE (EPA 551.1) as a technique to analyze chlorination DBPs in drinking water. Despite its advantages and important role in water analysis, LLE is unsustainable as it often requires consumption of large quantities of expensive highly pure organic solvents which poses health hazards to laboratory personnel, environment and extra cost for waste treatment. Additionally, it is very time-consuming due to slow phase separation, prone to emulsion formation, difficult to automate and overall, hardly suitable for a large number of samples and routine analysis.

Static headspace and purge-and-trap are headspace gas extraction techniques suitable for volatiles and semi-volatiles in water. In static headspace, a sample is placed in a vial that is sealed and heated. The volatile components migrate out of the sample matrix into the headspace of the vial. A portion of the headspace is then directly sampled by a gas-tight syringe and transferred to a GC for analysis. In modern automated headspace systems, the syringe is typically replaced with a heated transfer line and the sample vial is pressurized above the capillary column head pressure. This permits rapid sample transfer

and equilibration for interfacing the sampling device with the GC. The most important parameters that must be established for precise and quantitative analysis are temperature of the sample, volume of the sample and the vial used, injection volume, ionic strength and pH. These parameters should be optimized to maximize the concentration of the volatile components in the headspace and minimize interference from other compounds in the sample matrix. Because of its limited sensitivity, static headspace technique can be employed for applications in the ppb ranges. The detection limits can be decreased when HS-GC is combined with sensitive detectors such as MS.

The purge-and-trap (P&T) procedure is a dynamic headspace technique which involves bubbling and continuous flow of an ultra-pure inert gas, such as helium or nitrogen, through an aqueous sample. The purging gas liberates the volatile components into the headspace above the sample and then transfers them in a tube containing suitable sorbent materials, where they are trapped and concentrated. When purging is complete the sorbent tube is rapidly heated and the volatile components are desorbed and backflushed with carrier gas into a GC for analysis. A high flow-rate is necessary to achieve an exhaustive extraction from the sample in a reasonable time and this requires an adsorption trap with a sufficiently big capacity to avoid breakthrough during the purge time. Efficient desorption also requires high flow rate to avoid band broadening and high sensitivity. To achieve this and maintain the separation efficiency of capillary columns, additional cryogenic trapping may become necessary²⁷. Overall, the procedure prevents unwanted non-volatile and high molecular weight compounds from contaminating the GC column and produces a simplified chromatogram of only the volatiles. It has automation capability and is more sensitive than LLE and static headspace technique, due to the concentration aspect. P&T was the approach used to identify the first DBPs (THMs) in mid 1970s. It also has been prescribed in several EPA methods. Method 502.2 (1986) employs P&T technique combined with PID and ELCD detectors in series. The PID detects aromatic and double-bond compounds, and the ELCD detects halogenated compounds. Method 524.2 (1983), which is also used by Health Canada for analysis of THMs, employs a purge and trap concentrator combined with GC/MS detection. Despite its applicability to THMs and other volatile DBPs, P&T technique has a few shortcomings, including possibility of losses of very volatile compounds, foaming of

sample, cross-contamination in the purging vessel and sorbent bleeding during thermal desorption. Additionally, the technique is often useful for concentrating the volatiles that are insoluble or poorly soluble in water and have boiling points below 200°C. The efficiency of the technique is much lower for water soluble and semi-volatile analytes. Generally, longer purging times and heating the sample are required to increase the purging efficiency of these compounds.

Solid phase extraction is a newer and more popular technique in water analysis^{28, 29}. In SPE procedure^{30, 31}, an aqueous sample is passed over a sorbent packed cartridge or disk, which has initially been conditioned by one or more solvents. The analytes are thus adsorbed and retained on the sorbent. After washing and drying steps of the sorbent bed with ultra-pure water, solvents and vacuum or nitrogen, the analytes are recovered by eluting with a small volume of appropriate organic solvent through the cartridge or disk. The extract is then filtered and evaporated to the desired volume before chromatographic separation. SPE tends to be less selective, and matrix components can be extracted as well. Thus, the choice of elution solvent can be critical, particularly if the analytes are highly volatile. The solvent should be sufficiently volatile and nonpolar, and it should be able to elute the target analytes from the SPE sorbent in a small volume. Compared to the other conventional techniques, SPE offers higher sensitivity due to its exhaustive extraction nature, decreased use of organic solvents, shorter analysis times, automation capability and suitability for field analysis. Also, with a wide range of stationary phases now available, including hydrophilic and dual-type stationary phases, SPE can be tailored to extract a broader range of polar and non-polar analytes which is an advantage for profiling type of analysis, i.e. when all or most of the sample components are of interest. SPE can increase the concentration factor for target analytes by more than 3 orders of magnitude, achieving low parts per trillion (ng/L) detection¹⁹. Therefore, it is well suited for trace and ultra-trace analysis in water. The EPA Method 552.1 (1992) employs a SPE disk, esterification and capillary column GC/ECD for determination of regulated haloacetic acids in water. Method 521 (2004) uses SPE with capillary column GC/CI/MS/MS for determination of unregulated nitrosamines in drinking water. Despite its advantages, SPE has a few drawbacks including its multi-step procedure, low breakthrough volumes for very polar analytes, unsuitability for volatiles, possibility of

clogging of extraction cartridges by matrix components, and sometimes poor reproducibility due to batch-to-batch sorbent variation. Also, the amount of solvent needed for SPE might still be significant, e.g. 85 mL organic solvent prescribed for the SPE procedure in the EPA method 3535 versus 180 mL organic solvent requirement for the corresponding LLE procedure in the EPA method 3510³². Moreover, high pre-concentration of analytes requires further evaporation of the eluent after extraction.

1.2.4 Trends in new sample preparation techniques

Sample preparation has been recognized as the main bottleneck of the analytical process in many applications accounting for over 60% of the total analysis³³. It is often the slowest, most complicated step in the analytical procedures that has a direct impact on precision, accuracy, quantitation limits and overall performance. Despite advances and sophistication in analytical instrumentation, most classical techniques still suffer from the time-consuming methods used for sample preparation, which slows down the total analysis³³. Therefore, increasing efforts have been devoted to the search for simpler, faster, efficient, cost-effective and more sustainable techniques that could replace the time- and labor-intensive traditional methods. These efforts have been mainly toward miniaturized, solvent-free (or reduced) and automated techniques with fewer steps to be less prone to loss of analytes and cross contamination. Clearly, the trend of implementing green analytical chemistry favors elimination and/or reduction of organic solvents in new or revised methods. Also, there are advantages offered through miniaturization. First, it largely facilitates on-line coupling and automation, which in turn provides high sample throughput and unattended operation. Additionally, automation permits the use of closed analytical systems, leading to better control of contamination in trace analysis, safer handling of samples and better accuracy and precision due to more reproducible operation. Second, miniaturized portable extraction devices facilitate on-site analysis, thereby furnishing real-time data and minimizing problems of loss of analytes and appearance of artifacts during sample transportation and storage. Obviously, obtaining real time data is advantageous in that it enables detection of disturbances in the initial steps and in the course of a process (e.g. water treatment), and thus provides a chance for

proper reaction such as stopping the process or changing the operational parameters. Miniaturization of a procedure can be achieved by reducing the dimensions of the systems used in earlier approaches or by developing completely new set-up or techniques. Both strategies have been studied during the past two decades, leading to developments of novel microextraction techniques.

1.3 Microextraction techniques

The drive towards miniaturization and greener extraction techniques has led to remarkable reductions in the volume of extraction phase so that a sub-microliter of a sorbent material or a microliter (μL) of a solvent is sufficient for sample preparation. Such small volumes of extraction phase in μL range or lower and non-exhaustive nature of extraction are representative of most analytical microextraction techniques. Despite the fact that only a small fraction of the analytes in the sample is often recovered, the enrichment by the techniques is remarkably high without the need for further concentration, due to significant decrease in the phase volume ratio. The amount extracted is determined by the partitioning of analyte between the extraction phase and the sample. The higher the affinity the analyte has for the extraction phase, the larger is the amount of analyte extracted. Based on the type of extracting phase, sorbent or solvent, these techniques can be classified into two main categories of liquid phase microextraction (LPME) and solid phase microextraction (SPME).

1.3.1 Liquid phase microextraction (LPME)

The LPME techniques require a highly pure solvent which should be immiscible with water if in direct contact with the sample. The solvent should also have much higher affinity to dissolve the analytes than the aqueous sample. The main advantages of these techniques are their low cost, very low organic solvent consumption and the availability of a wide range of solvents. Also, carryover and memory effects normally associated with the sorbent-based techniques are avoided in that fresh solvent is used each time. Additionally, it is possible to add one or more chemicals, for example a derivatization or complexation reagent, to the extraction solvent to provide additional functionality. The

methods can be combined with different chromatographic and analytical techniques, depending on the nature of the solvent. However, when using GC as chromatographic separation system there may be a limit in detecting analytes due to the solvent peak, which may obscure early eluting volatile analytes. Several methodologies for LPME have been developed, two-phase and three-phase systems, which can be divided into three main categories; single drop microextraction (SDME), hollow-fiber liquid phase microextraction (HFLPME) and dispersive liquid–liquid microextraction (DLLME).

1.3.1.1 Single drop microextraction (SDME)

SDME is the simplest mode of LPME which is usually operated in two-phase mode. In this technique, analytes are normally partitioned between a stirring aqueous sample and a drop of extracting solvent^{34, 35}, often suspended from the tip of a conventional microsyringe needle by surface tension³⁶. After extraction, direct immersion (DI)³⁶ or headspace (HS)³⁷ for a set period of time, the drop is retracted into the syringe and injected into a chromatographic system, often GC. The effectiveness of extraction in SDME process is influenced by factors such as physical and chemical properties of the solvent, drop volume, extraction time and temperature, stirring rate, ionic strength of the solution and type of extraction, i.e. static or dynamic^{38, 39}. Clearly, the choice of solvent is critical in that it should have sufficient viscosity to prevent loss of the drop. Also, the solvent should not be too volatile in the headspace applications, because otherwise the drop will evaporate during the extraction. At the same time the solvent should not elute together with the target analytes. Typically, n-octyl acetate, isoamyl alcohol, undecane, octane, nonane and ethylene glycol are the conventional organic solvents used in SDME. Drop volumes are normally 1-3 μL as solvent drops of these volumes are relatively stable and less prone to fall off the needle. Also, the extraction is usually done at room temperature because increasing temperature may lead to drop instability and thus to lower reproducibility. As well, stirring should be done at low to medium speed because otherwise it affects the stability of the drop. Solvents other than conventional organic such as ionic liquids (ILs)^{40, 41} and even water in the headspace mode^{42, 43} have been practiced. Polar ILs not only provide better drop stability⁴⁴ but also significantly enhance the range of extractable analytes, e.g. metal ions^{40, 45}, as well as the range of analytical

techniques that can be coupled to SDME such as high performance liquid chromatography (HPLC)^{42, 43}, ultra-high performance liquid chromatography (UPLC)⁴⁶, capillary electrophoresis (CE)^{41, 47} and inductively coupled plasma⁴⁰. However, ILs cannot be used for GC applications unless a special interface is used or the injection port is modified to prevent them from entering the GC⁴⁸. SDME also can be operated in three-phase mode with back-extraction, in which analytes are extracted from an aqueous sample into an organic phase confined inside a small Teflon ring, and then back-extracted into a drop of aqueous phase suspended inside the organic phase from the tip of a microsyringe needle⁴⁹. This approach permits the extraction of ionizable analytes such as phenols and amines by adjustment of pH gradient in the sample and the aqueous microdrop, and again allows the final extract to be analyzed by HPLC or CE^{50, 51}. However, the three-phase mode operation requires careful manipulation of the extraction system. Applications of SDME for water samples have been reviewed in the literature^{52, 53}, including analysis of VOCs⁵⁴, phenols^{41, 43, 55}, chlorobenzenes⁵⁶, polycyclic aromatic hydrocarbons (PAHs)^{42, 57}, short-chain aliphatic amines⁵⁸, pesticides^{59, 60}, HAAs⁶¹, HNMs⁶² and THMs^{48, 63-65} in drinking water. SDME offers speed, ease of operation, automation and on-line coupling capability^{41, 45, 66, 67} and obviating the need for any complicated equipment and interface for sample introduction, which considerably lowers the cost of analysis and makes it affordable to any analytical lab. However, problems of drop instability and poor precision have often been reported for DI-SDME, particularly when fast stirring rates and prolonged extraction times are used which result in drop dissolution and/or dislodgment^{35, 44, 68}. On the other hand, HS-SDME is only applicable for volatile analytes and it limits the choice of extracting solvent due to evaporation problem. To address these problems, dynamic procedures with microsyringe were proposed. These procedures can be performed either by repeated withdrawal and expulsion of few μL of sample (or its headspace) into the microsyringe barrel preloaded with a solvent⁶⁹⁻⁷¹ or by repeatedly exposing a solvent microdrop to the headspace above sample and withdrawing it into the barrel of the syringe for a predetermined period of time⁶⁶, allowing extraction of analytes into a renewable organic solvent film (OSF) formed along the wall of the barrel. During the expulsion of sample or withdrawal of the microdrop, the OSF recombines with the bulk solvent in the syringe and the extracted

analytes are trapped in the bulk organic phase. With the dynamic procedures, the loss of solvent microdrop is less likely and the kinetics of extraction is improved as a result of increase in the extractive surface and better agitation of the two phases^{53, 72}. However, operation of the dynamic modes is more complicated and possible water residue in the microsyringe may cause problem with the final analysis with GC and/or MS systems. Another development of SDME is solidified floating organic drop microextraction (SFODME). In this variation, a microdrop of a water-immiscible organic solvent with a melting point near room temperature (10 – 30 °C) is floated on the surface of an agitated aqueous sample^{73, 74}. The droplet is suspended in a top-center position on the surface of the stirred aqueous sample during the procedure. After extraction for a selected time at a given temperature, the sample container is placed into an ice bath where the organic solvent solidifies. Then, the solidified solvent is transferred into a small conical vial for immediate melting and injection into an analytical system. The solvents used in this method, typically 1-undecanol and 1-dodecanol, have lower densities than water so they can remain on the surface of the sample during extraction. This approach does not need any support such as a microsyringe needle, polymer rod or other supporting materials. However, limitation on the choice of proper solvent, possibility of overlapping of the solvent peak with analytes peaks, the need for freezing step and manual collection of the solidified solvent can be mentioned as its drawbacks.

1.3.1.2 Hollow-fiber liquid phase microextraction (HFLPME)

Another methodology to perform LPME is application of a hollow fiber membrane (HFM) with minimal dimensions to enhance the stability of microvolume extracting solvent⁷⁵. In HFLPME, analytes are extracted from aqueous sample through a thin layer of organic solvent (or an IL) impregnated in the pores in the wall of a small hollow fiber, and further into an acceptor phase present inside the lumen of the hollow fiber. The acceptor phase can be different from the one impregnated in the HFM providing a three-phase extraction system^{75, 76}, or the same resulting in a two-phase system^{77, 78}. Prior to use, the hollow fiber, typically made of polypropylene, is cut into an appropriate length segment and sonicated in a suitable solvent (e.g. acetone) for several minutes to remove any contaminants and then dried. For solvent impregnation, the hollow fiber is usually

immersed into the organic solvent (or IL) for several seconds to ensure that the pores of the membrane are filled with the solvent. After that, the extra solvent on the surface and inside the hollow fiber is removed by small air flow, water flush or sonication. Then, a predetermined volume of the acceptor phase is carefully injected into its lumen using a microsyringe. For extraction, different set-ups may be used. In the simplest one, a rod configuration with a sealed bottom⁷⁹⁻⁸² is used in which the pretreated hollow fiber is exposed to the stirred sample solution or its headspace in a tightly closed screw cap vial while remaining attached to the loading microsyringe already passed through the cap PTFE-silicone septum. The microsyringe functions as a holder and a device for sample introduction to the chromatographic system. If desired, it can also be used for dynamic extraction⁸⁰. In another set-up with longer HFM segments, a U-shape configuration^{75, 77}, both ends of the hollow fiber are connected to guiding tubes, typically syringe needles initially passed through the vial septum, one serving to introduce the acceptor phase into the hollow fiber before extraction and the other for collecting it after extraction. The prepared U-shape hollow fiber assembly is then inserted in the vial containing sample solution with the screw cap tightly closed for immediate extraction. Longer HFM segments allow higher extracting phase volume, and thus higher absolute mass extracted with better sensitivity. In a third configuration, the acceptor phase is confined in the hollow fiber by sealing the open ends, making a solvent bar microextraction (SBME) device^{83, 84}. The extraction can take place either in headspace mode or by total immersion of the hollow fiber in the stirred sample solution. In the case of SBME, tumbling of the extraction device inside the sample solution facilitates extraction. The mass transfer is driven largely by the differences between the donor and the acceptor phases, such as analytes partitioning, salting out effect in the donor side, pH gradient (acid-base reaction) or addition of a proper reagent like complex reagent for the analytes. After extraction for a set period of time, the hollow fiber is detached from the syringe needles or its ends are trimmed off and an aliquot of the analyte-enriched solvent is either withdrawn by a GC or HPLC syringe for manual injection or totally collected in micro-insert vials for automated analysis⁷⁷. Since the acceptor phase in the three-phase system is often aqueous, the extract of these systems is usually analyzed by HPLC or CE. However, if an IL is used as the supported liquid membrane (SLM) the accepting phase and the final extract can be

organic, thus allowing GC analysis by the three-phase mode⁸⁵. With all the set-ups mentioned above, the micro amount of the extracting solvent is protected against mechanical disturbance within the confines of the hollow fiber, allowing higher stirring speed, longer sampling time and even higher extraction temperature. Using SBME format relatively better enrichment factors were reported, as compared with SDME and other HFLPME techniques⁸³. Dynamic approach has also been applied using HFM-attached microsyringe to move in-and-out the acceptor phase within the HFM lumen, and claimed to provide better extraction efficiency and improved reproducibility as compared with the static mode^{80, 86-90}. Basically, the two-phase HFLPME is suitable for extraction of neutral hydrophobic analytes, and the three-phase system for ionizable and ionic compounds. So far, limited applications for water analysis have been reported in the literature. Examples include PAHs^{80, 89, 91, 92}, BTEX⁹², chlorobenzenes⁸³, THMs⁸², HAAs^{93, 94}, phenols^{43, 88, 95}, aromatic amines^{87, 96}, herbicides⁹⁰, pesticides⁸⁶ and insecticides⁸¹. Typically, the volume of organic solvent immobilized in the pores of a HFM ranges between 5 and 30 μL . Also, in the two-phase system the volume of the organic acceptor phase inside lumen of the hollow fiber is ranging from 2 to 30 μL . Therefore, the total consumption of organic solvent per analysis in HFLPME normally ranges between 5 and 60 μL , which is still an extremely low level and provide high analyte enrichment⁹⁷. The low cost and disposable nature of the hollow fiber also allow single use which eliminates the possibility of sample carryover. Further, the small pore size of the membrane prevents particles and large molecules in the sample from entering the acceptor phase, thereby yielding very clean extracts and more selectivity. There are a few disadvantages, however, including slow kinetics and relatively long extraction times⁹⁸. Usually, equilibrium extraction times range between 15 and 45 minutes for sample volumes below 2 mL⁹⁹, whereas for 1 L samples even 2 hours may be required to reach equilibrium⁹⁷. The second disadvantage of the technique is the multi-steps of membrane handling, including the need for preconditioning and removal of excess organic solvent from the outer and/or inner side of hollow membrane which is cumbersome and can affect recovery and precision of extraction¹⁰⁰. Also, decreased reproducibility due to blockage of pores or creation of air bubbles/segments on the surface and the inner side of the hollow fiber has been reported^{73, 100}. Air segments inside

the hollow fiber may be introduced during filling of the acceptor solution or generated during extraction, which should be avoided requiring careful execution. From the practical point of view, the set-ups and operation of HSLPME are more difficult and longer than those of SDME, but HSLPME technique is more robust for high stirring speed, longer sampling time and avoidance of emulsion formation, and suitable more for complicated aqueous matrices such as wastewater and biological samples.

1.3.1.3 Dispersive liquid–liquid microextraction (DLLME)

Another type of microscale LLE is dispersive liquid–liquid microextraction (DLLME)¹⁰¹. In this method, a water-immiscible extracting phase in μL range and a disperser solvent are introduced simultaneously to an aqueous sample. The disperser solvent is miscible with both the aqueous sample and the extracting solvent, and represents 97–99 % of the total volume of extracting mixture⁴⁴. As a result, the extracting solvent is dispersed in the bulk of the aqueous sample as fine droplets forming a cloudy solution. Partitioning of analytes and equilibration between the extraction phase and the sample takes place in a very short time, typically less than two minutes, due to significantly large interface area between the two phases and fast mass-transfer. After extraction, the analytes-enriched solvent is separated from the sample by centrifugation in a conical tube. Since a denser chlorinated solvent is usually used for extraction, the solvent is normally sedimented at the bottom of the tube. After collecting, the solvent is injected, with or without further work-up, into a proper chromatographic system for analysis. Typical dispersers are polar solvents such as acetone, ethanol, methanol, acetonitrile and tetrahydrofuran. The performance of DLLME has been illustrated with the determination of organic compounds in water samples such as PAHs¹⁰¹, organophosphorus pesticides¹⁰², chlorophenols¹⁰³, triazine herbicides¹⁰⁴, anilines¹⁰⁵, polar compounds¹⁰⁶, phthalate esters^{107, 108} and metallic ions^{109, 110}. The combination of SPE with DLLME for the selective determination of chlorophenols in aqueous samples with more complex matrices¹¹¹ and application of an IL-based ultrasound-assisted procedure without a solvent disperser have also been reported¹¹². In addition to the merits of other LPME methods such as low cost, very low organic consumption and high enrichment, DLLME is quite efficient and notably rapid. However, it still has some

drawbacks, including non-selectivity of extraction and interferences from the matrix co-extractives, the need for centrifugation and the difficulty for automation, decrease in the partitioning of the analytes into the extracting solvent as a result of the presence of the disperser, application of toxic chlorinated solvents, and additional work-up that may be necessary to remove the water residue before final analysis^{44, 113}. To overcome the problem of toxic chlorinated solvents, combination of DLLME with SFODME has been proposed¹¹⁴⁻¹¹⁶. With this approach the analytes-enriched solvent is accumulated on the surface of the sample upon centrifugation due to its lower density than water. This along with the solvent solidification at low temperature facilitates the phase transfer¹¹⁵. However, this variation suffers from the limitations of the conventional SFODME, that are the limited choice of proper solvent, possibility of overlapping of solvent peak with some analytes peaks and the need for extra freezing step of the extract.

1.3.2 Solid phase microextraction (SPME)

The interest for microextraction techniques in analytical chemistry was initiated by the invention of SPME^{117, 118}, a small thin sorbent material coated on a fiber support. Since its introduction in 1989, this sorbent-based microextraction technique has been evolving very quickly, appearing in almost every field of analytical chemistry from environmental analysis¹¹⁹⁻¹²⁴ to food¹²⁵⁻¹³³, drug¹³⁴⁻¹⁴⁰ and in vivo analysis of biological samples¹⁴¹⁻¹⁴⁸. Also, it became the standard that other microextraction techniques such as LPME have tried to emulate and outdo. Thousands of articles about SPME have so far been published, of which approximately 40 % focus on environmental applications¹²³, including air¹⁴⁹⁻¹⁵⁶, soil and sediment¹⁵⁷⁻¹⁶⁴, and particularly water samples¹⁶⁵⁻¹⁷⁸. SPME has addressed the need for a simple, rapid, sample preparation method as it integrates sampling, isolation, enrichment and sample introduction into a single solvent-free step¹⁷⁹. Low sample volume requirement, automation, field sampling capability and large reduction of the solvent peak interfering with early eluting analytes, which is inherently associated with LPME techniques, are among other features of SPME^{180, 181}. Unlike SDME, it does not have the problem of extraction phase instability under high stirring speed and/or longer sampling time. As for limitations¹⁸², each SPME application involving different target analytes and sample matrices requires its own separate method

development. In addition, the limited volume of SPME fiber coatings might result in poorer sensitivity when analytes with low distribution constants are extracted. The robustness and durability of fused-silica type fibers might be an issue in sample sequences involving large number of samples. Limited range of commercial fibers and possibility of carryover between analyses are also stated as its drawbacks. Nevertheless, this microextraction technique is now firmly established and proved to be a powerful alternative to the conventional extraction methods¹⁸³. The technique has received continuous developments over the past two decades, including construction of new and improvement of existing devices, commercialization of more robust fiber assemblies with Stableflex and metal cores and automation for both GC and LC applications¹⁸³. Currently, research trends in SPME are focused on development of new types of coatings with selectivity or suitability for specific applications, derivatization strategies, and development of new devices to improve the extraction efficiency¹⁸³⁻¹⁸⁶.

1.3.2.1 Theoretical and practical aspects

SPME theory has been developed for ideal extraction conditions, i.e. trace concentrations and simple matrices, by applying principles of thermodynamics and mass-transfer¹⁷⁹. This theory can be very accurate for clean matrices such as drinking water with trace levels of DBPs under ambient conditions. Even when the conditions are more complex, the theory can approximate well some of the parameters such as extraction times and amounts of analytes extracted. Therefore, an understanding of SPME theory and its effective use provides insight and direction when developing and optimizing methods. Here, those aspects of particular interests for drinking water analysis are reviewed.

1.3.2.1.1 SPME device

The most commonly used form of SPME is fiber geometry, in which a thin layer of a polymeric material, neat or blended with solid particles, is coated and immobilized on a bare fiber support (e.g. fused silica or metal) for extraction purpose. To protect the fiber, an assembly has been designed that contains a septum piercing needle and inner needle tubing to which the coated fiber is attached. The outer needle is sealed with a septum to

keep it from leaking during extraction and desorption. Figure 1.2 illustrates the design of a manual fiber assembly and its holder made by Supelco¹⁷⁹. The manual fiber assembly contains a spring that helps to retract the fiber after exposure for extraction or desorption. The inner needle has a color-coded screw-type hub at the end, which indicates the type of coating and facilitates attachment of the assembly to the holder.

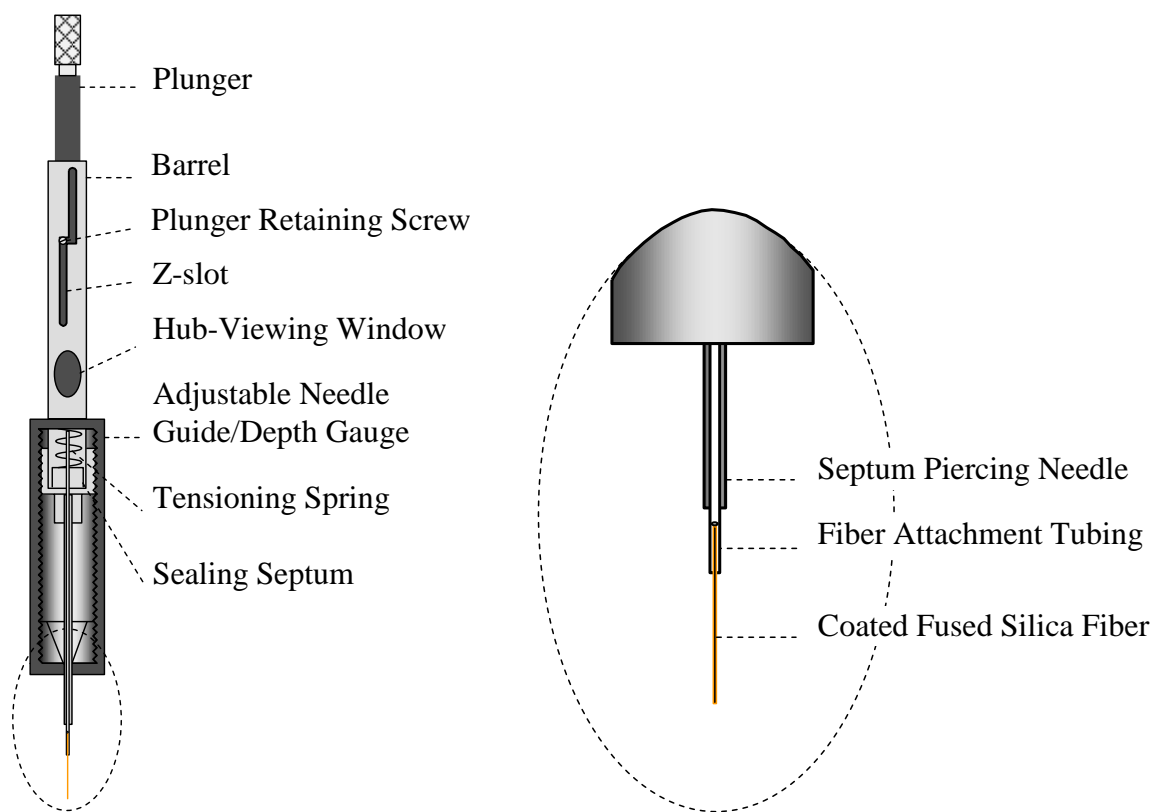


Figure 1.2 Design of the commercial SPME device made by Supelco (Sigma-Aldrich)¹⁷⁹.

A similar assembly is used for the autosamplers except that it does not have a spring. In addition to the fiber geometry, other formats of SPME are also available such as in-tube coated capillary, coated stir-bar and thin film membrane¹⁸³. Application of the SPME device does not require high laboratory skills. For a typical laboratory application, the piercing needle is passed through the vial septum and the plunger is depressed. By depressing the plunger, the fiber is extended outside the needle and exposed to the sample

matrix. After extraction for a set period of time, the fiber is withdrawn into the needle by pulling the plunger and taken for next step, analyte desorption. Although SPME field sampler devices have some modifications to protect the fiber during sampling, storage, and transportation¹⁸⁷⁻¹⁸⁸, their operating principles are similar to the conventional SPME device described.

1.3.2.1.2 Procedure and modes of extraction

SPME procedure includes two main steps that are (i) extraction of analytes by the coating from sample and (ii) desorption of the extracted analytes from the coating. The extraction process is carried out either by direct immersion of the fiber into the sample or by its exposure to the headspace above it, as illustrated in Fig. 1.3. The latter mode is usually applicable to volatile and semi-volatile species, while the former can be applied regardless of analyte volatility. Headspace mode is advantageous in that it allows longer lifetime of SPME fiber and modification of the matrix, such as pH adjustment and salt addition without damaging the fiber.

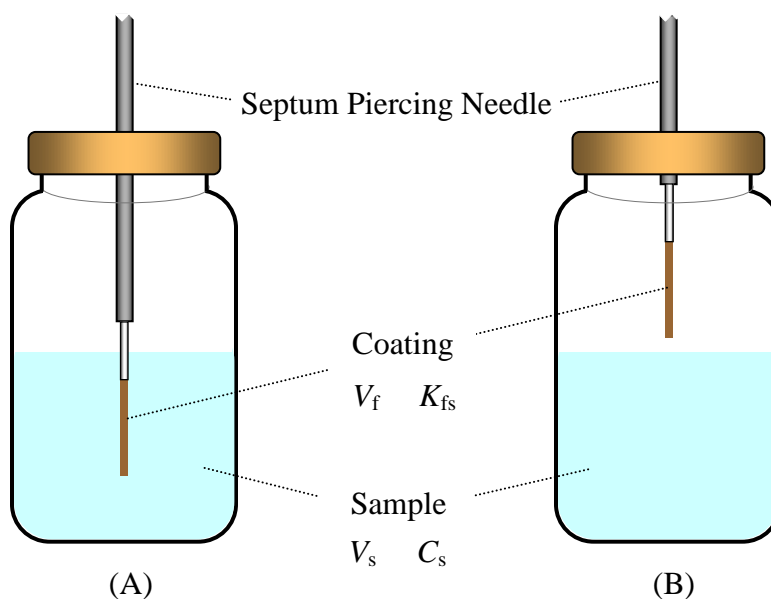


Figure 1.3 (A) Direct immersion and (B) headspace SPME.

Occasionally when target analytes are poorly volatile or non-volatile and sample contains high molecular weight interfering compounds, such as humic acids or proteins, a membrane-protected direct approach can be used¹⁸⁹. Typically, a cellulose hollow membrane with a molecular weight cut-off (e.g.18000 Da) can be used to cover the SPME fiber forming a concentric sheath around it, which allows target analytes to diffuse through while excluding the high molecular weight interfering compounds. Despite the advantage of fiber protection, the membrane-protected approach slows down mass transfer during direct SPME. Hence, it should be used only for complex matrices where application of direct or headspace SPME are both challenging. Irrespective of the mode of operation, the extraction is carried out via equilibrium-based absorptive and/or adsorptive mechanisms, depending on the nature of the coating. After extraction, analytes are desorbed thermally in the hot injection port of a GC, or by a small amount of solvent, either off-line or on-line, to be injected in a HPLC or capillary electrophoresis instrument for separation and subsequent detection. Although the sample capacity of SPME is low and in most cases a small portion of analyte is extracted and transferred, it is normally sufficient to produce a significant analytical signal with modern detectors.

1.3.2.1.3 Equilibrium extraction

The most widely used SPME technique consists of direct immersion of fiber coating into the sample for a predetermined amount of time (Fig. 1.3 A). Immediately after exposing the fiber coating to the sample, partitioning of analyte begins rapidly between the two phases. The amount of analyte extracted depends on the exposure time at initial stages of extraction. If a sufficient time is allowed for the equilibrium to be established, further increases in extraction time do not affect the amount of analyte extracted and microextraction is considered complete. When two phases are involved, the equilibrium sampling can be described by Equation 1.1 according to the law of mass conservation:

$$C_0V_s = C_f^\infty V_f + C_s^\infty V_s \quad (1.1)$$

where C_0 is the initial concentration of the analyte in the sample; C_f^∞ and C_s^∞ are the equilibrium concentrations of the analyte in the fiber coating and in the sample, respectively; V_s and V_f are the volumes of the sample and the fiber coating, respectively.

Partitioning of the analyte between the sample and the fiber coating is governed by the partition coefficient, K_{fs} , also called the distribution constant as given by:

$$K_{fs} = \frac{C_f^\infty}{C_s^\infty} \quad (1.2)$$

Equations 1.1 and 1.2 can be combined and rearranged into:

$$C_f^\infty = \frac{K_{fs} V_s}{K_{fs} V_f + V_s} C_0 \quad (1.3)$$

Finally, the number of moles of the analyte extracted by the coating at equilibrium, $n^\infty = C_f^\infty V_f$, can be calculated by multiplying the sides of Equation 1.3 by V_f :

$$n^\infty = \frac{K_{fs} V_f V_s}{K_{fs} V_f + V_s} C_0 \quad (1.4)$$

It follows from Equation 1.4 that the amount of analyte extracted by the coating at equilibrium is linearly proportional to the initial concentration of analyte in the sample, and that the amount is independent of extraction time. Hence, Equation 1.4 provides an analytical basis for quantification using SPME. Moreover, when the term $K_{fs} V_f$ (fiber capacity) is insignificant relative to V_s , then V_s cancels out and the amount of analyte extracted at equilibrium is no longer dependent on the sample volume. This way Equation 1.4 is simplified as Equation 1.5, which is important from the perspective of integrating sampling and sample preparation when the volume of the sample is very large or when the analyte partition coefficient into the coating is very low:

$$n^\infty = K_{fs} V_f C_0, \quad (K_{fs} V_f \ll V_s) \quad (1.5)$$

In practice, the fiber can be exposed directly to an undefined sample volume such as water streams, ambient air, etc. This facilitates in-field or on-site analysis by simplifying the sampling step, accelerating the whole analytical process and preventing the errors associated with a defined collection of sample. Equations 1.4 and 1.5 indicate that the efficiency of the extraction process is dependent on the fiber coating/sample matrix distribution coefficient. This is a characteristic parameter that describes properties of a

coating and its selectivity toward a specific analyte versus other matrix components. The magnitude of K_{fs} is impacted by the properties of sample matrix such as temperature, pH, addition of organic solvent and ionic strength. Therefore, it is important to keep these parameters constant during sample analysis. Equations 1.4 and 1.5 also demonstrate that increasing the coating volume can improve the sensitivity of the SPME method which is directly proportional to the number of moles extracted from the sample. However, as will be discussed later, increases in the extraction phase volume in the form of thicker coatings will cause equilibration times to be excessively long. Occasionally, when the sample volume is very small and the partition coefficient between the coating and the sample matrix is very large, that is when $V_s \ll K_{fs}V_f$, then the term $K_{fs}V_f$ cancels out and Equation 1.4 is simplified as Equation 1.6:

$$n^\infty = C_0 V_s, \quad (V_s \ll K_{fs}V_f) \quad (1.6)$$

Equation 1.6 implies that all of the analyte in the sample matrix is extracted into the coating (exhaustive extraction) and the initial concentration of the analyte can be easily calculated from the amount extracted by the coating and the volume of the sample.

When headspace is present and analytes have low affinity for that, its presence causes no complications for the extraction and may be disregarded. This is the case for non-volatile compounds whose Henry's law constants are so low that their amounts in the headspace can be neglected. Volatile compounds, however, have a significant concentration present in the headspace. Under these circumstances, the mass balance equation at equilibrium can be re-written as:

$$C_0V_s = C_f^\infty V_f + C_s^\infty V_s + C_h^\infty V_h \quad (1.7)$$

where C_h^∞ is the equilibrium concentration of the analyte in the headspace and V_h is the headspace volume. If we define the coating/gas distribution constant as $K_{fh} = C_f^\infty / C_h^\infty$ and the gas/sample matrix distribution constant as $K_{hs} = C_h^\infty / C_s^\infty$, the number of moles of the analyte extracted by the coating at equilibrium, $n^\infty = C_f^\infty V_f$, can be expressed as:

$$n^{\infty} = \frac{K_{fh} K_{hs} V_f V_s C_0}{K_{fh} K_{hs} V_f + K_{hs} V_h + V_s} \quad (1.8)$$

Considering $K_{fs} = K_{fh} K_{hs}$ ¹⁷⁹, Equation 1.8 can be further simplified as:

$$n^{\infty} = \frac{K_{fs} V_f V_s C_0}{K_{fs} V_f + K_{hs} V_h + V_s} \quad (1.9)$$

Equation 1.9 states that the amount of analyte extracted at equilibrium is proportional to the analyte initial concentration in the sample as long as the volumes of sample, headspace and the fiber coating and distribution constants are kept constant. Since at equilibrium the chemical potentials of the analyte in all three phases (water sample, headspace and fiber coating) must be the same by definition^{157,190}, the amount of analyte extracted at equilibrium is independent of the location of the fiber in the system, headspace or the sample itself.

Compared with Equation 1.4, described for a two-phase system, the difference is the additional term $K_{hs}V_h$ in the denominator of Equation 1.9, which is referred to as headspace capacity. For volatile compounds K_{hs} is usually close to one¹⁹⁰, which means that headspace volume cannot be neglected unless it is close to zero (a two-phase system). Semi-volatile compounds, on the other hand, have much lower K_{hs} values. Therefore, the $K_{hs}V_h$ term may be negligibly small. However, this assumption should always be verified.

1.3.2.1.4 Pre-equilibrium extraction

The equilibrium extraction is advantageous in that it provides improved precision and high method sensitivity. However, the time needed to reach equilibrium during SPME may sometimes be very long up to several hours, depending on the physiochemical properties of analyte, extraction phase, sample matrix and agitation conditions. Therefore, it may be desirable to shorten extraction time at the cost of reduced sensitivity where it is not a serious concern. Under these circumstances, quantification is still feasible using pre-equilibrium sampling, provided that the SPME conditions (agitation, temperature, etc.) and the sampling time are held constant, according to Equation 1.10¹⁹¹:

$$n = n^{\infty} (1 - e^{-at}) \quad (1.10)$$

where t is the sampling or extraction time, n is the pre-equilibrium amount of analyte extracted and a is a time constant representing how fast an equilibrium can be reached. Equations 1.10 and 1.4 can be combined into Equation 1.11:

$$n = (1 - e^{-at}) \frac{K_{fs} V_f V_s C_0}{K_{fs} V_f + V_s} \quad (1.11)$$

which states that there is still a linear relationship between the amount of analyte on the fiber coating and its initial concentration in the sample even when extraction process is interrupted before equilibrium condition is reached. When the extraction time is long enough, that is $t \rightarrow \infty$, Equation 1.11 turns into Equation 1.4, characterizing equilibrium extraction.

1.3.2.1.5 Matrix effect

Matrix effect on SPME is less pronounced for clean matrices such as drinking waters with low DBPs levels than complex matrices such as waste waters, soils and biological samples. Humic substances, inorganic salts and suspended particles, if any, are the potential matrix components that may interfere with SPME water analysis. Humic compounds and inorganic salts can damage the SPME fiber by fouling. The high molecular weight humic components may also remain in the GC system and deteriorate its performance, resulting in poor analytical performance. The typical approach used to reduce fouling involves introduction of a barrier between the sample matrix and SPME extraction phase to prevent transport of high molecular weight interferences. This barrier can be headspace above sample or a porous membrane surrounding SPME fiber (headspace or membrane-protected approach).

Suspended particles in water sample, if present, may also interfere with SPME analysis by adsorbing analytes onto their surface. In general, any additional phase present in the sample having a significant affinity for the analyte of interest can compete with the SPME extraction phase. Where additional competing phases are present, Equation 1.1 and Equation 1.2 can be re-written to include the impact of each additional phase:

$$C_0 V_s = C_f^\infty V_f + C_1^\infty V_1 + C_2^\infty V_2 + C_3^\infty V_3 + \dots + C_n^\infty V_n + C_s^\infty V_s \quad (1.12)$$

$$n^\infty = \frac{K_{fs} V_f V_s C_0}{K_{fs} V_f + K_{1s} V_1 + K_{2s} V_2 + K_{3s} V_3 + \dots + K_{ns} V_n + V_s} \quad (1.13)$$

A detail discussion of Equation 1.13 has been published¹⁷⁹. This equation indicates that composition of sample matrix can affect the amount of analyte extracted by SPME when dealing with complex heterogeneous samples.

1.3.2.1.6 Kinetics

The bottleneck of SPME procedure is the extraction kinetics. The mathematical descriptions of the kinetics of mass transfer for perfectly agitated and static solutions were developed and compared with experimental results^{179, 192}. The theory developed indicates that the speed of extraction is primarily controlled by diffusion coefficient of analyte in the polymer coating and/or the sample matrix. According to the theory, upon exposure of the fiber to the sample, a mass-transfer process begins and analytes cross the interface from the sample matrix into the fiber stationary phase. The mass transferred to the fiber is rapidly increased at the beginning, but the rate of increase then slows, and eventually reaches equilibrium. Theoretically, the time required to reach equilibrium is infinitely long. In practice, microextraction is considered to be complete if a sufficient exposure time is allowed to reach plateau conditions. Under these circumstances, further increase of extraction time does not result in an increase in the amount extracted within the limits of experimental error, which is typically about 5%. Therefore, the equilibrium extraction is assumed to be achieved when 95% of the equilibrium amount of the analyte is extracted. This is illustrated in Fig. 1.4 for a perfectly agitated solution¹⁷⁹, where the aqueous phase moves very rapidly with respect to the fiber so that all analytes present in the sample have immediate access to the fiber coating.

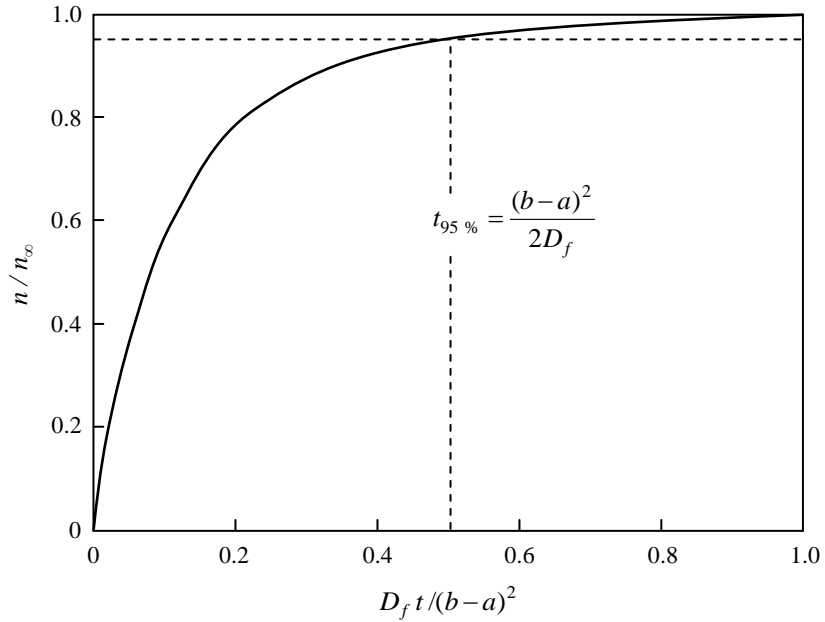


Figure 1.4 Universal profile of mass extracted versus time for a perfectly agitated sample solution of infinite volume; a , bare fiber radius; b , coated fiber radius; $(b-a)$, coating thickness; D_f , analyte diffusion coefficient in the fiber coating; $t_{95\%}$, practical equilibrium extraction time.

The graph in Fig. 1.4 is a universal extraction time profile since both the mass and time axes have dimensionless scales. The time required to reach equilibrium ($t_{95\%}$) can be estimated from the graph, as shown by Equation 1.14:

$$t_e = t_{95\%} = \frac{(b-a)^2}{2D_f} \quad (1.14)$$

which indicates that the speed of extraction is controlled by the analyte diffusion coefficient in the coating (D_f) and its thickness ($b-a$) under perfect agitation. Although such a system does not exist practically, the above equation can be used to estimate the shortest possible equilibration time.

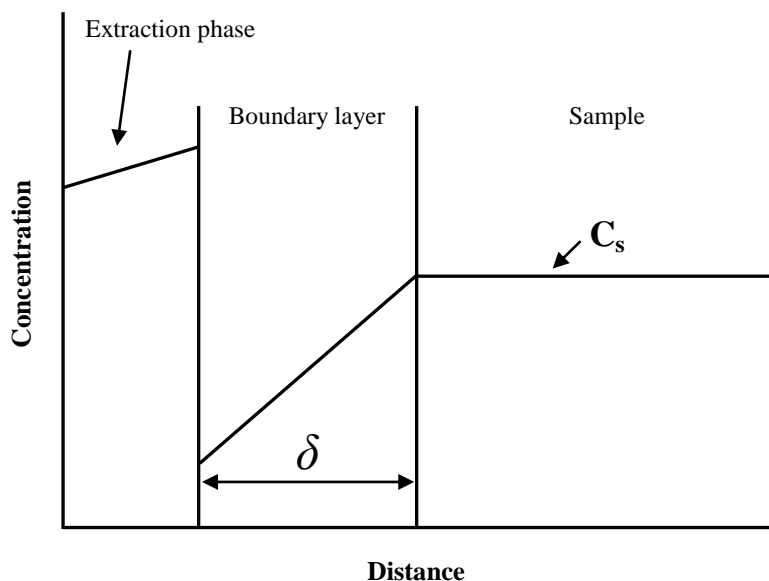


Figure 1.5 Boundary layer model configuration; regions and concentrations versus radius profile.

For practical agitation a boundary layer model was presented¹⁷⁹. According to the boundary layer model, the layer of the fluid contacting the fiber surface is always stationary, independent of the agitation level. As distance from the fiber surface increases the fluid movement increases gradually until it reaches the bulk flow level in the sample (Fig. 1.5). The thickness of this static layer (δ) called the boundary layer is controlled by agitation level (convection rate) and diffusion coefficient of the analyte in the sample (D_s). Where the system is completely static, the thickness of the boundary layer is comparable to the radius of the sampling vial¹⁷⁹. Therefore, to facilitate mass transfer to the vicinity of the fiber and rapid extraction some levels of agitation are often required, which can be in the form of fast sample flow, rapid fiber movement, stirring or sonication¹⁸¹. An illustration of kinetics of extraction for practical agitation is presented in Fig. 1.6¹⁷⁹.

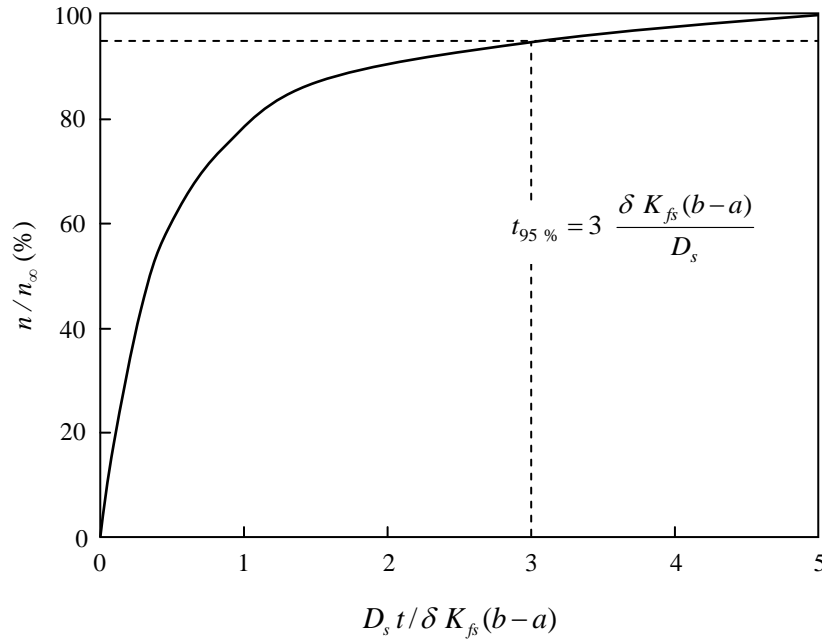


Figure 1.6 Universal extraction time profile for a practically agitated sample solution of infinite volume, when the boundary layer controls the extraction rate; δ , boundary layer thickness; K_{fs} , distribution coefficient of the analyte between the fiber coating and the sample; $(b-a)$, coating thickness; D_s , analyte diffusion coefficient in the sample; $t_{95\%}$, practical equilibrium extraction time.

This is again a universal extraction time profile, since both the mass and time axes have dimensionless scales. Similar to the case of perfect agitation, the time required to reach equilibration can be estimated from the graph in Fig. 1.6, as shown in Equation 1.15:

$$t_{95\%} = 3 \frac{\delta K_{fs} (b-a)}{D_s} \quad (1.15)$$

where δ is the boundary layer thickness; K_{fs} is distribution coefficient of the analyte between the fiber coating and the sample; $(b-a)$ is the coating thickness and D_s is the analyte diffusion coefficient in the sample fluid. Equation 1.15 indicates that the equilibrium extraction time is longer for analytes with higher K_{fs} values. Also, a decrease in the coating thickness and/or an increase in agitation speed shorten the equilibrium

extraction time. Moreover, an increase in extraction temperature translates to a decreased K_{fs} value and an increased diffusion coefficient, both leading to shorter equilibrium time. The kinetics of extraction in the headspace is generally faster than the extraction in the aqueous sample. The boundary layer is not present when sampling from headspace. In addition, the diffusion coefficients of analytes in the gas phase are much higher than those in liquid media, typically four orders of magnitude. Therefore, addition of a gaseous headspace as an intermediate phase may be an interesting means of accelerating the extraction, particularly for volatile analytes which have high Henry's law constants. When the fiber coating is in the headspace, analytes are indirectly extracted from the sample matrix through the headspace. If the headspace-sample distribution coefficient (equal to dimensionless Henry's law constant) is low and K_{fs} is large, such as the case of semi-volatiles, the equilibration process is very slow. Initially, the analyte is extracted only from the gaseous phase and a rapid increase in the amount extracted is observed. As soon as the headspace concentration of the analyte falls below the equilibrium level with respect to the aqueous phase, the increase in the amount extracted slows down and the trend continues for a long time. Under these circumstances, the analyte molecules start to move from the aqueous sample to the headspace. Yet, at any given moment there is only a limited amount of analytes in the headspace, because the rate of analyte evaporation is low. As a result, the extraction rate is limited by mass transfer rate from the sample to the headspace and the equilibration process is very slow. On the other hand, if the amount of the analyte extracted by the fiber at equilibrium is negligible compared with the amount present in the headspace, then only a very small amount of the analyte has to be transported from the aqueous sample through the headspace to the fiber coating. As a consequence, the analyte is extracted almost exclusively from the gaseous phase, and the extraction is much faster than the case previously described. Considering the limits of experimental error for trace SPME-GC analysis which is usually a 5% difference, then the condition that must be fulfilled for the extracted amount to be negligible compared with the amount present in the headspace can be described according to Equation 1.16 :

$$R = \frac{K_{fs}V_f}{K_{hs}V_h} = \frac{K_{fs}V_f}{K_{hs}aV_s} \leq 0.05 \quad , \quad (a = \frac{V_h}{V_s}) \quad (1.16)$$

Equation 1.16 indicates that the headspace capacity ($K_{hs}V_h$) must be at least 20 times larger than the capacity of the fiber ($K_{fs}V_f$) to achieve rapid extraction. For a given sample volume (V_s), this can be achieved by using a sufficiently large headspace volume (corresponding to a large headspace-to-sample volume ratio, a), or by increasing K_{hs} . The latter may be accomplished by increasing the temperature or by salting the analyte out of the aqueous phase. When the condition described by Equation 1.16 is fulfilled, equilibration can take as little as a few minutes, and is almost independent of the agitation conditions, provided that the analyte is equilibrated between the sample and its headspace before the extraction begins¹⁹⁰.

It should be emphasized that the presence of headspace and increase in its capacity causes loss of method sensitivity. In three-phase systems, the analyte is distributed between all three phases involved (aqueous sample, headspace and fibre coating). Consequently, the amount of an analyte extracted by the fiber at equilibrium in three-phase systems can only be smaller than or equal to the amount extracted when no headspace is present. Still, increasing the headspace capacity, as described above, might dramatically shorten the equilibration times for some semi-volatile analytes while maintaining sufficient sensitivity. Both these effects need to be taken into account when developing a method involving headspace extraction.

1.3.2.1.7 Adsorption versus absorption extraction

SPME extraction takes place via absorption and/or adsorption mechanisms depending on the nature of coating, which can be liquid polymer, solid particles suspended in liquid polymer (mixed-phase) or merely a layer of solid material. The two mechanisms and performance characteristics of liquid and solid SPME coatings are substantially different. When extraction begins analyte molecules initially get attached to the surface of the coating regardless of its nature. Whether they migrate to the bulk of the coating or remain at its surface depends on the magnitude of the diffusion coefficient of the analyte in the coating. Diffusion coefficients of organic molecules in liquid polymers such as polydimethylsiloxane (PDMS) are relatively high and close to those of organic solvents. These polymers are homogeneous, usually non-porous and in a gum-like or liquid-like state, which can dissolve analytes and behave similarly to organic solvents. As a result,

analytes can partition into these coatings via absorption (Equation 1.4) and their molecules are retained by solvation. Through absorption, analytes can penetrate the entire volume of a liquid polymer coating. Hence, liquid polymer coatings can provide high extraction capacity which is proportional to their volumes (or thicknesses). Another advantage of liquid polymer coatings is linearity of extracted amount over a wide range of analyte and interference concentrations. With these coatings nonlinear behavior happens only if the properties of bulk coating are changed by the extracted components. This occurs only when the amount extracted is a substantial portion of the liquid polymer extraction phase¹⁸¹, which is unlikely when dealing with analytes present at trace levels. The limitation is that they often provide higher detection limits and lower sensitivity for trace analysis, compared to the solid coatings.

The situation is different with solid coatings. These coatings often consist of porous solid particles, embedded into a liquid polymer such as PDMS. The solid nature of particles substantially reduces the diffusion coefficients within the coating structure. As a result, within the time span of the experiment, sorption occurs only in the pores of the coating surface by physical trapping or intermolecular forces such as Van der Waals or dipole-dipole interactions, as depicted in Fig. 1.7¹⁹³. Therefore, analyte extraction with solid coatings is mainly governed by adsorption mechanism. An equilibrium theory was developed for adsorption extraction by SPME porous solid coatings with intermediate to large pore sizes that cannot cause capillary condensation to occur¹⁹³. According to the theory, the amount of analyte extracted at equilibrium can be calculated using Equation 1.17:

$$n^{\infty} = \frac{K_A V_f V_s (C_{f_{\max}} - C_f^{\infty})}{V_s + K_A V_f (C_{f_{\max}} - C_f^{\infty})} C_0 \quad (1.17)$$

where, $C_{f_{\max}}$ is the maximum concentration of active sites on the coating, C_f^{∞} is the equilibrium concentration of analyte on the fibre, and K_A is the analyte adsorption equilibrium constant rather than partitioning constant described in Equation 1.4. Equation 1.17 indicates that if the relative number of occupied sites is very low ($C_{f_{\max}} \gg C_f^{\infty}$), that is when analyte concentration in a sample and/or its affinity for the coating are very

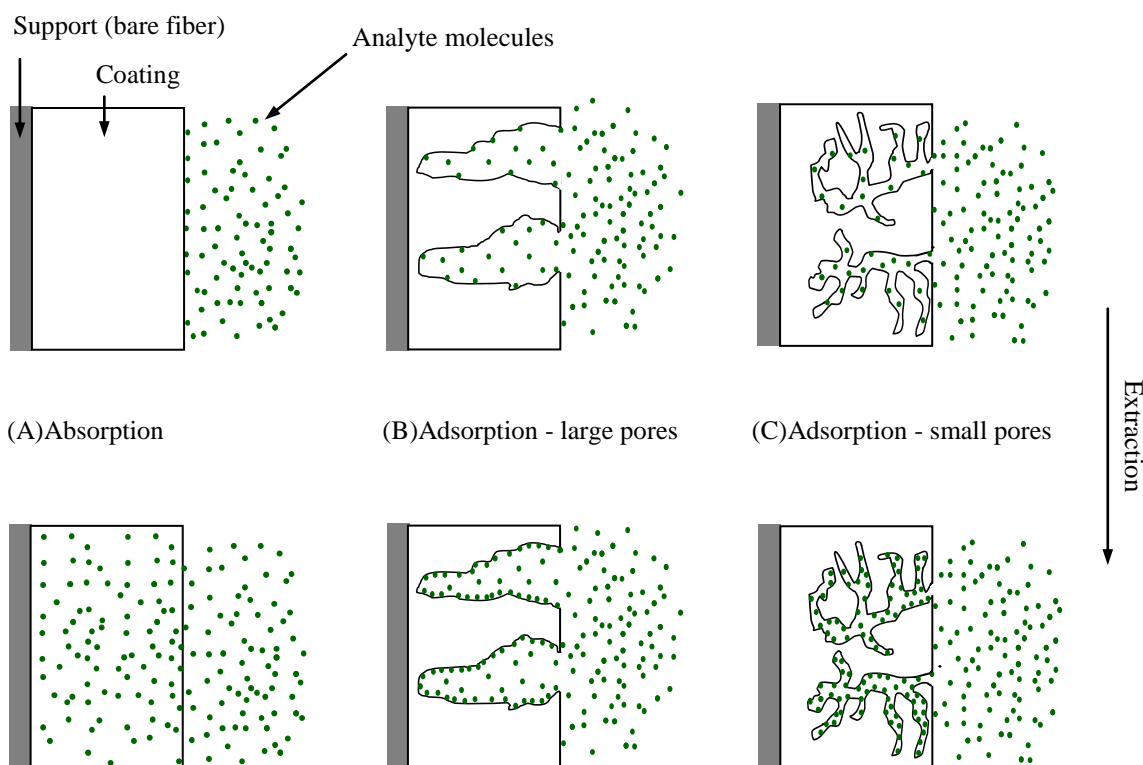


Figure 1.7 Comparison of (A) absorption and (B, C) adsorption extractions (cross-sections of the support or bare fiber)¹⁹³. Diagrams on the upper side illustrate the initial stages of the extractions. Diagrams on the lower side illustrate the equilibrium condition.

low, a linear dependence should be observed with the adsorptive solid coating. However, the number of surface sites in solid coatings where adsorption can take place is limited. When all the surface sites are occupied no more analyte can be trapped (unless it can condense into the small pores by the capillary condensation mechanism)¹⁹³. Consequently, the linear dependence is no longer observed. Moreover, after surface sites saturation, compounds with poor affinity toward the solid phase (low adsorption distribution constants) are frequently displaced by analytes characterized by stronger binding (higher adsorption distribution constants) or those present in the sample at high concentrations¹⁹⁴. Therefore, matrix composition can significantly affect the amount extracted by solid coatings and care should be exercised when performing quantitative

analysis with these coatings. In general, porous solid coatings can be expected to perform well for relatively clean matrices or matrices of constant composition, provided that the concentration of the analyte of interest is low. The common approach to avoid competition effects with these coatings is to use a sampling time less than the equilibration time, so that the total amounts of analytes extracted by the coating would be substantially below the saturation value. Long sampling times (days or weeks rather than hours) can cause the analytes molecules to diffuse into the bulk of solid coatings over very short distances, which would become noticeable as persistent carryover that is difficult to remove even with repeated desorptions. Nonetheless, solid coatings provide wider range of applications in terms of selectivity, polarity and molecular size of analytes that can be extracted by SPME fibers.

1.3.2.1.8 Calibration and quantification

As mentioned earlier, SPME is generally an equilibrium-based microextraction technique rather than an exhaustive method. Therefore, the SPME results must be calibrated to obtain the concentration of the analyte in the sample. Basically, calibration process serves to relate the measured analytical signal to the initial concentration of analyte in the sample matrix.

To obtain valid results, it is important that the calibration standards have the same composition as the test samples. Otherwise, if the calibration standards matrix differs from that of test samples, partitioning will not be the same and the calibration will not be valid. In addition to the sample composition, the volumes of all test samples and standards must be the same during analysis by SPME. When aqueous samples are analyzed by SPME a certain volume of headspace is often present in the vials. If the sample headspace exhibits a significant affinity for the analyte, that is normally when volatiles are present, the headspace volume must also be controlled. Two separate types of calibration are frequently performed when using SPME. The first one aims to calibrate the instrument response and calculate the amount of analyte extracted with SPME device. This is achieved by linear regression calibration curve of instrument response against the quantities of injected liquid standards and then correlating the instrument response obtained with the SPME device. The second calibration is for quantification and aims to

relate the measured signal of analyte extracted with SPME device to the initial concentration of the analyte in the sample. Several calibration techniques have been employed for quantification in SPME. The selection and suitability of a technique depends on the application, the number of samples to be analyzed and sample complexity. These calibration techniques include the followings:

(1) *External calibration curve* involves the preparation of several standard solutions using matrix-matched blank sample. The standards and samples are subsequently analyzed using the same extraction conditions to establish the relationship between the peak area responses and the analyte concentrations in the sample. The concentration of the target analyte is then calculated from the equation of the calibration curve. This is the simplest and most widely implemented calibration technique, especially for clean matrices. However, it may not be an appropriate method when reproducing sample matrix and extraction conditions is difficult or impossible to achieve.

(2) *Standard addition* method involves adding known quantities of the target analyte to the sample matrix containing an unknown concentration of the analyte. The analyte-added and the original samples are then analyzed using the optimized SPME procedure and a plot of the instrument responses against the range of known target analyte concentrations is produced. The unknown concentration of analyte in the original sample is then determined by the extrapolation of the response to zero. This approach requires extensive sample preparation, thus is not suitable when a large number of samples is intended for analysis. However, the technique is able to compensate for matrix effects, and therefore can be used for high-complexity sample matrices. As a general rule, the amount of organic solvent in spiked samples should be kept constant for all samples and all concentration levels tested to avoid precision problem.

(3) *Internal standard (IS)* approach involves the addition of a compound in a constant amount to the samples and standard solutions. The compound should mimic the behavior of the analyte during the extraction and can be well resolved chromatographically from the target analyte. Calibration then involves plotting the ratio of the analyte signal to the internal standard signal as a function of the analyte concentration of the standards. If an internal standard is properly chosen and used, the analyte and the

standard signals respond proportionally to random instrumental and method fluctuations and the ratio of their signals remain independent of these fluctuations. Therefore, it is preferable that internal standard selected relates closely to the analyte, particularly in terms of partition coefficient for the extraction and any competing phases. This approach shows significant advantages in terms of matrix effects, loss of target analytes during sample preparation and transportation processes as well as method precision issues. However, a major difficulty in applying this approach is that finding a suitable compound to serve as internal standard is not easy. As well, introducing the IS in both samples and standards in a reproducible way is difficult. Additionally, isotopically-labeled internal standards require MS analysis, are expensive and not always available.

(4) *Equilibrium extraction method* involves exposure of the liquid SPME coating to the sample matrix until the equilibrium between the coating and sample matrix is reached. The sample concentration can then be calculated from Equation 1.4 or 1.5. This calibration method is often used for on-site sampling. To use this method, the analytes distribution constants between the sample matrix and the coating must be known. These may be obtained from literature values or through well-established methods¹⁷⁹.

(5) *Exhaustive extraction calibration* is based on Equation 1.6, when the sample volume is very small and the partition coefficient between the coating and the sample matrix is very large. This happens when sampling semi-volatiles from small sample volumes or when sampling volatiles from small sample volumes using an internally-cooled fiber^{195, 196}. This calibration method is rarely used in SPME because it is only suitable for small sample volumes and very large distribution coefficients.

(6) *Kinetic calibration* is based on the dynamic model of SPME and symmetry of absorption and desorption in the SPME liquid coatings^{191, 197}. The kinetic calibration is particularly useful for on-site or *in vivo* sampling, where standard addition and external standard calibration methods are not practical to use. The approach can be performed using desorption of isotope-labeled standards pre-loaded in the extraction phase^{198, 199}, termed as the in-fiber standardization technique, according to Equation 1.18:

$$C_0 = \frac{q_0^n}{K_{fs} V_f (q_0 - q)} \quad (1.18)$$

where n is the amount of extracted analyte at time t , q_0 is the amount of pre-loaded standard and q is the amount of the standard remaining in the extraction phase after its exposure to the sample matrix for the extraction time, t . This technique can be used for both grab sampling and long term monitoring calibrating the effect of environmental factors such as temperature, turbulence and biofouling²⁰⁰. However, for some special situations, such as fast on-site sampling of the analytes with very large distribution coefficients, the pre-loaded standard approach might exhibit poor performance since the loss of the standard is too small (less than 5%, which is close to the RSD of the measurement) for proper quantification. The kinetic calibration can also be performed as a standard-free procedure using two samplings²⁰¹, which is a newer technique, according to Equation 1.19:

$$\frac{t_2}{t_1} \ln \left(1 - \frac{n_1}{n^\infty} \right) = \ln \left(1 - \frac{n_2}{n^\infty} \right) \quad (1.19)$$

where n_1 and n_2 are the amount of extracted analyte at sampling times t_1 and t_2 , respectively. Equation 1.19 can be used for the calculation of the amount of analyte extracted at equilibrium, n^∞ . Then, the initial concentration of the analyte in the sample can be calculated from Equation 1.4 or 1.5. The standard-free procedure obviates the need for an isotope-labeled standard and the use of a MS detector. As well, it facilitates direct quantification of all analytes with only two samplings without considering whether the system has reached equilibrium. This aspect of the technique is desirable for analytes with unknown or different equilibrium times, and particularly useful if a number of compounds are measured simultaneously. However, it is only applicable when the sampling rate remains constant such as the case for rapid on-site sampling²⁰⁰.

(7) *Diffusion-based calibrations* have also been developed for the quantification of SPME for on-site and *in vivo* sampling. Two approaches, interface model and cross-flow model, have been developed which are based on Fick's first law of diffusion and the kinetics of absorption/adsorption and desorption. These methods require additional equipment to control or measure the flow velocity of the sample matrix. A detailed discussion of diffusion-based calibration has been published²⁰⁰.

1.3.2.2 Method development

SPME Method development aims to achieve optimum experimental conditions for high sensitivity and good reproducibility. The steps and parameters that should potentially be considered for SPME method optimization include selection of separation/detection system, fiber coating, extraction mode, derivatization if necessary, sample volume, extraction time, agitation method, sample matrix parameters (e.g. temperature, pH and salt concentration), application of a different SPME configuration to increase sensitivity (e.g. stir bar or thin film) and desorption conditions. The choice of the separation/ detection system will largely depend on the goals of the analysis and the instrumentation available in the laboratory. As for the other steps, the selection depends on the properties and concentration of target analytes, required detection limits, and the complexity of sample matrix. The following discussion of method development strategies pertains to the parameters typically optimized for SPME with focus on GC applications. Additional information regarding LC and other applications can be obtained from literature²⁰².

1.3.2.2.1 Fiber coating

The sensitivity of SPME is significantly affected by the distribution coefficient of analyte between fiber coating and sample matrix. This coefficient, on the other hand, largely depends on the chemical properties of the analyte and the type of fiber coating. Hence, selecting an appropriate coating is the first step in SPME method development. This is normally accomplished by examination of various fibers and comparison of the extraction efficiencies under similar SPME conditions. When simultaneous determination of several analytes is of interest, selection is done based on the overall performance of the fibers.

Several fiber coatings have been commercialized which differ in nature (liquid or solid), polarity, thickness and length. Essentially, polarity of a coating enhances attraction of an analyte to the coating based on a simple general rule; ‘similar attracts similar’. Whether the analyte is efficiently retained by the coating or released depends primarily on the size (or volatility) of the analyte, the nature of coating and its thickness.

The commercial liquid polymer (absorbent type) fiber coatings include PDMS, Polyacrylate (PA) and Polyethylene glycol (PEG), also known as Carbowax (CW). Among these, the nonpolar PDMS fiber coating is the most frequently used one, which comes in different thicknesses and is suitable for the extraction of volatile and semi-volatile analytes with none or less polarity. Thin PDMS coatings (e.g. 7 μm) favor fast diffusion and release of semi-volatile and high molecular weight analytes, while thicker coatings (e.g. 100 μm) permit efficient retention of small size highly volatile analytes. Generally, thicker coatings offer higher capacity and increased sensitivity, but require longer equilibration times. Therefore, the thinnest coating which could achieve the required detection limits is favorable, particularly for analytes with larger distribution constants. PA is a moderately polar liquid polymer coating which is often suitable for extraction of a wide range of polar and nonpolar analytes. This coating has an affinity for aromatic compounds and oxygenated analytes, including phenols and PAHs. The PA polymer is more rigid than PDMS and polyethylene glycol (PEG), so absorption and desorption from the coating is slightly slower. The PEG, or Carbowax (CW), is the most polar coating currently available. This extraction phase tends to be more selective toward polar analytes. Also, it extracts smaller amounts of nonpolar analytes compared to nonpolar fiber coatings.

In addition to the liquid polymer coatings mentioned above, a limited number of mixed-phase coatings (adsorbent particles suspensions) are commercially available, in which PDMS usually serves as an adhesive to suspend and retain the adsorbent particles. The extraction capability of these solid coatings is largely determined by the degree of surface porosity and the average diameter of the pores of suspended particles²⁰³. The amount of porosity is measured as the pores volume per gram of adsorbent in mL/g. In terms of openings diameter, pores can be divided in three categories of macro, meso and micro. Macropores have openings with diameters larger than 50 nanometers (nm). The openings diameters of mesopores and micropores are in the ranges of 2-50 nm and 0.2-2 nm, respectively. The average size of the micropores diameters is important in determining the strength of an adsorbent. If the micropore volume is high, and the average diameter is small, the length of the micropores will be larger and the adsorbent has a high amount of microporosity. Two adsorbents commonly used for the preparation

of mixed-phase SPME fibers are a porous divinylbenzene (DVB) polymer, and a carbon molecular sieve, Carboxen 1006 (CAR). As shown in Table 1.2²⁰³, the porous DVB has a high degree of mesoporosity along with medium degree of macroporosity and some level microporosity. Because of this pore size distribution, the mixed-phase DVB coating (PDMS/DVB) is primarily used for extraction of semi-volatile and larger volatile analytes. In addition, a porosimetry study has shown that the micropores of the DVB material are fairly uniform²⁰³ resulting in possible competition and displacement effect among analytes.

Table 1.2 Physical characteristics of common adsorbents used in SPME fibers

| Material | Surface area (m ² /g) | Porosity (mL/g) | | | Average micropore | |
|----------------|-------------------------------------|----------------------|---------------------|-----------------------|-------------------|----------|
| | | Macropore > 50 nm | Mesopore 2-50 nm | Micropore 0.2-2 nm | Total | Diameter |
| Divinylbenzene | 750 | 0.58 | 0.85 | 0.11 | 1.54 | 1.6 |
| Carboxen 1006 | 950 | 0.23 | 0.26 | 0.29 | 0.78 | 1.2 |

Carboxen 1006 has a fairly even distribution of macro, meso and micro pores. The average diameter of micropores in this material is smaller compared to that of DVB. The micropores are narrow enough to retain analytes in the C3 range²⁰³. Because of the micropores size, Carboxen 1006 is an ideal adsorbent for extraction of volatile and small analytes. Additionally, the pores are not sealed in the material but pass entirely through the particle. As shown in Fig. 1.8, the pores taper down as they approach the center of the particle and then expand up as they approach the perimeter. The tapered pore structure allows analytes to be desorbed more efficiently by gas flow than with sealed pore structure, which is common with charcoals and other porous carbon materials. Because the pores are tapered, larger analytes can also be retained in the larger portion of the pores. However, the size of analytes that can be extracted and desorbed using Carboxen 1006 is limited. Large planar molecules exhibit strong interaction with the Carboxen 1006 surface. As a result, thermal desorption of these analytes from CAR/PDMS fiber is

very slow. To maximize the desorption efficiency, it is best to use a minimum temperature of 280 °C, which can be increased up to 320 °C without damaging the coating.

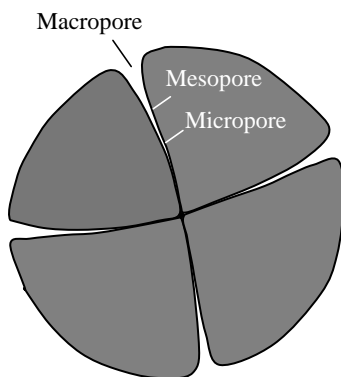


Figure 1.8 Schematic drawing of a tapered pore in a Carboxen 1006 particle²⁰³.

To take the advantage of both DVB and Carboxen 1006 adsorbents, a three-component fiber (DVB/CAR/PDMS) has been developed²⁰³. This fiber coating is composed of a layer of DVB/PDMS (55 μm) over a layer of Carboxen 1006/PDMS (30 μm). Because the coatings are layered, the larger analytes migrate slowly through DVB/PDMS layer and are retained in the meso and marco pores of DVB particles (or migrate very slightly into the Carboxen layer). The smaller analytes, on the other hand, penetrate faster and deeper into the Carboxen layer and are trapped in its micro pores. There is a reduction in the amount of analyte retained compared to the thicker single adsorbent. Still, with the two adsorbent beds, the DVB/CAR/PDMS fiber enables extraction of wider range of analytes from complex samples at low concentration levels.

In addition to commercial fibers, custom-made coatings can be developed to achieve more selectivity and higher sensitivity of SPME for specific analytes or applications. With the many possibilities of adsorbents, custom-made approach provides access to a wide range of SPME solid coatings. Nevertheless, one must consider not only the size and polarity of analytes when selecting a coating for SPME application, but also the concentration range and the detection limits that are intended for analysis. There is no need to use an adsorbent type fiber for extraction of analytes at high concentration levels,

nor when an absorbent type can provide the required sensitivity. However, if trace detection limits are intended, the adsorbent type fibers can be employed.

One last thing to consider is the lower precision encountered by fiber-to-fiber variation. SPME fiber manufacturing has improved over the years to afford fibers with almost identical properties, but even so, the highest reproducibility is obtained when all calibrations and measurements are performed continuously with the same fiber.

1.3.2.2.2 Analyte derivatization

Derivatization is used to transform an analyte into a compound with different physical and chemical properties such as volatility, polarity, solubility, etc. This is employed for the analysis of nonvolatile, highly polar and ionic species, which are hard to extract or less amenable to gas chromatographic separation. If performed before and/or during extraction, the derivatization step can enhance the extraction efficiency and the method sensitivity. Post-extraction approach, on the other hand, only improves chromatographic behavior and detection only. The incorporation of the derivatization step often complicates the SPME method and can introduce additional sources of interferences and errors. Therefore, it should only be considered when necessary.

1.3.2.2.3 Extraction mode

Among the three modes offered by SPME, the DI and HS modes are extensively used for water analysis. As mentioned earlier, DI-SPME is often used for simpler sample matrices, whereas HS-SPME is preferentially used for the extraction of analytes from complex and dirty samples as it serves to protect the fiber coating from damage by high molecular mass and other nonvolatile interferences present in the sample matrix. HS-SPME also offers a faster sampling and shorter equilibration times for highly volatile compounds compared to less volatile ones, owing to the higher concentration of these analyte in the headspace and higher diffusion coefficients in gaseous phase as compared with the aqueous phase.

1.3.2.2.4 Sample and headspace volumes

SPME method sensitivity is directly proportional to the amount of the analyte extracted from a sample. The amount extracted increases as the sample volume increases up to a point, beyond that it becomes steady and independent of the sample volume¹⁹⁰. For two-phase systems, this is the point where the fiber capacity ($K_{fs}V_f$) becomes significantly smaller than the volume of the sample (V_s), due to either a very low coating-sample partition coefficient or a very large sample volume (Equations 1.4 and 1.5). In field applications, the sample volume is usually significantly larger than the fiber capacity. However, in laboratory experiments, it is often limited by the size of vials employed or autosampler characteristics. Therefore, its effect on method sensitivity, quantification and precision of results should not be neglected, particularly for compounds with high K_{fs} values. If we assume that the effect of sample volume is negligible when it is large enough that the amount extracted is equal or smaller than 1% of the initial amount of the analyte in the sample, then the condition for the method sensitivity and precision to be independent of sample volume is :

$$C_f^\infty V_f \leq 0.01 C_0 V_s \quad (1.20)$$

The Equation 1.20 can be rearranged to yield¹⁹⁰:

$$100 \frac{C_f^\infty}{C_0} V_f \leq V_s \cong 100 K_{fs} V_f \leq V_s, \quad (C_0 \cong C_s^\infty) \quad (1.21)$$

For a 100 μm fiber coating, whose volume is approximately 0.65 μL , Equation 1.21 can be written as:

$$V_s \geq 0.065 K_{fs} [\text{mL}] \quad (1.22)$$

It follows from Equation 1.22 that even for analytes whose K_{fs} values are as low as 100, the minimum sample volume extracted by a 100 μm thick coating should be 6.5 mL if the effect of sample volume on the amount extracted or the sensitivity is to be neglected. Similarly, if the condition is set for the sample volume to be infinitely large when the amount extracted is equal or lower than 5% of the initial amount of the analyte in the sample, then the condition can be expressed as Equation 1.23:

$$20 K_{fs} V_f \leq V_s \quad (1.23)$$

This means that for K_{fs} up to 150 and 100 μm fiber coating, 2 mL sample volume is sufficient to give maximum sensitivity and best precision. With this assumption, the limiting sample volume is 12.9 mL for $K=1000$ or 1.29 L for $K=100000$. Generally, the higher the K_{fs} of the target analyte, the more pronounced is the effect of sample volume. It is also possible to calculate the sample volume from which 50% of the initial amount of the analyte is extracted at equilibrium, i.e. $n^\infty = C_f^\infty V_f = 0.5 C_0 V_s$. For this case, Equation 1.4 can be written as:

$$0.5 C_0 V_s = \frac{K_{fs} V_f V_s}{K_{fs} V_f + V_s} C_0 \quad (1.24)$$

in which $C_0 V_s$ can be cancelled out from the sides of the equation and with a few arrangements, the final expression can be written as:

$$V_s^{50\%} = K_{fs} V_f \quad (1.25)$$

It follows from Equation 1.25 that when 10 mL samples are analyzed with 100 μm fiber coatings ($\sim 0.65 \mu\text{l}$), 50% of the initial amount of the analyte will be extracted at equilibrium when the K_{fs} value is ~ 15500 . For higher K_{fs} values, the percentage of the extracted amount will be higher.

For three-phase systems containing headspace, similar reasoning can be employed to calculate the minimum sample volume necessary for the amount extracted by the fiber to be insignificant compared with the amount remaining in the sample after extraction. Again, it can be assumed that the condition is fulfilled when the amount extracted is equal or smaller than 1% of the initial amount of the analyte in the sample i.e., $C_f^\infty V_f \leq 0.01 C_0 V_s$. However, in this case, the assumption that $C_0 \cong C_s^\infty$ cannot be justified, because even if the amount extracted by the fiber constitutes only 1% of the initial amount of the analyte, a significant portion of the analyte might be present in the headspace. Therefore, Equation 1.9 can be used to calculate the criterion:

$$C_f^\infty V_f = \frac{K_{fs} V_f V_s C_0}{K_{fs} V_f + K_{hs} V_h + V_s} \leq 0.01 C_0 V_s \quad (1.26)$$

Then, rearrangements of Equation 1.26 will yield the final criterion:

$$V_s \geq \frac{99 K_{fs} V_f}{1 + a K_{hs}} \quad , \quad (a = \frac{V_h}{V_s}) \quad (1.27)$$

Compared with Equation 1.21, the major difference is the additional term, aK_{hs} , in the denominator of Equation 1.27. For non-zero headspace volumes this term is always greater than zero, which means that the sample volume fulfilling the condition is smaller in three-phase systems than in two-phase systems. This can be attributed to the lower equilibrated amount of analyte in the sample after extraction, due to presence of headspace, which ultimately determines the extract amount of analyte at equilibrium. As described earlier, this amount is lower in three-phase systems than in two-phase systems, Since the analyte is distributed between all three phases involved (aqueous sample, headspace and fibre coating). As a consequence, the equilibrated amount of analyte in the sample can only be lower than, or equal to, that of the case for two-phase (DI- SPME). By using Equation 1.9 and a similar procedure presented for two-phase systems, the sample volume from which 50% of the analyte is extracted at equilibrium by the SPME fiber can be determined for systems including headspace. The final criterion in this case is given by:

$$V_s^{50\%} = \frac{K_{fs} V_f}{1 + a K_{hs}} \quad , \quad (a = \frac{V_h}{V_s}) \quad (1.28)$$

Equation 1.28 indicates that the sample volume from which 50% of the initial amount of the analyte is extracted at equilibrium by the SPME fiber decreases as the headspace–sample partition coefficient, K_{hs} , or the headspace–to–sample volume ratio, a , increases.

1.3.2.2.5 Matrix conditions

Optimization of matrix conditions such as temperature, pH and ionic strength may improve method performance, depending on analytes. Elevated extraction temperatures

in headspace approach can reduce the extraction time and make the whole procedure faster by increasing the analytes diffusion coefficients and/or headspace capacity. This is helpful for extraction of semi-volatile analytes with low gas-sample distribution constants. However, increasing the extraction temperature will also lower the fiber coating-headspace distribution constant which negatively affects method sensitivity. Therefore, increasing temperature may be done up to a level, as far as the reduced sensitivity can be tolerated.

Since only neutral species are extracted in SPME, pH adjustment can improve method sensitivity for compounds that are prone to dissociation in water. It is clear that low pH values are in favor of acidic compounds and high pH ranges suitable for extraction of basic compounds. Extreme pH values are not recommended for direct immersion sampling and the adjustment is often practiced for HS approach because direct contact of the fiber coating with very low or very high pH levels can damage the fiber coating.

The addition of a soluble salt into the sample increases the ionic strength of the sample solution. Except for highly polar compounds, the aqueous solubility of analytes usually decreases when salt is added to the sample. With the decreased aqueous solubility, the fiber coating-sample distribution constant, K_{fs} , increases and consequently, method sensitivity is improved. The salts commonly used to increase the extraction efficiency are NaCl, Na₂SO₄, K₂CO₃ and NH₂SO₄¹⁸². In some cases, the addition of salts may decrease the amount of analyte extracted. This depends on the nature of target analyte and the salt concentration. Therefore, when salt addition is of interest, its actual effect on the extraction efficiency for a particular analyte should be determined experimentally. The addition of salts is often performed for HS-SPME, which avoids fiber damaging by salts solutions through sampling depth adjustment in vials. If salt effect is employed during DI-SPME, an additional washing step of fiber in deionized water should be done before its injection in GC systems.

1.3.2.2.6 Agitation method

To ensure fast mass transport and rapid extraction of analytes from sample matrix

some level of agitation is required for SPME. This can be done with flow-through stirring, magnetic stirring, fiber movement or sonication. The choice of agitation method depends on the availability of equipments, number of samples and nature of analysis. Flow-through technique offers efficient agitation, especially at rapid sample flow rates, but requires additional care and facilities to ensure constant sample flow rate and avoidance of cross-contamination. Magnetic stirring is simple and doesn't need expensive equipments. However, a stir-bar needs to be inserted in the sample vessel, which can introduce unwanted contamination and interferences to the sample. Where small sample volumes are to be analyzed and an autosampler is available, fiber movement is the preferred agitation method over magnetic stirring, especially for trace analysis. Sonication is an efficient agitation technique but additional care must be exercised to prevent increase of sample temperature which can cause precision issues. It should be noted that when pre-equilibrium extraction is used, the agitation conditions should be kept constant for all test samples and standard solutions.

1.3.2.2.7 Extraction time

In most applications, the sample extraction is the time-limiting step of the SPME procedure, often more time demanding than sample pre-incubation, desorption step or fiber conditioning. Therefore, optimization of extraction time is important in terms of speed of analysis. In principle, the objective of SPME experiments is to achieve equilibrium conditions in the system. This provides maximum method sensitivity and high precision with minimal relative errors, as discussed in the earlier sections. Usually, an extraction time profile curve is constructed for the analyte by preparing a set of vials containing similar standard solutions and then extracting them for progressively longer period of time. The curve obtained will show the optimum extraction time for equilibration conditions. Pre-equilibrium approach with shorter extraction times may also be selected in the case of long equilibration time. Nevertheless, both equilibrium and pre-equilibrium samplings need precise and repeatable timing. This is more critical for latter approach, in which the chosen extraction time is in the steep area of extraction time profile curve and a small error in timing may cause much higher relative error in analyte sorption, as compared with equilibrium extraction. In such cases, the use of an

autosampler can provide well-repeatable timing for extraction. In practice, pre-equilibrium methods are usually optimized so that extraction and analysis times are similar. This way, by using an autosampler the procedure is continuous, with the analysis occurring concurrently with the extraction of next sample thus enhancing sample throughput.

1.3.2.2.8 Desorption conditions

Unlike the liquid injection, the SPME fiber is not removed immediately after injection into GC systems and is left in the injector for a few minutes to allow complete thermal desorption of the analytes. The length of desorption time, i.e. the time duration over which the fiber is exposed to the injector hot zone, depends on the volatility of analytes, coating thickness, the injector temperature and the flow rate of the carrier gas, defined by the geometry of the injector or the glass liner. Longer desorption times are required for less volatile analytes and thicker coatings. The injector temperature can shift the gas-coating distribution coefficient of the analyte in favor of the gaseous phase. Consequently, the higher the temperature, the faster is the desorption process. However, high temperatures can also cause increased fibre background levels, acceleration of coating deterioration and potential degradation of less thermally stable analytes. The GC injector design can also affect the desorption process. The flow rate of the carrier gas along the fiber is largely determined by the inner diameter (ID) of the glass liner. This flow rate should be as high as possible for efficient desorption, therefore the ID of the liner should be the smallest possible, typically 0.75 mm, which is ideal for SPME. In addition to the ID of the glass insert, non-uniformity of temperature distribution in the injector may affect the fiber desorption. Therefore, it is important to position the fiber in the injector in a way that it is subjected to nominal injector temperature. Lower temperature may cause unnecessarily slow desorption, while excessively high temperature may damage the coating.

1.3.2.3 Stir-bar sorptive configuration

Fiber geometry is the most commonly used form of SPME, owing to its small size and ease of application. Another configuration which is more recent and offers increased

extraction ability is stir-bar sorptive extraction (SBSE)²⁰⁴. SBSE uses a thick film of PDMS on a glass-coated magnetic stirring bar for microextraction from aqueous samples. The sample is simply stirred with the coated bar, commercially known as Twister, for a pre-determined extraction time. Afterwards, the stir-bar is removed and dried with a soft tissue, and then analytes are either desorbed thermally in a GC system or back extracted with an organic solvent for large-volume GC injections or LC application. The twisters are available in 10 and 20 mm length, 0.5 and 1 mm phase thickness, corresponding to phase volumes ranging from 25 to 125 μL , approximately. The thin glass coating that covers the stirring bar is essential in the twister construction in that it effectively prevents thermal decomposition of the PDMS layer, catalyzed by the metal of magnetic bar. Where the commercial twisters are not available, a custom-made version can be made by inserting a small stir bar into a short length of PDMS tubing.

The theoretical aspects of SBSE are the same as SPME. However, compared to the fiber geometry the extraction time is longer for SBSE, typically 30 minutes to several hours, owing to the greater amount of coating. As well, the desorption process is slower in this case, likewise due to the greater amount of coating. Typical desorption times are around 10 min, which means that the desorbed analytes must be reconcentrated before the GC separation. This can be achieved using an interface with a programmed temperature vaporizer (PTV) and cryogenic cooling. The commercial twister thermal desorption unit (TDU) interface enables temperatures as low as $-150\text{ }^{\circ}\text{C}$ with liquid nitrogen cooled injection system (CIS) to trap volatile analytes²⁰⁵.

Compared with the fiber geometry, higher enrichment factors and sensitivities (~ 50 to 300 times more) can be achieved with SBSE. When combined with GC-MS systems, SBSE enables detection limits down to the low ng/L levels²⁰⁶. Additionally, quantitative recoveries may be achievable with SBSE owing to its high coating capacity. In this regard, the octanol–water distribution coefficient (K_{ow}) and the thickness of coating often serve as good indicators of how well, if at all, a given analyte can be quantitatively recovered from a specific sample volume with SPME or SBSE. For 100 μm PDMS fiber and a typical sample volume of 10 mL, quantitative recovery is only achievable for compounds with $\log K_{ow}$ values above 5. In the case of SBSE with 65 μL phase volume, quantitative recovery is possible for compounds with $\log K_{ow}$ values above 3²⁰⁶. Several

applications of SBSE to the analysis of pesticides, PAHs and volatiles in food, beverage and water samples have been reported²⁰⁶. Despite its high extraction capacity, the SBSE configuration is limited to few types of coating. The PA and PEG/PDMS twisters have recently become available for application with polar analytes²⁰⁷, yet mixed-phase coating options with solid particles are not available in SBSE configuration, perhaps due to the problem of friction and less physical stability during stirring. Further, the extraction is often performed off-line and the stir bar must be manually transferred from the sample vial to the GC liner tray, which prevents a fully automated procedure.

1.3.2.4 Thin film membrane configuration

Another SPME configuration with increased extraction ability is a thin layer of PDMS membrane²⁰⁸, which is sometimes referred to as thin film microextraction (TFME). The thin film membrane (TFM) is simply cut into a house-like or rectangular shape with a typical size of 2 cm × 3 cm and then mounted onto a stainless steel wire for support. After conditioning, the TFM can be used for both active and passive sampling, especially for field applications²⁰⁹. Similar to SBSE, the TFM configuration allows high extraction capacity when compared with PDMS fiber geometry. However, unlike SBSE thick coatings, the TFM exhibits higher extraction rates owing to the larger surface-to-volume ratio of PDMS extraction phase²¹⁰, as illustrated by Equation 1.29:

$$\frac{dn}{dt} = \frac{D_s A}{\delta} C_s \quad (1.29)$$

where dn/dt is the initial rate of extraction, D_s is the analyte diffusion coefficient in the sample fluid, A is the surface area of the extraction phase, C_s is the analyte concentration in the sample and δ is the boundary layer thickness. Equation 1.29 indicates that the initial rate of SPME extraction is proportional to the surface area of the extraction phase. Additionally, as shown by Equation 1.15, extraction phases of thinner thicknesses provide shorter equilibration times. Therefore, the thin film approach facilitates higher extraction efficiency and sensitivity without sacrificing the overall analysis time. Although the TFM requires relatively shorter desorption times compared to SBSE, the thermal desorption of analytes from the thin film device still needs several minutes to

complete. As a result, the desorbed analytes must be cryofocused before the GC separation. This can be achieved with the same interface (TDU-CIS) used for SBSE. After extraction for a pre-determined time under adequate agitation, the TF is dried with a soft tissue and simply rolled into a TDU liner with the attached wire for subsequent thermal desorption, cryogenic reconcentration and GC analysis. The TFM approach has been successfully applied for determination of PAHs in water samples²¹⁰. The drawbacks of the TFM technique are increased complexity of introduction and desorption in the analytical instrument, lack of full automation and limitation of commercial membranes to only PDMS material, which restricts wider application of the technique.

1.3.4.2.1 Methods for thin film preparation

Polymer thin film membranes can be prepared by different techniques, The most commonly used methods are spray coating, dip coating and spin coating. In spray coating, a stream of liquid polymer dissolved in solvent is dispersed over a substrate using a small nozzle or spray gun. The nozzle or the spray tip converts the flow of polymer solution into fine tiny droplets or aerosols toward the substrate. The quality of coating and its thickness on the substrate is controlled by the nozzle design, spray rate and the polymer viscosity. Solid particles can be suspended in the polymer solution before spray process to produce composite or mixed-phase thin layer coatings. After solvent evaporation and curing, the polymer thin film is prepared. Spray process reduces the amount of time required to coat per unit surface and is cost effective, particularly for large scale thin film production. However, highly uniform thin film preparation by spray process may be difficult to achieve. Coating can also be applied onto flat or cylindrical substrates by dipping procedure. The substrate is immersed in the solution of the coating material at a constant speed and remained inside the solution for a while. A thin layer of coating deposits itself on the substrate while it is pulled up. The solvent is allowed to evaporate from the coating before curing step. For volatile solvents, evaporation starts already during the deposition and drainage steps. The withdrawing of substrate should be carried out at a controlled speed to avoid any jitters on the coating. The thickness of the coating is primarily controlled by viscosity of coating solution and the withdrawing speed. Coating thickness generally increases with faster withdrawal speed. A faster

withdrawal pulls more fluid up onto the surface of the substrate before it has time to flow back down into the solution. The applied coating may be cured by a variety of means including conventional thermal, UV, or IR techniques depending on the coating solution formulation. Once a layer is cured, another layer may be applied on top of it with another dip-coating and curing process. In this way, a multi-layer coating can be constructed. While dip coating is a popular way of creating thin films for research purposes, it requires precise control of the procedure.

Spin coating is another method for producing thin film coatings. In this case, the coating solution is deposited onto a flat substrate already mounted horizontally on a rotating platform. The substrate then spins very rapidly and the coating solution is dispersed onto it. The high-speed rotation throws off most of the solution, leaving behind a thin, uniform coating. The coating thickness is precisely controlled by the rotation speed and its duration. Faster rotations result in thinner coating layers. Advantages of spin coating include fast process time (a few seconds to a minute per coating) and high uniformity over the substrate surface. A major limitation, however, is the lack of material efficiency. A substantial excess of coating solution need to be applied compared to the amount that is required. Typically, less than 50 % of the material loaded onto the substrate is utilized, while the remaining spins off the substrate edge during the procedure and is disposed. Another limitation is that no lateral resolution is possible. Also, as substrate size gets larger the throughput of the spin coating process decreases. Large substrates cannot be spun at a sufficiently high rate in order to allow the film to thin and dry in a timely manner, resulting in decreased throughput. In applications where either spinning or dipping can be used, it may be preferential to use spin coating in low volume operations and dip coating in high volume operations.

1.3.4.2.2 Spin coating

Spin coating is a batch process consisting in transient flow of a thick layer of viscous fluid on a rotating disk, of which the final result is a uniform thin film of the fluid. The process can be divided into four basic stages that are (1) deposition of coating fluid, often containing an organic solvent, on a substrate, (2) spin up, (3) spin off, and (4) evaporation and film casting, as shown in Fig. 1.9. The deposition process involves loading an

excessive amount of the coating fluid onto the center of a stationary or slowly spinning flat substrate such as a silicon wafer disk. The fluid deposition can be done either manually or by a robotic arm. An excessive amount of the fluid and a proper solvent, if any, should be used to prevent premature discontinuation of coating process caused by the fluid front drying prior to reaching the wafer edge. The adequate volume can range from 1 to 10 mL depending on the viscosity of the fluid and the size of the wafer to be coated. Higher viscous fluids and larger wafers require a larger amount of fluid to ensure full coverage of the wafer during the high speed spin step. The deposition process may be done dynamically while the wafer is spinning at low speed. This usually results in lower amounts of coating material wasted from the wafer since it is not necessary to load as much fluid on the wafer as is used in a static approach. Also, it is beneficial when the fluid or the wafer itself has poor wetting abilities.

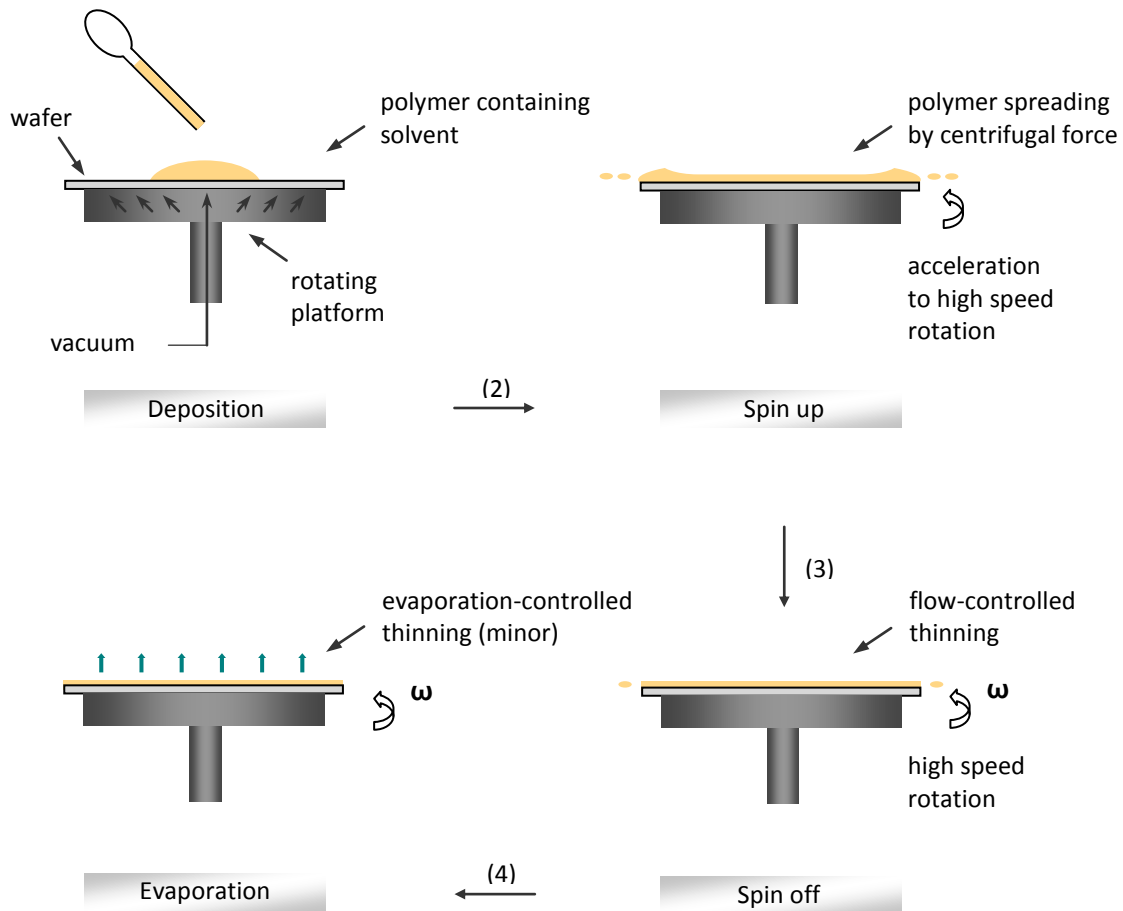


Figure 1.9 Schematic representation of stages in spin coating process.

The spin up is the stage in which the wafer is accelerated to a high rotation speed in order to spread the coating fluid over the entire wafer and make it thinner near its final desired thickness. Once the wafer is accelerated to its final spin speed a radial wave front forms and flows away to the wafer edge by centrifugal force, leaving a fairly uniform thin layer of coating behind that tends to become even more uniform as it thins further. Typical final high spin speeds range from 1000 to 6000 revolutions per minute (rpm), depending on the properties of the fluid and the size of wafer.

The spin off stage is characterized by constant high speed rotation and gradual thinning of the fluid by the radial flow. The excess amount of the fluid flies off the edge of rotating disk as small droplets. The film thinning continues further until a point that the radial force can no longer appreciably move the fluid over the surface. At this point, the film thickness will not decrease significantly with increased spin time and solvent evaporation dominates a minor fluid thinning behavior which helps with film casting and stabilizing on the wafer. Solvent evaporation occurs throughout the spin coating process. The transition point between the spin off and the evaporation stages is the point where the thinning rate due to evaporation becomes the same as the thinning rate due to centrifugal force.

The prepared thin film may still remain wet for several minutes until the residual solvent evaporates. The solvent removal can be aided by a separate drying step at lower spin speeds, following the high speed main procedure. This will increase the physical stability of the film, particularly thicker ones, before handling. Typically, a moderate spin speed of about 25% of the high speed stage will generally suffice to aid in drying the film without significantly changing the film thickness²¹¹. The final film thickness by spin coating process is determined by spin parameters (speed and duration) and physical properties of the fluid, including viscosity, density and nature of solvent.

A number of modelings have been developed for spin coating process²¹²⁻²¹³. When film thinning is only due to radial out-flow and effect of solvent evaporation is negligible, mathematical description of film thickness on a spinning disk of hypothetically, infinitely large can be described as Equations 1.30 and 1.31²¹²:

$$-\frac{dh}{dt} = \frac{2\rho\omega^2 h^3}{3\mu} \quad (1.30)$$

$$h = h_0(1 + 4K h_0^2 t)^{-1/2}, \quad K = \frac{\rho\omega^2}{3\mu} \quad (1.31)$$

where h is film thickness, t is spinning time, h_0 is initial film thickness ($t = 0$), ω is spin speed, ρ and μ are the fluid density and viscosity, respectively. Equations 1.30 and 1.31 show the film thickness decreases as the spin speed, spin time and the fluid density increase, and as the fluid viscosity decreases. Equation 1.31 corresponds to deposition of a perfectly uniform fluid with equal thickness distribution of $h = h_0$ on the substrate. According to the equation, if the initial distribution of fluid is uniform before spin process, it will remain so, as the thickness of fluid film is decreased by centrifugal force. This implies that ultimate uniformity in thin films is assured if the initial fluid distribution, before spinning, can somehow be made uniformly. Irregular fluid distributions of non-uniform depositions also tend toward uniformity under centrifugation and become increasingly more uniform as spinning continues²¹². Equation 1.31 also shows that the fluid layer thickness decreases by a factor $1/\sqrt{2}$ in a time, $t = 1/4Kh_0^2$, which indicates that thick layer depositions (higher h_0) thin out more rapidly than thin ones.

When the effect of solvent evaporation is significant, the modeling of spin coating process becomes complex due to coupling of radial flow and solvent evaporation. A simple mathematical expression of this situation with constant solvent evaporation has been driven with the assumption that fluid flow and solvent evaporation are independent parameters²¹³, as described by Equation 1.32:

$$h_w = \left[\left(\frac{3\mu_0}{2\rho\omega^2} \right) k(\chi_l^0 - \chi_l^\infty) \right]^{1/3} \quad (1.32)$$

where h_w is a wet film thickness, μ_0 is initial fluid viscosity, k is the mass transfer coefficient, χ_l^0 is the initial solvent mass fraction in the coating solution, and χ_l^∞ is the solvent mass fraction that would be in equilibrium with the solvent mass fraction in the

gas phase. Since further film thinning is due only to evaporation, the final film thickness, h_f , can be expressed as:

$$h_f = (1 - \chi_l^0) h_w \quad (1.33)$$

This model has been shown to predict film thickness values within 10% of the experimental results for thicknesses up to around $30 \mu\text{m}$ ²¹³. A more detailed modeling of spin coating requires mathematical treatment of the effects of solvent evaporation on the fluid flow and vice versa. However, this approach involves complex numerical methods and often includes parameters which are difficult to estimate²¹³.

It is evident from the discussions and models presented above that the major parameters that control film thickness and reproducibility of spin coating are spin speed, fluid viscosity and spin time. Among these, spin speed has a higher impact on film thickness and precision. Typically, variations of ± 50 rpm at high spin speed stage can result in thickness change of 10%. The range of film thicknesses that can be easily achieved by spin coating is $1\text{--}200 \mu\text{m}$ ²¹¹. For thicker films, high viscosity, low spin speed, and a short spin time may be used, but these can adversely affect the uniformity of the film coating. Multiple coating is usually a preferred choice for making thicker thin films. The viscosity can be reduced by addition of an organic solvent. However, the effect of evaporation rate should not be neglected during the spin process. The evaporation rate depends on the volatility of the solvent used as well as the space surrounding the substrate during the spin process. If significant evaporation happens prematurely during the procedure, non-uniformities appear on the film surface resulting in coating defects. It is important that the air flow and turbulence above the substrate be minimized, or at least held constant, during the spin process. Modern commercial spin coating machines, or spin coaters, employ a closed bowl design to ensure quality and uniformity of thin films. The closed chamber design not only prevents undesired air flow and turbulence above the substrate, but also slows down solvent evaporation rate which results in increased thin film uniformity. Spin coating within a close chamber also provides a dust-free atmosphere for clean thin film preparation.

1.4 Research objectives

The ultimate purpose of the analytical methods for DBPs studies is to support the relevant toxicology studies and drinking water regulations, and to monitor the DBPs concentrations in water treatment plants and distribution systems to ensure that they comply with the regulated levels. On the other hand, the current DBPs health-effects assessments and regulations are pushing the sample preparation techniques to new levels of sophistication and sensitivity at part-per-trillion levels monitoring. Moreover, the trend of implementing green analytical chemistry favors the use of “solvent-free” sample preparation methods. SPME complies with the solvent-free requirement and affords the promise for rapid cost-effective sample handling along with good sensitivity and automation capability for drinking water analysis. With these in mind, the present thesis aimed at evaluating SPME of DBPs in several aspects. Firstly, optimization of the fiber technique for selected priority DBPs to allow successful application of the technique for the selected analytes. Secondly, development and construction of novel thin film samplers with mixed-phase (particle-loaded) coatings to allow lower detection ability for the challenging DBPs such as N-nitrosamines that are hard to extract from water due to their hydrophilicity and polarity. Thirdly, demonstration of the performance and accuracy of the fiber technique for selected DBPs with real-world drinking water samples analysis and comparing the results with those of the standard LLE technique currently employed by Health Canada laboratories.

1.5 References

1. Rook JJ. 1974. Formation of haloforms during chlorination of natural waters. *Water Treat. Exam.* 23: 234–243.
2. Bellar TA, Lichtenberg JJ, Kroner RC. 1974. Occurrence of organohalides in chlorinated drinking water. *J. Am. Water Works Assoc.* 66: 703–712.
3. Kopfler FC, Melton RG, Lingg RD, Coleman WE. 1976. GC/MS determination of volatiles for the national organics reconnaissance survey (NORS) of drinking water. in: *Identification and Analysis of Organic Pollutants in Water*, Ed. Keith LH, Ann Arbor Science, Ann Arbor, MI, pp. 87–104.
4. National Cancer Institute. 1976. Report on the carcinogenesis bioassay of chloroform. National Cancer Institute, TR-000 NTIS Rpt No. PB264018, Bethesda, MD.
5. Loper JC. 1980. Mutagenic effects of organic compounds in drinking water. *Mutat. Res.* 76: 241–268.
6. Christman RF, Johnson JD, Norwood DL, Liao WT, Hass JR, Pfaender FK, Webb MR, Bobenreith MJ. 1979. Chlorination of Aquatic Humic Substances; final report of USEPA project R-804430, US Environmental Protection Agency: Cincinnati, OH.
7. Richardson SD. 1998. Drinking water disinfection by-products. In: *Encyclopedia of environmental analysis and remediation* vol. 3, Ed. Meyers RA, Wiley, New York, 1398–1421.
8. Weisburger EK. 1977. Carcinogenicity studies on halogenated hydrocarbons. *Environ. Health Perspect.* 21: 7–16.

9. Bull RJ, Meier JR, Robinson M, Ringhand HP, Laurie RD, Stober JA. 1985. Evaluation of mutagenic and carcinogenic properties of brominated and chlorinated acetonitriles: byproducts of chlorination. *Fundam. Appl. Toxicol.* 5: 1065–1074.
10. Boorman GA, Dellarco V, Dunnick JK, Chapin RE, Hunter S, Hauchman F, Gardner H, Cox M, Sills RC. 1999. Drinking water disinfection byproducts: Review and approach to toxicity evaluation. *Environ. Health Perspect* 107: 207–217.
11. Muellner MG, Wagner ED, Mccalla K, Richardson SD, Woo YT, Plewa MJ. 2007. Haloacetonitriles vs. regulated haloacetic acids: Are nitrogen-containing DBPs more toxic. *Environ. Sci. Technol.* 41: 645–651.
12. US EPA. 2009. Information Collection Rule: Disinfection byproduct health effects. Available on-line at:
http://www.epa.gov/enviro/html/icr/dbp_health.html [accessed: 15 October 2011].
13. Krasner SW, Weinberg HS, Richardson SD, Pastor SJ, Chinn R, Scilimenti MJ, Onstad GD, Thruston Jr AD. 2006. Occurrence of a new generation of disinfection byproducts. *Environ. Sci. Technol.* 40: 7175–7185.
14. Richardson SD, Plewa MJ, Elizabeth D, Wagner ED, Schoeny R, DeMarini DM. 2007. Occurrence, genotoxicity, and carcinogenicity of regulated and emerging disinfection by-products in drinking water: A review and roadmap for research, *Mutation Research* 636: 178–242.
15. US EPA. 2006. National Primary Drinking Water Regulations: Stage 2 Disinfectants and Disinfection Byproducts Rule; Final Rule, 2006. Available on-line at:
<http://www.epa.gov/fedrgstr/EPA-WATER/2006/January/Day-04/w03.pdf>
[accessed: 15 October 2011].

16. Yang X, Shang C, Westerhoff P. 2007. Factors affecting formation of haloacetonitriles, haloketones, chloropicrin and cyanogen halides during chloramination. *Water Research* 41: 1193–1200.
17. Zwiener C, Richardson SD. 2005. Analysis of disinfection by-products in drinking water by LC–MS and related MS techniques. *Trends Anal. Chem.* 24 (7): 613–621.
18. Lebel GL, Williams DT. 1995. Differences in chloroform levels from drinking water samples analyzed using various sampling and analytical techniques. *Intern. J. Environ. Anal. Chem.* 60: 213–220.
19. Weinberg HC. 2009. Modern approaches to the analysis of disinfection by-products in drinking water. *Phil. Trans. R. Soc. A* 367: 4097–4118.
20. Cavanagh JE, Weinberg HS, Gold A, Sangaiah R, Marbury D, Glaze WH. 1992. Ozonation by-products: identification of bromohydrins from the ozonation of natural waters with enhanced bromide levels. *Environ. Sci. Technol.* 26: 1658–1682.
21. Hong Y, Liu S, Song H, Karanfil T. 2007. HAA formation during chloramination: Significance of monochloramine's direct reaction with DOM. *J. AWWA* 99: 57–69.
22. Krasner SW, Pastor S, Chinn R, Scilimenti MJ, Weinberg HS, Richardson SD, Thruston Jr AD. 2001. The occurrence of a new generation of DBPs (beyond the ICR). *Proc. AWWA Water Quality Technology Conf.*, Denver.
23. Chinn R, Lee T, Krasner SW, Dale M, Richardson SD, Pressman J, Speth T, Miltner R, Simmons JE. 2007. Solid-phase extraction of 35 DBPs with analysis by GC/ECD and GC/MS. *Proc. AWWA Water Quality Technology Conf.* Denver.

24. Koudjonou B, Lebel, GL. 2003. Application of a consolidated method (LLE-GC/ECD) for the determination of halogenated acetaldehydes (HA) in Canadian drinking water. *Proc. Water Quality Technology Conference*, 2169–2184.
25. Brophy KS, Weinberg HS, Singer PC. 1999. Quantification of nine halogenated acetic acids in drinking water using gas chromatography with electron capture detection. *Book of Abstracts, 217th ACS National Meeting*, Anaheim, California.
26. Karsten L. 2002. Sample preparation for water analysis. In: *Comprehensive Analytical Chemistry*, vol. xxxvii, *Sampling and sample preparation for field and laboratory*, Ed. Pawliszyn J., Elsevier, Netherlands, 721–778.
27. Kolb B. 1999. Headspace sampling with capillary columns. *J. Chromatogr. A* 842: 163–205.
28. Koester CJ. 2005. Trends in environmental analysis. *Anal. Chem.* 77: 3737–3754.
29. Richardson SD. 2010. Environmental mass spectrometry: Emerging contaminants and current issues. *Anal. Chem.* 82: 4742–4774.
30. Thurman EM, Mills MS. 1998. *Solid-phase extraction: Principles and practice*. Wiley, New York, p. 384.
31. Fritz JS. 1999. *Analytical solid-phase extraction*. Wiley, New York.
32. Jonsson JA, Mathiasson L. 2000. Membrane-based techniques for sample enrichment. *J. Chromatogr. A* 902: 205–225.
33. Hyoetylaeinen T, Riekkola ML. 2008. Sorbent- and liquid-phase microextraction techniques and membrane-assisted extraction in combination with gas chromatographic analysis: A review. *Anal. Chim. Acta* 614: 27–37.

34. Liu H, Dasgupta PK. 1996. Analytical chemistry in a drop: solvent extraction in a microdrop. *Anal. Chem.* 68: 1817–1821.
35. Jeannot MA, Cantwell FF. 1996. Solvent microextraction into a single drop. *Anal. Chem.* 68: 2236–2240.
36. Jeannot MA, Cantwell FF. 1997. Mass transfer characteristics of solvent extraction into a single drop at the tip of a syringe needle. *Anal. Chem.* 69: 235–239.
37. Theis AL, Waldack AJ, Hansen SM, Jeannot MA. 2001. Headspace solvent microextraction. *Anal. Chem.* 73: 5651–5654.
38. Liu H, Dasgupta PK. 1996. Analytical chemistry in a drop. *Trends Anal. Chem.* 15: 468–475.
39. Ligor T, Buszewski B. 2000. Extraction of trace organic pollutants from aqueous samples by a single drop method. *Chromatographia* 51: 279–282.
40. Xia L, Li x, Wu Y, Hu B, Chen R. 2008. Ionic liquids based single drop microextraction combined with electrothermal vaporization inductively coupled plasma mass spectrometry for determination of Co, Hg and Pb in biological and environmental samples. *Spectrochimica Acta Part B* 63: 1290–1296.
41. Wang Q, Qiu H, Li J, Liu X, Jiang S. 2010. On-line coupling of ionic liquid-based single-drop microextraction with capillary electrophoresis for sensitive detection of phenols. *J. Chromatogr. A* 1217: 5434–5439.
42. Wu Y, Xia L, Chen R, Hu B. 2008. Headspace single drop microextraction combined with HPLC for the determination of trace polycyclic aromatic hydrocarbons in environmental samples. *Talanta* 74: 470–477.

43. Wu Y, Hu B, Hou Y. 2008. Headspace single drop and hollow fiber liquid phase microextractions for HPLC determination of phenols. *J. Sep. Sci.* 31: 3772–3781.
44. Sarafraz-Yazdi A, Amiri A. 2010. Liquid-phase microextraction. *Trends Anal. Chem.* 29: 1–14.
45. Anthemidis AN, Adam, ISI. 2009. Development of on-line single-drop microextraction sequential injection system for electrothermal atomic absorption spectrometric determination of trace metals. *Anal. Chim. Acta* 632: 216–220.
46. Batlle R, Lopez P, Nerin C, Crescenzi C. 2008. Active single-drop microextraction for the determination of gaseous diisocyanates. *J. Chromatogr. A* 1185: 155–160.
47. Choi K, Kim SJ, Jin YG, Jang YO, Kim JS, Chung DS. 2009. Single drop microextraction using commercial capillary electrophoresis instruments. *Anal. Chem.* 81: 225–230.
48. Aguilera-Herrador E, Lucena R, Cardenas S, Valcarcel M. 2010. The roles of ionic liquids in sorptive microextraction techniques. *Trends Anal. Chem.* 29: 602–616.
49. Ma M, Cantwell FF. 1999. Solvent microextraction with simultaneous back-extraction for sample cleanup and preconcentration: Preconcentration into a single microdrop. *Anal. Chem.* 71: 388–393.
50. Zhao L, Lee HK. 2001. Determination of phenols in water using liquid phase microextraction with back extraction combined with high-performance liquid chromatography. *J. Chromatogr. A* 931: 95–105.
51. Zhu L, Tay CB, Lee HK. 2002. Liquid–liquid–liquid microextraction of aromatic amines from water samples combined with high-performance liquid chromatography. *J. Chromatogr. A* 963: 231–237.

52. Lambropoulou DA, Konstantinou IK, Albanis TA. 2007. Recent developments in headspace microextraction techniques for the analysis of environmental contaminants in different matrices. *J. Chromatogr. A* 1152: 70–96.
53. Xu L, Basheer C, Lee HK. 2007. Developments in single-drop microextraction. *J. Chromatogr. A* 1152: 184–192.
54. Buszewski B, Ligor T. 2002. Single-drop extraction versus solid-phase microextraction for the analysis of VOCs in water. *LC GC Europe* 15: 92–97.
55. Saraji M, Bakhshi M. 2005. Determination of phenols in water samples by single-drop microextraction followed by in-syringe derivatization and gas chromatography–mass spectrometric detection. *J. Chromatogr. A* 1098: 30–36.
56. Psillakis E, Kalogerakis N. 2002. Developments in single-drop microextraction. *Trends Anal. Chem.* 21: 53–63.
57. Shariati-Feizabadi S, Yamini Y, Bahramifar N. 2003. Headspace solvent microextraction and gas chromatographic determination of some polycyclic aromatic hydrocarbons in water samples. *Anal. Chim. Acta* 489: 21–31.
58. Deng CH, Li N, Wang L, Zhang XM. 2006. Development of gas chromatography–mass spectrometry following headspace single-drop microextraction and simultaneous derivatization for fast determination of short-chain aliphatic amines in water samples. *J. Chromatogr. A* 1131: 45–50.
59. De Jager LS, Andrews ARJ. 1999. Solvent microextraction of chlorinated pesticides. *Chromatographia* 50: 733-738.
60. Lambropoulou DA, Albanis TA. 2007. Liquid-phase micro-extraction techniques in pesticide residue analysis. *J. Biochem. Biophys. Met.* 70:195–228.

61. Saraji M, Bidgoli AAH. 2009. Single-drop microextraction with in-microvial derivatization for the determination of haloacetic acids in water sample by gas chromatography–mass spectrometry. *J. Chromatogr. A* 1216: 1059–1066.
62. Montesinos I, Cardador MJ, Gallego M. 2011. Determination of halonitromethanes in treated water. *J. Chromatogr. A* 1218: 2497–2504.
63. Zhao RS, Lao WJ, Xu XB. 2004. Headspace liquid-phase microextraction of trihalomethanes in drinking water and their gas chromatographic determination. *Talanta* 62: 751–756.
64. Zhao RS, Wang XT, Wei AX, Xu XB. 2004. Determination of trihalomethanes in drinking water from Beijing, People’s Republic of China. *Bull. Environ. Contam. Toxicol.* 73: 111–116.
65. Tor A, Aydin ME. 2006. Application of liquid-phase microextraction to the analysis of trihalomethanes in water. *Anal. Chim. Acta* 575: 138–143.
66. Ouyang G, Zhao W, Pawliszyn J. 2005. Kinetic calibration for automated headspace liquid-phase microextraction. *Anal. Chem.* 77: 8122–8128.
67. Kokosa JM. 2007. Automation of liquid phase microextraction. United States Patent US 7,178,414 B1.
68. Psillakis E, Kalogerakis N. 2001. Solid-phase microextraction versus single-drop microextraction for the analysis of nitroaromatic explosives in water samples. *J. Chromatogr. A* 938: 113–120.
69. He Y, Lee HK. 1997. Liquid-Phase Microextraction in a single drop of organic solvent by using a conventional microsyringe. *Anal. Chem.* 69: 4634-4640.

70. Shen G, Lee HK. 2003. Headspace Liquid-Phase Microextraction of chlorobenzenes in soil with gas chromatography-electron capture detection. *Anal. Chem.* 75: 98–103.
71. Saraji M. 2005. Dynamic headspace liquid-phase microextraction of alcohols. *J. Chromatogr. A* 1062: 15–21.
72. Nerin C, Salafranca J, Aznar M, Batlle R. 2009. Critical review on recent developments in solventless techniques for extraction of analytes. *Anal. Bioanal. Chem.* 393: 809–833.
73. Khalili Zanjani, MR, Yamini Y, Shariati S, Jonsson JA. 2007. A new liquid-phase microextraction method based on solidification of floating organic drop. *Anal. Chim. Acta* 585: 286–293.
74. Dadfarnia S, Salmanzadeh AM, Shabani AMH. 2008. A novel separation/preconcentration system based on solidification of floating organic drop microextraction for determination of lead by graphite furnace atomic absorption spectrometry. *Anal. Chim. Acta* 623: 163–167.
75. Pedersen-Bjergaard S, Rasmussen KE. 1999. Liquid-liquid-liquid microextraction for sample preparation of biological fluids prior to capillary electrophoresis. *Anal. Chem.*, 71: 2650–2656.
76. Jonsson JA, Mathiasson L. 2000. Membrane-based techniques for sample enrichment. *J. Chromatogr. A* 902: 205–225.
77. Rasmussen KE, Pedersen-Bjergaard S, Krogh M, Ugland HG, Gronhaug T. 2000. Development of a simple in-vial liquid-phase microextraction device for drug analysis compatible with capillary gas chromatography, capillary electrophoresis and high-performance liquid chromatography. *J. Chromatogr. A* 873: 3–11.

78. Pedersen-Bjergaard S, Rasmussen KE. 2008. Liquid-phase microextraction with porous hollow fibers, a miniaturized and highly flexible format for liquid-liquid extraction. *J. Chromatogr. A* 1184: 132–142.
79. De Jager LS, Andrews ARJ. 2001. Preliminary studies of a fast screening method for cocaine and cocaine metabolites in urine using hollow fibre membrane solvent microextraction (HFMSME). *Analyst* 126: 1298–1303.
80. Zhao L, Lee HK. 2002. Liquid-phase microextraction combined with hollow fiber as a sample preparation technique prior to gas chromatography/mass spectrometry. *Anal. Chem.* 74: 2486–2492.
81. Lambropoulou DA, Albanis TA. 2005. Application of hollow fiber liquid phase microextraction for the determination of insecticides in water. *J. Chromatogr. A* 1072: 55–61.
82. Vora-adisak N, Varanusupakul P. 2006. A simple supported liquid hollow fiber membrane microextraction for sample preparation of trihalomethanes in water samples. *J. Chromatogr. A* 1121: 236–241.
83. Jiang X, Lee HK. 2004. Solvent bar microextraction. *Anal. Chem.* 76: 5591–5596.
84. Guo L, Lee HK. 2011. Ionic liquid based three-phase liquid–liquid–liquid solvent bar microextraction for the determination of phenols in seawater samples. *J. Chromatogr. A* 1218: 4299–4306.
85. Basheer C, Alnedhary AA, Rao BSM, Balasubramanian R, Lee HK. 2008. Ionic liquid supported three-phase liquid–liquid–liquid microextraction as a sample preparation technique for aliphatic and aromatic hydrocarbons prior to gas chromatography-mass spectrometry. *J. Chromatogr. A* 1210: 19–24.

86. Hou L, Shen G, Lee HK. 2003. Automated hollow fiber-protected dynamic liquid-phase microextraction of pesticides for gas chromatography-mass spectrometric analysis. *J. Chromatogr. A* 985: 107–116.
87. Hou L, Lee HK. 2003. Dynamic three-phase microextraction as a sample preparation technique prior to capillary electrophoresis. *Anal. Chem.* 75: 2784–2789.
88. Jiang X, Oh SY, Lee HK. 2005. Dynamic liquid-liquid-liquid microextraction with automated movement of the acceptor phase. *Anal. Chem.* 77: 1689–1695.
89. Jiang X, Basheer C, Zhang J, Lee, HK. 2005. Dynamic hollow fiber-supported headspace liquid-phase microextraction. *J. Chromatogr. A* 1087: 289–294.
90. Wu J, Ee KH, Lee HK. 2005. Automated dynamic liquid-liquid-liquid microextraction followed by high-performance liquid chromatography-ultraviolet detection for the determination of phenoxy acid herbicides in environmental waters. *J. Chromatogr. A* 1082: 121–127.
91. Wang X, Mitra S. 2006. Enhancing micro-scale membrane extraction by implementing a barrier film. *J. Chromatogr. A* 1122: 1–6.
92. Ouyang G, Zhao W, Pawliszyn J. 2007. Automation and optimization of liquid-phase microextraction by gas chromatography. *J. Chromatogr. A* 1138: 47–54.
93. Kou D, Wang X, Mitra S. 2004. Supported liquid membrane microextraction with high-performance liquid chromatography-UV detection for monitoring trace haloacetic acids in water. *J. Chromatogr. A* 1055: 63–69.

94. Varanusupakul P, Vora-adisak N, Pulpoka B. 2007. In situ derivatization and hollow fiber membrane microextraction for gas chromatographic determination of haloacetic acids in water. *Anal. Chim. Acta* 598: 82–86.
95. Zhu L, Zhu L, Lee HK. 2001. Liquid-liquid-liquid microextraction of nitrophenols with a hollow fiber membrane prior to capillary liquid chromatography. *J. Chromatogr. A* 924: 407–414.
96. Zhao L, Zhu L, Lee HK. 2002. Analysis of aromatic amines in water samples by liquid-liquid-liquid microextraction with hollow fibers and high-performance liquid chromatography. *J. Chromatogr. A* 963: 239–248.
97. Ho TS, Vasskog T, Anderssen T, Jensen E, Rasmussen KE, Pedersen-Bjergaard S. 2007. 25,000-fold preconcentration in a single step with liquid-phase microextraction. *Anal. Chim. Acta* 592: 1–8.
98. Lee J, Lee HK, Rasmussen KE, Pedersen-Bjergaard S. 2008. Environmental and bioanalytical applications of hollow fiber membrane liquid-phase microextraction: A review. *Anal. Chim. Acta* 624: 253–268.
99. Ho TS, Pedersen-Bjergaard S, Rasmussen KE. 2002. Liquid-phase microextraction of protein-bound drugs under non-equilibrium conditions. *Analyst* 127: 608–613.
100. Baardstu, KF, Ho TS, Rasmussen KE, Pedersen-Bjergaard S, Jonsson JA. 2007. Supported liquid membranes in hollow fiber liquid-phase microextraction (LPME) - practical considerations in the three-phase mode. *J. Sep. Sci.* 30: 1364–1370.
101. Rezaee M, Assadi Y, Milani Hosseini MR, Aghaee E, Ahmadi F, Berijani S. 2006. Determination of organic compounds in water using dispersive liquid-liquid microextraction. *J. Chromatogr. A* 1116: 1–9.

102. Berijani S, Assadi Y, Anbia M, Hosseini MRM, Aghaee E. 2006. Dispersive liquid-liquid microextraction combined with gas chromatography-flame photo-metric detection. Very simple, rapid and sensitive method for the determination of organophosphorus pesticides in water. *J. Chromatogr. A* 1123: 1–9.
103. Fattahi N, Assadi Y, Hosseini MRM, Jahromi EZ. 2007. Determination of chlorophenols in water samples using simultaneous dispersive liquid-liquid microextraction and derivatization followed by gas chromatography-electron-capture detection. *J. Chromatogr. A* 1157: 23–29.
104. Nagaraju D, Huang SD. 2007. Determination of triazine herbicides in aqueous samples by dispersive liquid-liquid microextraction with gas chromatography-ion trap mass spectrometry. *J. Chromatogr. A* 1161: 89–97.
105. Chiang JS, Huang SD. 2008. Simultaneous derivatization and extraction of anilines in waste water with dispersive liquid-liquid microextraction followed by gas chromatography-mass spectrometric detection. *Talanta* 75: 70–75.
106. Hu XZ, Wu JH, Feng YQ. 2010. Molecular complex-based dispersive liquid-liquid microextraction: Analysis of polar compounds in aqueous solution. *J. Chromatogr. A* 1217: 7010–7016.
107. Farahani H, Norouzi P, Dinarvand R, Ganjali MR. 2007. Development of dispersive liquid-liquid microextraction combined with gas chromatography-mass spectrometry as a simple, rapid and highly sensitive method for the determination of phthalate esters in water samples. *J. Chromatogr. A* 1172: 105–112.
108. Liang P, Xu J, Li Q. 2008. Application of dispersive liquid-liquid microextraction and high-performance liquid chromatography for the determination of three phthalate esters in water samples. *Anal. Chim. Acta* 609: 53–58.

109. Jahromi EZ, Bidari A, Assadi Y, Hosseini MRM, Jamali MR. 2007. Dispersive liquid-liquid microextraction combined with graphite furnace atomic absorption spectrometry. *Anal. Chim. Acta* 585: 305–311.
110. Shokoufi N, Shemirani F, Memarzadeh F. 2007. Fiber optic-linear array detection spectrophotometry in combination with cloud point extraction for simultaneous preconcentration and determination of cobalt and nickel. *Anal. Chim. Acta* 601: 204–211.
111. Fattahi N, Samadi S, Assadi Y, Hosseini MRM. 2007. Solid-phase extraction combined with dispersive liquid-liquid microextraction-ultra preconcentration of chlorophenols in aqueous samples. *J. Chromatogr. A* 1169: 63–69.
112. Li S, Cai S, Hu W, Chen H, Liu H. 2009. Ionic liquid-based ultrasound-assisted dispersive liquid-liquid microextraction combined with electrothermal atomic absorption spectrometry for a sensitive determination of cadmium in water samples. *Spectrochimica Acta, Part B: Atomic Spectroscopy* 64B: 666–671.
113. Dadfarnia S, Shabani AMH. 2010. Recent development in liquid phase microextraction for determination of trace level concentration of metals: A review. *Anal. Chim. Acta* 658: 107–19.
114. Leong MI, Huang SD. 2008. Dispersive liquid-liquid microextraction method based on solidification of floating organic drop combined with gas chromatography with electron-capture or mass spectrometry detection. *J. Chromatogr. A* 1211: 8–12.
115. Xu H, Ding Z, Lv L, Song D, Feng YQ. 2009. A novel dispersive liquid-liquid microextraction based on solidification of floating organic droplet method for determination of polycyclic aromatic hydrocarbons in aqueous samples. *Anal. Chim. Acta* 636: 28–33.

116. Asadollahi T, Dadfarnia S, Shabani AMH. 2010. Separation/preconcentration and determination of vanadium with dispersive liquid–liquid microextraction based on solidification of floating organic drop (DLLME-SFO) and electrothermal atomic absorption spectrometry. *Talanta* 82: 208–212.
117. Belardi RP, Pawliszyn J. 1989. The application of chemically modified fused silica fibers in the extraction of organics from water matrix samples and their rapid transfer to capillary columns. *Water Pollut. Res. J. Can.* 24: 179–191.
118. Arthur CL, Pawliszyn J. 1990. Solid phase microextraction with thermal desorption using fused silica optical fibers. *J. Anal. Chem.* 62: 2145–2148.
119. Zhang Z, Pawliszyn J. 1993. Analysis of organic compounds in environmental samples by headspace solid phase microextraction. *J. High Resolut. Chromatogr.* 16: 689–692.
120. Shirey RE. 1995. Rapid analysis of environmental samples using solid-phase microextraction (SPME) and narrow bore capillary columns. *J. High Resolut. Chromatogr.* 18: 495–499.
121. Penalver A, Pocurull E, Borrull F, Marce RM. 1999. Trends in solid-phase microextraction for determining organic pollutants in environmental samples. *Trends Anal. Chem.* 18: 557–568.
122. Zygmunt B, Jastrzebska A, Namiesnik J. 2001. Solid phase microextraction – A convenient tool for the determination of organic pollutants in environmental matrices. *Crit. Rev. Anal. Chem.*, 31: 1–18.
123. Ouyang G, Pawliszyn J. 2006. SPME in environmental analysis. *Anal. Bioanal. Chem.* 386: 1059–1073.

124. Lambropoulou DA, Konstantinou IK, Albanis TA. 2007. Recent developments in headspace microextraction techniques for the analysis of environmental contaminants in different matrices. *J. Chromatogr. A* 1152: 70–96.
125. Hawthorne SB, Miller DJ, Pawliszyn J, Arthur CL. 1992. Solventless determination of caffeine in beverages using solid-phase microextraction with fused-silica fibers. *J. Chromatogr.* 603: 185–191.
126. Page BD, Lacroix G. 1993. Application of solid-phase microextraction to the headspace gas chromatographic analysis of halogenated volatiles in selected foods. *J. Chromatogr.* 648: 199–211.
127. Braggins TJ, Grimm CC, Visser FR. 1999. Analysis of food volatiles using SPME. In: *Applications of solid phase microextraction*, Ed. Pawliszyn J., The Royal Society of Chemistry, Cambridge, 407–422.
128. Yang KW, Eisert R, Lord H, Pawliszyn J. 1999. Determination of pesticides in foods by automated SPME-GC-MS. In: *Applications of solid phase microextraction*, Ed. Pawliszyn J., The Royal Society of Chemistry, Cambridge, 435–447.
129. Kataoka H, Lord HL, Pawliszyn J. 2000. Applications of solid-phase microextraction in food analysis. *J. Chromatogr. A* 880: 35–62.
130. Wardencki W, Michulec M, Curylo J. 2004. A review of theoretical and practical aspects of solid-phase microextraction in food analysis. *Int. J. Food Sci. Technol.* 39: 703–717.
131. Riu-Aumatell M, Castellari M, Lopez-Tamames E, Galassi S, Buxaderas S. 2004. Characterization of volatile compounds of fruit juices and nectars by HS/SPME and GC-MS. *Food Chemistry* 87: 627–637.

132. Jelen HH. 2006. Solid-phase microextraction in the analysis of food taints and off-flavors. *J. Chromatogr. Sci.* 44: 399–415.
133. Balasubramanian S, Panigrahi S. 2011. Solid-phase microextraction (SPME) techniques for quality characterization of food products: A review. *Food Bioprocess Technol.* 4: 1–26.
134. DeBruin LS, Josephy PD, Pawliszyn J. 1998. Solid-phase microextraction of monocyclic aromatic amines from biological fluids. *Anal. Chem.* 70: 1986–1992.
135. Kataoka H, Lord H, Yamamoto S, Narimatsu S, Pawliszyn J. 2000. Development of automated in-tube SPME / LC / MS method for drug analysis. *J. Microcolumn Sep.* 12: 493–500.
136. Lord H, Pawliszyn J. 2000. Microextraction of drugs. *J. Chromatogr. A* 902: 17–63.
137. Ulrich S. 2000. Solid-phase microextraction in biomedical analysis. *J. Chromatogr. A* 902: 167–194.
138. Mullett WM, Pawliszyn J. 2002. Direct Determination of Benzodiazepines in Biological Fluids by Restricted-Access Solid-Phase Microextraction. *Anal. Chem.* 74: 1081–1087.
139. Kumazawa T, Lee XP, Sato K, Suzuki O. 2003. Solid-phase microextraction and liquid chromatography/mass spectrometry in drug analysis. *Anal. Chim. Acta* 492: 49–67.
140. Pragst F. 2007. Application of solid-phase microextraction in analytical toxicology. *Anal. Bioanal. Chem.* 388: 1393–1414.

141. Lord H, Grant RP, Walles M, Incledon B, Fahie B, Pawliszyn J. 2003. Development and evaluation of a solid-phase microextraction probe for in vivo pharmacokinetic studies. *Anal. Chem.* 75: 5103–5115.
142. Djozan D, Baheri T, Farshbaf R, Azhari S. 2005. Investigation of solid-phase microextraction efficiency using pencil lead fiber for in vitro and in vivo sampling of defensive volatiles from insects scent gland. *Anal. Chim. Acta* 554: 197–201.
143. Musteata FM, Musteata ML, Pawliszyn J. 2006. Fast in vivo microextraction: A new tool for clinical analysis. *Clinical Chemistry* 52: 708–715.
144. Musteata ML, Musteata FM, Pawliszyn, J. 2007. Biocompatible solid-phase microextraction coatings based on polyacrylonitrile and solid-phase extraction phases. *Anal. Chem.* 79: 6903–6911.
145. Musteata FM, Pawliszyn J. 2007. In vivo sampling with solid phase microextraction. *J. Biochem. Bioph. Methods* 70: 181–193.
146. Musteata FM, Pawliszyn J. 2007. Bioanalytical applications of solid-phase microextraction. *Trends Anal. Chem.* 26: 36–45.
147. Zhou SN, Oakes KD, Servos MR, Pawliszyn J. 2008. Application of solid-phase microextraction for in vivo laboratory and field sampling of pharmaceuticals in fish. *Environ. Sci. Technol.* 42: 6073–6079.
148. Vuckovic D, Zhang X, Cudjoe E, Pawliszyn J. 2010. Solid-phase microextraction in bioanalysis: New devices and directions. *J. Chromatogr. A* 1217: 4041–4060.
149. Chai M, Arthur CL, Pawliszyn J. 1993. Determination of volatile chlorinated hydrocarbons in air and water with solid-phase microextraction. *Analyst* 118: 1501–1505.

150. Chai M, Pawliszyn J. 1995. Analysis of environmental air samples by solid-phase microextraction and gas chromatography/ion trap mass spectrometry. *Environ. Sci. Technol.* 29: 693–701.
151. Grote C, Pawliszyn J. 1997. Solid-phase microextraction for the analysis of human breath. *Anal. Chem.* 69: 587–596.
152. Gorlo D, Zygmunt B, Dudek M, Jaszek A, Pilarczyk M, Namiesnik J. 1999. Application of solid-phase microextraction to monitoring indoor air quality. *Fresenius J. Anal. Chem.* 363: 696–699.
153. Koziel JA, Pawliszyn J. 2001. Air sampling and analysis of volatile organic compounds with solid phase microextraction. *J. Air & Waste Manage. Assoc.* 51: 173–184.
154. Chen Y, Pawliszyn J. 2003. Time-weighted average passive sampling with a solid-phase microextraction device. *Anal. Chem.* 75: 2004–2010.
155. Ras MR, Marce RM, Borrull F. 2008. Solid-phase microextraction gas chromatography to determine volatile organic sulfur compounds in the air at sewage treatment plants. *Talanta* 77: 774–778.
156. Lamas JP, Sanchez-Prado L, Lores M, Garcia-Jares C, Llompart M. 2010. Sorbent trapping solid-phase microextraction of fragrance allergens in indoor air. *J. Chromatogr. A* 1217: 5307–5316.
157. Zhang Z, Pawliszyn J. 1993. Headspace solid-phase microextraction. *Anal. Chem.* 65: 1843–1852.

158. Popp P, Kalbitz K, Oppermann G. 1994. Application of solid-phase microextraction and gas chromatography with electron-capture and mass spectrometric detection for the determination of hexachlorocyclohexanes in soil solutions. *J. Chromatogr. A* 687: 133–140.
159. James KJ, Stack MA. 1996. The determination of volatile organic compounds in soils using solid phase microextraction with gas chromatography-mass spectrometry. *J. High Res. Chromatogr.* 19: 515–519.
160. Hawthorne SB, Grabanski CB, Hageman KJ, Miller DJ. 1998. Simple method for estimating polychlorinated biphenyl concentrations on soils and sediments using subcritical water extraction coupled with solid-phase microextraction. *J. Chromatogr. A* 814: 151–160.
161. Moder M, Popp P, Eisert R, Pawliszyn J. 1999. Determination of polar pesticides in soil by solid phase microextraction coupled to high-performance liquid chromatography-electrospray/mass spectrometry. *Fresenius J. Anal. Chem.* 363: 680–685.
162. Llompart M, Li K, Fingas M. 1999. Headspace solid-phase microextraction for the determination of polychlorinated biphenyls in soils and sediments. *J. Microcolumn Sep.* 11: 397–402.
163. Herbert P, Morais S, Paiga P, Alves A, Santos L. 2006. Analysis of PCBs in soils and sediments by microwave-assisted extraction, headspace-SPME and high resolution gas chromatography with ion-trap tandem mass spectrometry. *Intern. J. Environ. Anal. Chem.* 86: 391–400.
164. Parkinson DR, Warren JM, Pawliszyn J. 2010. Analysis of ergosterol for the detection of mold in soils by automated on-fiber derivatization headspace extraction-SPME-GC/MS. *Anal. Chim. Acta* 661: 181–187.

165. Arthur CL, Pratt K, Motlagh S, Pawliszyn J, Belardi RP. 1992. Environmental analysis of organic compounds in water using solid phase micro extraction. *J. High Res. Chromatogr.* 15: 741–744.
166. Arthur CL, Killam LM, Motlagh S, Lim M, Potter DW, Pawliszyn J. 1992. Analysis of substituted benzene compounds in groundwater using solid-phase microextraction. *Environ. Sci. Technol.* 26: 979–983.
167. Buchholz KD, Pawliszyn J. 1993. Determination of phenols by solid phase microextraction and gas chromatographic analysis. *Environ. Sci. Technol.* 27: 2844–2848.
168. Potter DW, Pawliszyn J. 1994. Rapid determination of polyaromatic hydrocarbons and polychlorinated biphenyls in water using solid phase microextraction and GC/MS. *Environ. Sci. Technol.* 28: 298–305.
169. Nilsson T, Pelusio F, Montanarella L, Carsen B, Facchetti S, Madsen JO. 1995. An evaluation of solid-phase microextraction for analysis of volatile organic compounds in drinking water. *J. High Res. Chromatogr.* 18: 617–624.
170. Wittkamp BL, Tilotta DC. 1995. Determination of BTEX compounds in water by solid-phase microextraction and Raman spectroscopy. *Anal. Chem.* 67: 600–605.
171. Langenfeld JJ, Hawthorne SB, Miller DJ. 1996. Quantitative analysis of fuel-related hydrocarbons in surface water and wastewater samples by solid-phase microextraction *Anal. Chem.* 68: 144–155.
172. Llompарт M, Li K, Fingas M. 1998. Solid-phase microextraction and headspace solid-phase microextraction for the determination of polychlorinated biphenyls in water samples. *Anal. Chem.* 70: 2510–2515.

173. Doong RA, Chang SM, Sun YC. 2000. Solid-phase microextraction and headspace solid-phase microextraction for the determination of high molecular-weight polycyclic aromatic hydrocarbons in water and soil samples. *J. Chromatogr. Sci.* 38: 528–534.
174. Chang WY, Sung YH, Huang SD. 2003. Analysis of carcinogenic aromatic amines in water samples by solid-phase microextraction coupled with high-performance liquid chromatography. *Anal. Chim. Acta* 495: 109–122.
175. Aulakh JS, Malik AK, Kaur V, Schmitt-Kopplin P. 2005. A review on solid phase micro extraction high performance liquid chromatography (SPME-HPLC) analysis of pesticides. *Crit. Rev. Anal. Chem.* 35: 71–85.
176. Antoniou CV, Koukouraki EE, Diamadopoulos E. 2007. Analysis of volatile and semivolatile organic compounds in municipal wastewater using headspace solid-phase microextraction and gas chromatography. *Water Environ. Res.* 79: 921–930.
177. Chen W, Zeng J, Chen J, Huang X, Jiang Y, Wang Y, Chen X. 2009. High extraction efficiency for polar aromatic compounds in natural water samples using multiwalled carbon nanotubes/Nafion solid-phase microextraction coating. *J. Chromatogr. A* 1216: 9143–9148.
178. Basaglia G, Pasti L, Pietrogrande MC. 2011. Multi-residual GC-MS determination of personal care products in waters using solid-phase microextraction. *Anal. Bioanal. Chem.* 399: 2257–2265.
179. Pawliszyn J. 1997. *Solid Phase Microextraction: Theory and Practice*. Wiley-VCH, New York.
180. Shirey R, Mani V, Mindrup R. 1998. On-site sampling for volatiles and pesticides using solid-phase microextraction. *American Environmental Laboratory* 10: 21–22.

181. Lord H, Pawliszyn J. 2000. Evolution of solid-phase microextraction technology. *J. Chromatogr. A* 885: 153–193.
182. Risticovic S, Lord H, Gorecki T, Arthur CL, Pawliszyn J. 2010. Protocol for solid-phase microextraction method development. *Nature Protocols* 5: 122–139.
183. Risticovic S, Niri VH, Vuckovic D, Pawliszyn J. 2009. Recent developments in solid-phase microextraction. *Anal. Bioanal. Chem.* 393: 781–795.
184. Spietelun A, Pilarczyk M, Kloskowski A, Namiesnik J. 2010. Current trends in solid-phase microextraction (SPME) fiber coatings. *Chem. Soc. Rev.* 39: 4524–4537.
185. Turiel E, Martin-Esteban A. 2010. Molecularly imprinted polymers for sample preparation: A review. *Anal. Chim. Acta* 668: 87–99.
186. Vuckovic D, Zhang X, Cudjoe E, Pawliszyn J. 2010. Solid-phase microextraction in bioanalysis: New devices and directions. *J. Chromatogr. A* 1217: 4041–4060.
187. Muller L, Gorecki T, Pawliszyn J. 1999. Optimization of the SPME device design for field applications. *Fresenius J. Anal. Chem.* 364: 610–616.
188. Chen Y, Pawliszyn J. 2004. Solid phase microextraction field sampler. *Anal. Chem.* 76: 6823–6828.
189. Zhang Z, Poerschmann J, Pawliszyn J. 1996. Direct solid phase microextraction of complex aqueous samples with hollow fibre membrane protection. *Anal. Commun.* 33: 219–221.

190. Gorecki T, Pawliszyn J. 1997. Effect of sample volume on quantitative analysis by solid-phase microextraction. Part 1. Theoretical considerations. *Analyst* 122: 1079–1086.
191. Ai J. 1997. Solid phase microextraction for quantitative analysis in nonequilibrium situations. *Anal. Chem.* 69: 1230–1236.
192. Louch D, Motlagh S, Pawliszyn J. 1992. Dynamics of organic compound extraction from water using liquid-coated fused silica fibers. *Anal. Chem.* 64: 1187–1199.
193. Gorecki T, Yu X, Pawliszyn J. 1999. Theory of analyte extraction by selected porous polymer SPME fibres. *Analyst* 124: 643–649.
194. Ruthven D. 1984. Principles of Adsorption & Adsorption Process. John Wiley & Sons, NY.
195. Zhang Z, Pawliszyn J. 1995. Quantitative Extraction Using an Internally Cooled Solid Phase Microextraction Device. *Anal. Chem.* 67: 34–43.
196. Chen Y, Pawliszyn J. 2006. Miniaturization and Automation of an Internally Cooled Coated Fiber Device. *Anal. Chem.* 78: 5222–5226.
197. Ai J. 1997. Headspace solid phase microextraction. Dynamics and quantitative analysis before reaching a partition equilibrium. *Anal. Chem.* 69: 3260–3266.
198. Chen Y, O'Reilly J, Wang Y, Pawliszyn J. 2004. Standards in the extraction phase, a new approach to calibration of microextraction processes. *Analyst* 129: 702–703.
199. Chen Y, Pawliszyn J. 2004. Kinetics and the on-site application of standards in a solid-phase microextraction fiber. *Anal. Chem.* 76: 5807–5815.

200. Ouyang G. 2009. Calibration. In: *Handbook of Solid Phase Microextraction*, Ed. Pawliszyn J., Chemical Industry Press, Beijing.
201. Ouyang G, Cai J, Zhang X, Li H, Pawliszyn J. 2008. Standard-free kinetic calibration for rapid on-site analysis by solid-phase microextraction. *J. Sep. Sci.* 31: 1167–1172.
202. Kudlejova L, Risticovic S, Vuckovic D. 2009. Solid-phase microextraction method development. In: *Handbook of Solid Phase Microextraction*, Ed. Pawliszyn J., Chemical Industry Press, Beijing.
203. Shirey RE. 2009. SPME commercial devices and fibre coatings. In: *Handbook of Solid Phase Microextraction*, Ed. Pawliszyn J., Chemical Industry Press, Beijing.
204. Baltussen E, Sandra P, David F, Cramers C. 1999. Stir bar sorptive extraction (SBSE), a novel extraction technique for aqueous samples: theory and principles. *J. Microcolumn Sep.* 11: 737–747.
205. Sandra P, Tienpont B, David F. 2003. Multi-residue screening of pesticides in vegetables, fruits and baby food by stir bar sorptive extraction-thermal desorption-capillary gas chromatography-mass spectrometry. *J. Chromatogr. A* 1000: 299–309.
206. David F, Tienpont B, Sandra P. 2003. Stir-bar sorptive extraction of trace organic compounds from aqueous matrices. *LCGC North America* 21(2): 108, 111–112, 114, 116–118.
207. Nie YY, Kleine-Benne E. 2011. Using three types of twister phases for stir bar sorptive extraction of whisky, wine and fruit Juice. *GERSTEL Application Note* AN/2011/03, 1–13.

208. Bruheim I, Liu X, Pawliszyn J. 2003. Thin-Film Microextraction. *Anal. Chem.* 75: 1002–1010.
209. Bragg L, Qin Z, Alaei M, Pawliszyn J. 2006. Field sampling with a polydimethylsiloxane thin-film. *J. Chromatogr. Sci.* 44: 317–323.
210. Qin Z, Bragg L, Ouyang G, Pawliszyn J. 2008. Comparison of thin-film microextraction and stir bar sorptive extraction for the analysis of polycyclic aromatic hydrocarbons in aqueous samples with controlled agitation conditions, *J. Chromatogr. A* 1196-1197: 89–95.
211. Brewer Science Inc. 2011. Spin Coating Theory.
Available on-line at:
<http://www.brewerscience.com/research/processing-theory/spin-coater-theory>
[accessed: 15 October 2011].
212. Emslie AG, Bonner FT, Peck LG. 1958. Flow of a viscous liquid on a rotating disk. *J. Appl. Phys.* 29: 858–862.
213. Hall DB, Underhill P, Torkelson JM. 1998. Spin coating of thin and ultrathin polymer films. *Polym. Eng. Sci.* 38(12): 2039–2045.

Chapter 2

Solid phase microextraction of N-nitrosamines: Development of mixed- phase (particle-loaded) thin films as novel sampling and sample preparation devices

2.1 Introduction

Occurrence of N-nitrosamines (NAs) in source and treated drinking water is an issue of environmental and public health concern. Many NAs have shown to induce tumors in laboratory animals and are considered to be probable (B2) human carcinogens by US EPA¹. N-nitrosodimethylamine (NDMA), the simplest dialkyl nitrosamine was first detected in the water supply for the Village of Ohsweken in Ontario (Canada) in December 1989 during routine monitoring under the Ontario Ministry of Environment and Energy (MOEE) Drinking Water Surveillance Program (DWSP)². Around the same time, it was detected as an industrial pollutant in a groundwater source in Elmira³,

Ontario. Afterwards, NDMA was repeatedly found in treated drinking water throughout North America²⁻⁴. Public health concerns were then increased after the observation that other NAs are generated as DBPs in finished drinking water both at the treatment plant and in the distribution system. *N*-nitrosopiperidine (NPIP), *N*-nitrosopyrrolidine (NPYR), *N*-nitrosodiethylamine (NDEA), *N*-nitroso-morpholine (NMOR), *N*-nitrosodiphenylamine (NDPHA), *N*-nitrosodipropylamine (NDPA) and *N*-nitrosodibutylamine (NDBA) were detected in drinking water⁵⁻⁹. Moreover, it was revealed that these DBPs could continue to form in the drinking water distribution system in increased levels compared to the amounts in the treatment plant⁵⁻⁷. In addition to the drinking water, NDMA, NDEA, NPYR, NPIP, NDPA and NDBA were found in treated wastewater in higher concentrations⁸. This raised another concern about the intentional and unintentional reuse of municipal wastewater¹⁰. As a result, legislations and recommendations about the presence of NAs in drinking water were implemented in different states and countries. The province of Ontario set a maximum acceptable concentration of 9 ng/L for NDMA in 1991¹¹. Health Canada has recently proposed a Canadian drinking water guideline for the same compound at a maximum acceptable limit of 40 ng/L¹². World Health Organization (WHO) has a drinking water guideline of 100 ng/L¹³. The California Department of Health Services (CDHS) has established a notification level of 10 ng/L for NDMA, NDEA and NDPA, and response levels based on a 10^{-4} cancer risk (at which CDHS recommends removing the source from service) of 200, 100 and 500 ng/L, respectively⁸. The US EPA has added NDMA, NDEA, NPYR, NDP, NDBA and *N*-nitrosomethylethylamine (NMEA) to the list of Unregulated Contaminants Monitoring Rule 2 (UCMR-2)¹⁴, indicating the importance of monitoring these compounds. As for wastewaters, a regulatory level of 200 ng/L in effluents was established for NDMA by the Ontario Ministry of Environment and Energy¹¹. The concentrations of the NAs detected in drinking water at different locations are generally less than 100 ng/L and often below 10 ng/L^{4, 8}. Higher concentrations up to 180 ng/L were also found in some drinking water plants and distribution systems⁵⁻⁷. Recent measurements have shown that the *N*-nitrosamines formation can exceed 100 ng/L during chlorination of wastewater effluents¹⁵.

The observation of NAs at low ng/L concentrations in source and treated drinking water has been largely due to improved analytical techniques. Many of these compounds are polar with hydrophilic character, owing to the presence of N–nitroso group (–N–N=O) and an amine group (–NR₂) in their chemical structure. As a result, their efficient extraction from water is a major analytical challenge. In the past, LLE technique was usually employed for preconcentration of these analytes. Water samples of approximately 1 liter volume were serially or continuously extracted with a total of 100–500 mL of an organic solvent, often methylene chloride, using a separatory funnel (e.g. EPA method 3510C)¹⁶, or a continuous extractor to obtain better efficiency and avoid emulsion formation (e.g. EPA method 3520C)¹⁷. The organic solvent extract(s) were then dried and concentrated to 1 mL of the same solvent or a different one (e.g. methanol), using rotary evaporators or a stream of nitrogen, before chromatographic separation. Although LLE technique may still be practiced for extraction of NAs, it suffers from large amounts of organic solvent usage, the relevant health hazards, and prolonged procedure (sometime 24 h or more), including careful cleaning of all glasswares before analysis which is tedious and labor intensive.

The more recent methods for preconcentration of NAs are mainly based on adsorption technique using granular adsorbent beads^{11, 18, 19}, SPE disk²⁰, or SPE cartridge (EPA method 521)²¹. Water samples of approximately 0.5–1 liter volume are extracted by shaking or passing through 0.2–2 grams of an adsorbent, normally a carbonaceous type such as Ambersorb 572 resin or coconut charcoal. The extracted analytes are desorbed or eluted from the adsorbent by 0.5–12 mL of solvent (e.g. methylene chloride) and then concentrated to approximately 1 mL. To ensure removal of residual water the adsorbent or the eluted solvent is dried either before desorption or the after elution, depending on the procedure.

For analytical determination of NAs, the concentrated extract derived from SPE or LLE methods is subjected to chromatographic separation, usually capillary gas chromatography (GC), with different detection systems, such as nitrogen–phosphorus detector (NPD) (EPA method 8070A)²², nitrogen chemiluminescence detector (NCD), also known as nitrogen-mode thermal energy analyzer (TEA)^{23, 24}, and mass spectrometry (MS)^{25, 26}. NPD and NCD detectors are less sensitive than MS detector and

generally suitable for analysis of moderate to high concentrations of NAs, such as those found in wastewater²⁷. For monitoring of ultra trace concentration in drinking water, MS approach is usually used in combination with chemical ionization (CI/MS)^{5, 10}, or with CI and tandem mass spectrometry (CI/MS/MS)^{21, 28}. Alternatively, high-resolution mass spectrometry (HRMS) can be used for increased selectivity^{8, 11}. Liquid chromatography–tandem mass spectrometry (LC/MS/MS) has also been applied to the analysis of NAs in water samples⁶ to address better detection of thermally liable nitrosamines such as NDPHA. The SPE-based methods offer reduction of methylene chloride usage and typical method detection limits around 1 ng/L of NAs in water using sensitive mass spectrometry^{8, 21}. However, similar to the LLE technique, the SPE approach requires large volume of samples and its set-up is not very simple.

There are few studies concerning application of solid-phase microextraction (SPME) for extraction and determination of NAs in water. Grebel et al.²⁹ reported a method with detection limits in the range of 30–138 ng/L obtained for the compounds using an adsorption commercial fiber (CAR/PDMS) combined with gas chromatography and CI mass spectrometry (GC/CI/MS). Parallel to this thesis research, lower detection limits in the range of 1-5 ng/L were reported using adsorption commercial fibers (CAR/PDMS and DVB/CAR/PDMS) and more sensitive GC/CI/MS/MS detection approach^{30, 31}. While these recent studies indicate the feasibility of conventional SPME fiber technique for analysis of NAs in water at low ng/L range, they rely on highly sensitive CI/MS/MS detection. An alternative way to improve the analytical sensitivity is to develop a microextraction device having larger extraction phase with adsorption properties appropriate for these analytes. Clearly, a device with large surface-to-volume ratio such as thin film configuration is more efficient than simply a thick spherical or rod shape in that it can enhance the extraction capacity while providing faster extraction rates. To date, such thin film device has only been available with polydimethylsiloxane (PDMS) as extraction phase³²⁻³⁴ and no mixed-phase similar type has been developed for microextraction purposes. This study describes development and construction of mixed-phase (particle-loaded) thin films as novel solvent-free sampling/sample preparation devices and feasibility of their application for NAs analysis in water.

2.2 Experimental

2.2.1 Safety considerations

N-nitrosamines (NAs) are probable human carcinogens and must be handled with extreme care inside a fume hood with ventilation. Safety precautions were taken when these compounds were used and waste disposal followed proper safety procedures.

2.2.2 Chemicals and supplies

A standard mix solution of *N*-nitrosamines (EPA 521) [*N*-nitrosodimethylamine, *N*-nitrosomethylethylamine, *N*-nitrosodiethylamine, *N*-nitrosopyrrolidine, *N*-nitrosodipropylamine, *N*-nitrosopiperidine and *N*-nitrosodibutylamine] containing 2000 µg/mL of each compound in methylene chloride from Supelco (Bellefonte, USA) was used to prepare secondary stock solutions in methanol. The stock solutions in methanol were stored at 4 °C in amber vials in refrigerator. Standard aqueous solutions were prepared by spiking appropriate volumes of the stock solutions into ultra-pure water. The volume of spiked water samples were 10 mL and 5 mL for direct immersion (DI) and headspace (HS) SPME, respectively, and 240 mL for direct thin film microextraction (TFME). Ultra-pure water was obtained from a Barnstead/Thermodyne water system (Dubuque IA, USA). High density polydimethylsiloxane gum (PDMS), Carboxen 1006 (CAR) and divinylbenzene (DVB) particles, dimethyldichlorosilane (DMDCS 5% in toluene), sodium chloride, vials (10 & 20 mL) and the commercial SPME fibers used in this study including polyacrylate (PA 85µm), polydimethylsiloxane (PDMS 100µm), polydimethylsiloxane/divinylbenzene (PDMS/DVB 65µm), divinylbenzene/carboxen/polydimethylsiloxane (DVB/CAR/PDMS 50/30µm) and carboxen/polydimethylsiloxane (CAR/PDMS 75µm) were all supplied by Supelco (Bellefonte, USA). Sylgard 184 PDMS gum was provided by Dow Corning (Midland, USA). Commercial PDMS thin film (75 µm) was purchased from Specialty Silicone Products Inc (Ballston NY, USA). HPLC grade methanol and glass bottles (250 mL) were purchased from Fisher Scientific (Ottawa, Canada). Ultra-pure Helium for gas chromatography and liquid nitrogen for cryogenic trapping were supplied by Praxair (Kitchener, Canada). Glass wool fabric mesh (58 µm)

were provided by BGF (Greensboro, NC, USA). Stainless steel cotter pins were supplied by Spaenaur (Kitchener, Canada). Teflon holder and custom-made thin film cutters were created by University of Waterloo Science Shop (ON, Canada). A Mitutoyo 293 series MDC-Lite digital micrometer (Tools & Instruments, Toronto, Canada) was used to estimate the thickness of PDMS thin film area cuts (round-shape, 1 cm i.d.) by placing them between two square-shape pieces of wafer (1 cm x 1 cm) and measuring the net thickness. The thin film-to-fiber volume ratio of similar coatings was estimated indirectly by weighing using a Radwag MXA 21 microbalance (North Miami Beach, FL).

2.2.3 GC-MS analysis

The SPME analyses were carried out using a Varian 3800 gas chromatograph coupled with a 4000 ion trap MS detector (Varian, Mississauga, Canada). Automated analyses were performed using a CTC Analytics CombiPAL autosampler equipped with a temperature-controlled SPME agitator (Zwingen, Switzerland) and Cycle Composer software (Version 1.4.0). The injection port was equipped with a SPME insert and was kept splitless during injection. The chromatographic separation was performed on a 30m x 0.25mm x 0.25 μ m RTX-5 amine capillary column from Restek (Bellefonte, PA, USA). The column was initially set at 45 °C for 1 min, ramped at 5 °C/min to 100 °C and held for 1 min, then ramped at 1°C/min to 105 °C. Temperature was held at 105 °C for 1 min, then ramped at 30 °C/min to 250 °C and held for 3.17 min giving a total GC run of 28 min. The Helium carrier gas flow rate was constant at 1 ml/min. The mass spectrometry was performed using full scan mode with electron impact ionization (EI). Data acquisition was started after 2 min. The NAs were identified using the mass spectra library of the National Institute of Standard and Technology (NIST, USA) and their retention times. The quantifications were done using selected ion for each compound. The ions used were 74 for NDMA, 88 for NMEA, 102 for NDEA, 100 for NPYR, 70 for NDPA, 114 for NPIP and 84 for NDBA.

The thin film analyses were carried out using an Agilent 6890 GC coupled with a 5973 MSD system. The Agilent GC was equipped with a MPS-2 multipurpose autosampler and a TDS-2 thermal desorption system (Gerstel GmbH, Mullheim, Germany) which was mounted on the GC via a CIS-4 cooled injection system inlet. The

thermal desorption unit (TDU) served as large volume injection (LVI) unit and the CIS-4 as a programmed temperature vaporizer (PTV) with cryogenic trapping capability. The analytes desorption was performed under TDU-splitless/CIS-split mode under high gas flow rate (80mL/min). The TDU initial temperature, delay time and desorption time were set as 30 °C, 2 min and 7 min, respectively. The transfer line situated between the TDU and the CIS was set at 300 °C. The CIS-4 cryogenic cooling temperature for all thin film analyses was set at –150 °C. The chromatographic separation was performed on a 30m x 0.25mm x 0.25µm SLB-5MS capillary column from Supelco (Bellefonte, USA) with a Helium constant carrier gas flow rate at 1.6 mL/min. The column was initially set at 40 °C for 2 min, ramped at 5 °C/min to 75 °C and held for 5 min, then ramped at 25 °C/min to 200 °C and held for 6 min, giving a total GC run of 25 min. The mass spectrometry was performed using selected ion monitoring (SIM) mode with electron impact ionization (EI). The ion used for quantification and qualification were 74 and 42 for NDMA, 88 and 42 for NMEA, 102 and 42 for NDEA, 100 and 68 for NPYR, 70 and 130 for NDPA, 114 and 55 for NPIP, 84 and 57 for NDBA, respectively. Data acquisition was started after 3 min.

2.2.4 Spin coating instrument

A Cee Model 200 precision spin coater (Brewer Science Inc, Rolla MO, USA) was used for preparation of mixed-phase (particle-loaded) thin films. Silicon wafer disks (4 inches) were supplied by Montco Silicon (PA, USA).

2.2.5 Fabrication of mixed-phase thin films (MPTFs)

The mixed-phase thin films (MPTFs) were prepared by spin coating technique. At first, PDMS gum (0.25 gram) was diluted in methylene chloride (5–10 times) in a 10 mL screw cap vial. Fine particles of the adsorptive material (divinylbenzene or carboxen 1006) were then suspended in the diluted PDMS at desired ratios by vigorous shaking for a few hours. After complete dispersion of the particles in PDMS, the curing agent was added and the mixture was vortexed for a few minutes. The solvent was then allowed to evaporate so that the viscosity of mixture was adjusted to the desired level. Approximately 1.5 mL the coating mixture was deposited on the center of a 4 inches

wafer, over the spin chuck, using a disposable pipette. The spin coater lid was then closed and the wafer was accelerated to the desired speed, typically 1000–1250 rpm, and kept rotating for a set period of time (30–40 sec). Following the spin cycle, the lid was opened and the coated wafer was transferred into a vacuum oven. The thin film coating was thermally cured (80°C) under vacuum for approximately 2 hours. Afterwards, the prepared thin film was removed carefully from the wafer and transferred over a thin sheet of Teflon. The thin film was then cut into a house shape at the desired size (2 cm × 2 cm square with a 1 cm height triangle on top), using a custom-made cutter. In order to have a fair comparison of extraction performance between the prepared MPTF samplers and the commercial SPME fibers, samples were prepared with particles-to-PDMS ratios similar to those of commercial fiber coatings (property of Supelco, Bellefonte, USA). For these coatings, the wafer was initially covered with a thin layer of silanized glass wool (GW) fabric mesh, which served as a substrate for the thin film coatings (Fig. 2.1).

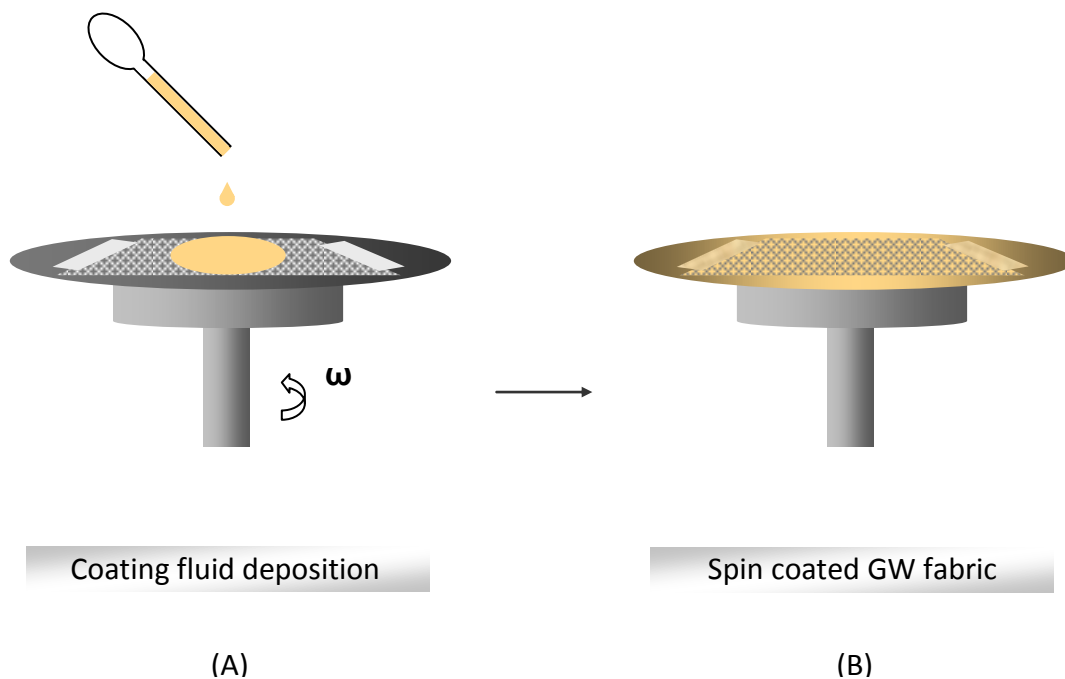


Figure 2.1 Schematic representation of thin film fabrication; (A) coating fluid deposition, (B) spin coated GW fabric mesh.

Before use, the mesh was treated by 20% HCl for a few hours, rinsed with ultra-pure water, dried and then silanized (30 min) using dimethyldichlorosilane (DMDCS 5% in toluene) to mask the polar Si–OH groups at its surface. After treatment the mesh was rinsed with toluene and thereafter with methanol, and finally dried at 70 °C in a vacuum oven before final use.

2.2.6 Scanning electron microscopy (SEM)

Surface characterization of the mixed-phase thin film devices was performed on a LEO 1530 field emission SEM (Carl Zeiss NTS GmbH, Germany) using 10 nm of gold deposition on the surface before the microscopy.

2.2.7 SPME procedure

All SPME fibers were conditioned before use, according to the manufacturer's instructions. Automated extractions were performed in triplicate using spiked water samples of 10 mL for DI mode and 5 mL for HS mode in 10 mL vials at 30 °C unless otherwise stated. The agitation speed was 250 rpm and the incubation and desorption times were 5 and 2 minutes, respectively. The desorption temperature was set at 265 °C for all of the fibers except for PA and CAR/PDMS fiber, which was set at 290 °C and 300 °C, respectively.

2.2.8 TFME set-up and procedure

All thin film samplers were conditioned before use. The conditioning was done under stream of Helium in a tube inside an oven and later in a large volume GC injection port for a minimum of 1 hour at temperatures typical of similar commercial SPME fiber coatings. The TDU liners containing conditioned thin film samplers were stored in sealed 20 mL vials to minimize contamination from air. Prior to extraction, the thin film samplers were re-conditioned for 15 min, at temperatures appropriate of each coating. Extractions were performed manually by direct immersion in 250 mL glass bottles containing 240 mL of spiked water samples. A magnetic stirrer and Teflon-coated stir bar (4 cm length) were used for agitation. To facilitate thin film handling, each sampler was

attached to a stainless steel cotter pin (Fig. 2.2), initially cleaned by sonication, water and methanol. To position and hold the thin film samplers inside water samples in a reproducible way during extraction, a specially designed Teflon-made holder (Fig. 2.2), which was created by the University of Waterloo Science Shop, Waterloo, ON, Canada. The Teflon holder comprised of a thin disk at the upper part and a grooved rod at the lower part with a separate tube movable along the rod. The disk had a diameter equal to inner size of the bottle screw cap which was settled at the top of the bottle serving to hold the assembly during extraction and to seal the bottle. The grooved rod at the lower part was used for fitting the cotter pin. The movable tube served to tighten or loose the cotter pin inside the groove by moving along the rod.

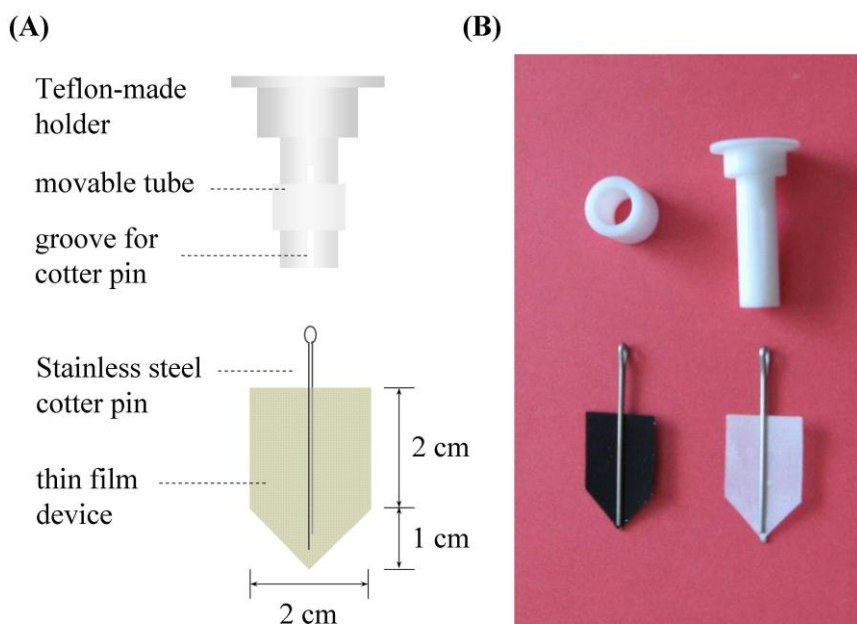


Figure 2.2 (A) Schematic representations and (B) images of house-shape thin film sampler with cotter pin and Teflon-made holder.

Immediately after exposing the thin film device to the sample, the bottle was tightly capped and extraction began for a set period of time. After extraction, the thin film assembly was removed from the bottle and the sampler with the cotter pin was detached from the Teflon holder. The thin film sampler was then dried gently and thoroughly by a

soft lint-free tissue and rolled into a TDU glass liner (60 mm length, 6 mm o.d. and 4.8 mm i.d.) for TDU-CIS-GC-MS analysis. A schematic representation and image of the set-up used for thin film extraction is presented in Fig. 2.3. The sealed bottle set up used is also advantageous where headspace TFME is intended. After placing the thin film sampler into the TDU liner in the MPS-2 tray, the liner containing the sampler was transferred into the TDU by the autosampler, where it was heated to desired temperature (265 °C for PDMS/DVB or PDMS thin films, 300 °C for CAR/PDMS thin film) to desorb and transfer the analytes to the pre-cooled (–150 °C) CIS-4 liner.

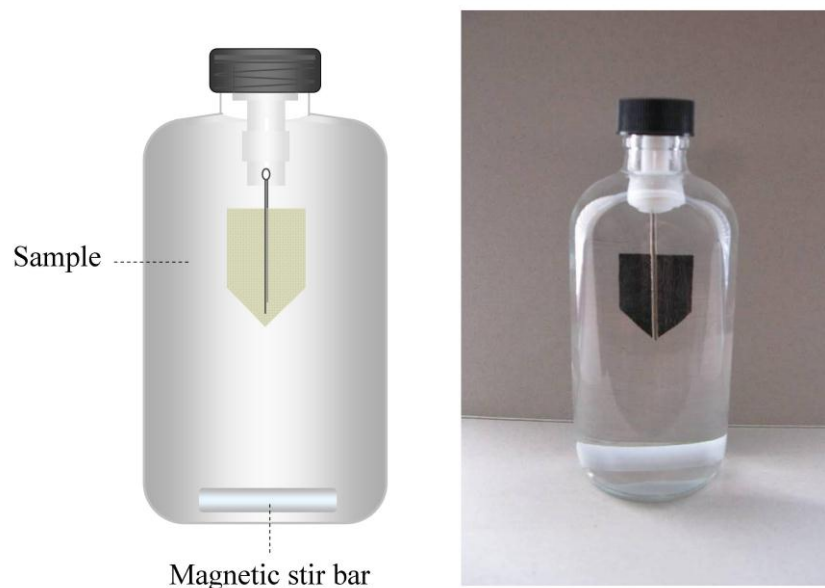


Figure 2.3 Schematic representation and image of set-up for thin film extraction.

For efficient desorption of analytes from the thin films, a TDU-splitless/CIS-split mode with high gas flow rate (80 mL/min) was used. This combination mode with the two split points and a narrow liner cold trap (0.75 mm i.d. packed with silanized glass wool) placed between enabled high flow rate desorption of analytes without losing them in the CIS-4 split during desorption, as shown in Fig. 2.4. After desorption, the TDU liner containing the sampler was cooled and transferred back to the TDU tray by the autosampler. The CIS split was then closed and the trap temperature was rapidly increased automatically to transfer the analytes to the GC column.

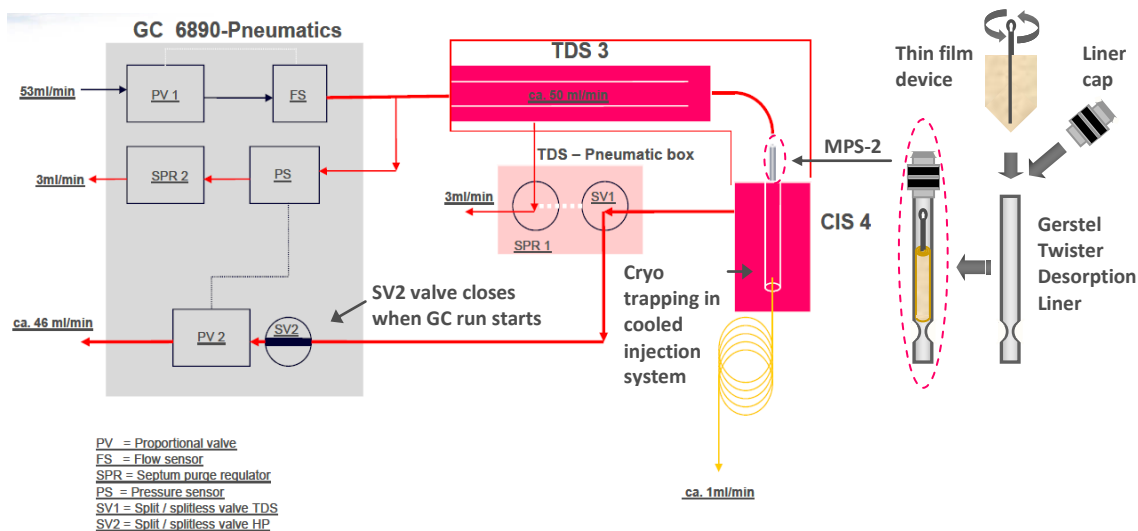


Figure 2.4 Schematic representation of thin film desorption in TDU-CIS-GC system.

2.3 Results and Discussion

2.3.1 Analytes description and properties

The *N*-nitrosamines studied in this research were a group of seven analytes included in the EPA method 521²¹. Table 2.1 presents the analytes description, acronym, Chemical Abstracts Service Registry Number (CASRN), and their properties such as molecular weight (MW), boiling point (b.p.), solubility in water, Henry's law constant (H) and log of octanol-water partition coefficient ($\log K_{ow}$)³⁵⁻³⁷. The value of the Henry's law constant provides an indication of partitioning from water to air (i.e. a measure of volatility). The value of $\log K_{ow}$ is a measure of the preference of the compound for the organic phase (lipophilic compounds) or the water phase (hydrophilic compounds). As is seen from the table, these analytes exhibit different volatility, lipophilicity and solubility in water, which affect their extraction from water.

Table 2.1 Description and properties of N–nitrosamines (EPA 521)

| Compound | Formula | Acronym | CASRN | MW g/mol | b.p. ^a (°C) | Solubility in ^b Water (g/L) | H^c atm.m ³ /mole | Log K_{ow}^d |
|---------------------------|--|---------|------------|-------------|---------------------------|---|-----------------------------------|----------------|
| N–nitrosodimethylamine | (CH ₃) ₂ –N(NO) | NDMA | 62-75-9 | 74.08 | 152 | 740 | 1.82 x 10 ⁻⁶ | - 0.57 |
| N–nitrosomethylethylamine | (CH ₃)(C ₂ H ₅)–N(NO) | NMEA | 10595-95-6 | 88.11 | 161 | 292 | 4.25 x 10 ⁻⁷ | - 0.24 |
| N–nitrosodiethylamine | (C ₂ H ₅) ₂ –N(NO) | NDEA | 55-18-5 | 102.14 | 177 | 95 | 3.63 x 10 ⁻⁶ | 0.48 |
| N–nitrosopyrrolidine | C ₄ H ₈ –N(NO) | NPYR | 930-55-2 | 100.12 | 214 | 399 | 4.89 x 10 ⁻⁸ | - 0.19 |
| N–nitrosodipropylamine | (C ₃ H ₇) ₂ –N(NO) | NDPA | 621-64-7 | 130.19 | 206 | 12 | 5.38 x 10 ⁻⁶ | 1.36 |
| N–nitrosopiperidine | C ₅ H ₁₀ –N(NO) | NPIP | 100-75-4 | 114.15 | 220 | 44 | 8.44 x 10 ⁻⁷ | 0.63 |
| N–nitrosodibutylamine | (C ₄ H ₉) ₂ –N(NO) | NDBA | 924-16-3 | 158.25 | 237 | 1.2 | 1.32 x 10 ⁻⁵ | 1.92 |

^a Ref.35 (760 torr); ^b Ref.36 (25 °C, calculated from the log of S_w); ^c Ref.37 (25 °C); ^d Ref.38 (25 °C).

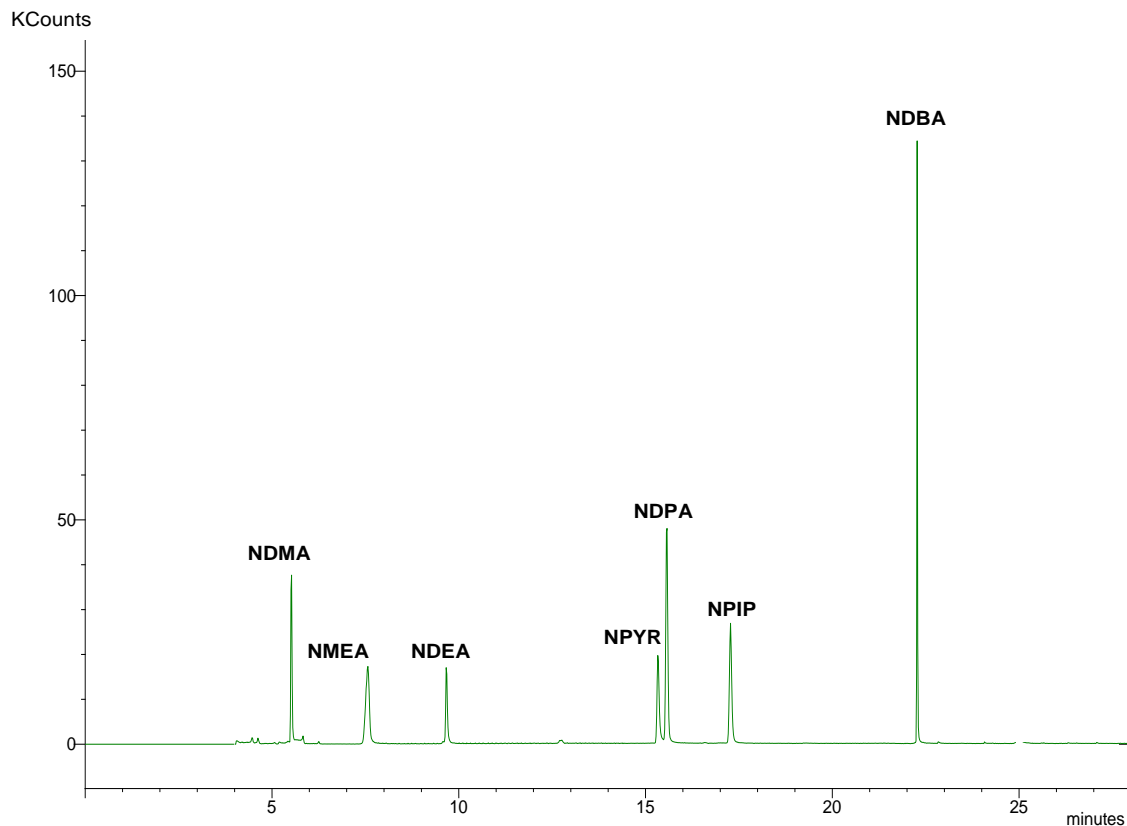


Figure 2.5 Liquid injection GC-MS chromatogram of N-nitrosamines (0.5 μ L of 10 μ g/mL solution in methanol).

2.3.2 Separation and identification

Figure 2.5 presents a typical liquid injection GC-MS chromatogram of the NAs under the temperature program used. The chromatogram shows that the analytes were clearly separated and identified using their mass spectra.

2.3.3 SPME fibers evaluation

Five different commercial fibers including PA, PDMS, CAR/PDMS, DVB/CAR/PDMS and PDMS/DVB were evaluated to find the most appropriate fiber coatings for extraction of the NAs from water. Figure 2.6 shows a comparison of the efficiencies of the fibers for the extraction of selected NAs under similar experimental conditions. Each fiber was examined with 30 min direct immersion extraction in triplicates. As shown, effective extraction of the small molecular size NDMA was

achieved by the Carboxen containing fibers with the CAR/PDMS (75 μm) fiber several times more efficient than DVB/CAR/PDMS (50/30 μm) fiber under the experimental conditions. This can be attributed to the small pores in Carboxen particles which make this carbon molecular sieve suitable for extracting the small molecular size NAs. The outperformance of CAR/PDMS fiber for NDMA is in agreement with the recent findings of Grebel et al. (2006)²⁹ and Hung et al. (2010)³⁰.

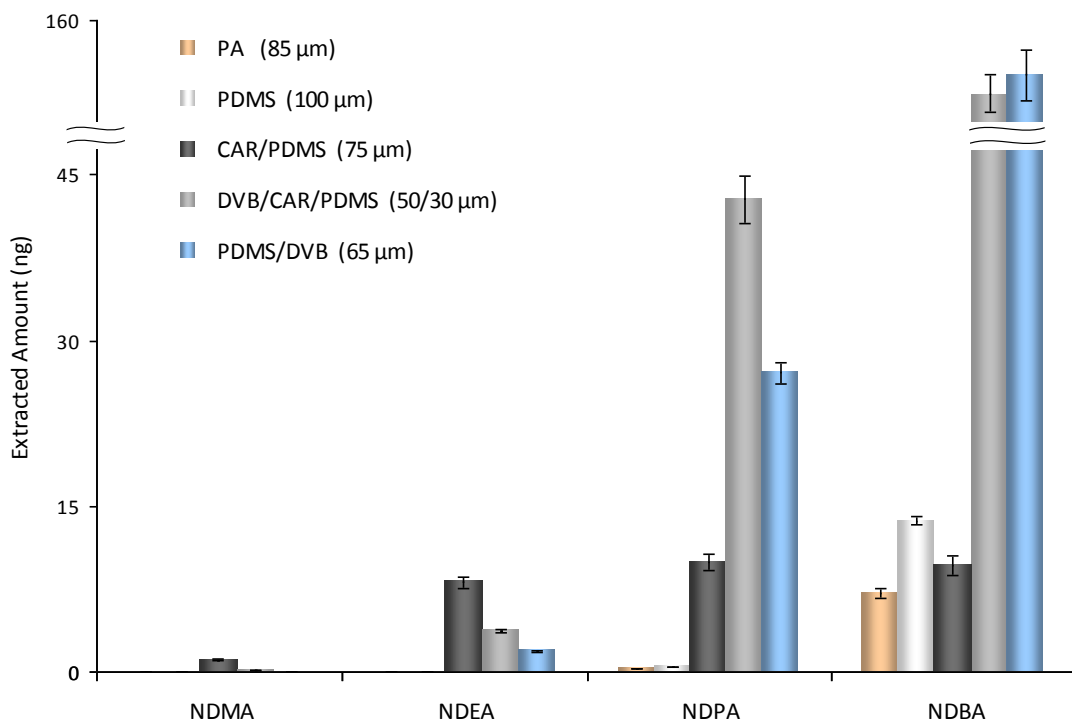


Figure 2.6 Comparison of different SPME fiber coatings for the extraction of selected *N*-nitrosamines; 50 $\mu\text{g/L}$ spiked water sample, 30 min direct extraction at 30°C, $n = 3$.

The CAR/PDMS fiber also exhibited higher extraction efficiency for NDEA and moderate to low efficiency for the large molecular size NDPA and NDDBA, owing to presence of a variety of pore sizes in the Carboxen material. These analytes, however, were more efficiently extracted with the fibers containing divinylbenzene/polydimethylsiloxane mixed-phase. DVB particles have a mesoporous structure with a moderate amount of macropores which enable extraction of the bigger size, more lipophilic NAs.

The extraction of NDBA, which was the heavier studied analyte and the one having the highest log K_{ow} , was much greater with the fibers containing DVB.

2.3.4 Extraction mode (CAR/PDMS fiber)

Selection of extraction mode in SPME is based on the analytes volatilities and sample matrix. Headspace extraction is preferable for volatiles and dirty samples to allow faster kinetics and to prevent fiber damage by fouling. For semi-volatiles and clean matrices such as drinking water direct immersion can be used. Figure 2.7 compares the headspace and direct immersion sampling of the NAs from spiked water sample (pH = 6.5) for 30 min pre-equilibrium extraction under similar experimental conditions. According to the SPME theory, the amount of analyte extracted by a fiber at equilibrium is independent of location of fiber, whether in the sample or its headspace. However, for pre-equilibrium extractions the amount extracted via the two modes may be different.

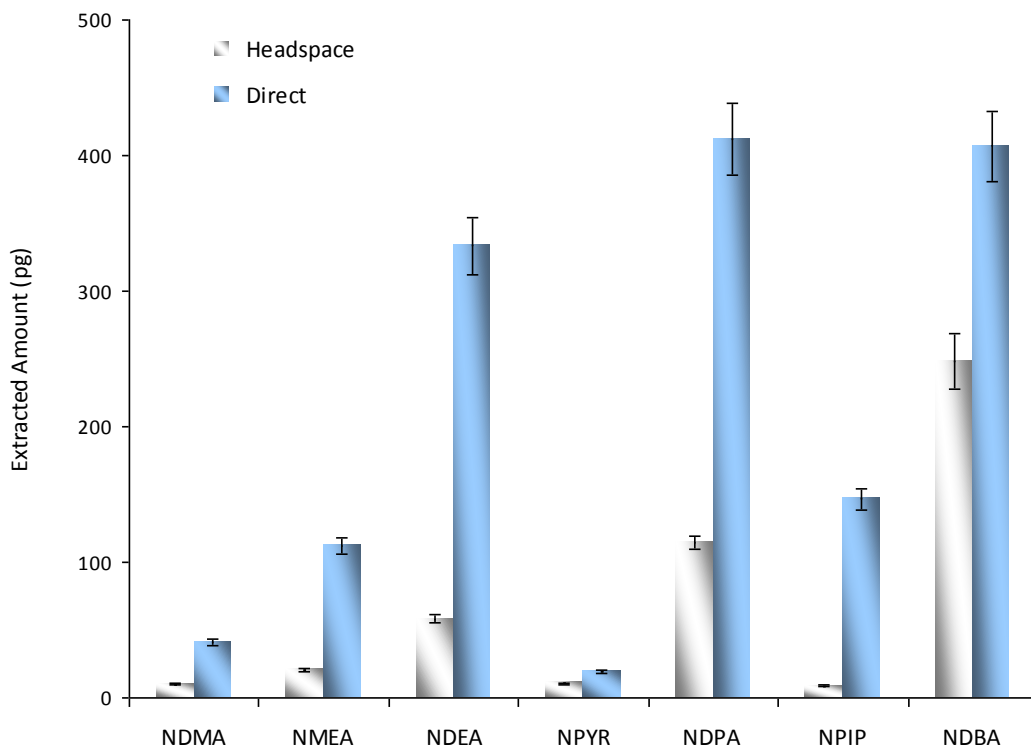


Figure 2.7 Direct versus headspace extraction of N–nitrosamines with CAR/PDMS fiber; 2 µg/L spiked water sample, 30 min extraction at 30°C, n = 3.

As is seen in Fig. 2.7, for 30 min sampling at 30°C the amounts of analytes extracted via direct immersion were considerably greater for all the analytes compared to the headspace mode. Since volatility of the target analytes was expected to increase at higher temperature, headspace extraction under increased temperatures was also investigated. Three temperatures of 30°C, 50°C and 70°C were compared. The results are presented in Fig. 2.8.

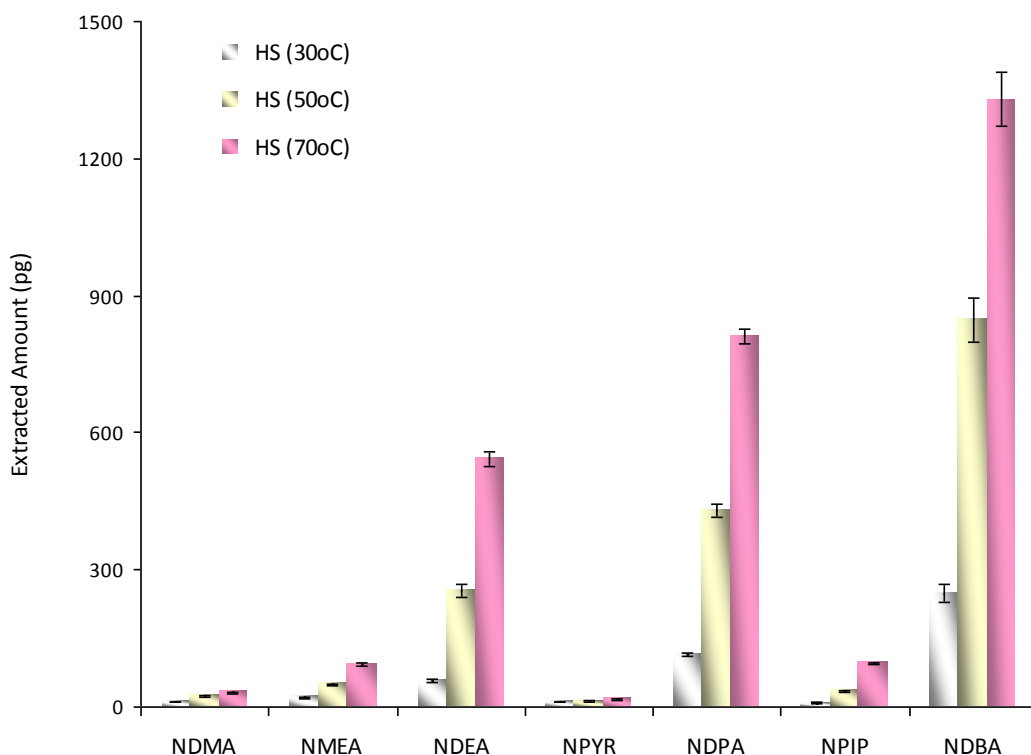


Figure 2.8 Headspace extraction of N–nitrosamines at different temperatures with CAR/PDMS fiber; 2 µg/L spiked water sample, 30 min extraction, n = 3.

As is seen, increasing the temperature caused increases in the amounts extracted in the headspace with the highest amounts at 70°C. However, for the highly soluble NAs (NDMA, NMEA and NPYR), the increased amounts were lower compared to the other analytes. These amounts were then compared with those of direct immersion at 30°C. As shown in Fig. 2.9, the results obtained by the two approaches were not significantly

different for the highly soluble NAs. Thus, the headspace extraction at elevated temperature appeared to offer no advantage over direct immersion for the very soluble NAs under the experimental conditioned used.

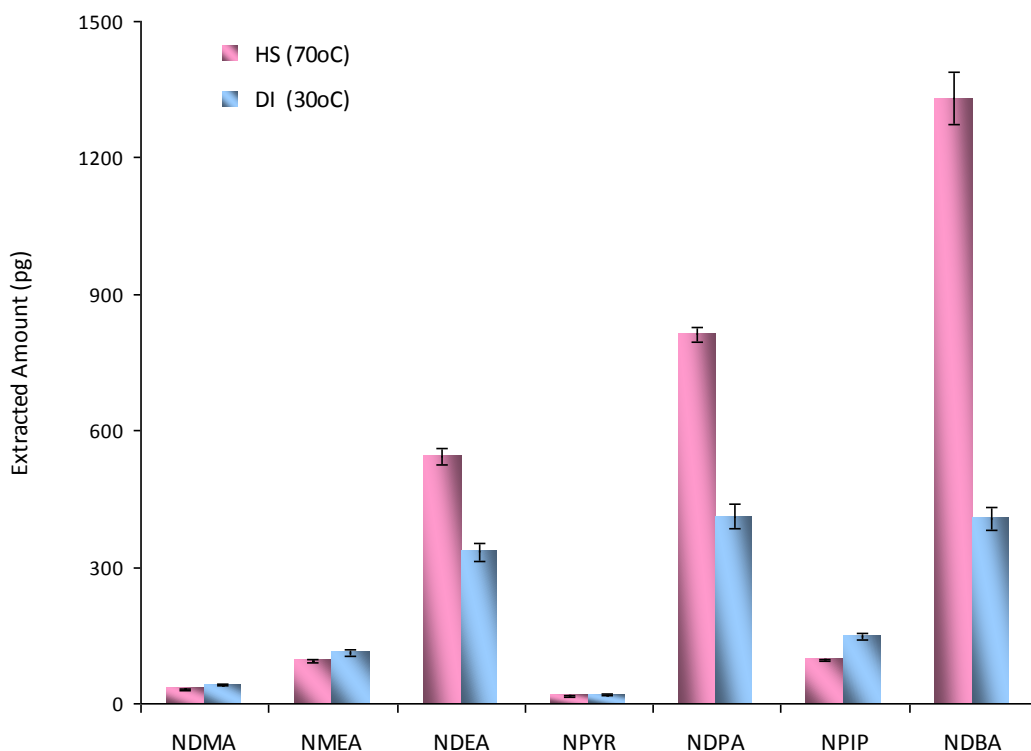


Figure 2.9 Direct versus headspace extraction (elevated temperature) of N–nitrosamines with CAR/PDMS fiber; 2 µg/L spiked water sample, 30 min extraction, n = 3.

2.3.5 Extraction time (CAR/PDMS fiber)

The equilibrium extraction is generally preferred in SPME process, owing to higher sensitivity and precision. When the equilibration times are too long for analytes, pre-equilibrium approach with shorter extraction time can be used for quantification purposes. To determine the length of time necessary for equilibrium extraction of the NAs, different extraction times were examined up to 960 min using CAR/PDMS fiber. The equilibration times appeared to be long and the extracted amounts by the fiber were

still progressively increasing after 960 min under the experimental conditions, as shown in Fig. 2.10. Prolonged equilibrium extraction times were also reported with the headspace extraction by other workers³¹. Therefore, to adopt a fast procedure, 30 min was selected as the extraction time. This time nearly matched the GC run time (28 min) allowing little gap between analyses.

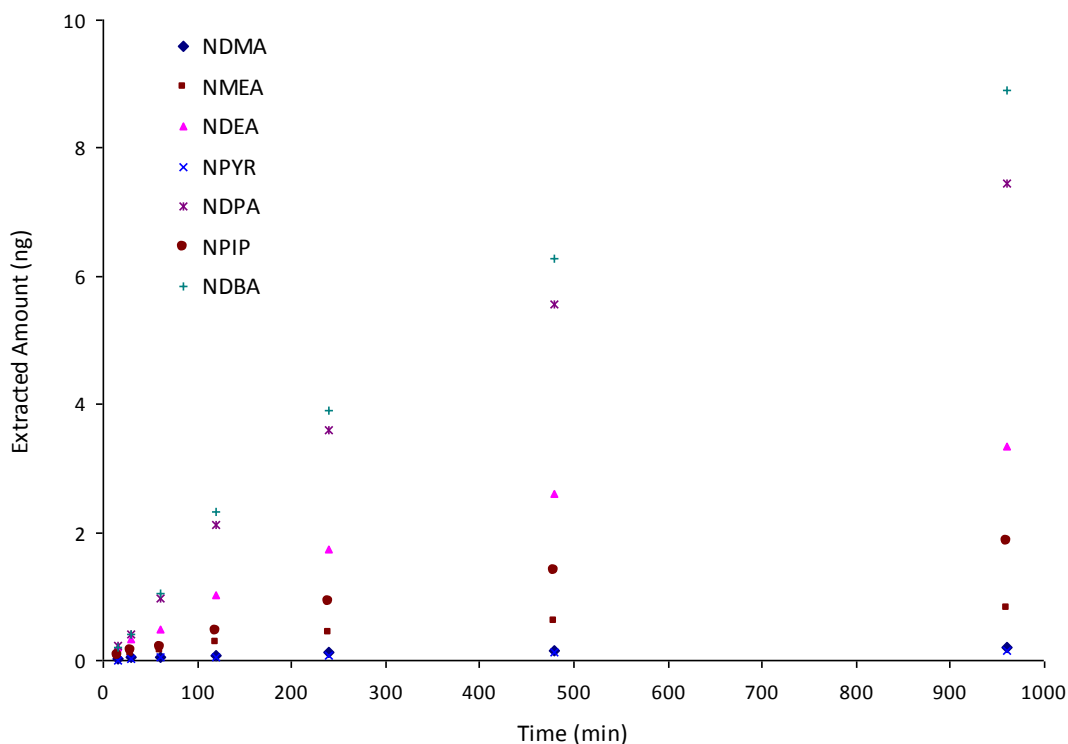


Figure 2.10 Extraction time profile of *N*-nitrosamines for direct immersion SPME with CAR/PDMS fiber; 2 $\mu\text{g/L}$ spiked water sample, extraction temperature 30°C, 250 rpm stirring rate.

2.3.6 pH effect

N-nitrosamines are very much weaker bases than the parent amines ($\sim 10^{10}$ less basic) and they undergo protonation only in super acid solutions³⁹⁻⁴⁰. As well, in alkaline solution, they exhibit very weak acidity of hydrogens at α -carbon positions⁴⁰.

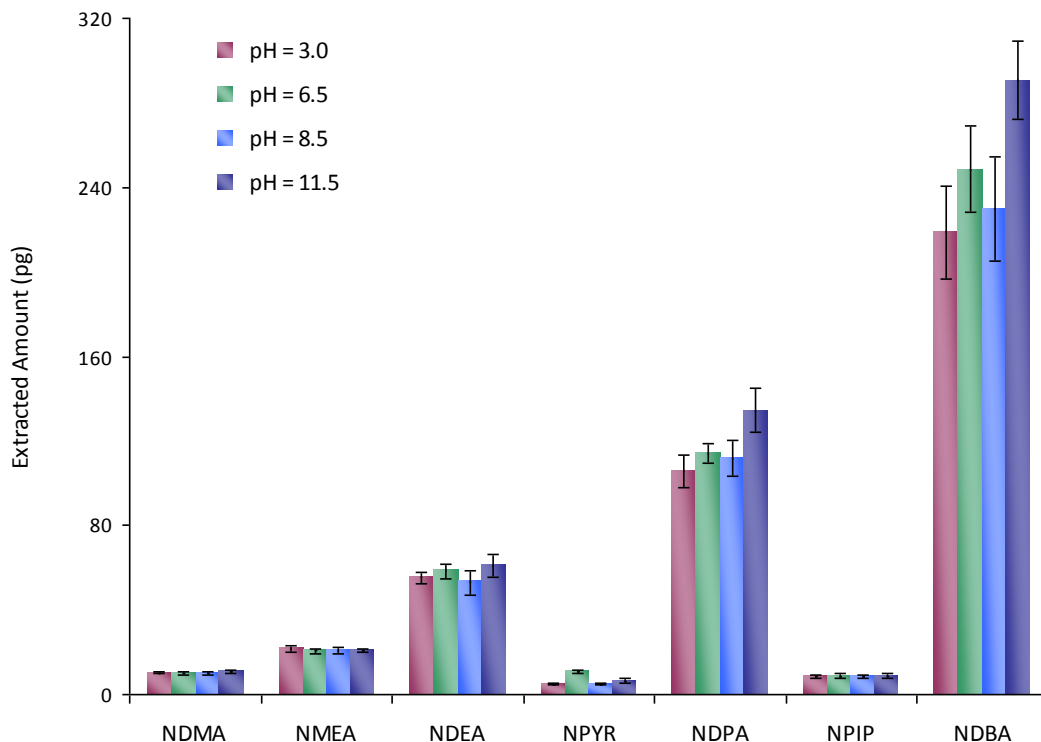


Figure 2.11 Effect of pH on the extraction of N-nitrosamines with CAR/PDMS fiber; 2 µg/L spiked water sample, 30 min headspace extraction at 30°C, n = 3.

To ensure that pH has no significant effect on the SPME extraction efficiency, four pH levels of 3, 6.5, 8.5 and 11.5 were studied under similar experimental conditions using CAR/PDMS fiber (Fig. 2.11). For comparison, headspace extraction was used to avoid damaging the fiber. The results confirmed that pH didn't have significant effect on the extraction of the analytes.

2.3.7 Salt addition effect

The effect of salt addition was also investigated for both direct and headspace extraction modes. It was found that 25% salt amount (~ 3.4 g NaCl in 10 mL water) had the highest effect on the extraction of small molecular size highly soluble N-nitrosamines. However, the effects were not similar for all the compounds. As shown in Fig. 2.12, for NDMA, NMEA and NPIP the extraction efficiency was increased by approximately a factor of 2 – 5 times for the headspace and 2 – 3 times for direct

immersion. For NDEA, an increase of more than 2 times in the extraction efficiency was observed with the headspace mode while there was no considerable change through the direct extraction. The change in the extracted amount due to salt addition was not substantial for NPYR, neither with the headspace nor with the direct immersion mode. For more lipophilic NDPA and NDBA, the extracted amount was increased with salt addition through headspace as roughly 4 and 3 times more, respectively. However, the efficiency was decreased with salt addition through direct mode by approximately 29% and 47%, respectively.

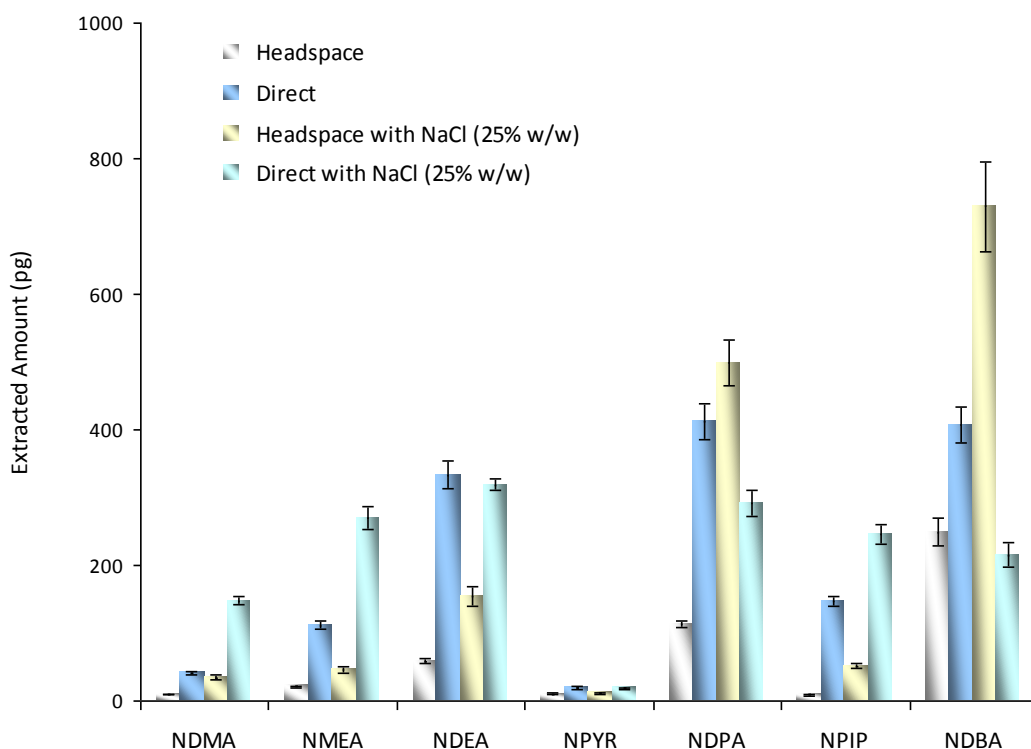


Figure 2.12 Effect of salt addition on the extraction of N-nitrosamines with CAR/PDMS fiber; 2 µg/L spiked water sample, 30 min extraction at 30°C, n = 3.

2.3.8 Thermal degradation on CAR/PDMS coating

Non polar organic compounds containing C-C and C-H bonds are usually stable toward GC hot injection temperatures. Polar molecules, on the other hand, especially

those with functional groups containing nitrogen and sulfur, contain weaker bonds in their structure and are prone to thermal degradation. In aliphatic and heterocyclic *N*-nitrosamines, for example, the N–NO bond enthalpies are of the order of 215–217 kJ/mol. These are considerably lower than the values for C–N, C–C or C–H bonds which lie in the range of 250–450 kJ/mol³⁹. Therefore, it was rational to consider likely degradation of the NAs during thermal desorption from the carbon-based CAR/PDMS coating, which requires around 300 °C for effective desorption of the analytes. To evaluate the possibility of thermal degradation, desorption of the analytes (25 ng) along with two thermally stable compounds, *p*-xylene and mesitylene (5 ng), pre-loaded by microsyringe on CAR/PDMS and PDMS/DVB coatings were investigated. The amounts desorbed were calibrated by GC liquid injections and the results were compared (Fig. 2.13).

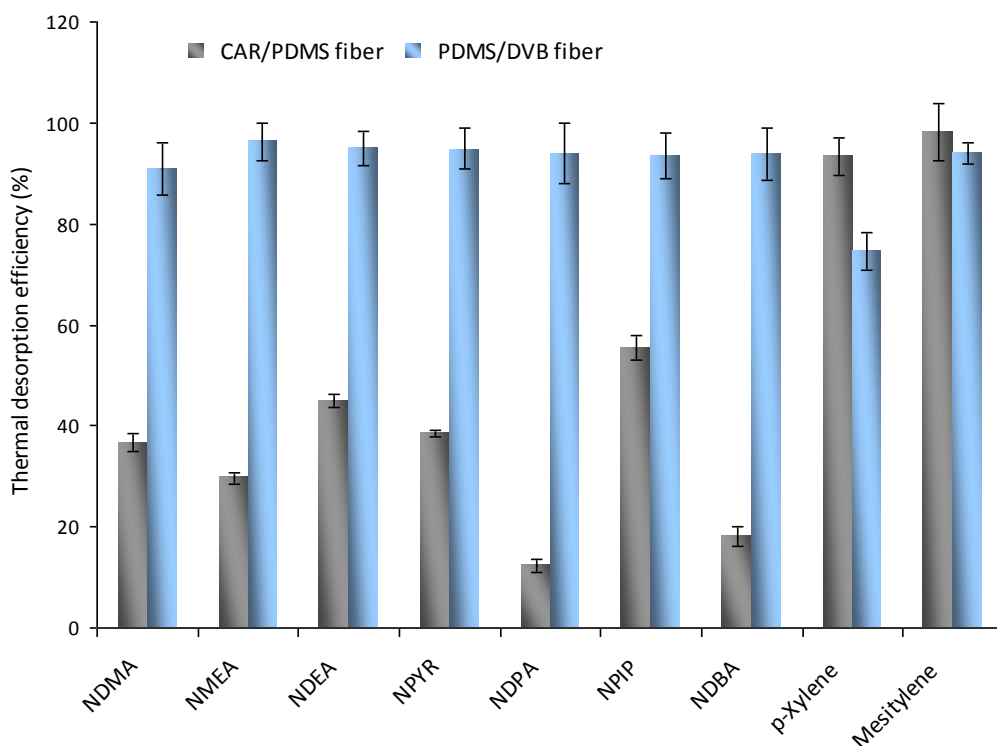


Figure 2.13 Thermal desorption efficiency of *N*-nitrosamines (25 ng), *p*-xylene and mesitylene (5 ng) from SPME fibers; direct loading, *n* = 3.

As can be seen from the graph in Fig. 2.13, the thermal desorption efficiencies of the N-nitrosamines from CAR/PDMS fiber were around 55% or lower while the desorption efficiencies from PDMS/DVB fiber were above 90%. On the other hand, the thermal desorption efficiency of *p*-xylene and mesitylene from CAR/PDMS fiber were above 94%. Additionally, the desorption efficiency of less volatile mesitylene from the both fibers were comparable with each other. These results collectively suggest that the N-nitrosamines are partially decomposed during thermal desorption from CAR/PDMS coating. Despite this fact, as will be described in the next section, the quantification of the analytes using CAR/PDMS fiber was satisfactory.

2.3.9 Analytical parameters (CAR/PDMS fiber)

The analytical performance of CAR/PDMS fiber for the extraction of the NAs from spiked water samples was evaluated in combination with GC/MS (Table 2.2). The calibration curves for the compounds were established in concentration ranges varying between 0.2 and 20 µg/L. All the compounds exhibited good linearity with correlation coefficients (R^2) exceeding 0.9946. The precision of the measurements represented by relative standard deviation percentage (RSD %) of three replicates ranged between 5 and 8 % at 2 µg/L spike level for the analytes. The method detection limits (MDLs) were determined as 3.14 times the standard deviation for seven replicates at low concentrations close to the detection limits. The analytical data in Table 2.2 indicate that quantification of the NAs using SPME/GC/MS with CAR/PDMS fiber is reliable. However, the method detection limits obtained with the fiber were far above the current regulatory levels of N-nitrosamines in drinking water. The detection limits of the analytes can be lowered instrumentally using more sensitive mass detection such as CI/MS/MS³⁰⁻³¹. Another approach to obtain lower detection limits is to increase extraction efficiency through development of a higher capacity sampling device of similar coating.

2.3.10 Precision and quality of spin coating

Initial work began with the assessment of precision and quality of spin coating. Particle-free PDMS (Sylgard 184) thin films were prepared at three different spin speeds (550, 650 and 750 rpm) and equal spin time (1min). After preparation and thermal curing,

Table 2.2 Analytical data for SPME-GC-MS of the N-nitrosamines (EPA 521) in water using CAR/PDMS fiber ^a

| Compound | Symbol | Linear range ($\mu\text{g/L}$) | Correlation coefficient (R^2) | MDL (ng/L) | RSD ^b (%) |
|---------------------------|--------|-------------------------------------|--------------------------------------|--------------------------|-------------------------|
| N-nitrosodimethylamine | NDMA | 0.5 – 20 | 0.9957 | 90 | 5 |
| N-nitrosomethylethylamine | NMEA | 0.5 – 20 | 0.9976 | 80 | 5 |
| N-nitrosodiethylamine | NDEA | 0.2 – 20 | 0.9992 | 70 | 6 |
| N-nitrosopyrrolidine | NPYR | 2.0 – 20 | 0.9946 | 680 | 8 |
| N-nitrosodipropylamine | NDPA | 0.2 – 20 | 0.9983 | 60 ^c | 6 |
| N-nitrosopiperidine | NPIP | 0.5 – 20 | 0.9955 | 110 | 5 |
| N-nitrosodibutylamine | NDBA | 0.2 – 20 | 0.9974 | 70 ^c | 6 |

^a Direct sampling from 10 mL spiked water samples at 30 °C, 30 min, 25% w/w NaCl.

^b Relative standard deviation (n=3) for 2 $\mu\text{g/L}$ spiked water sample.

^c Without salt effect.

the PDMS thin films were separated from the surface of wafers and transferred over a flat narrow sheet of Teflon. Area cuts of constant size (round-shape, 1cm i.d.) were made on the thin films along with the support sheet at 5 different locations on each sample using a cutting tool. The area cuts were then separated from the Teflon support and measured by weigh and thickness.

Table 2.3 Precision of PDMS thin film preparation by spin coating

| Spin speed (rpm) | Sample cut average wt (mg) | RSD% (n=5) | Average thickness (µm) |
|------------------|----------------------------|------------|------------------------|
| 550 | 9.5 | 2 | 120 |
| 650 | 8.2 | 1 | 101 |
| 750 | 6.6 | 1 | 84 |

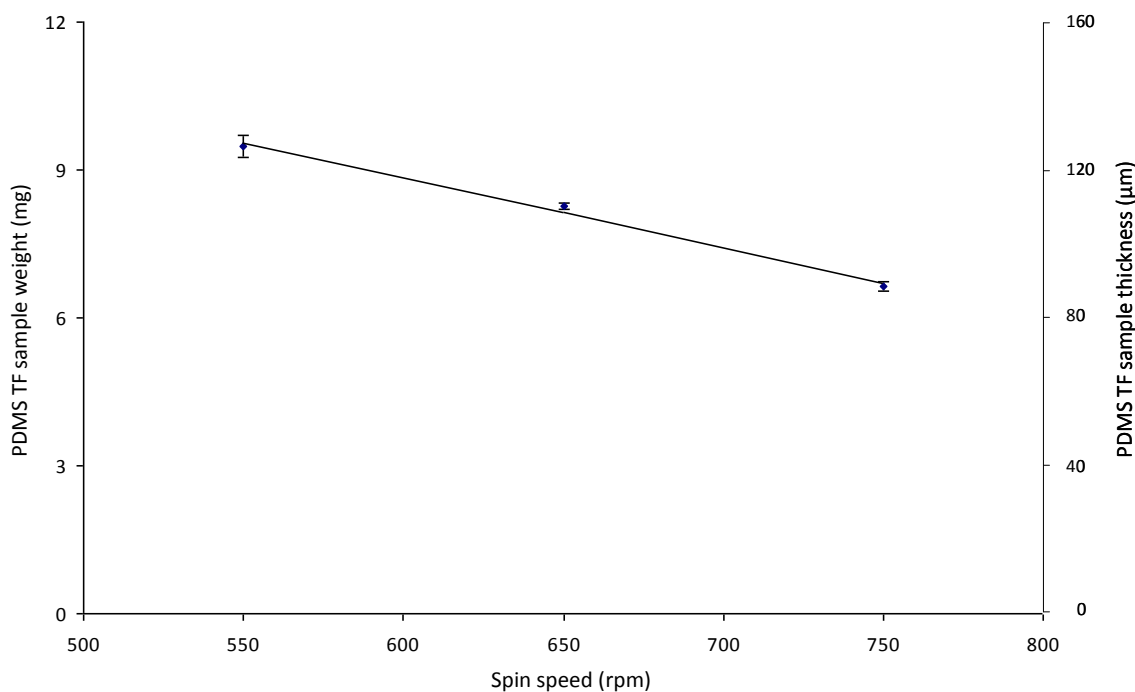


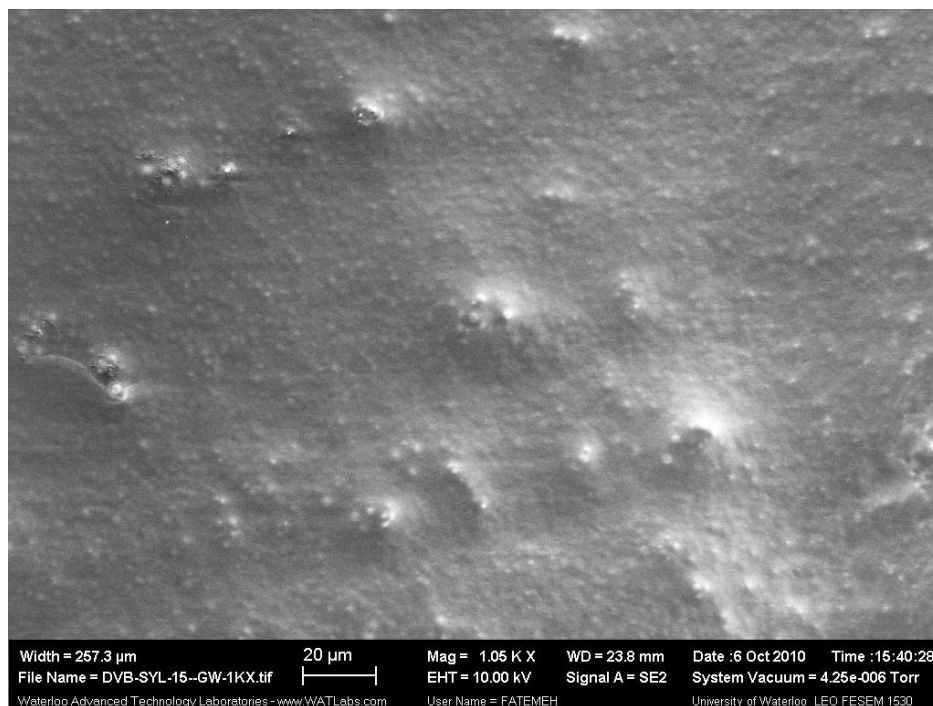
Figure 2.14 PDMS thin film sample cut weight/thickness versus spin speed (n = 5).

As shown by the results in Table 2.3, spin coating produced PDMS thin films of excellent uniformity with a thickness variation of 2% or less ($n = 5$) within the film. Additionally, as shown in Fig. 2.14, higher spin speeds led to thinner thin film samples. Each 100 rpm increase in spin speed caused a resulting thickness decrease of approximately 16-17%.

2.3.11 Development of mixed-phase thin film (MPTF) devices

In the course of preparation of the MPTF devices, several different particle-to-PDMS ratios were tested. Figure 2.15 shows SEM images of the PDMS/DVB thin film samples prepared at 0.15 and 0.20 w/w ratios by spin coating technique. These images exemplify the surface characteristic of the samples of lower particle contents. The particles are well-dispersed in the samples, though not clearly visible due to larger amounts of PDMS. In these samples, the PDMS elasticity and strength were less affected by mixing with the particles. On the other hand, the MPTF coatings prepared with higher loads of particles exhibited poor elasticity and cohesion, to the extent that they were not practical without a support. Therefore, an inert thermally resistant support needed to be devised in order to make such MPTF devices. In search for a suitable support, thin samples of stainless-steel mesh, Teflon sheet and glass wool fabric mesh were examined. Among these, the latter was found to be a better support with more flexibility and ease of handling during extraction and analysis. Since one of the objectives of this work was to compare the extraction efficiencies of MPTF devices with those of the commercial SPME fibers, samples were prepared with particles-to-PDMS ratios similar to those of commercial fiber coatings using the mesh support. Figures 2.16-2.18 present SEM images of the prepared CAR/PDMS and PDMS/DVB MPTF devices which were fabricated using spin coating technique. As shown, the coatings were quite uniform and the particles were tightly dispersed in PDMS. The particles and their porous surface are clearly visible in some images, owing to relatively lower amounts of PDMS in these samples. Both Carboxen and DVB particles are shown to be spherical with a diameter of less than 5 μm .

(A)



(B)

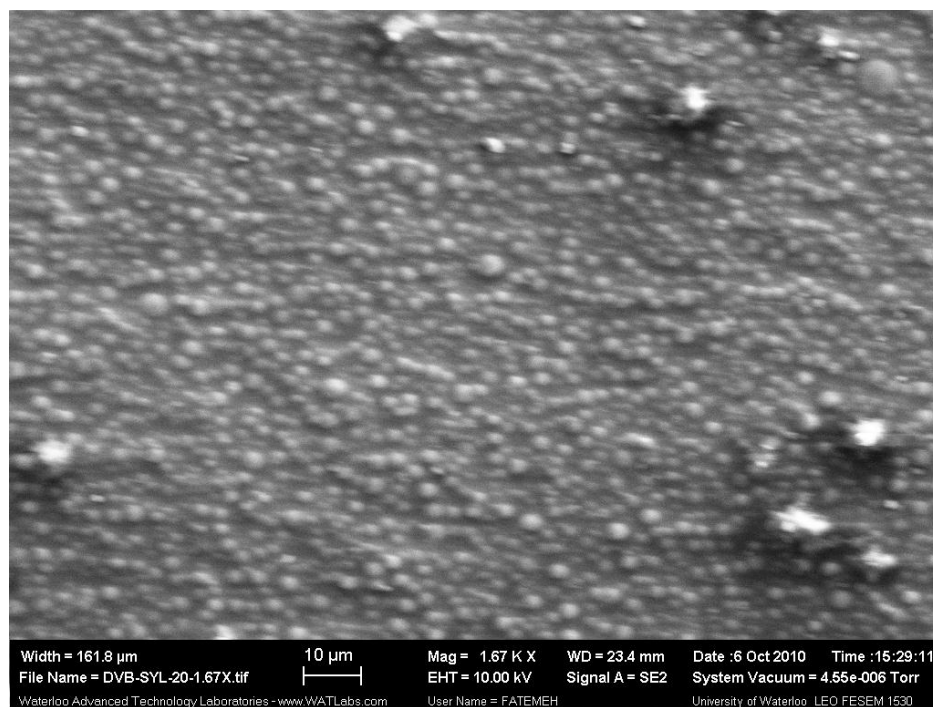


Figure 2.15 SEM surface images of PDMS/DVB thin films; (A) 0.15 w/w, (B) 0.20 w/w particle-to-PDMS ratio.

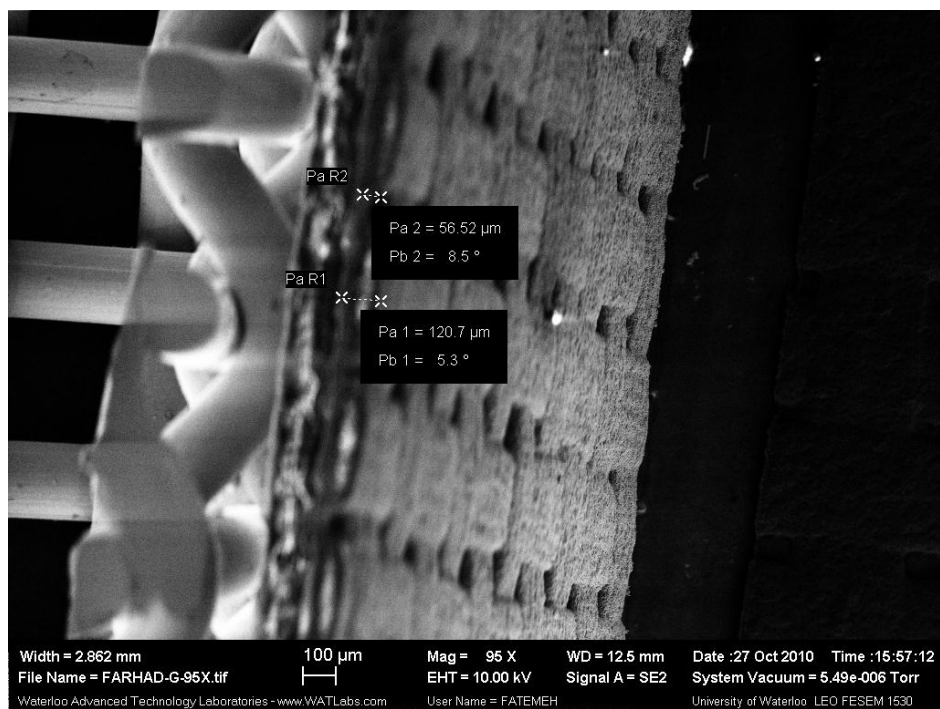
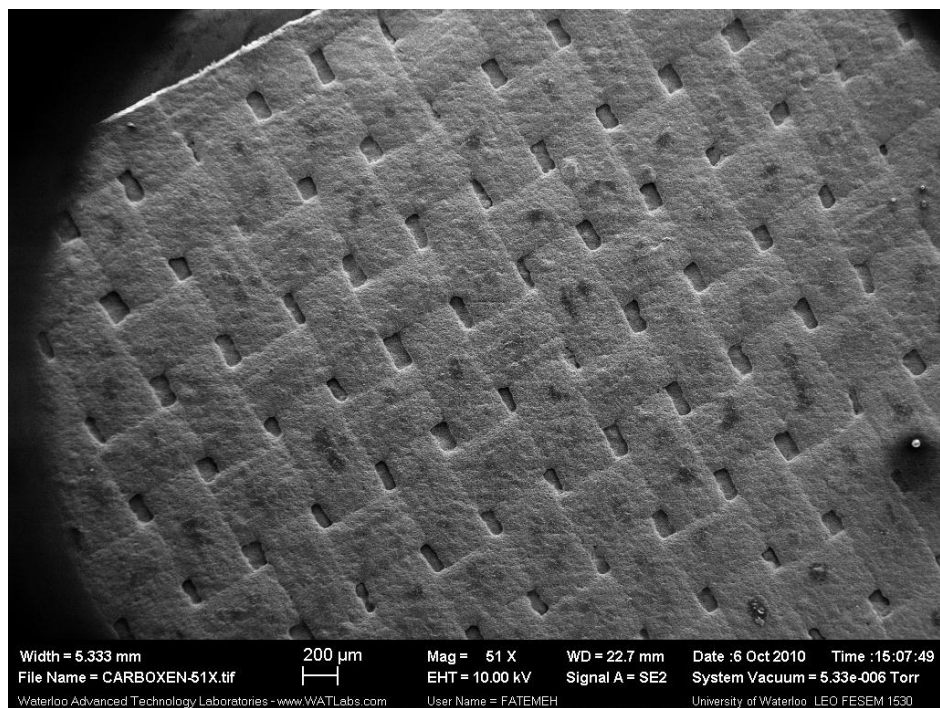


Figure 2.16 SEM images of CAR/PDMS mixed-phase thin film device using GW fabric mesh; particle-to-PDMS ratio equal to that of the commercial fiber coating.

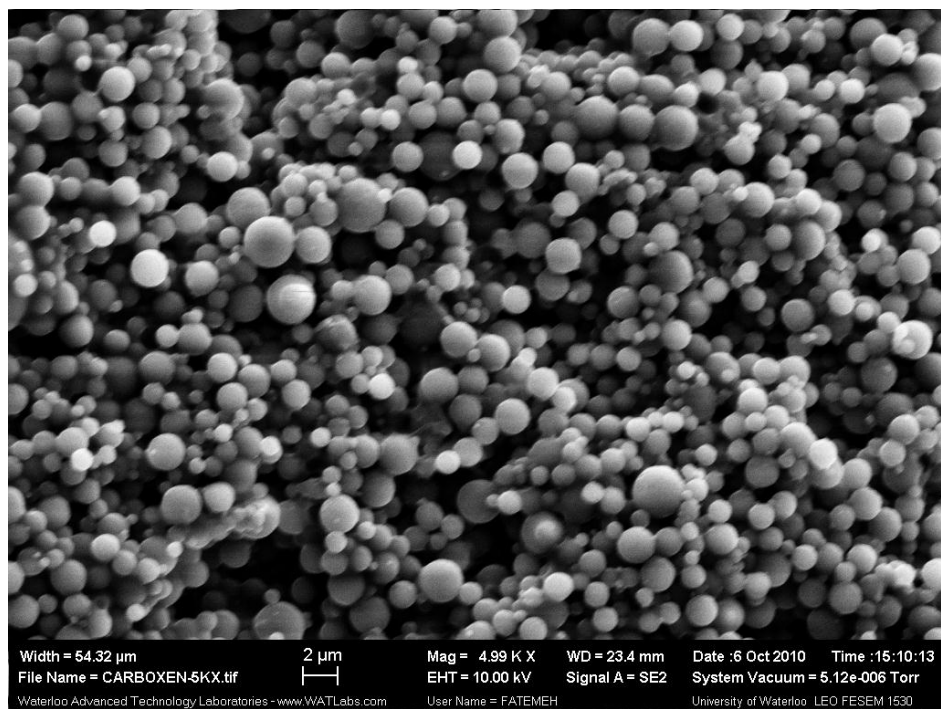
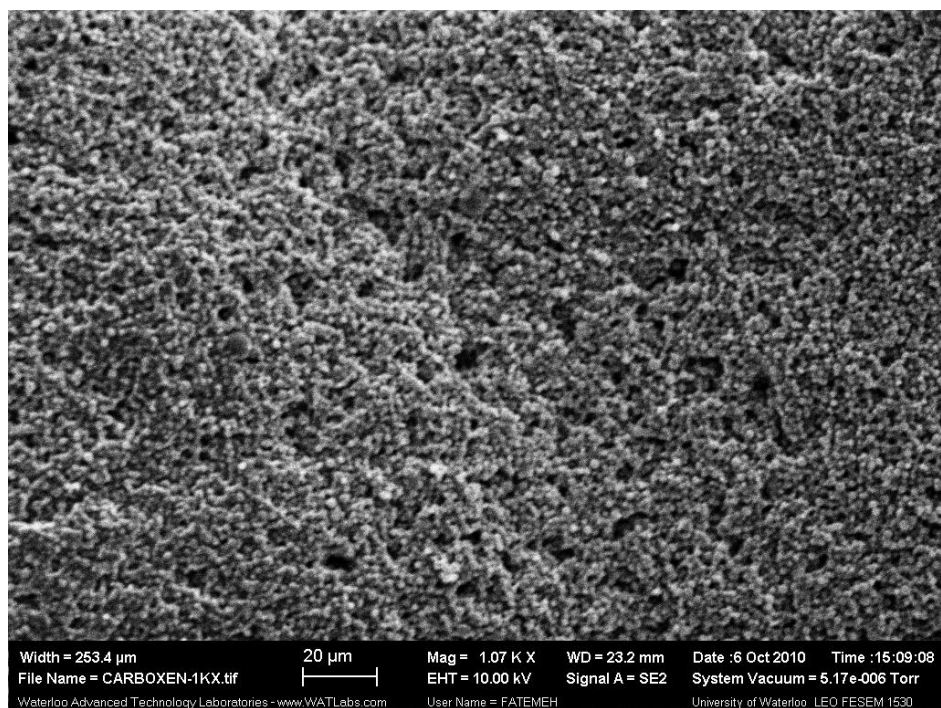


Figure 2.17 SEM surface images of CAR/PDMS mixed-phase thin film device; particle-to-PDMS ratio equal to that of the similar commercial fiber coating.

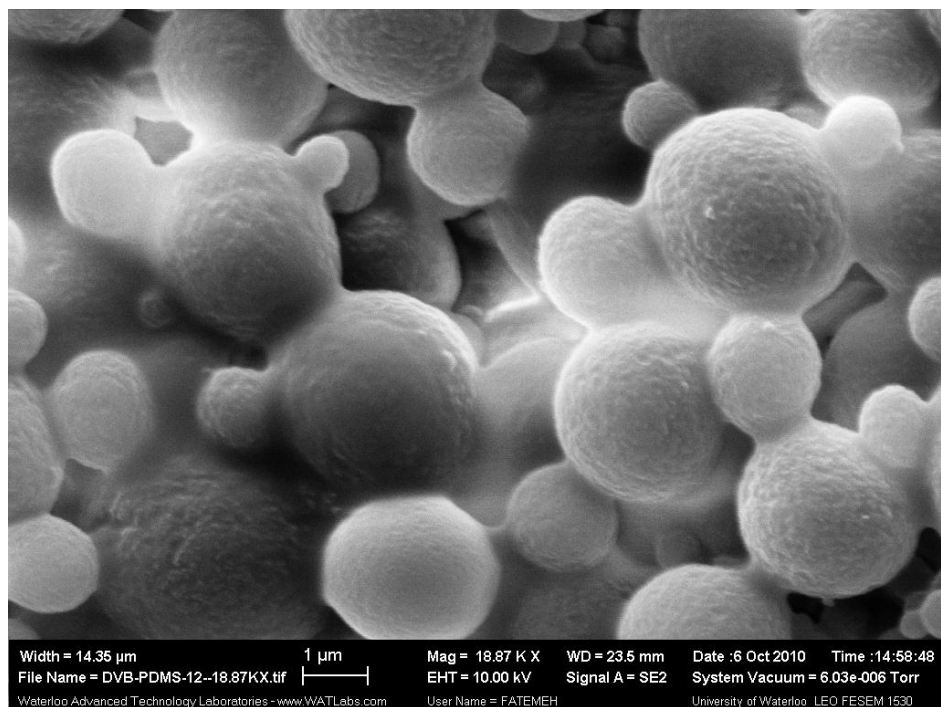
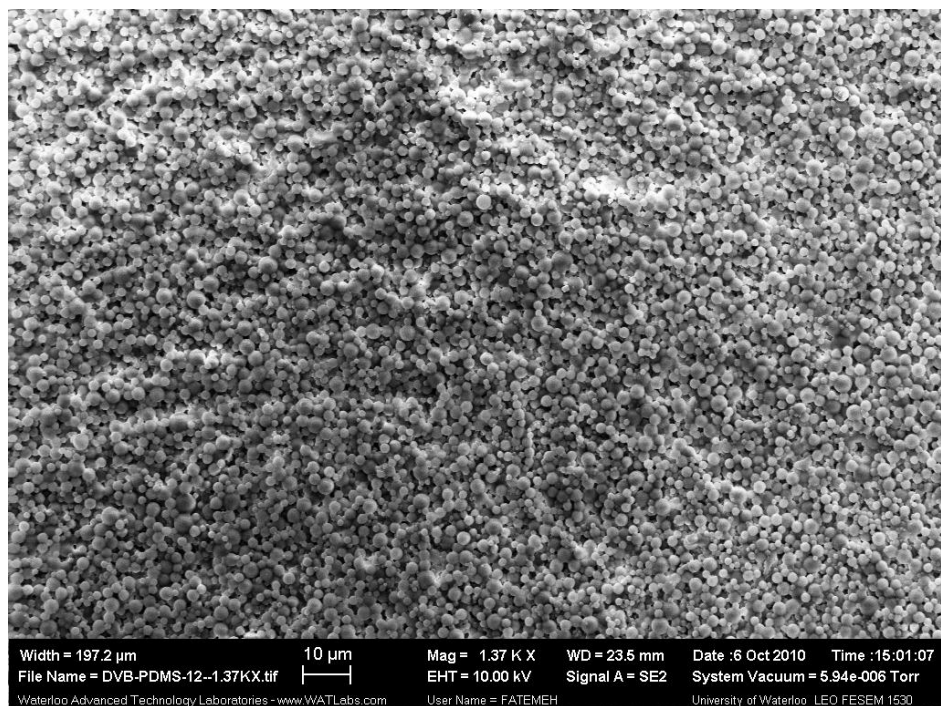


Figure 2.18 SEM surface images of PDMS/DVB mixed-phase thin film device; particle-to-PDMS ratio equal to that of the similar commercial fiber coating.

2.3.12 Thin film reinforcement by incorporation of glass wool fabric mesh

The incorporation of glass wool fabric mesh in the structure of thin film device, developed in this research, also addressed the problem of thin film sampler twisting during extraction with high rotational speed, which is encountered with commercial PDMS thin film membranes. These samplers are too much flexible and cannot maintain a flat-shape at rotational speeds commonly used for extraction³⁴. This causes a reduction in effective extraction surface area and consequently a decrease in the extraction rate³⁴. As a result, an extra framed holder is necessary in order to preserve the flat-shape of these thin film samplers during extraction³⁴. In an assessment of the flat-shape stability during rotation in water, it was observed that the commercial PDMS thin film (75 μ m) began to twist around itself even at a low stirring rate of 50 rpm. However, a PDMS sampler of similar thickness fabricated with the glass wool fabric mesh preserved its absolute flat-shape up to 800 rpm stirring and only slightly twisted at 2000 rpm. Similar stabilities were observed of the MPTF devices during rotation in water (see Appendices A-C for a video illustration). This contribution is clearly an advantage for fast active thin film microextraction by obviating the need for a framed holder during extraction.

2.3.13 Analytical performance of MPTF technique

2.3.13.1 Stability and extraction repeatability of MPTFs

The stability of the coating is an important factor in the performance of MPTF devices. The MPTF samplers fabricated in this research exhibited good mechanical stability during extraction and analysis. No cracking of the coating was observed due to stirring and the particles were not detached from the coatings during extraction. Further, the MPTF devices showed no deterioration after 50 times extraction. Another key factor which ensures the practicability of MPTF devices as analytical tools is the repeatability of extraction. Figures 2.19 A and B show the percent relative standard deviations (RSD %) for replicate extractions of the NAs from water ($n = 7$) by the CAR/PDMS and PDMS/DVB TFs, respectively. As shown, the devices exhibited good extraction repeatability for the analytes with RSD% range of 3–8% and 2–5%, respectively.

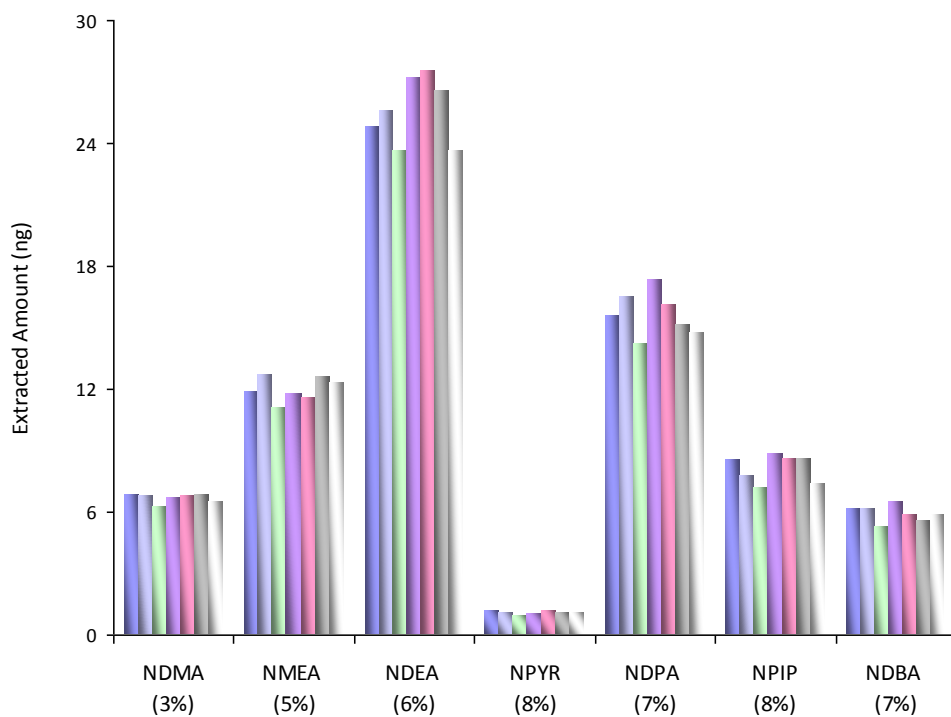
2.3.13.2 Extraction time profiles of *N*-nitrosamines with MPTFs

Extraction time profiles of the NAs using the MPTFs were investigated up to 16 hours. Three replicates, whose RSD were below 10%, were performed for each extraction time. The profiles for the CAR/PDMS TF and the PDMS/DVB TF are shown in Fig. 2.20 A and B, respectively. The equilibration times using the CAR/PDMS TF were generally long and not completely achieved for all analytes after 16 hours. However, in contrast with the SPME fiber, for some analytes (NDMA, NMEA, NDPA, NDBA) the extracted amounts decreased after 2 hours and the equilibrium appeared to have reached in 4 hours. This can be attributed to the difference between the geometries of the two devices, which affect the kinetics of extractions. In the case of the PDMS/DVB TF, the equilibration times for the extraction of more lipophilic NAs (NDPA, NDBA) were again long and not fully achieved after 16 hours (Fig. 2.20 B). As a result, pre-equilibrium approach with a shorter extraction time (30 min) was still preferable with the MPTS devices.

2.3.13.3 Extraction efficiencies of MPTFs versus SPME fibers and PDMS thin film

The extracted amount of analyte is affected by several factors, including distribution coefficient between extraction phase and sample matrix, extraction phase and sample volumes, concentration of the analyte in the sample and duration of extraction as long as equilibrium condition does not exist. To obtain an estimate of comparative efficiencies of the MPTF devices with those of SPME fibers, the extracted amounts were compared under similar experimental conditions except for sample volumes which were 240 mL and 10 mL for the MPTF devices and the SPME fibers, respectively. As shown in Fig. 2.21 A and B, a marked difference in the extraction efficiencies was observed, with more than one order of magnitude enhancement by the MPTF devices in most cases, including the hydrophilic analytes. This can be attributed to the increase in the extraction phase volume in the MPTFs, which was estimated to be 40 and 50 times higher than the volumes of CAR/PDMS and PDMS/DVB fiber coatings, respectively. In another assessment, the efficiencies of the PDMS/DVB TF and a commercial PDMS TF were compared for the extraction of NDPA and NDBA, the NAs having the highest log K_{ow} values in the group, under similar experimental conditions. Figures 2.22 A and B present the extraction time profiles of the two analytes using the commercial PDMS thin film

(A)



(B)

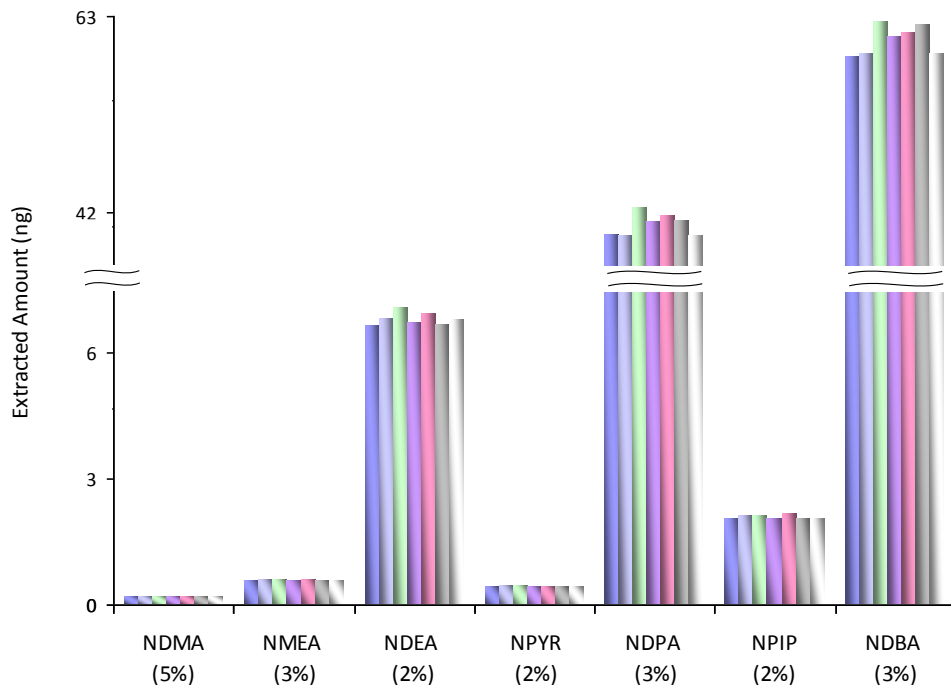
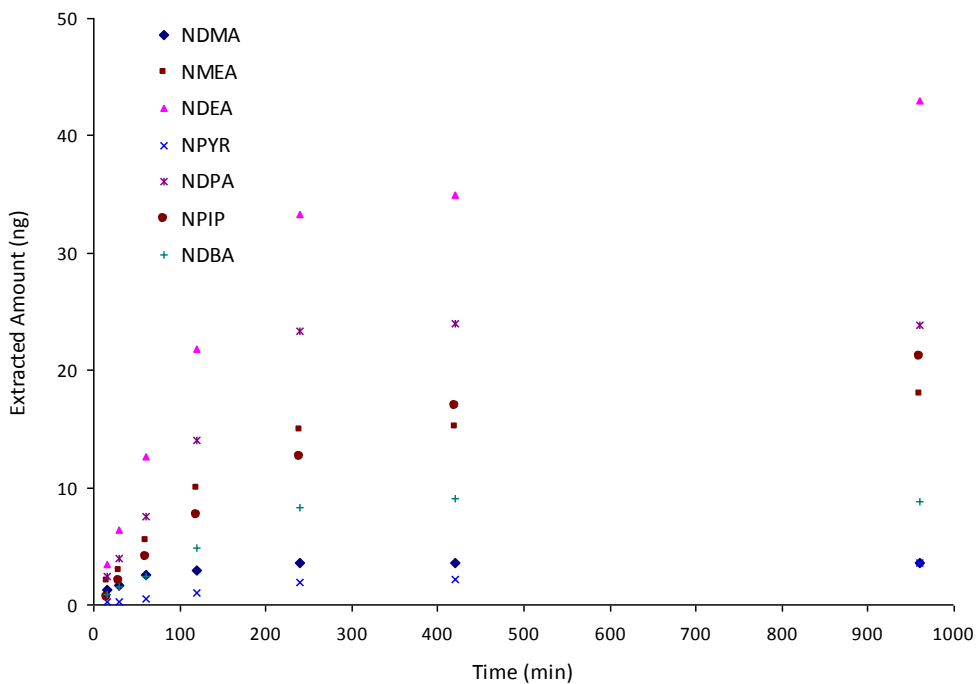


Figure 2.19 Repeatability of extraction using MPTF devices; (A) CAR/PDMS TF, (B) PDMS/DVB TF; 2 $\mu\text{g/L}$ *N*-nitrosamines in water, 30 min extraction room temp., $n = 7$.

(A)



(B)

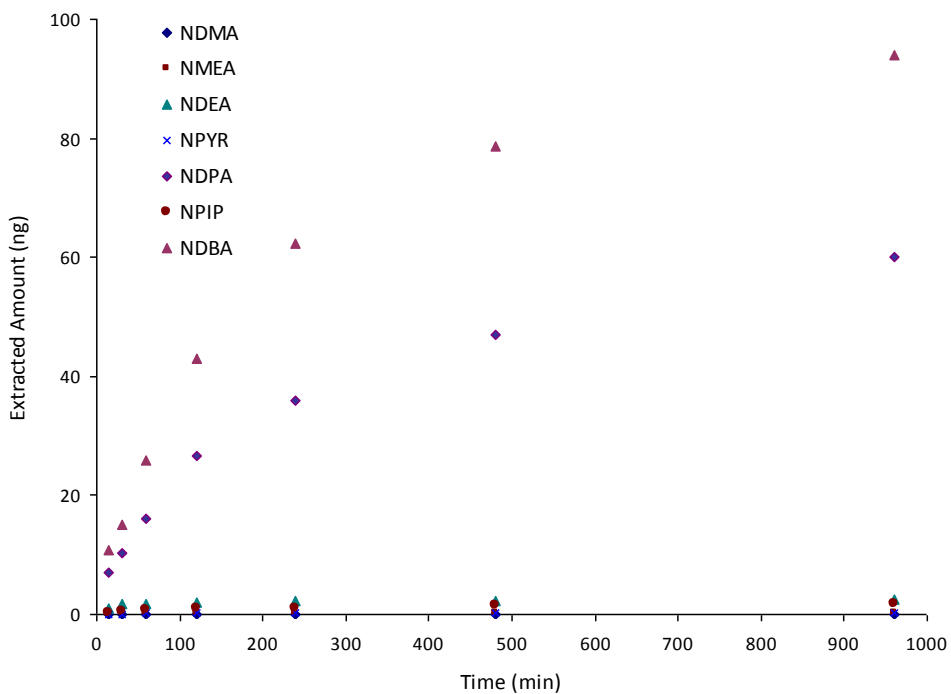
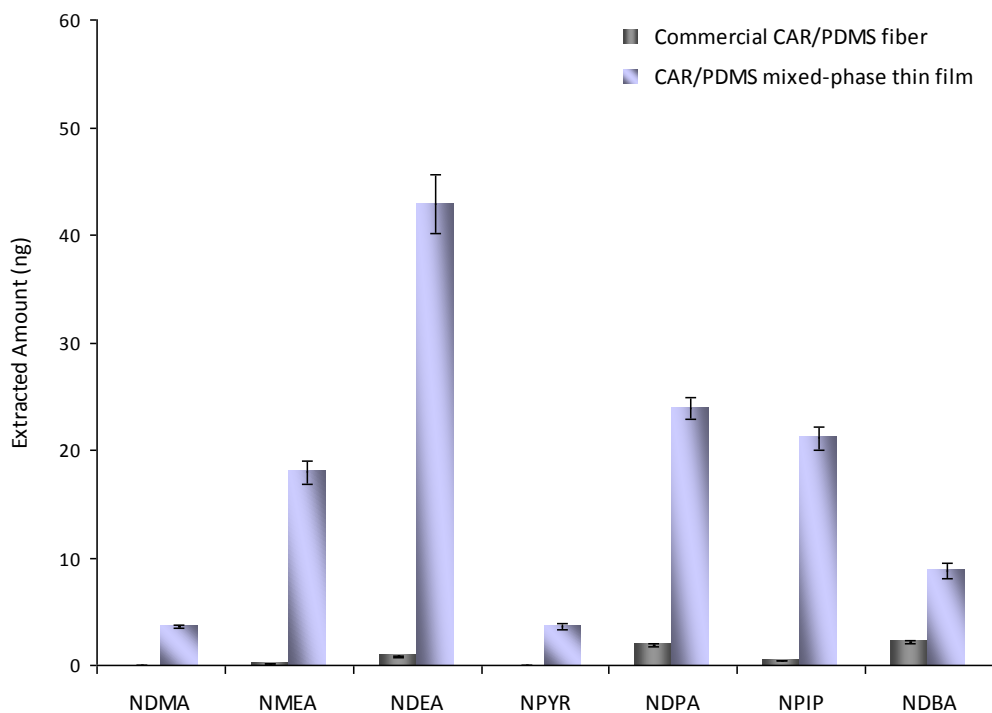


Figure 2.20 Extraction time profiles of *N*-nitrosamines in water with MPTF devices; (A) CAR/PDMS TF, (B) PDMS/DVB TF; 500 ng/L spiked water sample, room temp, 250 rpm.

(A)



(B)

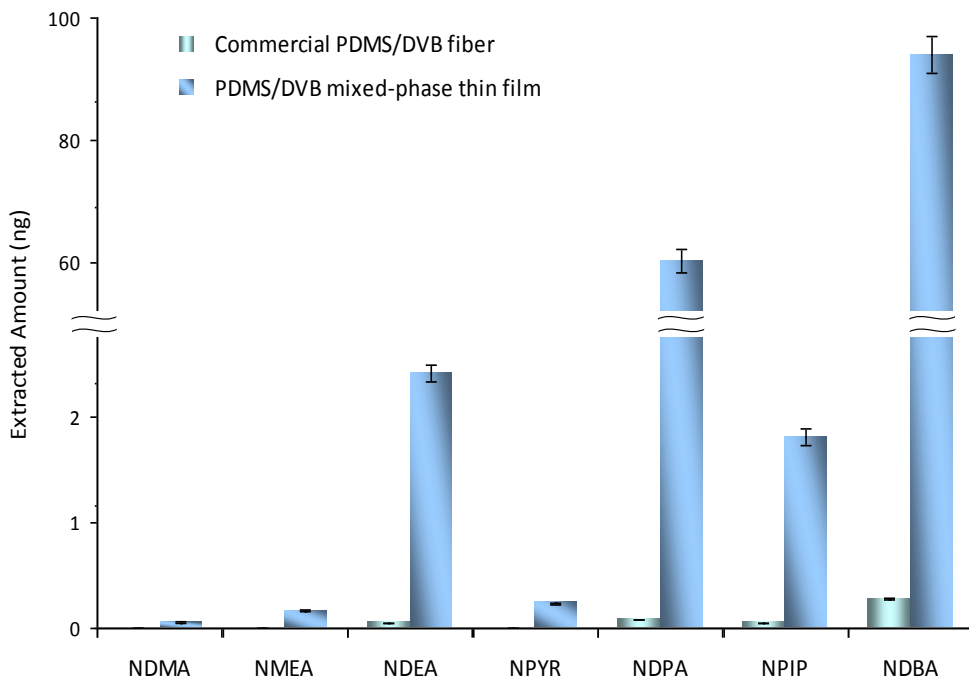
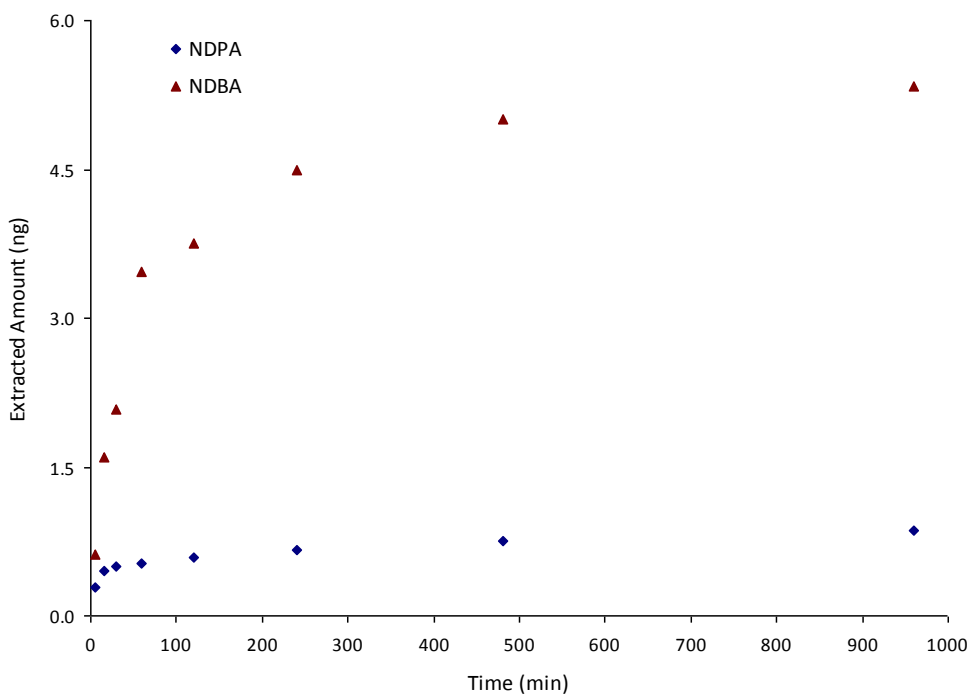


Figure 2.21 Extraction efficiencies of MPTF device vs. SPME fiber; (A) CAR/ PDMS coating, (B) PDMS/ DVB coating; 500 ng/L *N*-nitrosamines in water, 16 h, room temp.

(A)



(B)

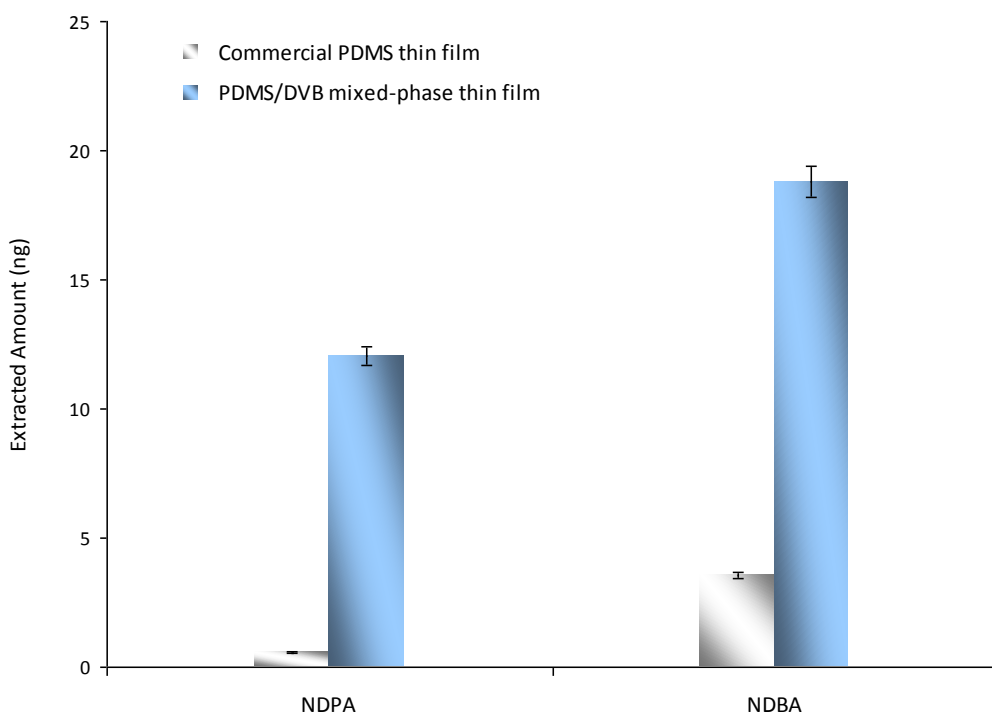


Figure 2.22 (A) Extraction time profiles of NDPA and NDBA in water with commercial PDMS thin film; (B) Extraction efficiency of PDMS/DVB TF vs. commercial PDMS TF; (A, B) 100 ng/L spiked water sample, 250 rpm; (B) 16 h, room temp.

sampler and the comparative extraction efficiencies of the two devices, respectively. As shown in Fig. 2.22 B, the PDMS/DVB TF was several times to more than of one order of magnitude more efficient for the extraction of the analytes compared to the commercial PDMS TF.

2.3.13.4 Linearity and lowest detectable levels using MPTFs

Table 2.3 lists analytical parameters for the extraction of the NAs from spiked water samples using the MPTFs combined with GC/MS. The calibration curves for the compounds were established in concentration ranges varying between 0.01 and 5 µg/L, depending on the analyte and the type of coating. Good linearities were obtained with both CAR/PDMS and PDMS/DVB TFs with correlation coefficients (R^2) exceeding 0.9923 and 0.9962, respectively. The lowest detectable level (LDL) for NDEA, NPIP, NDMA and NMEA were in the range of 2-10 ng/L using CAR/PDMS TF. The LDLs for NDPA and NDBA were 3 ng/L and for NPYR 40 ng/L using PDMS/DVB TF. These LDLs were a result of detector signal responses at low concentrations that were 3 times the noise level (signal-to-noise ratios of 3). The precision of the technique represented by relative standard deviation percentage (RSD %) of seven replicates at 2 µg/L spike level was 8 % or better for the CAR/PDMS TF and 5 % or better for PDMS/DVB TF. The analytical data in Table 2.3 indicate that quantification of the NAs using MPTF technique is reliable and more sensitive than SPME fibers for the determination of the NAs in water.

2.4 Conclusions

A new technique for sample preparation and trace analysis of organic pollutants in water using mixed-phase thin film (MPTF) devices, combined with direct thermal desorption, cold trapping, gas chromatography-mass spectrometry was presented. Highly particle-loaded Carboxen/PDMS and PDMS/DVB thin film samplers coated on a deactivated glass wool fabric mesh substrate by spin coating were developed. The MPTF samplers were easy to prepare by spin coating and could be tailored in thickness by the spin procedure and in size and shape by cutting tools. The samplers were durable and

exhibited enhanced flat-shape stability induced by incorporation of glass wool fabric mesh in their thin film structure. This characteristic is advantageous in that it makes the sampler more robust and user-friendly and obviates the need for a framed thin film holder to maintain enhanced extraction kinetics. The results of this study firmly establish analytical performance of the novel MPTF samplers and marked enhancement of sensitivity over the fiber approach. On the basis of ease of preparation, proved analytical performance, higher sensitivity and wider range of application offered by mixed-phase coatings, the novel MPTF devices are promising for rapid sampling and sample preparation of trace levels of polar organic pollutants in water. The user-friendly format and robustness of the novel devices are also advantageous for on-site applications, which is the ultimate use of thin film samplers. Additionally, the thin film fabrication approach developed in this study offers the possibility of making other novel samplers with PDMS or different absorptive polymers such as polyacrylate (PA) and polyethylene glycol (PEG) as particle-free, or as particle-loaded thin films with a variety of adsorptive solid particles.

Table 2.3 Analytical data for TFME-GC-MS of the N-nitrosamines (EPA 521) in water using mixed-phase thin films[†]

| Compound | Linear range (µg/L) | | Correlation coefficient (R ²) | | LDL (ng/L) | | Repeatability (RSD %) [‡] | |
|----------|---------------------|----------|---|----------|------------|----------|------------------------------------|----------|
| | CAR/PDMS | PDMS/DVB | CAR/PDMS | PDMS/DVB | CAR/PDMS | PDMS/DVB | CAR/PDMS | PDMS/DVB |
| NDMA | 0.04 – 2 | 0.50 – 5 | 0.9974 | 0.9969 | 10 | 160 | 3 | 5 |
| NMEA | 0.04 – 5 | 0.20 – 5 | 0.9935 | 0.9963 | 10 | 70 | 5 | 3 |
| NDEA | 0.01 – 5 | 0.02 – 2 | 0.9979 | 0.9962 | 2 | 7 | 6 | 2 |
| NPYR | 0.20 – 5 | 0.10 – 5 | 0.9923 | 0.9975 | 70 | 40 | 8 | 2 |
| NDPA | 0.02 – 5 | 0.01 – 2 | 0.9989 | 0.9992 | 7 | 3 | 7 | 3 |
| NPIP | 0.02 – 5 | 0.10 – 5 | 0.9984 | 0.9995 | 7 | 20 | 8 | 2 |
| NDBA | 0.10 – 2 | 0.01 – 2 | 0.9991 | 0.9981 | 20 | 3 | 7 | 2 |

[†] Direct sampling from 240 mL spiked water samples at room temperature, 30 min.

[‡] Relative standard deviation (n=7) for 2 µg/L spiked water sample.

2.5 Reference

1. U.S. EPA Integrated Risk Information System (IRIS), 2011. Available on-line at: <http://www.epa.gov/iris/index.html> [Last updated: 03 October 2009; accessed: 6 October 2011].
2. Jobb DB, Hunsinger RB, Meresz O, Taguchi V. 1994. Removal of N-nitrosodimethylamine from the Ohsweken (Six Nations) water supply: Final report. Ontario Ministry of Environment and Energy, Toronto, ON, ISBN 0-7778-3439-1.
3. Health Canada, 2011. N-Nitrosodimethylamine (NDMA) in Drinking Water. Available on-line at: http://www.hc-sc.gc.ca/ewh-semt/consult/_2010/ndma/draft-ebauche-eng.php [Last modified: 21 April 2010; accessed: 6 October 2011].
4. Richardson SD. 2003. Disinfection by-products and other emerging contaminants in drinking water. *Trends Anal. Chem.* 22(10): 666–684.
5. Charrois JW, Arend MW, Froese KL, Hrudey SE. 2004. Detecting N-nitrosamines in drinking water at nanogram per liter levels using ammonia positive chemical ionization. *Environ. Sci. Technol.* 38: 4835–4841.
6. Zhao YY, Boyd J, Hrudey SE, Li XF. 2006. Characterization of new nitrosamines in drinking water using liquid chromatography tandem mass spectrometry. *Environ. Sci. Technol.* 40: 7636–7641.
7. Zhao YY, Boyd JM, Woodbeck M, Andrews RC, Qin F, Hrudey SE, Li XF. 2008. Formation of N-nitrosamines from eleven disinfection treatments of seven different surface waters. *Environ. Sci. Technol.* 42: 4857–4862.

8. Planas C, Palacios O, Ventura F, Rivera J, Caixach J. 2008. Analysis of nitrosamines in water by automated SPE and isotope dilution GC/HRMS. *Talanta* 76(4): 906–913.
9. Pozzi R, Bocchini P, Pinelli F, Galletti GC. 2011. Determination of nitrosamines in water by gas chromatography/chemical ionization/selective ion trapping mass spectrometry. *J. Chromatogr. A* 1218(14): 1808–1814.
10. Mitch WA, Sedlak DL. 2002. Factors controlling nitrosamine formation during wastewater chlorination. *Water Sci. Technol. Water Supply* 2(3): 191–198.
11. Taguchi VY, Jenkins SWD, Wang DT, Palmentier JPPF, Reiner EJ. 1994. Determination of N-nitrosodimethylamine by isotope dilution, high-resolution mass spectrometry. *Can. J. Appl. Spectrosc.* 39(3): 87–93.
12. Health Canada, 2010. Guidelines for Canadian Drinking Water Quality: Guideline Technical Document – N-Nitrosodimethylamine. Water, Air and Climate Change Bureau, Healthy Environments and Consumer Safety Branch, Health Canada, Ottawa, Ontario. (Catalogue No H128-1/11-662E). Available on-line at: http://www.hc-sc.gc.ca/ewh-semt/alt_formats/hecs-sesc/pdf/pubs/water-eau/ndma/ndma-eng.pdf
[Posted: 31 August 2011; accessed: 11 October 2011].
13. WHO, 2008. World Health Organization Guidelines for Drinking-Water Quality, 3rd ed. including 1st and 2nd addenda. Available on-line at: http://www.who.int/water_sanitation_health/dwq/chemicals/ndmasummary_2ndadd.pdf
[Posted: 2011; accessed: 27 July 2011].
14. Unregulated Contaminant Monitoring Regulation (UCMR) for Public Water Systems Revisions. 2007. US EPA, 40 CFR Parts 9, 141 and 142 [Docket No. OW-2004-0001; FRL-8261-7] RIN 2040-AD93

Available on-line at:

<http://www.epa.gov/fedrgstr/EPA-WATER/2007/January/Day-04/w22123.htm>

[Accessed: 6 October 2011].

15. Najm I, Trussell RR. 2001. NDMA formation in water and wastewater. *J. Am. Water Works Assoc.* 93: 92–99.
16. U.S. EPA. 1996. Method 3510C: Separatory Funnel Liquid-Liquid Extraction. Available on-line at:
<http://www.epa.gov/osw/hazard/testmethods/sw846/pdfs/3510c.pdf>
[Last updated: 27 July 2011; accessed: 11 October 2011].
17. U.S. EPA Method 3520C. 1998. Continuous Liquid-Liquid Extraction. Available on-line at:
<http://www.epa.gov/osw/hazard/testmethods/sw846/pdfs/3520c.pdf>
[Last updated: 27 July 2011; accessed: 11 October 2011].
18. Jenkins SWD, Koester CJ, Taguchi VY, Wang DT, Palmentier JPFP, Hong KP. 1995. N-Nitrosodimethylamine determination in drinking water using a rapid, solid-phase extraction method. *Environ. Sci. Pollut. Res. Int.* 2(4): 207–210.
19. Choi J, Duirk SE, Valentine RL. 2002. Mechanistic studies of N-nitrosodimethylamine (NDMA) formation in chlorinated drinking water. *J. Environ. Monit.* 4: 249–252.
20. Tomkins BA, Griest WH. 1996. Determinations of N-nitrosodimethylamine at part-per-trillion concentrations in contaminated ground waters and drinking waters featuring carbon-based membrane extraction disks. *Anal. Chem.* 68: 2533–2540.

21. U.S. EPA Method 521. 2004. Determination of Nitrosamines in Drinking Water by Solid Phase Extraction and Capillary Column and Solid Phase Extraction and Capillary Column Gas Chromatography. Available on-line at:
http://www.epa.gov/microbes/m_521.pdf
[Last updated: 8 November 2011; accessed: 11 October 2011].
22. U.S. EPA Method 8070A. 1996. Nitrosamines by Gas Chromatography. Available on-line at:
<http://www.epa.gov/osw/hazard/testmethods/sw846/pdfs/8070a.pdf>
[Last updated: 27 July 2011; accessed: 11 October 2011].
23. Fine DH, Rufeh F, Lieb D, Rounbehler DP. 1975. Description of the thermal energy analyzer (TEA) for trace determination of volatile and nonvolatile N-nitroso compounds. *Anal. Chem.* 47(7): 1188–1191.
24. Tomkins BA, Griest WH, Higgins CE. 1995. Determination of N-nitrosodimethylamine at part-per-trillion levels in drinking waters and contaminated ground waters. *Anal. Chem.* 67(23): 4387–4395.
25. Lesage S. 1991. Characterization of groundwater contaminants using dynamic thermal stripping and adsorption/thermal desorption-GC-MS. *Fresenius J. Anal. Chem.* 339(7): 516–527.
26. Mitch WA, Sedlak DL. 2002. Formation of N-nitrosodimethylamine (NDMA) from dimethylamine during chlorination. *Environ. Sci. Technol.* 36(4), 588–595.
27. Grebel JE, Suffet IH. 2007. Nitrogen-phosphorus detection and nitrogen chemiluminescence detection of volatile nitrosamines in water matrices: Optimization and performance comparison. *J. Chromatogr. A* 1175(1): 141–144.

28. Plomley JB, Koester CJ, March RE. 1994. Determination of N-nitrosodimethylamine in complex environmental matrixes by quadrupole ion storage tandem mass spectrometry enhanced by unidirectional ion ejection. *Anal. Chem.*, 66(24): 4437–4443.
29. Grebel JE, Young CC, Suffet IH. 2006. Solid-phase microextraction of N-nitrosamines. *J. Chromatogr. A* 1117: 11–18.
30. Hung HW, Lin TF, Chiu CH, Chang YC, Hsieh TY. 2010. Trace Analysis of N-Nitrosamines in Water Using Solid-Phase Microextraction Coupled with Gas Chromatograph-Tandem Mass Spectrometry. *Water, Air, & Soil Pollution* 213(1-4): 459–469.
31. Llop A, Borrull F, Pocurull E. 2010. Fully automated determination of N-nitrosamines in environmental waters by headspace solid-phase microextraction followed by GC-MS-MS. *J. Sep. Sci.* 33(23-24): 3692–3700.
32. Bruheim I, Liu X, Pawliszyn J. 2003. Thin-Film Microextraction. *Anal. Chem.* 75: 1002–1010.
33. Bragg L, Qin Z, Alae M, Pawliszyn J. 2006. Field sampling with a polydimethylsiloxane thin-film. *J. Chromatogr. Sci.* 44: 317–323.
34. Qin Z, Bragg L, Ouyang G, Pawliszyn J. 2008. Comparison of thin-film microextraction and stir bar sorptive extraction for the analysis of polycyclic aromatic hydrocarbons in aqueous samples with controlled agitation conditions, *J. Chromatogr. A* 1196-1197: 89–95.
35. CRC Handbook of Chemistry and Physics 89th Edition 2009

36. Abraham MH, Al-Husseini AJM. 2002. Solvation descriptors for N-nitrosodialkylamines; calculation of some of their properties of environmental significance *J. Environ. Monit.* 4: 743–746.

37. US National Library of Medicine (USNLM) 2011. *Hazardous Substances Data Bank*, Toxicology Data Network.
Available on-line at:
<http://toxnet.nlm.nih.gov/>
[Accessed: 20 October 2011].

38. Smith CJ, Hansch C. 2000. The relative toxicity of compounds in mainstream cigarette smoke condensate. *Food Chem. Toxicol.* 38(7): 637–646.

39. Layne WS, Jaffe HH, Zimmer H. 1963. Basicity of N-nitrosamines. II. Aqueous sulfuric acid solutions. *J. Am. Chem. Soc.* 85: 1816–1820.

40. Challis BC, Challis JA. 1982. N-nitrosamines and N-nitrosoimines. *In* The chemistry of amino, nitroso and nitro compounds and their derivatives. Part 2. Edited by Patai S, John Wiley & Sons.

Chapter 3

Solid phase microextraction of trihalomethanes in drinking water

3.1 Introduction

Chlorination is the most widely used method for drinking water disinfection around the world, owing to its proven effectiveness and low cost. A major class of chlorination by-products in drinking water is trihalomethanes (THMs), the first disinfection by-products (DBPs) identified in drinking water^{1, 2}. THMs together with haloacetic acids (HAAs) account for approximately 25% of the halogenated DBPs in drinking water³.

While THMs are primarily formed in chlorinated waters, they are also found in chloraminated drinking waters at lower levels. Disinfection with chlorine dioxide does not form the THMs. However, low THMs levels may be present due to chlorine impurities in chlorine dioxide³. Brominated THMs are also formed when elevated levels of natural bromide are present in source waters, particularly when ozone is used as disinfecting agent³. Higher levels of chlorination usually lead to greater amounts of THMs in drinking water. If residual chlorine exists in the water distribution system (as is

required for efficient disinfection), THMs formation will continue as long as organic matter is present and until the free chlorine supply is exhausted.

The primary THMs found in drinking water are chloroform (CHCl_3), bromodichloromethane (CHBrCl_2), dibromochloromethane (CHBr_2Cl), and bromoform (CHBr_3), which have been studied intensively over the past 30 years. All these THMs are carcinogenic in rodents and except chloroform they are all genotoxic³ and can cause mutation (change in DNA sequence) as well as DNA damage (DNA adducts, DNA strand breaks). As a result, they are potentially harmful for humans and may cause carcinogenic and adverse reproductive effects. The sum of concentrations of the four THMs represents the total amount of THMs in drinking water, which has been regulated in many countries. The U.S. EPA implemented a maximum contamination level (MCL) of 80 $\mu\text{g/L}$ for the total THMs under the Stage 1 DBPs Rule³. The EPA Stage 1 regulations required monitoring based on running annual averages, which represented averages of all samples collected in a utility's distribution system over a 1-year period. The EPA Stage 2 regulations (2006) maintained the Stage 1 MCL for the total THMs but required that the MCL be based on locational running annual averages, which means that each location in the distribution system needs to comply on a running annual average basis³. The maximum acceptable concentration (MAC) of the total THMs in drinking water in Canada is 100 $\mu\text{g/L}$ based on a locational running annual average of a minimum of quarterly samples taken at the point in the distribution system with the highest potential THM levels⁴. The European Union (EU) has a similar drinking water guideline of 100 $\mu\text{g/L}$ ³.

The potential adverse health implications of THMs and subsequent regulation of maximum total concentrations have prompted a search for simple, fast and reliable analytical methods for their determination. Various sample preparation methods have been used for THM analysis from chlorinated water (potable and recreational water). The EPA method 524.2 (1995)⁵ uses a purge and trap method for DBPs, including THMs analysis. The EPA Method 551.1 (1995)⁶ describes a liquid-liquid extraction (LLE) method for the analysis of DBPs (including THMs) from drinking water using methyl-t-butyl ether (MTBE) as extracting solvent combined with gas chromatography separation and electron capture detection (GC-ECD). The LLE approach has already been used to

determine a variety of DBPs, including THMs, in Canadian drinking waters⁷. Direct aqueous injection (DAI) and headspace methods have also been used by investigators to determine THMs in chlorinated waters^{8,9}.

Solid phase microextraction (SPME) has gained widespread acceptance for environmental analysis, particularly in the analysis of volatiles and semi-volatiles from water¹⁰⁻¹². Low sample volume requirement, automation capability of the entire analytical procedure, short analysis time and the possibility of headspace (HS) sampling recommend this one-step solvent-free sample preparation technique for the routine analysis of volatile trihalomethanes from water and a good replacement for the commonly used LLE technique. Although many investigators all over the world have used SPME to analyze THMs¹³⁻²¹, no study has compared real sample analysis results obtained by this technique to those produced using the more widely accepted EPA 551.1 method. In this research, THMs in source and drinking water samples from six water treatment and distribution systems in Canada, collected under similar sampling and sample stabilization protocol, were analyzed in parallel using an optimized headspace SPME method combined with gas chromatography separation and mass spectrometry (HS-SPME-GC-MS) in University of Waterloo (Waterloo, ON) and a LLE-GC-ECD method equivalent to EPA 551.1 in Health Canada laboratories (Ottawa, ON). The results obtained by the two methods were compared.

3.2 Experimental

3.2.1 HS-SPME-GC-MS method

3.2.1.1 Chemicals and supplies

A standard mix solution of trihalomethanes [trichloromethane (chloroform), bromodichloromethane, dibromochloromethane and tribromomethane (bromoform)] containing 2000 µg/mL of each compound in methanol from Supelco (Bellefonte, USA) was used to prepare secondary stock solutions in methanol. The stock solutions were stored at 4 °C in amber vials in refrigerator. Standard aqueous solutions for calibration in the range of 0.1–

100 µg/L were freshly prepared for each set of water samples, prior to analysis, by spiking appropriate volumes of the stock solutions into 5 ml of blank water. Natural spring water (ozonized), verified to be free of target analytes and interfering compounds, from Hichinbrooke, QC, bottled by Labrador Laurentienne Inc., Anjou, QC, was used for blanks and as matrix for fortified samples. The pH of the blank water was adjusted to 4.5 using 0.1 N HCl. Nano-pure water for preliminary experiments was obtained from a Barnstead/Thermodyne water system (Dubuque, USA). HPLC grade methanol, headspace vials (10ml) with screw cap and polytetrafluoroethylene (PTFE)-silicon septum, sodium chloride (NaCl) and the commercial SPME fibers used in the study including polydimethylsiloxane (PDMS 100µm), polydimethylsiloxane/divinylbenzene (PDMS/DVB 65µm), carboxen/polydimethylsiloxane (CAR/PDMS 75µm), divinylbenzene/carboxen/polydimethylsiloxane (DVB/CAR/PDMS 50/30µm), were all purchased from Supelco (Bellefonte, USA). Helium for gas chromatography was ultra-pure and supplied by Praxair (Kitchener, Canada).

3.2.1.2 Instrumentation

A Varian 3800 gas chromatograph coupled with a 4000 ion trap MS detector (Varian, Mississauga, Canada) was used. Automated analyses were performed using a CTC Analytics CombiPAL autosampler equipped with a temperature-controlled SPME agitator (Zwingen, Switzerland) and Cycle Composer software (Version 1.4.0). The injection port was equipped with a SPME insert and was kept splitless during injection. The chromatographic separation was carried out on a 30m x 0.25mm x 0.25 µm RTX-5 amine capillary column from Restek (Bellefonte, PA, USA). The column was initially set at 40 °C for 1 min, ramped at 20 °C/min to 50 °C and then at 30 °C/min to 70 °C. Temperature was held at 70 °C for 1 min, then ramped at 30 °C/min to 150 °C and held for 1.17 min giving a total GC run of 7 min. The Helium carrier gas flow rate was constant at 1 ml/min. The mass spectrometry was performed using full scan mode with electron impact ionization (EI). Data acquisition was started after 2 min. The THMs were identified using the mass spectra library of the National Institute of Standard and Technology (NIST, USA) and their retention times. The quantifications were done using selected ions for each compound. The ions used were 83 and 85 for chloroform, 83 and

85 for bromodichloromethane, 127 and 129 for Dibromochloromethane, 173 and 175 for bromoform.

3.2.1.3 SPME procedure

All SPME fibers were conditioned before use, according to the manufacturer's instructions. Headspace extractions (automated) were performed in triplicate using 5 mL samples and/or calibration standards in 10 mL sealed screw cap vials at 30 °C for 5 minutes. The agitation speed was 500 rpm and the incubation and desorption times were 5 and 1 minutes, respectively. The desorption temperature was set at 250 °C for PDMS and PDMS/DVB fibers, and at 260 °C and 300 °C for DVB/CAR/PDMS and CAR/PDMS, respectively.

3.2.2 LLE-GC-ECD method

3.2.2.1 Chemicals and supplies

Individual neat standards of chloroform, bromodichloromethane, dibromochloromethane and bromoform from Supelco (Oakville, ON) were used to prepare a standard mix stock solution of 1 mg/mL trihalomethanes in methanol. The surrogate standards (dibromo-methane and 1,2-dibromopropane) and the recovery standard (1,3-dibromopropane) were purchased from Sigma-Aldrich (Oakville, ON) and solutions of 1000 mg/ml were prepared in methanol. A mixed solution of 10 mg/L dibromomethane and 50 mg/L 1,2-dibromopropane was then prepared in MTBE. Preservative-free MTBE (99.0%) was purchased from Burdick & Jackson, Honeywell International Inc., Muskegon, MI. Sodium sulfate, anhydrous (baked at 400 °C for 3 hours) and sodium chloride, biological grade, containing minimal bromide ion (assayed at 0.001%) were purchased from Fisher Scientific (Fair Lawn, NJ). Deionized water (18 M Ω .cm) was obtained from Millipore Super-Q system. Purified water was prepared by the distillation of Super-Q water over KMnO_4 and H_2SO_4 . Natural spring water (ozonized), verified to be free of target analytes and interfering compounds, from Hichinbrooke, QC, bottled by Labrador Laurentienne Inc., Anjou, QC, was used for blanks and as matrix for fortified samples. Blank water pH was adjusted to 4.5 using 0.1

N HCl. Ascorbic acid from Fisher Scientific (Fair Lawn, NJ) was used to prepare a 0.114 M solution (0.500 mg/25mL) in purified water. This solution was used to quench residual chlorine at time of sample collection. Hydrochloric acid (HCl) 36.5–38 % was purchased from EMD Chemicals (Gibbstown, NJ) and diluted using purified water. A 0.1 N solution of HCl was used to adjust the pH of water samples to 4.5–5 in the field and also to adjust the pH of the natural spring water used for blanks. All gases were ultra-pure grade.

3.2.2.2 Instrumentation

A Varian CP-3800 gas chromatograph equipped with dual programmable injectors and ECD detectors was used. A DB-5 capillary column (30m x 0.25mm x 1 µm) was used as the main column and the confirmatory column was a DB-1 (30m x 0.25mm x 1 µm), both Agilent J&W columns from Agilent Technologies (Santa Clara, CA). Helium carrier gas flow and nitrogen make-up gas flow for the ECD were set at 1 ml/min and 30 ml/min, respectively. Injector temperature program was from 80 °C to 240 °C at a rate of 140 °C /min. Column oven temperature was initially set at temp 50 °C (hold 4 min), ramped at 1.5 °C /min to 65 °C (hold 1 min); ramped at 5 °C /min to 120 °C (hold 5 min) and finally ramped at 10 °C /min to 200 °C (hold 5 min). The conditions were the same for both columns.

3.2.2.3 LLE extraction

Samples were removed from cold storage and allowed to sit at ambient temperature for ca 30 minutes. 12 ml of each water sample was removed using a disposable pipette. 3 mL of extracting solvent (MTBE) containing a known concentration of the two surrogate standards 1,2-dibromomethane (surrogate standard-1), 1,3-dibromopropane (surrogate standard-2) were immediately added. Sodium chloride (16 g) was added to each bottle. Bottles were capped, shaken for 2x1.5 minutes and then allowed to stand 30 minutes for phase separation. The MTBE extract was transferred to a 4 mL vial, calibrated at 3.0 mL and diluted to the calibration mark with pure MTBE. Drying salt (Na₂SO₄, ca 0.1 g) was added and the vial was vortexed to allow thorough mixing. 15 µL of the recovery standard solution (50 ng/µL) was added to obtain 250 pg/µL in the final

extract. Extracts were thoroughly mixed by vortexing and stored in labeled vials at cold room temperature (ca 4 °C) until analysis by GC.

3.2.3 Water samples

Samples were collected from six public water treatment plants and distribution systems in the winter of 2009 by Health Canada. For each water system five samples were collected including a raw water sample before the treatment plant, a treated water sample at the plant and three samples at progressively distant points in the distribution system. Water samples were collected and stabilized under the same protocol for SPME and LLE analysis. The samples were collected in 65 ml amber bottles pre-loaded with 0.2 mL ascorbic acid solution (0.114 M) as a quencher and enough 0.1 N HCl solution to bring the sample at pH 4.5–5. The required HCl amount was pre-determined by titration for each water sample. The bottles were filled with no headspace from the water tap after running water for at least 5 minutes. Water samples were packed in ice-filled coolers and sent to both participating laboratories (at University of Waterloo for analysis by SPME-GC-MS method and at Health Canada for analysis by the LLE-GC-ECD method). Samples were analyzed less than 4 days after collection. Stability studies conducted previously in Health Canada show that water samples stabilized according to this protocol and kept in a cold, dark room are stable for at least 14 days (Health Canada, unpublished results).

3.3 Results and Discussion

3.3.1 Analytes description and properties

The THMs studied in this research were a group of four analytes commonly found in chlorinated waters. Table 3.1 presents the THMs description, acronym, Chemical Abstracts Service Registry Number (CASRN), and physical properties including molecular weight (MW), boiling point (b.p.), solubility in water, Henry's law constant (H) and log of octanol-water partition coefficient ($\log K_{ow}$)²²⁻²³. The value of the Henry's law constant provides an indication of likely partitioning from water to air (i.e.

Table 3.1 Description and properties of commonly found trihalomethanes (THMs) in drinking water

| Compound | Formula | Acronym | CASRN | MW g/mol | b.p. °C ^a | Solubility ^b g/L | H^b atm·m ³ /mole | Log K_{ow}^b (25°C) |
|----------------------|----------------------|---------|----------|-------------|----------------------|--------------------------------|-----------------------------------|--------------------------|
| Trichloromethane | CHCl ₃ | TCM | 67-66-3 | 119.38 | 61 | 7.95 (25°C) | 3.67 x 10 ⁻³ (24°C) | 1.97 |
| Bromodichloromethane | CHBrCl ₂ | BDCM | 75-27-4 | 163.83 | 90 | 3.97 (30°C) | 2.12 x 10 ⁻³ (25°C) | 2.00 |
| Dibromochloromethane | CHBr ₂ Cl | DBCM | 124-48-1 | 208.28 | 122 | 2.70 (20°C) | 7.83 x 10 ⁻⁴ (20°C) | 2.16 |
| Tribromomethane | CHBr ₃ | TBM | 75-25-2 | 252.73 | 149 | 3.10 (25°C) | 5.35 x 10 ⁻⁴ (25°C) | 2.40 |

^a Ref. 22 (760 torr). ^b Ref. 23.

a measure of volatility). The $\log K_{ow}$ is a measure of the preference of the compound for the organic phase (lipophilic compounds) or the water phase (hydrophilic compounds). As is seen from the table, the THMs exhibit high volatilities which favor their extraction from water by headspace SPME.

3.3.2 Separation and identification

A typical chromatogram of the four THMs is displayed in Fig. 3.1 illustrating clear separation and identification of the analytes using GC-MS.

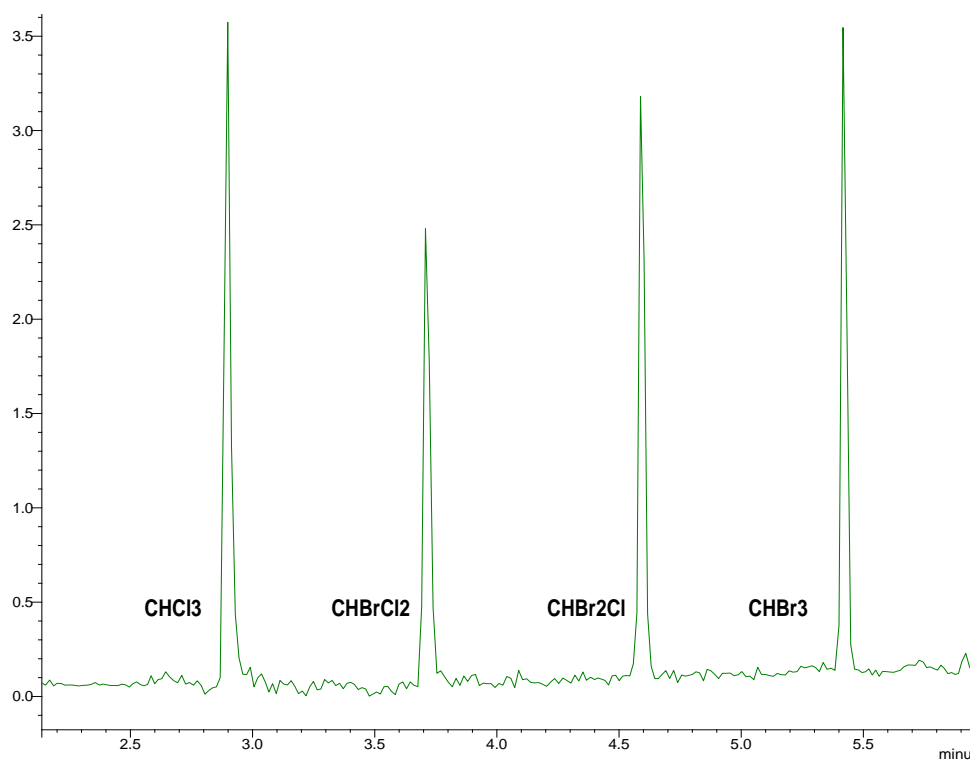


Figure 3.1 HS-SPME-GC-MS chromatogram of THMs in spiked water sample (1 μ g/L) using 100 μ m PDMS fiber.

3.3.3 Fiber selection

Selection of fiber coating in SPME is based on several factors including size, volatility and polarity of analytes as well as the concentration range and the detection limits that are intended for analysis. The nonpolar liquid polymer PDMS fiber is usually preferable for volatiles and semi-volatiles with none or less polarity. The 100 μm PDMS fiber, in particular, allows efficient retention of small size highly volatile analytes. These analytes can also be extracted with the Carboxen-containing fibers (CAR/PDMS and DVB/CAR/PDMS), owing to the presence of small pores in this carbon-based material. However, due to the predominance of adsorption mechanism, shorter linear range of quantification could be expected compared with the PDMS fiber. As a result, application of PDMS (or other absorbent type) fibers is preferable as far as they provide the required sensitivity. To compare the efficiencies of the commercial fibers for the extraction of THMs from water, an evaluation was made under similar extraction conditions of four different fibers, including PDMS, CAR/PDMS, DVB/CAR/PDMS and PDMS/DVB fibers. As shown in Fig. 3.2, the Carboxen-containing fibers exhibited the highest efficiencies for the analytes. The 75 μm -CAR/PDMS was the best fiber for TCM and BDCM, having 80% and 10% higher efficiency than the 50/30 μm -DVB/CAR/PDMS for the two analytes, respectively. As the $\log K_{ow}$ increases among the analytes, the DVB-containing coatings become more effective. The extraction efficiencies for tribromomethane (TBM), the THM having the highest $\log K_{ow}$, were increased according to the following order: 100 μm -PDMS < 75 μm -CAR/PDMS < 65 μm -PDMS/DVB < 50/30 μm -DVB/CAR/PDMS. Despite higher efficiencies of the Carboxen-containing fibers for the extraction of THMs in water, varying approximately between 1 to 2 orders of magnitude better than the 100 μm -PDMS fiber, the preliminary assessment of HS-SPME-GC-MS sensitivity using the PDMS fiber proved that this fiber could provide low ng/L detection of analytes in water at the levels comparable with LLE-GC-ECD method. Therefore, to take the advantage of a wider linear range offered by PDMS coating, the 100 μm PDMS fiber was selected for the rest of experiments.

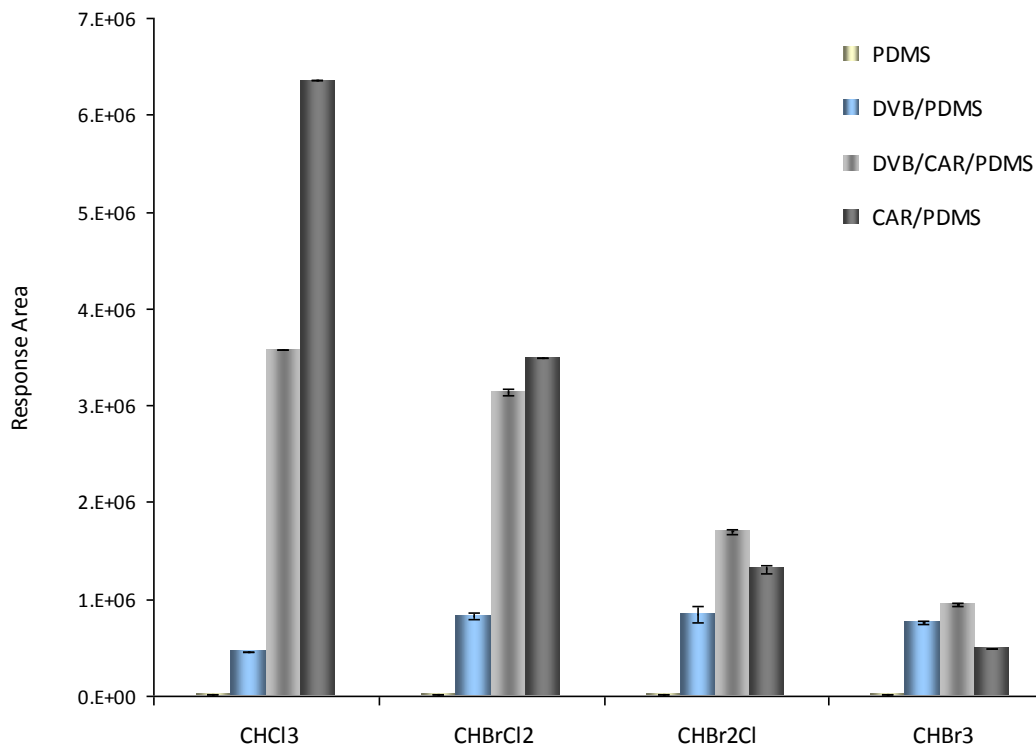


Figure 3.2 Comparison of different SPME fiber coatings for the extraction of selected THMs; 4 µg/L spiked water sample, 15 min headspace extraction at 30°C, n = 3.

3.3.4 Extraction time

Figure 3.3 illustrates the effect of extraction time on the extraction efficiency of the analytes for the headspace SPME. To obtain the time profile, extraction times of 15 sec, 30 sec, 45 sec, 1 min, 2 min, 3 min, 5 min and 15 min were tested using 1 µg/L spiked water samples. Based on the results, a 5 min extraction time was found adequate for equilibration, under the experimental conditions.

3.3.5 Desorption time

Desorption time and possible carryover of the analytes on the PDMS fiber were tested at the injection temperature, 250 °C. Since the analytes are very volatile, they are easily desorbed from the fiber. The optimum desorption time was found to be 1 min leading to complete removal of all analytes from the fiber without carryover.

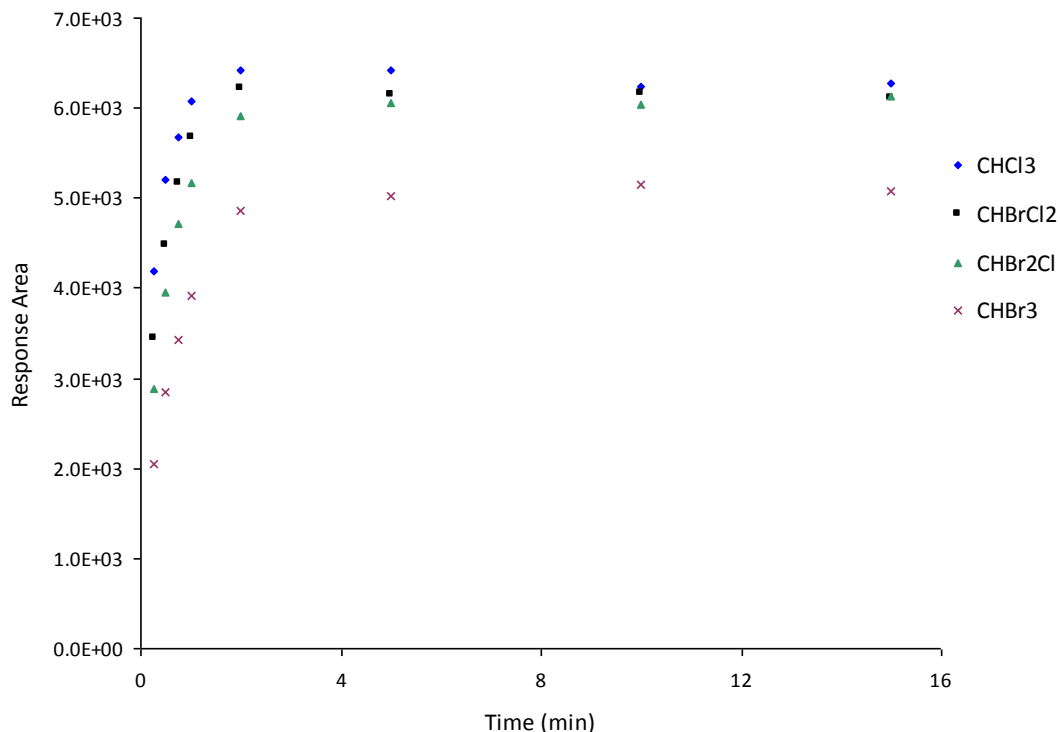


Figure 3.3 Extraction time profiles of THMs in water for HS-SPME with 100 µm PDMS fiber; 1 µg/L spiked water sample, extraction temperature 30°C.

3.3.6 Salt addition

The effect of salt addition on headspace extraction with PDMS fiber was investigated. Adding salt often increases the amount of analytes in the headspace due to salting effect. As shown in Fig. 3.4, the enhancement of the signal intensities of the THMs due to addition of salt (NaCl 25% w/w) for 1 µg/L spiked water sample was varying between 3 to 4 times, approximately.

3.3.7 Analytical parameters

Table 3.2 presents analytical parameters obtained by HS-SPME-GC-MS using a 100 µm PDMS fiber. The calibration curves for the THMs were established in a concentration range between 0.1 and 100 µg/L. All the THMs exhibited excellent linearity with

correlation coefficients (R^2) exceeding 0.9979. The precision of the measurements represented by relative standard deviation percentage (RSD %) of three replicates ranged between 1 to 4 % at 2 $\mu\text{g/L}$ spike level for the analytes. The method detection limits (MDLs) were determined for salt-free and salt added spiked samples as 3.14 times the standard deviation of seven replicates at low concentrations close to the detection limits. The MDLs obtained by the LLE-GC-ECD method in Health Canada laboratories are also listed in Table 3.2. As is seen, the values obtained for BDCM, DBCM and TBM by the two methods are comparable. Further, the MDL obtained for TCM by the SPME method was approximately 5 times lower than that obtained by the LLE method. The analytical data in Table 3.2 collectively indicate that quantification of the THMs using HS-SPME/GC/MS with the PDMS fiber is very reliable.

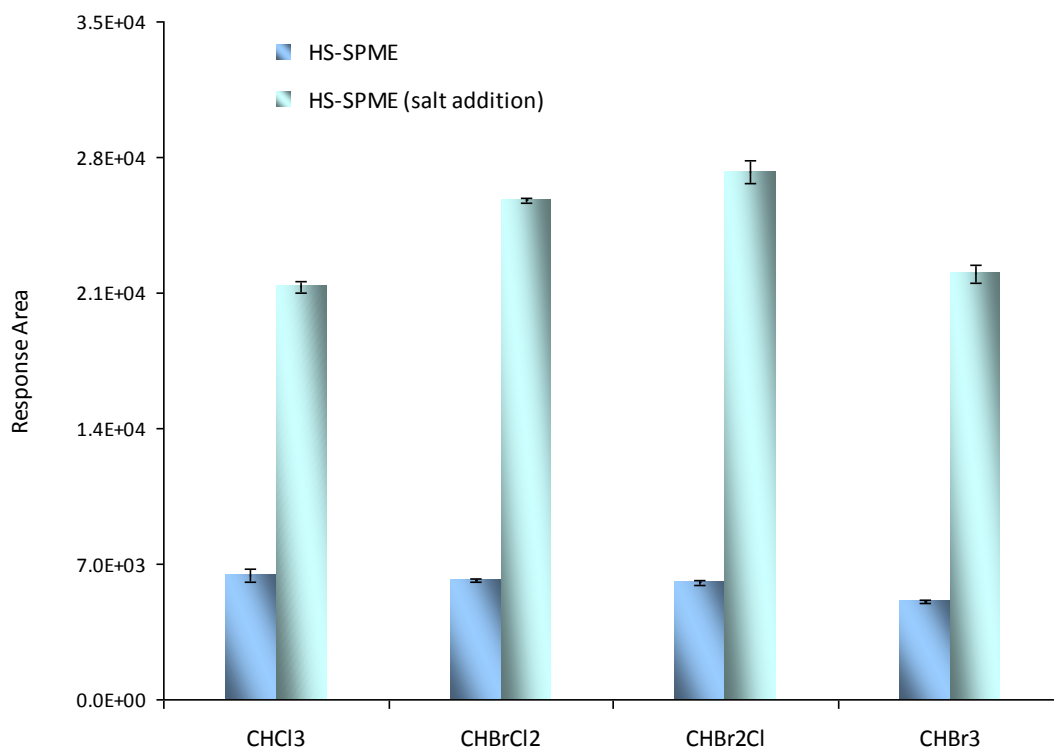


Figure 3.4 Effect of salt addition (NaCl 25% w/w) on HS-SPME extraction of THMs from water with PDMS fiber; 1 $\mu\text{g/L}$ spiked water sample, extraction temperature 30°C.

Table 3.2 Analytical data for selected trihalomethanes (THMs) in water

| Compound | Linear range (µg/L) | Correlation coefficient (R ²) | Repeatability (RSD %) ^a | MDL (ng/L) | | |
|----------------------|------------------------|--|---------------------------------------|-------------------|--------------------------------|------------------|
| | | | | SPME ^b | SPME (salt added) ^c | LLE ^d |
| Trichloromethane | 0.1 – 100 | 0.9999 | 1 | 23 | 10 | 150 |
| Bromodichloromethane | 0.1 – 100 | 0.9999 | 4 | 25 | 9 | 30 |
| Dibromochloromethane | 0.1 – 100 | 0.9999 | 4 | 22 | 8 | 30 |
| Tribromomethane | 0.1 – 100 | 0.9979 | 3 | 22 | 7 | 40 |

^a Relative standard deviation (n=3) for 2 µg/L spiked water samples; ^b HS-SPME-GC-MS; ^c 25% w/w NaCl; ^d LLE-GC-ECD with permission from Health Canada.

3.3.8 Sample analysis

The HS-SPME-GC-MS optimized method was applied for analysis of the THMs in real drinking water samples from six public water treatment and distribution systems in Canada. Table 3.3 describes the characteristics of the water samples including pH, turbidity, temperature and total chlorine as well as disinfection process and population at the region of each water treatment plant. For each water system five samples were collected including a raw water sample (R) before the treatment plant, a treated water sample (T) at the treatment plant and three samples at progressively distant locations in the distribution system (D1, D2, D3). The SPME results along with those obtained with the LLE-GC-ECD method in Health Canada laboratories were summarized in Table 3.4. As is seen, the values obtained by the two methods are in close agreement with each other. To compare the results graphically, a scattered plot was also derived by pooling the data, as shown in Fig. 3.5.

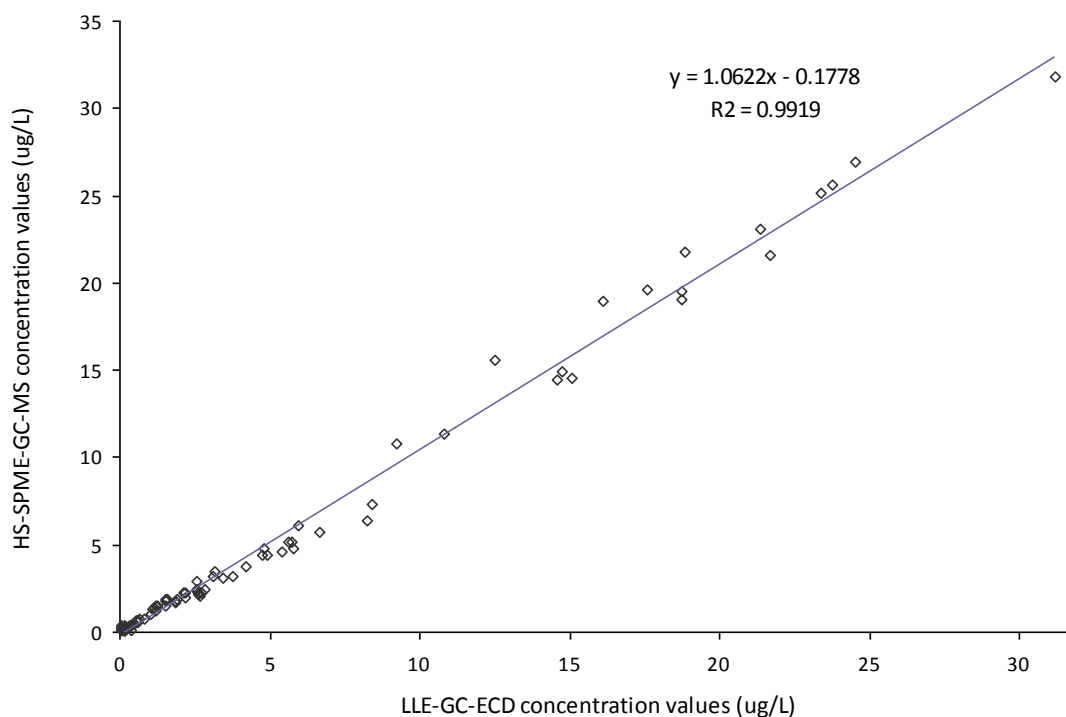


Figure 3.5 Scatter plot of the amounts of TCB, BDCM, DBCM and TBM detected in some Canadian water samples measured by HS-SPME-GC-MS and LLE-GC-ECD.

Table 3.3 Characteristics of the Canadian drinking water samples (Winter 2009)

| WTP - # | WTP-1 | WTP-2 | WTP-3 | WTP-4 | WTP-5 | WTP-6 |
|-------------------------------------|-----------------|--------------------------------------|--------------------|-------------------|--------------------|-----------------|
| Total population supplied | 98950 | 500000 | 800000 | 230000 | NA | 50000 |
| Raw water source | River | River | River | River | Lake | Lake |
| Raw water pH | 6.48 | 7.8 | 7.4 | 8.27 | 5.83 | 6.07 |
| Raw water turbidity | 8 | 12.7 | 11.44 | 5 | 0.48 | 0.42 |
| Raw water temp (°C) | 2 | 3.9 | 2.2 | 11 | 3.3 | --- |
| Treated water pH | 7.32 | 7.3 | 9.4 | 8.95 | 7.54 | 7.5 |
| Treated water temp (°C) | 1.5 | --- | 2.3 | 9 | 3.8 | 4 |
| Treated water total Cl ₂ | 1.08 | 2.4 | 1.29 | 1.92 | 2.03 | 1.55 |
| D1 total Cl ₂ | 0.95 | 1.65 | 1.11 | 2.02 | 1.89 | 1.14 |
| D2 total Cl ₂ | 0.78 | 1.29 | 1.12 | 1.65 | 1.34 | 1.32 |
| D3 total Cl ₂ | 0.97 | 1.32 | 1.08 | 1.73 | 1.73 | 0.97 |
| Pre-disinfection process | O ₃ | --- | --- | KMnO ₄ | --- | --- |
| Inter-disinfection process | --- | O ₃ | Cl ₂ | Cl ₂ | Cl ₂ | --- |
| Post-disinfection process | Cl ₂ | Cl ₂ , NH ₂ Cl | NH ₂ Cl | --- | NH ₂ Cl | Cl ₂ |

Note: WTP (water treatment plant); D1, D2, D3: treated water at three progressively distant locations in distribution system; total Cl₂ values in mg/liter.

Table 3.4 Results of drinking water sample analysis by the LLE and the SPME methods †

| WTP-# | THM (µg/L) | | CHCl ₃ | | CHBrCl ₂ | | CHBr ₂ Cl | | CHBr ₃ | |
|----------|-------------|-------|-------------------|------|---------------------|------|----------------------|------|-------------------|--|
| | Method | LLE | SPME | LLE | SPME | LLE | SPME | LLE | SPME | |
| WTP-1-R | | 0.06 | 0.20 | 0.03 | ND | 0.02 | 0.11 | ND | ND | |
| WTP-1-T | | 1.14 | 1.41 | 1.55 | 1.49 | 1.07 | 1.33 | 0.13 | 0.10 | |
| WTP-1-D1 | | 1.52 | 1.90 | 1.86 | 1.80 | 1.22 | 1.53 | 0.14 | 0.11 | |
| WTP-1-D2 | | 2.54 | 2.87 | 2.59 | 2.46 | 1.54 | 1.81 | 0.14 | 0.11 | |
| WTP-1-D3 | | 1.60 | 1.91 | 1.93 | 1.84 | 1.26 | 1.46 | 0.14 | 0.11 | |
| WTP-2-R | | 0.08 | 0.07 | 0.03 | ND | ND | ND | ND | ND | |
| WTP-2-T | | 2.56 | 2.33 | 2.70 | 2.04 | 1.22 | 1.19 | 0.14 | 0.36 | |
| WTP-2-D1 | | 3.13 | 3.16 | 2.85 | 2.41 | 2.16 | 2.22 | 1.05 | 1.07 | |
| WTP-2-D2 | | 5.94 | 6.10 | 5.38 | 4.57 | 2.12 | 2.23 | 0.35 | 0.33 | |
| WTP-2-D3 | | 10.80 | 11.32 | 8.39 | 7.36 | 3.18 | 3.51 | 0.36 | 0.06 | |
| WTP-3-R | | 0.07 | 0.29 | 0.04 | ND | 0.01 | ND | ND | ND | |
| WTP-3-T | | 9.24 | 10.81 | 1.87 | 1.67 | 0.12 | 0.09 | ND | ND | |
| WTP-3-D1 | | 14.60 | 14.43 | 2.60 | 2.20 | 0.14 | 0.10 | ND | ND | |
| WTP-3-D2 | | 14.72 | 14.95 | 2.62 | 2.29 | 0.15 | 0.12 | ND | ND | |
| WTP-3-D3 | | 15.07 | 14.54 | 2.71 | 2.26 | 0.16 | 0.12 | ND | ND | |
| WTP-4-R | | 0.07 | 0.36 | 0.02 | ND | ND | ND | ND | ND | |
| WTP-4-T | | 18.85 | 21.81 | 4.80 | 4.76 | 0.47 | 0.49 | ND | ND | |
| WTP-4-D1 | | 17.58 | 19.61 | 4.75 | 4.45 | 0.46 | 0.44 | ND | ND | |
| WTP-4-D2 | | 24.54 | 26.91 | 5.75 | 5.15 | 0.61 | 0.62 | ND | ND | |
| WTP-4-D3 | | 23.39 | 25.13 | 5.64 | 5.19 | 0.61 | 0.58 | ND | ND | |
| WTP-5-R | | 0.13 | 0.19 | 0.03 | ND | ND | ND | ND | ND | |
| WTP-5-T | | 12.48 | 15.53 | 2.20 | 1.99 | 0.20 | 0.19 | ND | ND | |
| WTP-5-D1 | | 18.74 | 19.08 | 3.46 | 3.09 | 0.30 | 0.25 | ND | ND | |
| WTP-5-D2 | | 21.35 | 23.05 | 4.19 | 3.77 | 0.38 | 0.35 | ND | ND | |
| WTP-5-D3 | | 21.69 | 21.54 | 3.77 | 3.15 | 0.31 | 0.27 | ND | ND | |
| WTP-6-R | | 0.18 | 0.25 | 0.05 | ND | 0.01 | ND | ND | ND | |
| WTP-6-T | | 16.12 | 18.94 | 4.91 | 4.37 | 0.56 | 0.63 | ND | ND | |
| WTP-6-D1 | | 23.75 | 25.63 | 6.68 | 5.71 | 0.68 | 0.73 | ND | ND | |
| WTP-6-D2 | | 18.75 | 19.49 | 5.77 | 4.75 | 0.60 | 0.63 | ND | ND | |
| WTP-6-D3 | | 31.20 | 31.79 | 8.24 | 6.40 | 0.81 | 0.78 | ND | ND | |

† Printed with permission from Health Canada; WTP: water treatment plant; R: raw water; T: treated water at the plant; D1, D2, D3: treated water at three progressively distant locations in the distribution system; ND: not detected.

The plot in Fig. 3.5 illustrates an excellent correlation ($R^2 = 0.9919$) between the results of sample analysis by the LLE and the SPME methods. The maximum amounts of TCM, BDCM, DBCM and TBM detected in the treated drinking water samples were around 31, 8, 3 and 0.3 $\mu\text{g/L}$, respectively. TBM was detected only in the samples treated with Ozone (O_3).

3.4 Conclusions

This study described a fast, sensitive automated HS-SPME-GC-MS method for determination of four regulated THMs commonly found in drinking water. The total analysis time including incubation, extraction and chromatographic run was 17 min. The method detection limits were in low ng/L levels using a 100 μm PDMS fiber. Excellent linearity for all the four THMs was obtained in 0.1-100 $\mu\text{g/L}$ range with correlation coefficients exceeding 0.9979. The method was reproducible with RSD % generally less than 4 %. The quantitative measurements of the THMs in real drinking water samples by the optimized HS-SPME-GC-MS method in the University of Waterloo and by the LLE-GC-ECD method (EPA 551.1) in Health Canada showed excellent agreement between the values obtained by the two analytical methods. The results obtained in this study along with the SPME method advantages, including ease of operation, solventless nature, short analysis time and fully-automated procedure, proved that the HS-SPME-GC-MS was a fast reliable alternative to the LLE-GC-ECD method for analysis of the THMs in the concentration ranges that are typical and relevant for drinking water samples.

3.5 References

1. Rook JJ. 1974. Formation of haloforms during chlorination of natural waters. *Water Treat. Exam.* 23: 234–243.
2. Bellar TA, Lichtenberg JJ, Kroner RC. 1974. Occurrence of organohalides in chlorinated drinking water. *J. Am. Water Works Assoc.* 66: 703–712.
3. Richardson SD, Plewa MJ, Elizabeth D, Wagner ED, Schoeny R, DeMarini DM. 2007. Occurrence, genotoxicity, and carcinogenicity of regulated and emerging disinfection by-products in drinking water: A review and roadmap for research, *Mutation Research* 636: 178–242.
4. Health Canada, 2006. Guidelines for Canadian Drinking Water Quality: Guideline Technical Document: Trihalomethanes. Federal-Provincial-Territorial Committee on Drinking Water, Health Canada, Ottawa, Ontario.
Available on-line at:
<http://www.hc-sc.gc.ca/ewh-semt/pubs/water-eau/trihalomethanes/index-eng.php>
[Last modified: 23 June 2010; accessed: 11 October 2011]
5. U.S. EPA Method 524.2. 1995. Measurement of Purgeable Organic Compounds in Water by Capillary Column Gas Chromatography/Mass Spectrometry. National Exposure Research Laboratory, U.S. EPA, Cincinnati, Ohio, 45268.
Available on-line at:
<http://www.epa.gov/sam/pdfs/EPA-524.2.pdf>
[Accessed: 11 October 2011].
6. U.S. EPA Method 551.1. 1995. Determination of Chlorination Disinfection Byproducts, Chlorinated Solvents, and Halogenated Pesticides/Herbicides in Drinking Water by Liquid-Liquid Extraction and Gas Chromatography with Electron-Capture Detection. National Exposure Research Laboratory, U.S. EPA, Cincinnati, Ohio.

Available on-line at:

<http://www.epa.gov/sam/pdfs/EPA-551.1.pdf>

[Accessed: 11 October 2011].

7. Williams DT, Lebel GL, Benoit FM. 1997. Disinfection byproducts in Canadian drinking water. *Chemosphere* 34: 299–316.
8. Wolska L, Olszewska C, Turska M, Zygmunt B, Namiesnik J. 1998. Volatile and semivolatile organohalogen trace analysis in surface water by direct aqueous injection GC-ECD. *Chemosphere* 37(13): 2645–2651.
9. Golfinopoulos SK, Lekkas TD, Nikolaou AD. 2001. Comparison of methods for determination of volatile organic compounds on drinking water. *Chemosphere* 45: 275–284.
10. Arthur CL, Pawliszyn J. 1990. Solid phase microextraction with thermal desorption using fused silica optical fibers. *J. Anal. Chem.* 62: 2145–2148.
11. Pawliszyn J. 1997. Solid Phase Microextraction: Theory and Practice. Wiley-VCH, New York.
12. Ouyang G, Pawliszyn J. 2006. SPME in environmental analysis. *Anal. Bioanal. Chem.* 386: 1059–1073.
13. Brand, G. 1995. Evaluation of solid phase microextraction (SPME) technology for applicability to drinking water analysis. *Proceedings – Water Quality Technology Conference* (Pt. 1), 273–283.
14. Chen, ML, Mao IF, Hsu CC. 1997. Determination of trihalomethanes in drinking water by solid-phase microextraction and gas chromatography with electron-captured detection. *Toxicol. Environ. Chem.* 60: 39–45.

15. Stack MA, Fitzgerald G, O'Connell S, James KJ. 2000. Measurement of trihalomethanes in potable and recreational waters using solid phase micro extraction with gas chromatography-mass spectrometry. *Chemosphere* 41(11): 1821–1826.
16. Cho DH, Kong SH, Oh SG. 2003. Analysis of trihalomethanes in drinking water using headspace-SPME technique with gas chromatography. *Water Research* 37(2): 402–408.
17. Cardinali FL, Ashley DL, Morrow JC, Moll DM, Blount BC. 2004. Measurement of trihalomethanes and methyl tertiary-butyl ether in tap water using solid-phase microextraction GC-MS. *J. Chromatogr. Sci.* 42(4): 200–206.
18. Nakamura S, Daishima S. 2005. Simultaneous determination of 22 volatile organic compounds, methyl-tert-butyl ether, 1,4-dioxane, 2-methylisoborneol and geosmin in water by headspace solid phase microextraction-gas chromatography-mass spectrometry. *Anal. Chim. Acta* 548(1–2): 79–85.
19. San Juan PM, Carrillo JD, Tena MT. 2007. Fibre selection based on an overall analytical feature comparison for the solid-phase microextraction of trihalomethanes from drinking water. *J. Chromatogr. A* 1139(1): 27–35.
20. Guimaraes AD, Carvalho JJ, Goncalves C, Alpendurada MF. 2008. Simultaneous analysis of 23 priority volatile compounds in water by solid-phase microextraction-gas chromatography-mass spectrometry and estimation of the method's uncertainty. *Inter. J. Environ. Anal. Chem.* 88(3): 151–164.
21. Niri VH, Bragg L, Pawliszyn J. 2008. Fast analysis of volatile organic compounds and disinfection by-products in drinking water using solid-phase microextraction-gas chromatography/time-of-flight mass spectrometry. *J. Chromatogr. A* 1201(2): 222–227.

22. CRC Handbook of Chemistry and Physics 89th Edition 2009

23. US National Library of Medicine (USNLM) 2011. *Hazardous Substances Data Bank*, Toxicology Data Network.
Available on-line at:
<http://toxnet.nlm.nih.gov/>
[Accessed: 20 October 2011].

Chapter 4

Solid phase microextraction of haloacetonitriles, halo ketones and chloropicrin in drinking water

4.1 Introduction

The predominant by-products that result from the chlorination of drinking water are trihalomethanes and haloacetic acids, which have been regulated in many countries. In addition to these, other disinfection by-products (DBPs) such as haloacetonitriles (HANs), halo ketones (HKs) and halonitromethanes can be formed in drinking water ^{1, 2}. The levels of HANs and other nitrogenous DBPs (N-DBPs) in treated waters are often increased when chloroamine is used as a disinfecting agent, or when nitrogen-containing compounds of natural origin are present in source waters ^{3, 4}.

Compared to carbon-based DBPs (i.e., DBPs without a nitrogen), the N-DBPs are more chemically reactive and thus potentially more toxic ⁴. As a result, the U.S.

Environmental Protection Agency (EPA) has cited the N-DBPs, including HANs, as research priorities⁵ and encouraged further toxicology studies, as well as development of new techniques for measurement and monitoring of these analytes in drinking water.

The frequently found HAN compounds in drinking water supplies are trichloroacetonitrile (TCAN), dichloroacetonitrile (DCAN), bromochloroacetonitrile (BCAN) and dibromoacetonitrile (DBAN)^{6, 7}. Toxicology studies on laboratory animals have shown that all the four HANs mentioned above may induce DNA sequence change and/or DNA damage in mammalian cells⁴. These, along with the commonly observed HKs, 1,1-dichloro-2-propanone (1,1-DCP) and 1,1,1-trichloro-2-propanone (1,1,1-TCP), and trichloronitromethane (chloropicrin) were included in the U.S. EPA Information Collection Rule (ICR 1996)⁸ and may be regulated in the future.

The conventional methods for sample preparation, pre-concentration and quantification of volatile chlorinated by-products in drinking water are based on liquid-liquid extraction (LLE - EPA method 551.1)⁹ or purge and trap (P&T - EPA method 524.2)¹⁰ followed by gas chromatography (GC) separation with electron capture (ECD) or mass spectrometry (MS) detection. Although reliable, the LLE technique is time consuming, labor intensive and requires organic solvents which are toxic and expensive to use. The P&T technique is more sensitive, but it has a few shortcomings including possibility of losses of very volatile compounds, foaming of sample, cross-contamination in the purging vessel and sorbent bleeding during thermal desorption. Simpler methods have also been used, including direct aqueous injection¹¹ and headspace method¹², however, they have the disadvantage of lower sensitivity.

Solid-phase microextraction (SPME)¹³ is the newest approach in the analysis of volatile chlorinated by-products in water¹⁴. The technique is simple, rapid, sensitive and solvent-free¹⁵. Ease of automation of the entire analytical procedure and low sample volume requirement are other advantages of this technique¹⁵. SPME has been successfully applied to analysis of THMs in water¹⁶⁻²³. Scilimenti et al.²⁴ reported an automated headspace SPME-GC-ECD method for the determination of several DBPs at 12 water treatment plants in the U.S. Antoniou et al.²⁵ described a manual headspace SPME-GC-ECD method for the determination of chlorinated volatile organic compounds

in water and municipal waste water, evaluating four SPME fibers. Although a wider range of DBPs were analyzed, the total analysis times of these two methods were both above 80 minutes. In this research, a faster automated HS-SPME-GC-MS method was optimized for the determination of seven target DBPs. Seven different SPME fibers, including a novel custom-made coating, were evaluated and the optimized method was then applied to the analysis of real samples. Source and drinking water samples from eight water treatment and distribution systems in Canada were analyzed in parallel by the optimized HS-SPME-GC-MS method in University of Waterloo (Waterloo, ON) and a LLE-GC-ECD method equivalent to EPA Method 551.1 in Health Canada laboratories (Health Canada, Ottawa, ON). The results obtained by the two methods were compared.

4.2 Experimental

4.2.1 HS-SPME-GC-MS method

4.2.1.1 Chemicals and supplies

A 2000 µg/mL halogenated volatiles mixed analytical standard (EPA 551B) [trichloroacetonitrile (TCAN), dichloroacetonitrile (DCAN), bromochloroacetonitrile (BCAN), dibromoaceto-nitrile (DBAN), chloropicrin (CP), 1,1-dichloro-2-propanone (1,1-DCP), 1,1,1-trichloro-2-propanone (1,1,1-TCP)] in acetone was purchased from Supelco (Bellefonte, USA). Secondary stock solutions in the range of 0.01–20 µg/mL were prepared in acetone and stored at 4 °C in amber vials in refrigerator. Standard aqueous solutions for calibration were freshly prepared for each set of water samples, prior to analysis, by spiking 5 µL of the appropriate stock solutions into 5 ml of blank water. Natural spring water (ozonized), verified to be free of target analytes and interfering compounds, from Hichinbrooke, QC, bottled by Labrador Laurentienne Inc. (Anjou, QC) was used for blanks and as matrix for fortified samples. The pH of the blank water was adjusted to 4.5 using 0.1 N HCl. Nano-pure water for preliminary experiments was obtained from a Barnstead/Thermodyne water system (Dubuque, USA). HPLC grade acetone, HPLC grade methanol for CI, headspace vials (10 ml) and the commercial SPME fibers used in this study including polyacrylate (PA 85µm), carbowax/divinyl-

benzene (CW/DVB 70 μ m), polydimethylsiloxane (PDMS 100 μ m), polydimethylsiloxane/divinylbenzene (PDMS/DVB 65 μ m), divinylbenzene/carboxen/polydimethylsiloxane (DVB/CAR/PDMS, 50/30 μ m), carboxen/polydimethylsiloxane (CAR/PDMS 75 μ m) were all purchased from Supelco. Oasis HLB particles (30 μ m) for the custom-made polydimethylsiloxane/divinylbenzene-N-vinylpyrrolidone (PDMS/DVB-NVP 70 μ m) fiber were purchased from Waters (Mississauga, Canada). Bulk PDMS was provided by Dow Corning Co. (Midland, USA). Helium for gas chromatography was ultra-pure and supplied by Praxair (Kitchener, Canada).

4.2.1.2 Instrumentation

A Varian 3800 gas chromatograph coupled with a 4000 ion trap MS detector (Varian, Mississauga, Canada) was used. Automated analyses were performed using a CTC Analytics CombiPAL autosampler equipped with SPME agitator (Zwingen, Switzerland) and Cycle Composer software (Version 1.4.0). The injection port was equipped with a SPME insert and was kept splitless during injection. The chromatographic separation was carried out on a 30m x 0.25mm x 0.25 μ m RTX-5 amine capillary column from Restek (Bellefonte, PA, USA). The column was initially set at 40 °C for 1 min, ramped at 20 °C /min to 200 °C and held for 1 min) giving a total GC run of 10 min. The Helium carrier gas flow rate was constant at 1 ml/min. The electron ionization (EI) segments were set for five analytes (TCAN, DCAN, CP, BCAN, DBAN). Methanol was used as CI reagent for the chemical ionization of 1,1-DCP and 1,1,1-TCP. Data acquisition was started after 2 min. The compounds were identified using the mass spectra library of the National Institute of Standard and Technology (NIST, USA) and their retention times. The quantifications were done using selected ion for each compound. Scanning electron microscopy was performed on a LEO 1530 field emission SEM (Carl Zeiss NTS GmbH, Germany) using 10 nm of gold deposition on the surface before the microscopy.

4.2.1.3 SPME procedure

All SPME fibers were conditioned before use, according to the manufacturer's instructions. The desorption temperature for each fiber was set at 5 °C below the

maximum operating temperature recommended by the manufacturer. The PDMS/DVB-NVP fiber was conditioned (30 min) at 250 °C and desorbed at the same temperature. Headspace extractions (automated) were performed in triplicate using 5 mL samples and/or calibration standards in 10 mL vials at 30 °C for 15 minutes. The agitation speed was 500 rpm and the incubation and desorption times were 5 and 2 minutes, respectively.

4.2.2 LLE-GC-ECD method

4.2.2.1 Chemicals and supplies

Disinfectant by-products mix (EPA 551B) (trichloroacetonitrile, dichloroacetonitrile, bromochloroacetonitrile, dibromoacetonitrile, chloropicrin, 1,1-dichloro-2-propanone, 1,1,1-trichloro-2-propanone) 1 mg/mL, in acetone was purchased from Accustandard (Newhaven, CN, USA). The surrogate standards (dibromomethane and 1,2-dibromopropane) and the recovery standard (1,3-dibromopropane) were purchased from Sigma-Aldrich (Oakville, ON) and solutions of 1000 mg/ml were prepared in acetone. A mixed solution of 10 mg/L dibromomethane and 50 mg/L 1,2-dibromopropane was then prepared in methyl-t-butyl ether (MTBE). MTBE (99.0%), preservative-free, was purchased from Burdick & Jackson, Honeywell International Inc., Muskegon, MI. Sodium sulfate, anhydrous (baked at 400 °C for 3 hours) and sodium chloride, biological grade, containing minimal bromide ion (assayed at 0.001%) were purchased from Fisher Scientific (Fair Lawn, NJ). Deionized water (18 M Ω .cm) was obtained from Millipore Super-Q system. Purified water was prepared by the distillation of Super-Q water over KMnO_4 and H_2SO_4 . Natural spring water (ozonized), verified to be free of target analytes and interfering compounds, from Hichinbrooke, QC, bottled by Labrador Laurentienne Inc. (Anjou, QC) was used for blanks and as matrix for fortified samples. Blank water pH was adjusted to 4.5 using 0.1N HCl. Ascorbic acid from Fisher Scientific (Fair Lawn, NJ) was used to prepare a 0.114 M solution (0.500mg/25mL) in purified water. This solution was used to quench residual chlorine at the time of sample collection. Hydrochloric acid (HCl) 36.5–38 % was purchased from EMD Chemicals (Gibbstown, NJ) and diluted using purified water. A 0.1 N solution of HCl was used to adjust the pH of water samples to 4.5–5 in the field and also to adjust the pH of the natural spring water used for blanks.

4.2.2.2 Instrumentation

A Varian CP-3800 gas chromatograph equipped with dual programmable injectors and ECD detectors was used. A DB-5 capillary column (30m x 0.25mm x 1 μ m) was used as the main column and the confirmatory column was a DB-1 (30m x 0.25mm x 1 μ m), both Agilent J&W columns from Agilent Technologies (Santa Clara, CA). Helium carrier gas flow and nitrogen make-up gas flow for the ECD were set at 1 ml/min and 30 ml/min, respectively. Injector temperature program was from 80 °C to 240 °C at a rate of 140 °C /min. Column oven temperature was initially set at temp 50 °C (hold 4 min), ramped at 1.5 °C /min to 65 °C (hold 1 min); ramped at 5 °C /min to 120 °C (hold 5 min) and finally ramped at 10 °C/min to 200 °C (hold 5 min). The conditions were the same for both columns.

4.2.2.3 LLE extraction

Samples were removed from cold storage and allowed to sit at ambient temperature for ca 30 minutes. 12 ml of each water sample was removed using a disposable pipette. 3 mL of extracting solvent (MTBE) containing a known concentration of the two surrogate standards 1,2-dibromomethane (surrogate standard-1), 1,3-dibromopropane (surrogate standard-2) were immediately added. Sodium chloride (16 g) was added to each bottle. Bottles were capped, shaken for 2 x 1.5 minutes and then allowed to stand 30 minutes for phase separation. The MTBE extract was transferred to a 4 mL vial, calibrated at 3.0 mL and diluted to the calibration mark with pure MTBE. Drying salt (Na₂SO₄, ca 0.1 g) was added and the vial was vortexed to allow thorough mixing. 15 μ L of the recovery standard solution (50 ng/ μ L) was added to obtain 250 pg/ μ L in the final extract. Extracts were thoroughly mixed by vortexing and stored in labeled vials at cold room temperature (ca 4 °C) until analysis by GC.

4.2.3 Water samples

Samples were collected from 8 public water treatment plants and distribution systems in the winter of 2010 by Health Canada. For each water system five samples were collected including a raw water sample before the treatment plant, a treated water sample

at the plant and three samples at progressively distant points in the distribution system. Water samples were collected and stabilized under the same protocol for SPME and LLE analysis. The samples were collected in 65 ml amber bottles preloaded with 0.2 mL ascorbic acid solution (0.114 M) as a quencher and enough 0.1 N HCl solution to bring the sample at pH 4.5–5. The required HCl amount was predetermined by titration for each water sample. The bottles were filled with no headspace from the water tap after running water for at least 5 minutes. Water samples were packed in ice-filled coolers and sent to both participating laboratories in University of Waterloo and Health Canada for analysis by SPME-GC-MS and LLE-GC-ECD methods, respectively. Samples were analyzed less than 4 days after collection. Stability studies conducted previously in Health Canada show that water samples stabilized according to this protocol and kept in a cold, dark room are stable for at least 14 days (unpublished results).

4.3 Results and Discussion

3.3.1 Analytes description and properties

The DBPs studied in this research were a group of seven analytes including selected haloacetonitriles, haloketones and chloropicrin. Table 4.1 presents the analytes description, acronym, Chemical Abstracts Service Registry Number (CASRN), and physical properties including molecular weight (MW), boiling point (b.p.), solubility in water, Henry's law constant (H) and log of octanol-water partition coefficient ($\log K_{ow}$)^{26, 27}. The value of the Henry's law constant serves as a measure of volatility of analyte while the $\log K_{ow}$ provides an indication of the preference of the compound for the organic phase (lipophilic compounds) or the water phase (hydrophilic compounds). As can be seen from the table, the analytes exhibit different volatility, lipophilicity and solubility in water, which affect their extraction from water.

4.3.1 Fiber selection

To select the most appropriate fiber for the extraction of the analytes, fibers with seven different coatings including PA, CW/DVB, PDMS, PDMS/DVB, CAR/PDMS,

Table 4.1 Description and properties of chloropicrin and commonly found haloacetonitriles and haloketones in drinking water

| Compound | Formula | Acronym | CASRN | MW g/mol | b.p.°C ^a | Solubility ^b g/L | <i>H</i> ^b atm·m ³ /mole | Log <i>K</i> _{ow} ^b |
|-----------------------------|-------------------------------------|-----------|------------|-------------|---------------------|--------------------------------|---|---|
| Chloropicrin | CCl ₃ NO ₂ | CP | 76-06-2 | 164.38 | 112 | 1.62 | 2.05 × 10 ⁻³ | 2.09 |
| Trichloroacetonitrile | CCl ₃ CN | TCAN | 545-06-2 | 144.39 | 86 | 0.72 | 1.34 × 10 ⁻⁶ | 2.09 |
| Dichloroacetonitrile | CHCl ₂ CN | DCAN | 3018-12-0 | 109.94 | 112 | 33.50 | 3.79 × 10 ⁻⁶ | 0.29 |
| Bromochloroacetonitrile | CHBrClCN | BCAN | 83463-62-1 | 154.41 | 139 | 18.70 | 1.24 × 10 ⁻⁶ | 0.38 |
| Dibromoacetonitrile | CHBr ₂ CN | DBAN | 3252-43-5 | 198.84 | 169 | 9.60 | 4.06 × 10 ⁻⁷ | 0.47 |
| 1,1-Dichloro-2-propanone | CHCl ₂ COCH ₃ | 1,1-DCP | 513-88-2 | 126.97 | 120 | 63.82 | 6.15 × 10 ⁻⁶ | 0.20 |
| 1,1,1-Trichloro-2-propanone | CCl ₃ COCH ₃ | 1,1,1-TCP | 918-00-3 | 161.41 | 149 | 7.45 | 2.17 × 10 ⁻⁶ | 1.12 |

^a Ref. 26 (760 torr). ^b Ref. 27 (25°C).

DVB/CAR/PDMS, and a custom-made polydimethylsiloxane/divinylbenzene-N-vinylpyrrolidone (PDMS/DVB-NVP, 70 μm) were tested. Figure 4.1 compares the performance of the various fibers for pre-equilibrium extraction (15 min) of the analytes. As shown, the commercial DVB/CAR/PDMS fiber was more suitable for the range of all analytes. The CAR/PDMS fiber was found to be 40% more efficient for the extraction of DCAN and 1,1-DCP compared with the DVB/CAR/PDMS fiber. The custom-made PDMS/DVB-NVP fiber was 80% more efficient for the extraction of the brominated acetonitriles (DBAN and BCAN). This fiber was prepared by coating a stainless steel wire (0.005”) with a thin film of PDMS diluted in hexane, covering it with the Oasis HLB

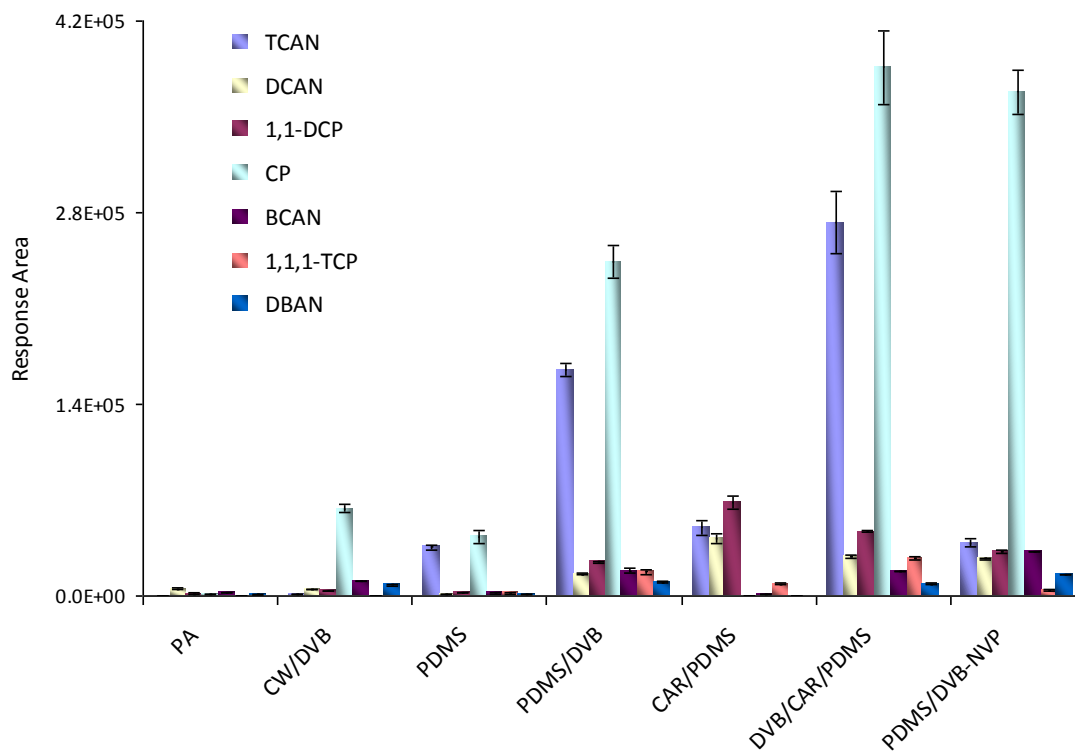


Figure 4.1 Evaluation of different SPME fibers for extraction of TCAN, DCAN, BCAN, DBAN, CP, 1,1-DCP and 1,1,1-TCP in water; 20 $\mu\text{g/L}$ spiked water samples, 15 min headspace extraction at 30°C, n = 3.

particles through shaking inside a small vial, and fixing the particles by PDMS thermal curing. Figure 4.2 shows the SEM image of the custom-made PDMS/DVB-NVP fiber. Based on the overall results and the versatility of the DVB/CAR/PDMS, this fiber was selected for the rest of experiments.

4.3.2 Extraction time

Figure 4.3 illustrates the effect of extraction time on the extraction efficiency of the analytes from water by the headspace SPME. To obtain the time profile, extraction times of 15s, 1 min, 2 min, 4 min, 8 min, 16 min, 30 min, 60 min and 120 min were examined using 20 µg/L spiked water samples. The equilibration times varied between 4 min for TCAN to more than 120 min for DBAN. Based on the results and considering the GC run time, a 15 min extraction time was found to be a good compromise allowing good sensitivity for all analytes.

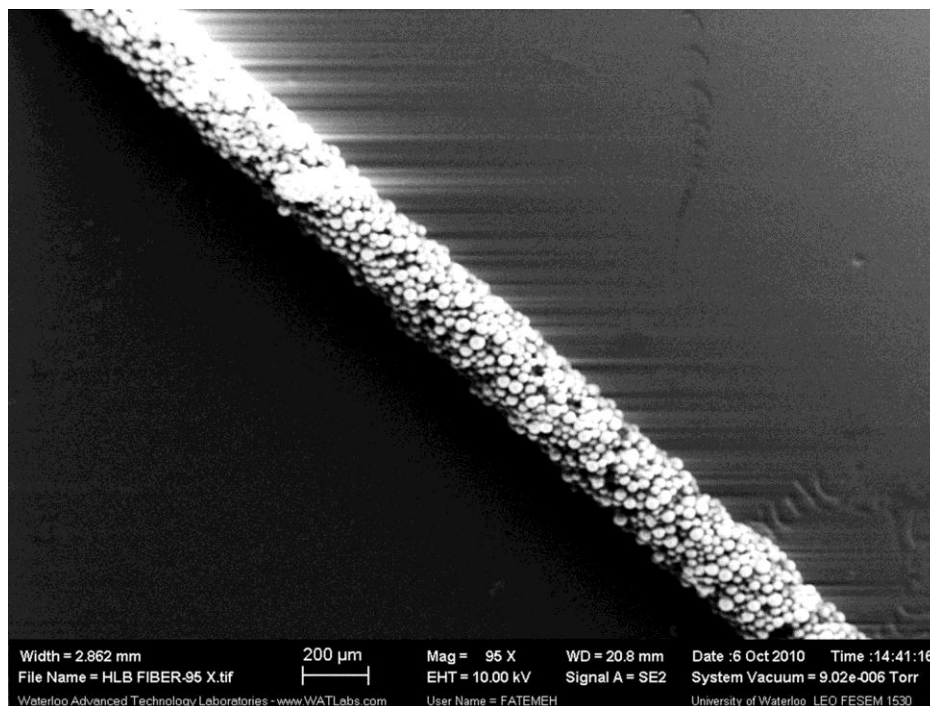


Figure 4.2 SEM image (95 magnifications) of the custom-made PDMS/DVB-NVP fiber.

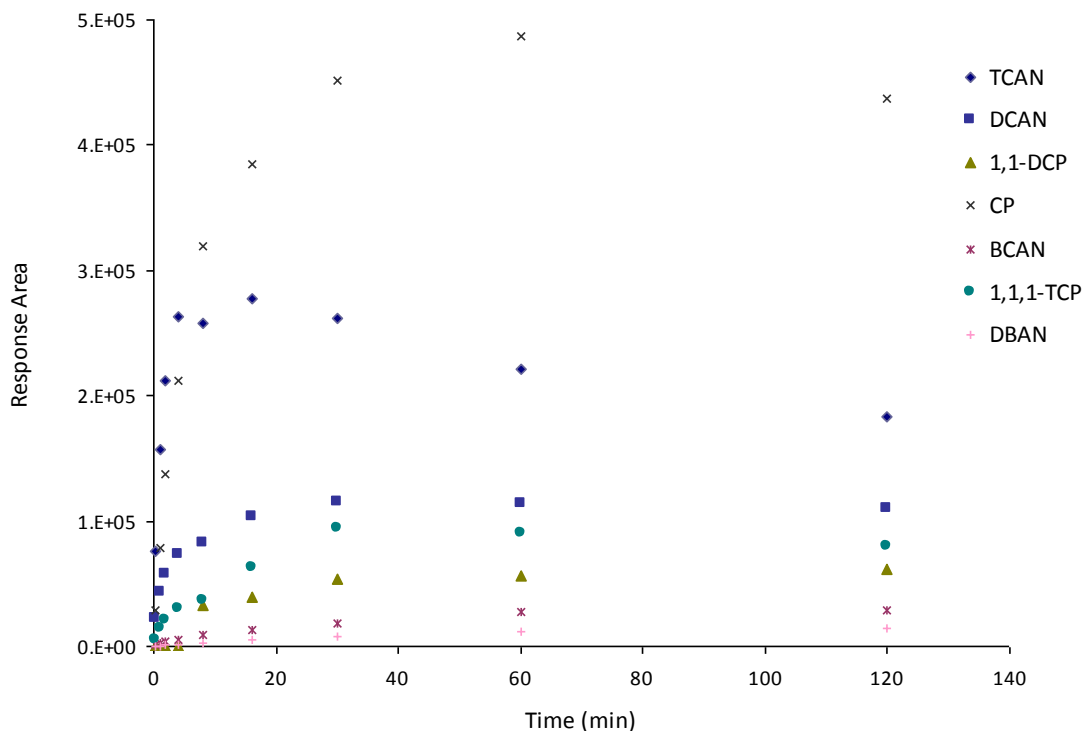


Figure 4.3 HS-SPME extraction time profiles of TCAN, DCAN, BCAN, DBAN, CP, 1,1-DCP and 1,1,1-TCP in water; DVB/CAR/PDMS fiber; 20µg/L spiked water samples, extraction temperature 30°C.

4.3.3 Desorption time

Desorption time and possible carryover of the analytes on the DVB/CAR/PDMS fiber were tested at the injection temperature, 265 °C. Since the analytes are very volatile, they are easily desorbed from the fiber. The optimum desorption time was found to be 2 min leading to complete removal of all analytes from the fiber without carryover.

4.3.4 Chemical ionization

During the optimization procedure it was found that significant background interference impacted the ability of the method to quantify 1,1-DCP and 1,1,1-TCP at low ppb levels in EI mode. At the same time, it was noticed that the major ion fragment on the

EI spectra of these analytes was $m/z = 43$ with an almost total absence of molecular ion. Therefore, chemical ionization with methanol as the reagent was considered as an option to improve the sensitivity. Since an ion trap collects ions over relatively long periods, collisions between analyte and reagent ions are increased. The increased collisions facilitate the possibility of using liquid reagents such as methanol because only low concentrations are needed. For the CI technique, no optimization was performed; rather the instrument was used under the established manufacturer default conditions. Figures 4.4 and 4.5 compare the detection of 1,1-DCP and 1,1,1-TCP for 50 $\mu\text{g/L}$ spiked water samples under EI and CI modes. As shown, the application of CI considerably improved the signal-to-noise ratio and the sensitivity of the method for these two analytes, with the molecular ions becoming significantly abundant. Therefore, CI with methanol was considered as part of optimized method for the two analytes.

4.3.5 Analytical parameters

The calibration curves for all the compounds were established in concentration ranges varying between 0.01 and 20 $\mu\text{g/L}$. The correlation coefficients (R^2) were satisfactory exceeding 0.9925 (Table 4.2). The precision of the measurements (RSD %) at 2 $\mu\text{g/L}$ spike level for three replicates ranged from 4 to 7 % indicating good repeatability of the method. The method detection limits (MDLs) were determined as 3 times the standard deviation of eight replicates at low concentrations close to the detection limits. The MDL for all analytes, including those obtained by the LLE-GC-ECD method, are shown in Table 4.2. The SPME method detection limits for TCAN and CP were lower and for DCAN comparable with those of the LLE method. The MDL values for the rest of analytes were higher than those obtained by the LLE-GC-ECD method.

4.3.6 Sample analysis

The HS-SPME-GC-MS optimized method was applied for analysis of the selected DBPs in real drinking water samples from eight public water treatment and distribution systems in Canada. Table 4.3 describes the characteristics of the water samples including pH, turbidity, temperature and total chlorine as well as disinfection process and population at the region of each water treatment plant.

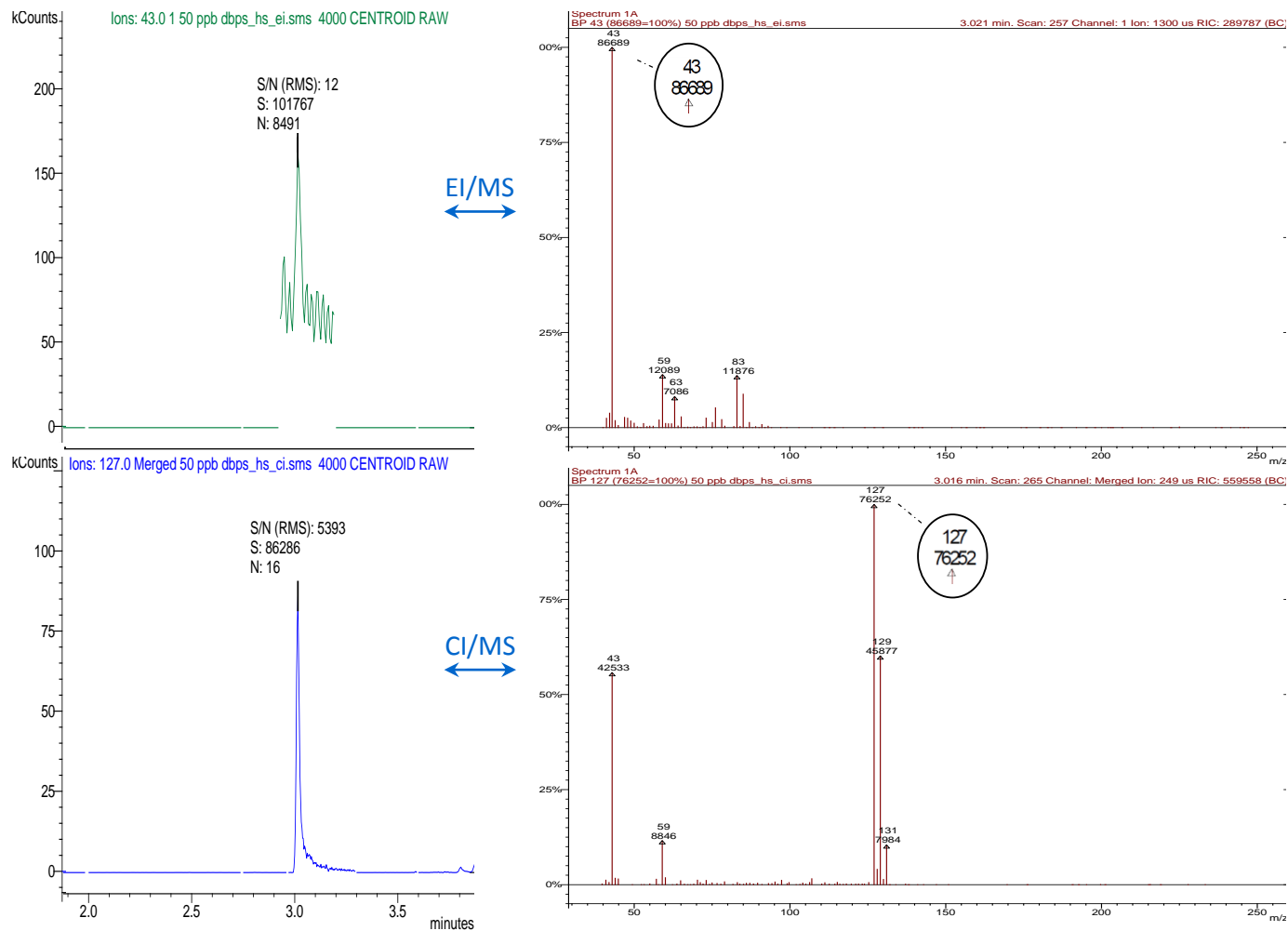


Figure 4.4 GC chromatograms and MS spectra of 1,1-DCP for 50 µg/L spiked water samples; EI (top) and CI (bottom). Molecular ion not observed in EI mode, signal-to-noise ratio significantly increased in CI mode.

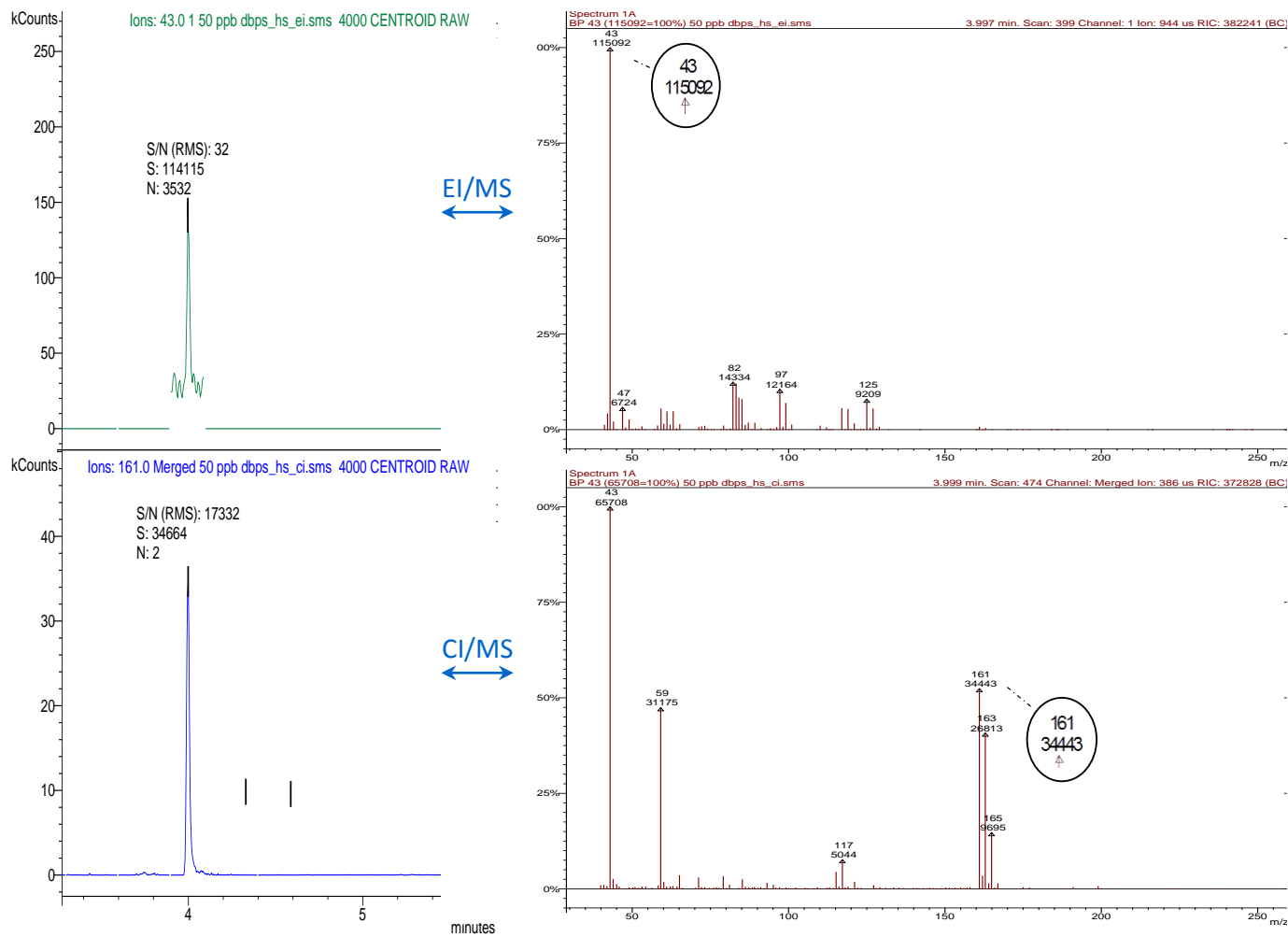


Figure 4.5 GC chromatograms and MS spectra of 1,1,1-TCP for 50 µg/L spiked water samples; EI (top) and CI (bottom). Molecular ion not observed in EI mode, signal-to-noise ratio significantly increased in CI mode.

Table 4.2 Analytical parameters using spiked water samples

| Compound | Quantification ion (m/z) | Linear range (µg/L) | Correlation coefficient (R ²) | RSD% (n=3) | SPME MDLs (ng/L) | LLE MDLs [†] (ng/L) |
|-----------------------------|--------------------------|---------------------|---|------------|------------------|------------------------------|
| Chloropicrin | 117 | 0.02-10 | 0.9959 | 4 | 7 | 40 |
| Trichloroacetonitrile | 108 | 0.01-20 | 0.9997 | 5 | 2 | 30 |
| Dichloroacetonitrile | 74 | 0.10-20 | 0.9990 | 4 | 40 | 40 |
| Bromochloroacetonitrile | 74 | 0.50-20 | 0.9925 | 5 | 160 | 30 |
| Dibromoacetonitrile | 118 | 0.50-20 | 0.9964 | 5 | 130 | 30 |
| 1,1-Dichloro-2-propanone | 127 | 0.30-5 | 0.9970 | 7 | 100 | 30 |
| 1,1,1-Trichloro-2-propanone | 161 | 0.60-10 | 0.9997 | 7 | 180 | 30 |

Note: Quantification, linear range, correlation coefficient and relative standard deviation (RSD%) data are of the SPME method.

[†] Printed with permission from Health Canada.

Table 4.3 Characteristics of the Canadian drinking water samples (Winter 2010)

| WTP - # | WTP-36 | WTP-46 | WTP-49 | WTP-53 | WTP-54 | WTP-55 | WTP-59 | WTP-60 |
|-------------------------------------|-----------------|-----------------|---------------------|-----------------|-----------------|-----------------|-----------------|-----------------|
| Total population supplied | 5000 | 35000 | 580000 | 70000 | 1421 | 10000 | 700000 | 6000 |
| Raw water source | River | River | Lake | Lake | Well | Well | River | Lake |
| Raw water pH | 7.11 | 8.11 | 7.35 | 6.34 | 6.71 | 7.69 | 8.20 | 7.91 |
| Raw water turbidity | 0.13 | 6.68 | 0.42 | 0.63 | 2.90 | 0.12 | 1.46 | 0.49 |
| Raw water temp | 2.5 | 1.5 | 3 | 3 | 6 | 7 | 1 | 1.5 |
| Treated water pH | 7.68 | 7.51 | 7.56 | 5.75 | 7.08 | 7.61 | 7.52 | 7.6 |
| Treated water turbidity | 0.70 | 0.12 | 0.14 | 0.75 | 0.62 | 0.17 | 0.08 | 0.06 |
| Treated water temp | 5.5 | 2 | 3 | 4 | 6 | 6.5 | 1 | 1.5 |
| Treated water total Cl ₂ | 0.90 | 1.95 | 1.34 | 2.78 | 0.26 | 0.65 | 0.79 | 0.68 |
| D1 total Cl ₂ | 0.70 | 2.10 | 1.01 | 1.73 | 0.36 | 0.39 | 0.69 | 0.65 |
| D2 total Cl ₂ | 0.65 | 1.62 | 0.88 | 1.46 | 0.26 | 0.37 | 0.88 | 0.74 |
| D3 total Cl ₂ | 0.54 | 1.39 | 0.39 | 0.67 | 0.28 | 0.38 | 0.84 | 0.61 |
| Post disinfection process | Cl ₂ | Cl ₂ | Cl ₂ | Cl ₂ | Cl ₂ | Cl ₂ | Cl ₂ | Cl ₂ |
| Other disinfection processes | --- | --- | O ₃ , UV | --- | --- | --- | --- | UV |

Note: WTP (water treatment plant); D1, D2, D3: treated water at three progressively distant locations in distribution system; total Cl₂ values in mg/liter.

For each water system five samples were collected including a raw water sample (R) before the treatment plant, a treated water sample (T) at the treatment plant and three samples at progressively distant locations in the distribution system (D1, D2, D3). The SPME results along with those obtained with the LLE-GC-ECD method in Health Canada laboratories were summarized in Table 4.4. For comparison of the results between the two methods, a scattered plot was derived by pooling the data. As illustrated in Fig. 4.6, there is good correlation ($R^2 = 0.9217$) between the results obtained by the two methods.

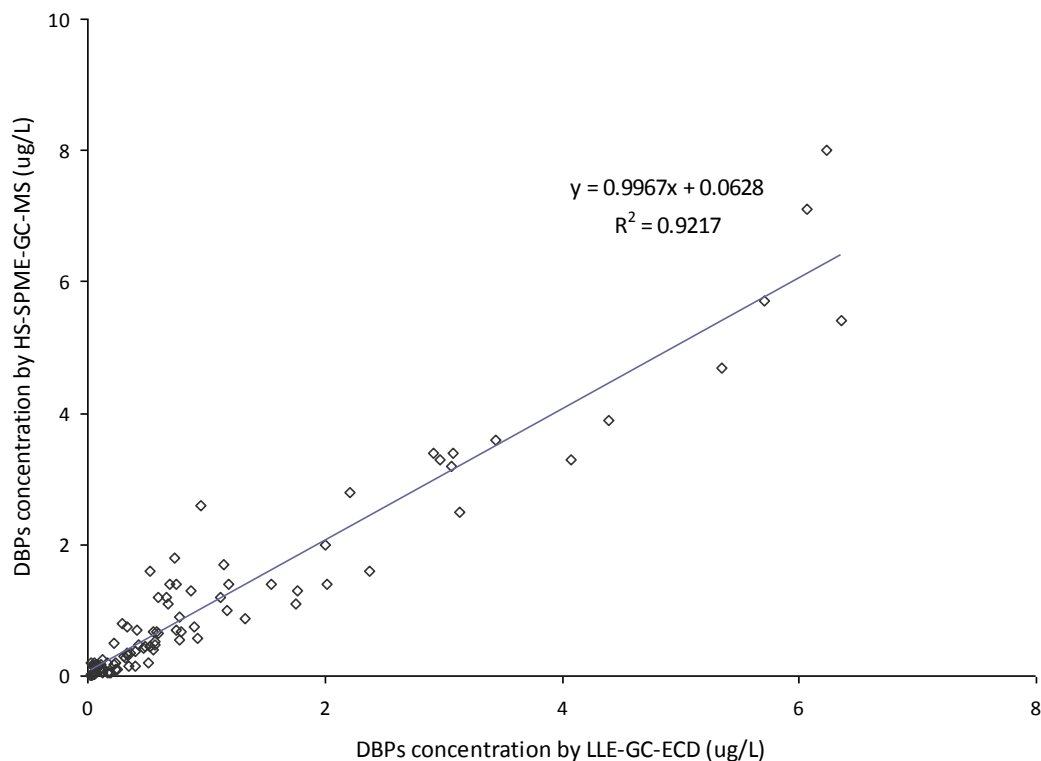


Figure 4.6 Scatter plot of amounts of TCAN, DCAN, BCAN, DBAN, CP, 1,1-DCP and 1,1,1-TCP detected in some Canadian water samples measured by HS-SPME-GC-MS and LLE-GC-ECD.

Table 4.4 Results of drinking water sample analysis by the LLE and the SPME methods[†]

| WTP-# | DBP (µg/L) | TCAN | | DCAN | | 1,1-DCP | | CP | | BCAN | | 1,1,1-TCP | | DBAN | |
|-----------|------------|------|------|------|------|---------|------|------|------|------|------|-----------|------|------|------|
| | Method | LLE | SPME | LLE | SPME | LLE | SPME | LLE | SPME | LLE | SPME | LLE | SPME | LLE | SPME |
| WTP-36-R | | ND | ND | ND | ND | ND | ND | ND | ND | ND | ND | ND | ND | ND | ND |
| WTP-36-T | | ND | ND | ND | ND | 0.11 | 0.10 | ND | ND | ND | ND | 0.20 | ND | ND | ND |
| WTP-36-D1 | | ND | ND | 0.22 | 0.17 | 0.11 | 0.18 | 0.05 | ND | ND | ND | 0.56 | 0.40 | ND | ND |
| WTP-36-D2 | | ND | ND | 0.37 | 0.34 | 0.09 | 0.16 | 0.06 | ND | ND | ND | 0.77 | 0.54 | ND | ND |
| WTP-36-D3 | | ND | ND | 0.47 | 0.43 | 0.07 | 0.18 | 0.07 | ND | ND | ND | 0.92 | 0.57 | ND | ND |
| WTP-46-R | | ND | ND | ND | ND | ND | ND | ND | ND | ND | ND | ND | ND | ND | ND |
| WTP-46-T | | 0.03 | ND | 1.76 | 1.1 | 0.57 | 0.52 | ND | 0.02 | 0.39 | ND | 1.19 | 1.4 | 0.62 | ND |
| WTP-46-D1 | | 0.04 | 0.02 | 2.38 | 1.6 | 0.60 | 0.64 | ND | 0.02 | 0.53 | 1.6 | 1.55 | 1.4 | 0.23 | 0.5 |
| WTP-46-D2 | | 0.05 | 0.04 | 3.14 | 2.5 | 0.60 | 1.2 | ND | 0.03 | 0.73 | 1.8 | 2.21 | 2.8 | 0.29 | 0.8 |
| WTP-46-D3 | | 0.04 | 0.02 | 4.08 | 3.3 | 0.34 | 0.75 | 0.05 | 0.03 | 0.96 | 2.6 | 3.44 | 3.6 | 0.41 | 0.7 |
| WTP-49-R | | ND | ND | ND | ND | ND | ND | ND | ND | ND | ND | ND | ND | ND | ND |
| WTP-49-T | | 0.04 | 0.02 | 2.00 | 2.0 | 0.78 | 0.9 | ND | ND | 0.08 | ND | 3.07 | 3.2 | ND | ND |
| WTP-49-D1 | | 0.04 | 0.02 | 2.98 | 3.3 | 0.68 | 1.1 | 0.16 | 0.04 | 0.15 | ND | 5.71 | 5.7 | ND | ND |
| WTP-49-D2 | | 0.03 | 0.02 | 3.09 | 3.4 | 0.74 | 1.4 | 0.18 | 0.05 | 0.16 | ND | 6.07 | 7.1 | ND | ND |
| WTP-49-D3 | | 0.03 | 0.01 | 2.92 | 3.4 | 0.69 | 1.4 | 0.20 | 0.06 | 0.14 | ND | 6.23 | 8.0 | ND | ND |
| WTP-53-R | | ND | ND | ND | ND | ND | ND | ND | ND | ND | ND | ND | ND | ND | ND |
| WTP-53-T | | ND | ND | 0.26 | 0.10 | 1.12 | 1.2 | 0.13 | 0.06 | ND | ND | 1.78 | 1.3 | ND | ND |
| WTP-53-D1 | | ND | 0.01 | 0.79 | 0.68 | 0.66 | 1.2 | 0.35 | 0.15 | ND | ND | 4.40 | 3.9 | ND | ND |
| WTP-53-D2 | | 0.04 | 0.02 | 1.33 | 0.88 | 0.87 | 1.3 | 0.41 | 0.15 | ND | ND | 5.35 | 4.7 | ND | ND |
| WTP-53-D3 | | 0.07 | 0.04 | 2.02 | 1.4 | 1.15 | 1.7 | 0.51 | 0.19 | 0.03 | ND | 6.36 | 5.4 | ND | 0.45 |

[†] Printed with permission from Health Canada; WTP: water treatment plant; R: raw water; T: treated water at the plan; D1, D2, D3: treated water at three progressively distant locations in distribution system; ND: not detected.

Table 4.4 (continued)

| WTP-# | DBP (µg/L) | TCAN | | DCAN | | 1,1-DCP | | CP | | BCAN | | 1,1,1-TCP | | DBAN | |
|-----------|------------|------|------|------|------|---------|------|------|------|------|------|-----------|------|------|------|
| | Method | LLE | SPME | LLE | SPME | LLE | SPME | LLE | SPME | LLE | SPME | LLE | SPME | LLE | SPME |
| WTP-54-R | | ND | ND | ND | ND | ND | ND | ND | ND | ND | ND | ND | ND | ND | ND |
| WTP-54-T | | ND | ND | ND | ND | ND | ND | ND | ND | 0.05 | ND | 0.04 | ND | 0.03 | ND |
| WTP-54-D1 | | ND | ND | 0.04 | ND | ND | ND | ND | ND | 0.04 | ND | 0.04 | ND | ND | ND |
| WTP-54-D2 | | ND | ND | 0.04 | ND | ND | ND | ND | ND | 0.05 | ND | 0.05 | ND | 0.03 | ND |
| WTP-54-D3 | | ND | ND | 0.06 | ND | ND | ND | ND | ND | 0.06 | ND | 0.06 | ND | 0.04 | ND |
| WTP-55-R | | ND | ND | ND | ND | ND | ND | ND | ND | ND | ND | ND | ND | ND | ND |
| WTP-55-T | | ND | ND | ND | ND | ND | ND | ND | ND | ND | ND | ND | ND | ND | ND |
| WTP-55-D1 | | ND | ND | 0.04 | ND | ND | ND | ND | ND | 0.03 | ND | 0.09 | ND | ND | 0.3 |
| WTP-55-D2 | | ND | ND | 0.07 | ND | ND | ND | ND | ND | 0.05 | ND | 0.11 | ND | ND | 0.4 |
| WTP-55-D3 | | ND | ND | 0.13 | 0.08 | ND | ND | ND | ND | 0.07 | ND | 0.23 | 0.20 | ND | 0.5 |
| WTP-59-R | | ND | ND | ND | ND | ND | ND | ND | ND | ND | ND | ND | ND | ND | ND |
| WTP-59-T | | ND | ND | 0.31 | 0.29 | 0.11 | 0.13 | ND | ND | ND | ND | 0.33 | 0.35 | ND | ND |
| WTP-59-D1 | | ND | ND | 0.53 | 0.44 | 0.06 | 0.15 | ND | ND | 0.03 | ND | 0.55 | 0.68 | ND | ND |
| WTP-59-D2 | | ND | ND | 0.41 | 0.38 | 0.08 | 0.15 | ND | ND | ND | ND | 0.43 | 0.48 | ND | ND |
| WTP-59-D3 | | ND | ND | 0.57 | 0.47 | 0.05 | 0.14 | ND | ND | 0.03 | ND | 0.58 | 0.67 | ND | ND |
| WTP-60-R | | ND | ND | ND | ND | ND | ND | ND | ND | ND | ND | ND | ND | ND | ND |
| WTP-60-T | | ND | ND | 0.23 | 0.10 | 0.17 | 0.2 | ND | ND | ND | ND | 0.52 | 0.46 | ND | ND |
| WTP-60-D1 | | ND | ND | 0.49 | 0.45 | 0.03 | 0.2 | 0.05 | ND | 0.03 | ND | 1.17 | 1.0 | ND | ND |
| WTP-60-D2 | | ND | ND | 0.32 | 0.27 | 0.06 | 0.2 | ND | ND | ND | ND | 0.75 | 0.70 | ND | ND |
| WTP-60-D3 | | ND | ND | 0.34 | 0.32 | 0.12 | 0.2 | 0.04 | ND | ND | ND | 0.91 | 0.76 | ND | ND |

† Printed with permission from Health Canada; WTP: water treatment plant; R: raw water; T: treated water at the plant; D1, D2, D3: treated water at three progressively distant locations in distribution system; ND: not detected.

4.4 Conclusions

This study describes a fast automated HS-SPME-GC-MS method for determination of the selected haloacetonitriles (HANs), halo ketones (HKs) and chloropicrin (CP) in drinking water with good sensitivity at ng/L levels using DVB/CAR/PDMS fiber. The total analysis time including extraction and chromatographic run was 30 min. Chemical ionization (CI) was essential to increase the sensitivity of the MS detection for the halo ketones. The novel custom-made PDMS/DVB-NVP fiber prepared in this study showed 80% more efficiency for the extraction of the brominated acetonitriles. The method exhibited good linearity in concentration ranges up to 20 µg/L with correlation coefficients exceeding 0.9925. The MDLs obtained by the SPME method for the trichloroacetonitrile and chloropicrin were lower, the one for dichloroacetonitrile was comparable, and those for brominated acetonitriles and halo ketones were higher than those obtained by the LLE-GC-ECD method. The results of sample analysis generated by the HS-SPME-GC-MS and the LLE-GC-ECD methods were in good agreement with each other indicating the applicability of the developed SPME method for rapid analysis of these disinfection by-products in drinking water samples.

4.5 References

1. Zhang X, Echigo S, Minear RA, Plewa MJ. 2000. Characterization and comparison of disinfection by-products of four major disinfectants, p. 299–314. In Barrett SW and Amy GL (ed.), *Natural Organic Matter and Disinfection By-Products: Characterization and Control in Drinking Water*. American Chemical Society, Washington, DC.
2. Yang X, Shang C, Westerhoff P. 2007. Factors affecting formation of haloacetonitriles, halo ketones, chloropicrin and cyanogen halides during chloramination. *Water Research* 41(6): 1193–1200.
3. Lipscomb JC, El-Demerdash E, Ahmed AE. 2009. Haloacetonitriles: metabolism and toxicity. *Rev. Environ. Contam. Toxicol.* 198: 169–200.
4. Richardson SD, Plewa MJ, Wagner ED, Schoeny R, DeMarini DM. 2007. Occurrence, genotoxicity, and carcinogenicity of regulated and emerging disinfection by-products in drinking water: A review and roadmap for research. *Mutation Research* 636(1–3): 178–242.
5. Weinberg HS, Krasner SW, Richardson SD, Thruston ADJ. 2002. The Occurrence of Disinfection By-Products (DBPs) of Health Concern in Drinking Water: Results of a Nationwide DBP Occurrence Study. EPA/600/R02/068, U.S. Environmental Protection Agency, Washington, DC.
6. Krasner SW, McGuire MJ, Jacangelo JG, Patania NL, Reagan KW, Aieta EM. 1989. The occurrence of disinfection by-products in US drinking water. *J. Am. Water Works Ass.* 81(8): 41–53.
7. Williams DT, Lebel GL, Benoit FM. 1997. Disinfection byproducts in Canadian drinking water. *Chemosphere* 34: 299–316.

8. U.S EPA Information Collection Rule, 1996. Final Rule. Federal Register, Vol. 61, No.94, 24354.
9. U.S. EPA Method 551.1. 1995. Determination of Chlorination Disinfection Byproducts, Chlorinated Solvents, and Halogenated Pesticides/Herbicides in Drinking Water by Liquid-Liquid Extraction and Gas Chromatography with Electron-Capture Detection. National Exposure Research Laboratory, U.S. EPA, Cincinnati, Ohio.
Available on-line at:
<http://www.epa.gov/sam/pdfs/EPA-551.1.pdf>
[Accessed: 11 October 2011].
10. U.S. EPA Method 524.2. 1995. Measurement of Purgeable Organic Compounds in Water by Capillary Column Gas Chromatography/Mass Spectrometry. National Exposure Research Laboratory, U.S. EPA, Cincinnati, Ohio, 45268.
Available on-line at:
<http://www.epa.gov/sam/pdfs/EPA-524.2.pdf>
[Accessed: 11 October 2011].
11. Wolska L, Olszewska C, Turska M, Zygmunt B, Namiesnik J. 1998. Volatile and semivolatile organohalogen trace analysis in surface water by direct aqueous injection GC-ECD. *Chemosphere* 37(13): 2645–2651.
12. Golfinopoulos SK, Lekkas TD, Nikolaou AD. 2001. Comparison of methods for determination of volatile organic compounds on drinking water. *Chemosphere* 45(3): 275–284.
13. Arthur CL, Pawliszyn J. 1990. Solid phase microextraction with thermal desorption using fused silica optical fibers. *J. Anal. Chem.* 62: 2145–2148.

14. Chai M, Arthur CL, Pawliszyn J, Belardi RP, Pratt KF. 1993. Determination of volatile chlorinated hydrocarbons in air and water with solid-phase microextraction. *Analyst* 118(12): 1501–1505.
15. Pawliszyn J. 1997. *Solid Phase Microextraction: Theory and Practice*. Wiley-VCH, New York.
16. Chen, ML, Mao IF, Hsu CC. 1997. Determination of trihalomethanes in drinking water by solid-phase microextraction and gas chromatography with electron-captured detection. *Toxicol. Environ. Chem.* 60: 39–45.
17. Stack MA, Fitzgerald G, O'Connell S, James KJ. 2000. Measurement of trihalomethanes in potable and recreational waters using solid phase micro extraction with gas chromatography-mass spectrometry. *Chemosphere* 41(11): 1821–1826.
18. Cho DH, Kong SH, Oh SG. 2003. Analysis of trihalomethanes in drinking water using headspace-SPME technique with gas chromatography. *Water Research* 37(2): 402–408.
19. Cardinali FL, Ashley DL, Morrow JC, Moll DM, Blount BC. 2004. Measurement of trihalomethanes and methyl tertiary-butyl ether in tap water using solid-phase microextraction GC-MS. *J. Chromatogr. Sci.* 42(4): 200–206.
20. Nakamura S, Daishima S. 2005. Simultaneous determination of 22 volatile organic compounds, methyl-tert-butyl ether, 1,4-dioxane, 2-methylisoborneol and geosmin in water by headspace solid phase microextraction-gas chromatography-mass spectrometry. *Anal. Chim. Acta* 548(1–2): 79–85.

21. San Juan PM, Carrillo JD, Tena MT. 2007. Fibre selection based on an overall analytical feature comparison for the solid-phase microextraction of trihalomethanes from drinking water. *J. Chromatogr. A* 1139(1): 27–35.
22. Guimaraes AD, Carvalho JJ, Goncalves C, Alpendurada MF. 2008. Simultaneous analysis of 23 priority volatile compounds in water by solid-phase microextraction-gas chromatography-mass spectrometry and estimation of the method's uncertainty. *Inter. J. Environ. Anal. Chem.* 88(3): 151–164.
23. Niri VH, Bragg L, Pawliszyn J. 2008. Fast analysis of volatile organic compounds and disinfection by-products in drinking water using solid-phase microextraction-gas chromatography/time-of-flight mass spectrometry. *J. Chromatogr. A* 1201(2): 222–227.
24. Scilimenti MJ, Krasner SW, Richardson SD. 2002. The determination of DBPs using a solid-phase microextraction (SPME)-GC/ECD technique, p. 1115–1134. Proceedings of Water Quality Technology Conference, American Water Works Association, Denver.
25. Antoniou CV, Koukouraki EE, Diamadopoulos E. 2006. Determination of chlorinated volatile organic compounds in water and municipal wastewater using headspace solid phase microextraction gas chromatography. *J. Chromatogr. A* 1132(1–2): 310–314.
26. CRC Handbook of Chemistry and Physics 89th Edition 2009
27. Hazardous Substances Data Bank (HSDB), 2011. Toxicology Data Network, US National Library of Medicine.
Available on-line at:
<http://toxnet.nlm.nih.gov/>
[Accessed: 20 October 2011].

Chapter 5

Summary and future directions

5.1 Summary

Sample preparation has been recognized as the main bottleneck of analytical procedures in many applications, comprising the slowest, most complicated step that has a direct impact on precision, accuracy, sensitivity and overall performance of analytical methods. The conventional sample preparation methods for analysis of DBPs in water are liquid-liquid extraction (LLE), solid phase extraction (SPE) and purge-and-trap (P&T). While these methods are frequently used for DBPs analysis they suffer from disadvantages such as the need for organic solvent, time-consuming and multi-step procedures, complicated set-ups and the cost associated with the techniques. To devise simpler, faster and more sustainable methods, several microextraction techniques have been developed in the past two decades. Among these, solid phase microextraction (SPME) in the form of coated fibers has been evolving very quickly, appearing in almost every field of analytical chemistry, particularly environmental and water analysis. SPME fibers with absorptive and/or adsorptive coatings have addressed the need for a rapid,

simple, automated sample preparation method by integrating sampling, isolation, enrichment and sample introduction into a single solvent-free step. The mixed-phase adsorptive fiber coatings have provided more selectivity and wider range of SPME application for analytes with different size and polarity, at the expense of narrower linear range. In some applications, SPME fiber approach may not provide the desired sensitivity for analysis due to the small volume of the coating (extraction phase) and low distribution coefficient of some analytes between the coating and sample matrix. To overcome this limitation, stir bar sorptive extraction (SBSE) and thin film microextraction (TFME) with large volume (typically 25-125 times more) polydimethylsiloxane (PDMS) as the extraction phase were developed by different workers, which proved to have considerable higher extraction efficiencies than SPME fibers in some applications. Further, the PDMS membrane TFME was shown to achieve higher extraction rates and shorter equilibration times than SBSE for aqueous samples, owing to larger surface-to-volume ratio of PDMS extraction phase. However, application of PDMS as extraction phase still limits the selectivity and sensitivity obtainable by these approaches.

To address this limitation and for effective preconcentration of polar DBPs in water samples, a new technique for sampling and sample preparation using novel mixed-phase thin film (MPTF) devices was presented in this research for the first time. Highly particle-loaded Carboxen/polydimethylsiloxane (CAR/PDMS) and polydimethylsiloxane/divinylbenzene (PDMS/DVB) thin films coated on a deactivated glass wool fabric mesh substrate by spin coating were developed. The thickness of thin film coating could be controlled by spin coating procedure and the samplers were easily tailored in shape and size by cutting tools for application using Gerstel TDU-CIS-GC-MS system. The MPTF samplers showed good durability and no deterioration after 50 times extractions. The incorporation of glass wool fabric mesh in the structure of thin film device, developed in this research, not only enabled fabrication of MPTF devices with high particle-to-PDMS weight ratios, but also addressed the problem of thin film membrane twisting during stirring which adversely affect extraction rate by reducing effective interface area. This contribution obviates the need for a framed holder to preserve thin film flat-shape during extraction and makes the thin film samplers more robust and user-friendly. The performance of the novel MPTF devices was illustrated by extraction and enrichment of

seven different N-nitrosamines from spiked water samples. These DBPs were initially found to be best extracted with CAR/PDMS and PDMS/DVB fiber coatings; the latter was suitable for extraction of the more lipophilic analytes. The N-nitrosamines were also found to be partially decomposed during thermal desorption from the CAR/PDMS coating, however, their quantification using the coating was still satisfactory. The N-nitrosamines were extracted by both CAR/PDMS and PDMS/DVB TF samplers followed by thermal desorption, cryofocusing in cooled injection system and GC-MS analysis. Due to the increased amount of extraction phase in the MPTF samplers (40-50 times), marked enhancement of extraction efficiencies (typically more than one order of magnitude) for the model compounds was obtained, under generally pre-equilibrium conditions, compared to the commercial SPME fibers. As well, marked enhancement on the extraction efficiency for the model compounds was observed with the PDMS/DVB TF sampler compared to the commercial PDMS TF. The satisfactory results obtained by the novel MPTF devices, including linearity, repeatability and lower detection ability at low ng/L for the tested compounds firmly establish analytical performance of the new thin film samplers with sensitivities higher than SPME fibers and with a wide application range typical of mixed-phase coatings. The user-friendly format and robustness of the novel devices are also promising for on-site applications, which is the ultimate use of thin film samplers.

Apart from development and evaluation of the MPTF samplers mentioned above, the performance and accuracy of the SPME fiber technique for selected DBPs were demonstrated with real drinking water samples analysis through collaborations and comparative studies with Health Canada. In the first study in 2009, four regulated trihalomethanes (THMs) in source and drinking water samples from six water treatment and distribution systems in Canada, collected under similar sampling and sample stabilization protocol, were analyzed in parallel using an optimized headspace SPME-GC-MS method in the University of Waterloo (UW) and a LLE-GC-ECD method equivalent to EPA 551.1 in Health Canada laboratories. In this study, a fast, sensitive automated HS-SPME-GC-MS method was developed for determination of these THMs in drinking water. The method detection limits were in low ng/L levels using a 100 μ m PDMS fiber. Excellent linearity ($R^2 \geq 0.9979$) for all the THMs was obtained in a wide

concentration range (0.1-100 µg/L) with repeatability of generally less than 4%. The quantitative measurements of the THMs in the real drinking water samples by the optimized HS-SPME-GC-MS and the LLE-GC-ECD methods showed excellent agreement between the values obtained by the two methods. The results of this study along with the SPME method advantages proved that the HS-SPME-GC-MS was a fast reliable alternative to the LLE-GC-ECD method for analysis of the THMs in the concentration ranges that are typical and relevant for drinking water samples.

In another study in 2010, seven target DBPs (four haloacetonitriles, two halo ketones and chloropicrin) in source and drinking water samples from eight water treatment and distribution systems in Canada were analyzed in parallel by an optimized HS-SPME-GC-MS method (in UW) and the LLE-GC-ECD method equivalent to EPA 551.1 (in Health Canada laboratories). This study presented a fast automated HS-SPME-GC-MS method for determination of the selected analytes in drinking water with good sensitivity at ng/L levels using DVB/CAR/PDMS fiber. Chemical ionization (CI) was employed to increase the sensitivity of the MS detection for the halo ketones. A novel custom-made PDMS/DVB-NVP fiber was prepared showing 80% more efficiency for the extraction of the brominated acetonitriles. Good linearity ($R^2 \geq 0.9925$) for the target analytes was obtained in concentration ranges up to 20µg/L, which were generally narrower than that obtained by the PDMS fiber for THMs. The results of real sample analysis generated by the HS-SPME-GC-MS and the LLE-GC-ECD methods were in good agreement with each other indicating the applicability of the developed SPME method for rapid analysis of these disinfection by-products in drinking water samples.

5.2 Future directions

Development and fabrication of the novel thin film samplers, presented in this thesis, is a remarkable contribution to thin film microextraction in that it expands application of the technique for a wider range of analytes in a more robust and user-friendly way and opens new areas of related research. Future contributions related to MPTF technique and TF fabrication by spin coating will include a number of different directions. Absorbent type (liquid-like) TF samplers other than PDMS such as polyacrylate (PA) and

polyethylene glycol (PEG) of desired thicknesses may be prepared as particle-free or particle-loaded form by spin coating. Other adsorptive particles such as Carbo-pack Z (a porous graphitized carbon material), hydrophilic-lipophilic balance (HLB) particles, e.g. divinylbenzene-N-vinylpyrrolidone (DVB-NVP) co-polymer, C18 and a wide variety of other particles can be used for fabrication of MPTF samplers. MPTF samplers with dual-type coating such as DVB/CAR/PDMS of desired thickness can be prepared by sequential spin coating procedures. These can be fabricated as either layer-over-layer or as individual layers coated on each side of TF sampler, which is an advantage in that it provides free access of analytes to each coating. The MPTF technique can be applied to other challenging DBPs and micropollutants in water for more sensitive extraction and analysis. MPTF samplers can also be used for gaseous or other samples. Liquid desorption can be examined instead of thermal desorption, followed by large volume injection, or in combination with liquid chromatography.

Appendix A

Video Illustration I

This appendix is a video file titled “Video illustration I - Novel CAR-PDMS thin film sampler coated on GW mesh substrate rotating in water”.

The file name of this video is “Video illustration I - Novel CAR-PDMS thin film sampler coated on GW mesh substrate rotating in water.mp4”.

This video illustrates flat-shape stability of the novel CAR-PDMS thin film sampler, coated on glass wool fabric mesh substrate, while rotating in water at increasing speed between 0 to 2000 rpm.

If you accessed this thesis from a source other than the University of Waterloo, you may not have access to this file. You may access it by searching for this thesis at <http://uwspace.uwaterloo.ca>.

Appendix B

Video Illustration II

This appendix is a video file titled “Video illustration II - Novel PDMS thin film sampler coated on GW mesh substrate rotating in water”.

The file name of this video is “Video illustration II - Novel PDMS thin film sampler coated on GW mesh substrate rotating in water.mp4”.

This video illustrates flat-shape stability of a novel PDMS thin film sampler, coated on glass wool fabric mesh substrate, while rotating in water at increasing speed between 0 to 2000 rpm.

If you accessed this thesis from a source other than the University of Waterloo, you may not have access to this file. You may access it by searching for this thesis at <http://uwspace.uwaterloo.ca>.

Appendix C

Video Illustration III

This appendix is a video file titled “Video illustration III - Commercial PDMS thin film membrane rotating in water”.

The file name of this video is “Video illustration III - Commercial PDMS thin film membrane rotating in water.mp4”.

This video illustrates lack of flat-shape stability of a typical commercial PDMS thin film membrane sampler while rotating in water at increasing speed between 0 to 2000 rpm.

If you accessed this thesis from a source other than the University of Waterloo, you may not have access to this file. You may access it by searching for this thesis at <http://uwspace.uwaterloo.ca>.